



Universitat Autònoma de Barcelona

ADVERTIMENT. L'accés als continguts d'aquesta tesi queda condicionat a l'acceptació de les condicions d'ús establertes per la següent llicència Creative Commons:  http://cat.creativecommons.org/?page_id=184

ADVERTENCIA. El acceso a los contenidos de esta tesis queda condicionado a la aceptación de las condiciones de uso establecidas por la siguiente licencia Creative Commons:  <http://es.creativecommons.org/blog/licencias/>

WARNING. The access to the contents of this doctoral thesis it is limited to the acceptance of the use conditions set by the following Creative Commons license:  <https://creativecommons.org/licenses/?lang=en>

The Small GTPase RHOA in cancer

By

Estefanía Anguita Espinosa

For the title of PhD

Biochemistry, Molecular Biology and Biomedicine doctorate program

Faculty of Medicine

Universitat Autònoma de Barcelona

The work was carried out at

Group of Biomedical Research in Digestive Tract Tumors

Vall d'Hebron Institut de Recerca (VHIR)

and

Group of Molecular Oncology

Institut de Recerca Biomèdica de Lleida Fundació Dr. Pifarré (IRBLleida)

March 2022

DIRECTOR

Dr. Diego Arango

DIRECTOR

Dr. Águeda Martínez

DIRECTOR

Dr. Jose Higinio Dopeso

TUTOR

Dr. Miquel Vila

PhD CANDIDATE

Estefanía Anguita

A mi trébol de cuatro hojas,

Mamá, papá, Almu y Patri

INDEX OF CONTENTS

ABSTRACT/RESUMEN/RESUM	13
------------------------------	----

CHAPTER I. FUNCTIONAL CHARACTERIZATION OF RHOA HOTSPOT MUTATIONS

ABSTRACT	21
----------------	----

INTRODUCTION	25
--------------------	----

1. General aspects of cancer	25
2. Signaling pathways in cancer and contribution of small GTPases	31
MAPK pathway	31
PI3K pathway	33
3. RHO GTPases	34
Structure	35
Activity regulation	36
Cellular functions	38
4. RHOA GTPase in cancer	42
RHOA as oncogene	42
RHOA as tumor suppressor	46
RHOA mutations in cancer	48

AIMS OF THE STUDY	57
-------------------------	----

MATERIALS AND METHODS	61
-----------------------------	----

Cell lines	61
Plasmids	61
1. RHOA expression	62
RHOA protein expression	62
RHOA mRNA expression	64
RHOA protein stability	65
2. RHOA subcellular localization	66
3. Analysis of RHOA cytoskeleton regulation	68
4. Analysis of the RHOA-dependent SRF and NFkB transcriptional regulation	69

5. RHOA known interactome analysis	70
RHOA binding capacity to Rhotekin through a pull-down assay.....	70
Analysis of RHOA binding to known effectors and regulatory proteins through a Yeast-Two-Hybrid Assay	71
RESULTS	77
1. Protein expression of RHOA hotspot mutants	77
2. Protein localization of RHOA hotspot mutants	85
3. Cytoskeleton regulation of RHOA hotspot mutants.....	87
4. Transcriptional regulation of SRF and NFκB by RHOA hotspot mutants.....	91
5. RHOA hotspot mutant interactome	93
Rhotekin binding capacity of RHOA hotspot mutants	93
Yeast two-hybrid screening of effectors binding to wild type and DGC and HNSCC hotspot <i>RHOA</i> mutants.....	94

CHAPTER II. RHOA IN HEAD & NECK CANCER

ABSTRACT	101
INTRODUCTION	105
1. Epidemiology	105
2. Histopathology	107
Pathogenesis of HNSCC	108
3. Molecular heterogeneity of HNSCC.....	109
HPV+ve HNSCC	111
HPV-ve HNSCC	113
4. Hallmarks of HNSCC.....	113
Limitless replicative potential.....	113
Self-sufficiency in growth signals	114
EGFR pathway.....	114
TGFβ pathway.....	115
Evading programmed cell-death	116
Phenotypic plasticity.....	117
Tissue invasion and metastasis	118
Sustained angiogenesis	119

Evasion of immune destruction.....	119
5. Head and neck cancer treatment	120
Treatment in HPV-associated tumors	120
Treatment in early-stage disease	121
Treatment in locally-advanced disease	121
Definitive concurrent chemoradiotherapy.....	121
Recurrent or metastatic disease.....	122
Targeted therapies and immuncheckpoint inhibitors.....	122
6. RHO signaling in HNSCC.....	122
AIMS OF THE STUDY	127
MATERIALS AND METHODS	131
1. Study of RHOA in HNSCC patient samples	131
Tissue microarray (TMA) analysis.....	131
TCGA RNA sequencing data analysis	131
2. Study of RHOA in HNSCC cell lines	132
Generation of isogenic HNSCC cell lines.....	133
<i>In vitro</i> cell growth.....	137
Clonogenicity assay	138
Migration (Wound-healing assay)	138
Matrigel invasion assay	138
<i>In vivo</i> cell growth in subcutaneous xenografts	139
Study of RHOA interactome by shotgun proteomics	140
RESULTS	147
1. Role of RHOA in HNSCC tumors.....	147
Study of RHOA in HNSCC patient samples	147
Study of the role of RHOA in the oncogenic process of HNSCC using cell lines...	160
2. RHOA mutations in HNSCC:	169
RHOA mutation profile in HNSCC patient tumors.....	169
The role of RHOA E40Q in HNSCC cell lines.....	170
3. Characterization of the interactome of RHOA wt and RHOA E40Q in HNSCC cell lines.....	178
DISCUSSION	183
1. Functional characterization of RHOA hotspot mutants	185

RHOA G17 mutants exhibit a lower protein stability	186
RHOA G17 mutants tend to localize into the nucleus.....	187
RHOA hotspot mutants display reduced cytoskeletal dynamics	188
RHOA hotspot mutations downregulate SRF and NFkB signaling.....	190
<i>RHOA</i> mutations affect the binding to known interactors.....	192
Overview and future perspectives	194
2. RHOA in head & neck squamous cell carcinoma.....	195
RHOA evaluation as a biomarker in HNSCC.....	196
RHOA role in HNSCC cell lines	198
RHOA E40Q mutation in HNSCC cancer cells	199
Overview and future perspectives	203
CONCLUSIONS	207
SUPPLEMENTARY RESULTS	209
BIBLIOGRAPHY	217

INDEX OF FIGURES

CHAPTER I. FUNCTIONAL CHARACTERIZATION OF RHOA HOTSPOT MUTATIONS

Figure 1. Classification of benign and malignant lesions according to the cell and tissue of origin.....	26
Figure 2. Incidence and mortality of the most common cancers..	27
Figure 3. Classification of tumor lesions according to the grade of differentiation..	28
Figure 4. Classification of tumor lesions according to the stage.....	29
Figure 5. Hallmarks of cancer and enabling characteristics.....	30
Figure 6. Principal signaling pathways driving tumorigenesis.....	31
Figure 7. MAPK signaling pathway.	32
Figure 8. PI3K signaling pathway.....	34
Figure 9. Domain organization of the Rho small GTPases.....	35
Figure 10. Structure of Rho GTPases.	36
Figure 11. Rho GTPase cycle and its regulation.....	37
Figure 12. Distribution of <i>RHOA</i> mutations in human malignancies..	49
Figure 13. pINDUCER20-GFP- <i>RHOA</i> plasmids.....	61
Figure 14. Assessment of <i>RHOA</i> subcellular localization.	67
Figure 15. Yeast-Two-Hybrid spot assay: fundamentals and workflow.....	73
Figure 16. Protein expression of GFP- <i>RHOA</i> wt and GFP- <i>RHOA</i> mutants in HEK293T cells.	79
Figure 17. Protein expression of GFP- <i>RHOA</i> wt and GFP- <i>RHOA</i> mutants in COS1 cells..	80
Figure 18. Protein expression of GFP- <i>RHOA</i> G17E and G17V in MKN45 and Jurkat cells.	81
Figure 19. GFP- <i>RHOA</i> mutants DNA and RNA levels in HEK293T cells.....	82
Figure 20. GFP- <i>RHOA</i> mutants DNA and RNA levels in COS1 cells.....	83
Figure 21. Half-life determination of <i>RHOA</i> G17E and G17V proteins in HEK293T cells..	84
Figure 22. <i>RHOA</i> wt and mutants nuclear localization in HEK293T cells..	87
Figure 23. <i>RHOA</i> hotspot mutants downregulate F-actin formation in COS1 cells..	88

Figure 24. HEK293T cell morphology and adhesion upon expression of GFP-RHOA wt and GPF-RHOA mutants..	90
Figure 25. Effects of GFP-RHOA mutants on SRF and NFκB transcriptional activity.....	92
Figure 26. Rhotekin binding of RHOA wt and mutants in HEK293T.....	94
Figure 27. Yeast-Two-Hybrid assay for testing protein-protein interactions between <i>RHOA</i> wild type and <i>RHOA</i> mutants to different binders..	96

CHAPTER II. RHOA IN HEAD & NECK CANCER

Figure 28. Anatomical sites of HNSCC development.....	105
Figure 29. Worldwide age-standardized incidence of HNSCC in 2020.....	106
Figure 30. Histology of the buccal oral mucosa.	107
Figure 31. Molecular carcinogenesis in HNSCC.....	108
Figure 32. Candidate therapeutic targets and driver oncogenic events in HNSCC according to TCGA..	110
Figure 33. Deregulated signaling pathways in HNSCC..	111
Figure 34. Deregulation of the cell cycle by HPV.	112
Figure 35. Canonical and non-canonical TGFβ signaling pathways.....	116
Figure 36. Matrigel invasion assay workflow.	139
Figure 37. Workflow for the identification of RHOA wt and RHOA E40Q interactors in HNSCC cell lines.	143
Figure 38. Survival of HNSCC patients with low and high tumor RHOA protein expression.....	149
Figure 39. RHOA tumor expression and survival outcomes according the grade of differentiation of primary HNSCC tumors.	151
Figure 40. Survival of oropharynx, hypopharynx and larynx tumor patients with low and high RHOA protein expression.	152
Figure 41. Survival of HNSCC patients as a function of RHOA mRNA expression.....	155
Figure 42. Survival of oral cavity, oropharynx and larynx cancer patients from the TCGA with low and high RHOA mRNA levels..	158
Figure 43. RHOA expression in HNSCC cell lines..	161
Figure 44. Validation of SCC25 RHOA KD, and SCC25 and JHU012 isogenic cell line models with targeted inactivation of RHOA by CRISPR/Cas9 technology..	163
Figure 45. Effects of RHOA expression downregulation through shRNA in cell growth and colony formation ability of SCC25 tongue cancer cells.	165

Figure 46. Effect of RHOA downregulation in the growth of SCC25 tongue cancer cells <i>in vivo</i>	166
Figure 47. Effect of knocking out RHOA on the growth of SCC25 cells.....	167
Figure 48. Effect of RHOA KO in cell growth, colony formation on solid substrate and cell migration in JHU012 larynx tumor cells.....	168
Figure 49. <i>RHOA</i> E40Q mutation in HNSCC patients from TCGA.	170
Figure 50. RHOA WT or E40Q mutant reintroduction in HNSCC RHOA KO cell lines...	172
Figure 51. Effect of GFP-RHOA wt and GFP-RHOA E40Q reintroduction in the SCC25 RHOA KO cell line model.	174
Figure 52. Effects of RHOA wt and RHOA E40Q reintroduction in JHU012 RHOA KO cell model.....	175
Figure 53. Functional analysis of the reintroduction of RHOA wt ^{UTRs} and RHOA E40Q ^{UTRs} in SCC25 and JHU012 RHOA polyKO cell line models.....	177
Figure 54. PKN1, PKN2 and RHOA pull down in HNSCC cells.	180
Figure 55. RHOA mutation mapper in different tumor types.	184
Figure 56. Signaling from RHOA to the cytoskeleton.....	189
Figure 57. Cytoskeletal dynamics and SRF signaling.	191
Figure 58. Distribution of mutations in <i>PI3KCA</i> oncogene, <i>TP53</i> tumor suppressor and <i>RHOA</i> along the coding sequence..	200

INDEX OF TABLES

CHAPTER I. FUNCTIONAL CHARACTERIZATION OF RHOA HOTSPOT MUTATIONS

Table 1. Main effectors of Rho GTPases.....	41
Table 2. Antibodies used in this study.....	63
Table 3. Oligos used in this study.....	65
Table 4. Interaction of <i>RHOA</i> mutants with canonical binders in the yeast two hybrid assay.....	97

CHAPTER II. RHOA IN HEAD & NECK CANCER

Table 5. HNSCC stages according to the TNM classification.....	121
Table 6. General information of cell lines used in the study.....	132
Table 7. Sequences of the primers used in this study.....	135
Table 8. Antibodies used in the study.....	137
Table 9. Clinicopathological features of the 360 HNSCC patients in the TMAs.....	150
Table 10. Clinicopathological features of the 135 larynx cancer patients in the HUCA/HUVH cohort and associations with RHOA protein expression.....	154
Table 11. Clinicopathological features of 520 HNSCC cancer patients from TCGA and association with RHOA transcript expression.....	156
Table 12. Clinicopathological features of 116 larynx cancer patients from TCGA and association with RHOA transcript expression.....	160
Table 13. Studies used to evaluate the mutational profile of RHOA in HNSCC.....	169
Table 14. RHOA interacting proteins identified by MS analysis.....	179
Table 15. Summary of the functional characterization studies and the interactome analysis for the different RHOA hotspot mutants.....	195
Table 16. Role of (bio)markers in HNSCC.....	197
Supplementary Table 1. Clinicopathological features of 182 oropharynx cancer patients and association with RHOA protein expression.....	209
Supplementary Table 2. Clinicopathological features of 49 hypopharynx cancer patients and association with RHOA protein expression.....	211
Supplementary Table 3. Clinicopathological features of 315 oral cavity cancer patients from TCGA and association with RHOA transcript expression. ^a Fisher's exact test.....	213
Supplementary Table 4. Clinicopathological features of 79 oropharynx cancer patients from TCGA and association with RHOA transcript expression.....	214

ABSTRACT

RHOA is a small GTPase with an important role in key cellular processes. RHOA expression levels and/or activity are altered in multiple cancers, but interestingly, recurrent and tissue-specific hotspot mutations have been recently identified in diffuse gastric cancer (DGC), head and neck squamous cell carcinoma (HNSCC), Burkitt lymphoma, adult T-cell leukemia/lymphoma and angioimmunoblastic T-cell lymphoma, suggesting a distinctive and tumor-dependent role of each mutant protein. In this work, seven recurrent RHOA mutations have been functionally characterized. Our results indicate that some RHOA mutants display lower protein stability and a predominant nuclear localization compared to the wild-type (wt) RHOA. Moreover, the evaluation of the effects of mutant RHOA overexpression on the cytoskeleton organization showed a general reduction in the formation of actin filaments, and a higher cell adhesion capacity. Finally, we observed a reduced NFkB and serum response factor signaling in most of the hotspot RHOA mutants studied.

To dissect the molecular mechanisms deregulated due to RHOA mutations, we investigated the protein interactome. Binding of the different RHOA mutants to Rhotekin effector protein through a pull-down assay was dependent on RHOA protein levels. A yeast-two-hybrid system approach between RHOA forms and the most common RHOA effector proteins, evidenced that all the studied DGC mutants were unable to bind to PKN1, whereas the HNSCC hotspot mutant RHOA E40Q failed to bind to NET1 and kinectin.

HNSCC is a very heterogeneous group of cancers. The lack of survival improvement and personalized treatments has promoted active research into the molecular mechanisms of HNSCC. RHOA is mutated only in around of 1.5% of the HNSCC cases, but interestingly, more than 60% of these mutations occur in E40Q, suggesting a possible active role in the tumorigenic process. Immunohistochemical analysis of RHOA expression in HNSCC tissue microarray indicated that RHOA expression is associated with shorter survival outcomes in patients with larynx tumors. To study the role of wt RHOA in HNSCC, we engineered isogenic cell line systems downregulated for RHOA through the directed targeting of RHOA by shRNA (RHOA KD) and by CRISPR/Cas9 technology (RHOA KO). Results showed an impairment of cell growth *in vitro* and *in vivo*, as well as a decrease of the migration potential *in vitro*, both in tongue and larynx-derived tumor cell lines. These results confirm that RHOA acts as an oncogene in HNSCC. Next, the role of E40Q hotspot mutation was evaluated in doxycycline-inducible RHOA overexpressing cell systems. Surprisingly, RHOA wt or E40Q overexpression in pharynx cells reduced cell growth *in vitro*. Hence, we decided to re-introduce RHOA wt or E40Q in tongue and larynx cell lines RHOA KD and RHOA KO cell

systems. Intriguingly, the reintroduction of RHOA wt and E40Q did not affect cell growth and migration capabilities of the cells.

Altogether, the unprecedented tumor-type-dependent complexity in the mutational landscape of RHOA and our results indicate that the different RHOA hotspot mutations exhibit different oncogenic roles. Furthermore, specifically in HNSCC we demonstrate that RHOA provides a growth advantage for the cancer cells supporting a possible oncogenic role of RHOA in this tumor type.

RESUMEN

RHOA es una proteína GTPasa con un papel relevante en importantes procesos celulares. Los niveles de expresión de RHOA y/o su actividad se encuentran alterados en muchos tipos de cáncer, pero curiosamente, se han encontrado mutaciones recurrentes y específicas de tumor en cáncer gástrico de tipo difuso (CGD), carcinoma de células escamosas de cabeza y cuello (CCECC), linfoma de Burkitt, leucemia/linfoma T del adulto y linfoma T angioinmunoblástico, sugiriendo un papel distinto y dependiente de tumor para cada proteína mutante. En este trabajo hemos caracterizado a nivel funcional siete de las mutaciones recurrentes en RHOA. Nuestros resultados indican que, algunos de los mutantes exhiben una disminución en la estabilidad de la proteína y una localización predominante en el núcleo en comparación con la proteína RHOA nativa. Además, la evaluación de los efectos de la sobreexpresión de las formas de RHOA mutadas en la organización del citoesqueleto mostró una reducción general en la formación de filamentos de actina, y una mayor capacidad de adhesión a sustrato. Finalmente, la mayoría de los mutantes estudiados mostraron una señalización dependiente de las vías NFκB y del factor de respuesta sérica reducida.

Para conocer los mecanismos moleculares desregulados por las mutaciones de RHOA, se evaluó su interactoma. La capacidad de unión de las diferentes proteínas mutantes de RHOA a Rhotekina resultó ser dependiente de su estabilidad proteica. Además, la evaluación de la interacción entre las diferentes proteínas RHOA y sus efectores más comunes mediante un sistema de doble híbrido en levadura, demostró la incapacidad de todos los mutantes de DGC estudiados de unir a PKN1. Sin embargo, el mutante de CCECC RHOA E40Q resultó deficiente en la unión a NET1 y kinectina.

El CCECC es un grupo muy heterogéneo de cánceres. Las carencias en la mejora de la supervivencia y en los tratamientos personalizados han promovido la investigación activa de los mecanismos moleculares asociados su desarrollo. Aunque RHOA está mutado sólo en el 1,5% de los pacientes de CCECC, más del 60% de estas mutaciones ocurren en E40Q, lo que sugiere un papel determinante en el proceso de carcinogénesis. La evaluación inmunohistoquímica de los niveles de RHOA en muestras de tejido de CCECC indicó que la expresión de RHOA se asocia con una peor supervivencia en pacientes con tumores de laringe específicamente. Para estudiar el papel de RHOA nativa en CCECC, se generaron líneas celulares isogénicas deplecionadas de RHOA mediante ARN de interferencia (RHOA KD) e inactivación genética mediante la tecnología CRISPR/Cas9 (RHOA KO). Los resultados mostraron una ralentización del crecimiento celular *in vitro* e *in vivo*, así como una disminución del potencial de migración *in vitro* en líneas celulares tumorales derivadas de lengua y laringe. Estos resultados confirman que RHOA actúa como un oncogén en CCECC.

Resum

Seguidamente, se evaluó el papel de la mutación E40Q en sistemas celulares de sobreexpresión de RHOA de manera inducible con doxiciclina. Sorprendentemente, la sobreexpresión de RHOA nativa o E40Q en células de faringe redujo el crecimiento celular *in vitro*. Por consiguiente, decidimos reintroducir RHOA nativa o E40Q en los sistemas celulares de lengua y laringe RHOA KD y RHOA KO generados previamente. Curiosamente, la reintroducción de RHOA nativa y E40Q no afectó el crecimiento celular ni las capacidades de migración de las células.

En conjunto, la complejidad del patrón mutacional de RHOA sin precedentes, específico del tipo de tumor, y nuestros resultados muestran que los distintos mutantes de RHOA presentan diferentes papeles oncogénicos. Además, demostramos que RHOA en CCECC proporciona una ventaja de crecimiento para las células tumorales que apoyan el posible papel oncogénico en este tipo tumoral.

RESUM

RHOA és una proteïna GTPasa amb un paper rellevant en importants processos cel·lulars. Els nivells d'expressió de RHOA i/o la seva activitat es troben alterats en molts tipus de càncer, però curiosament s'han trobat mutacions recurrents i específiques de tumor en càncer gàstric de tipus difús (CGD), carcinoma de cèl·lules escamoses de cap i coll (CCECC), limfoma de Burkitt, leucèmia/limfoma T de l'adult i limfoma T angioimmunoblàstic, suggerint un paper diferent y dependent de tumor per cada proteïna mutant. En aquest treball hem caracteritzat a nivell funcional set de les mutacions recurrents en RHOA. Els nostres resultats indiquen que, alguns dels mutants exhibeixen una disminució en l'estabilitat de la proteïna i una localització predominant al nucli en comparació amb la proteïna RHOA nativa. A més, l'avaluació dels efectes de la sobreexpressió de les formes de RHOA mutades en l'organització del citoesquelet va mostrar una reducció general en la formació de filaments d'actina i una major capacitat d'adhesió a substrat. Finalment, la majoria dels mutants estudiats mostraren una senyalització dependent de les vies NFkB i del factor de resposta sèrica reduïda.

Per conèixer els mecanismes moleculars desregulats per les mutacions de RHOA, s'avaluà l'interactoma. La capacitat d'unió de les diferents proteïnes mutants de RHOA a Rhotekina resultà ser dependent de la seva estabilitat proteica. A més, l'avaluació de la interacció entre les diferents proteïnes RHOA i els seus efectors més comuns mitjançant un sistema de doble híbrid en llevat, demostrà la incapacitat de tots els mutants de DGC estudiants d'unir PKN1. Tanmateix, el mutant de CCECC RHOA E40Q resultà deficient en la unió a NET1 y kinectina.

El CCECC és un grup molt heterogeni de càncers. Les mancances en la millora de la supervivència i en els tractaments personalitzats han promogut la investigació activa dels mecanismes moleculars associats al seu desenvolupament. Encara que RHOA està mutat en només l'1,5% dels pacients de CCECC, més del 60% d'aquestes mutacions succeeixen a E40Q, el que suggereix un paper determinant en el procés de carcinogènesi. L'avaluació immunohistoquímica dels nivells de RHOA en mostres de teixit de CCECC va indicar que l'expressió de RHOA s'associa amb una pitjor supervivència en pacients amb tumors de laringe específicament. Per estudiar el paper de RHOA nativa a CCECC, es van generar línies cel·lulars isogèniques deplecionades de RHOA mitjançant ARN d'interferència (RHOA KD) i inactivació genètica mitjançant la tecnologia CRISPR/Cas9 (RHOA KO). Els resultats van mostrar un alentiment del creixement cel·lular *in vitro* i *in vivo*, així com una disminució del potencial de migració *in vitro* en línies cel·lulars tumorals derivades de llengua i laringe. Aquests resultats confirmen que RHOA actua com un oncogen a CCECC. Seguidament, es va avaluar el paper de la mutació E40Q en sistemes cel·lulars de sobreexpressió de RHOA de manera induïble amb doxiciclina. Sorprenentment, la sobreexpressió de RHOA nativa o

Resum

E40Q en cèl·lules de faringe va reduir el creixement cel·lular in vitro. Per tant, vam decidir reintroducir RHOA nativa o E40Q en els sistemes cel·lulars de llengua i laringe RHOA KD i RHOA KO generats prèviament. Curiosament, la reintroducció de RHOA nativa i E40Q no va afectar el creixement cel·lular ni les capacitats de migració de les cèl·lules.

En conjunt, la complexitat del patró mutacional de RHOA sense precedents, específic del tipus de tumor, i els nostres resultats, mostren que els diferents mutants de RHOA presenten diferents papers oncogènics. A més, demostrem que RHOA a CCECC proporciona un avantatge de creixement per a les cèl·lules tumorals que donen suport al possible paper oncogènic en aquest tipus tumoral.

Chapter I

Functional Characterization of RHOA hotspot mutations

ABSTRACT

RHOA is a small GTPase with an important role as a molecular switch in key cellular processes, such as the regulation of cytoskeletal dynamics, transcription, cell cycle progression and cell transformation. RHOA expression levels and/or activity are altered in a wide variety of cancers, but interestingly, recurrent and tissue-specific hotspot mutations in RHOA have been recently identified in diffuse gastric cancer (DGC), head & neck squamous cell carcinoma (HNSCC), Burkitt lymphoma (BL), adult T-cell leukemia/lymphoma (ATLL) and angioimmunoblastic T-cell lymphoma (AITL), suggesting a distinctive role of each mutant in the carcinogenesis of each tumor type. To determine the impact of the most abundant *RHOA* mutations in the protein function, we conducted a systematic functional characterization. The specific mutations addressed in our study are the following: C16R (ATLL); G17V (AITL), R5Q (BL and DGC); G17E, L57V, Y42C (DGC); and E40Q (HNSCC).

Our results reveal that RHOA G17 mutants display lower protein stability and predominant nuclear localization compared to RHOA wild type. Furthermore, cytoskeleton rearrangement, one of the principal functions of Rho GTPases, was studied determining the ability of cells to form actin filaments (F actin), and cell adhesion properties under centrifugation forces. Our data indicates a widespread reduced ability of forming F actin and a higher adhesion capability for the RHOA mutants tested. Moreover, decreased NF κ B and serum response factor (SRF) activation was observed for some of the hotspot RHOA mutants when interrogated in luciferase reporter assays.

Finally, to dissect the molecular mechanisms deregulated as consequence of *RHOA* mutations, the interactome of RHOA hotspot mutants was evaluated through two different approaches. First a Rhotekin pull-down assay evidenced clear differences in the binding capacity of the mutants to Rhotekin, which was associated with the protein stability of the different RHOA forms. Moreover, the binding of RHOA mutants found in DGC (R5Q, G17E, L57V and Y42C) and HNSCC (E40Q) solid tumors to known RHOA interactors was investigated using a yeast-two-hybrid. Interestingly, all the DGC mutants assessed were unable to bind to the RHOA effector PKN1, whereas RHOA E40Q mutant (HNSCC) failed to bind to the guanidine nucleotide exchange factor NET1 and the kinectin effector protein.

According to our results, the unprecedented tumor-type-dependent complexity in the mutational landscape of RHOA leads to functional differences across mutants that may drive oncogenic programs through alternative but convergent signaling pathways. Therefore, the pathways deregulated as consequence of RHOA mutations could constitute new and exciting therapeutic targets for cancer treatment.

Chapter I

Functional Characterization of RHOA hotspot mutations

INTRODUCTION

INTRODUCTION

1. General aspects of cancer

Cancer is considered a group of diseases caused by genetic and epigenetic alterations that affect cell replication and cell death, producing an imbalance between these two processes.

Depending on the organ and the cell of origin, tumors are classified into four major groups (**Figure 1**):

1) **Carcinomas:** originate from the cells that line the outer or inner surface of organs, which are known as epithelial cells. There are three major types of carcinomas according to the biological functions associated with epithelia.

- **Adenocarcinoma:** this is the neoplasia of an epithelial tissue that has glandular origin, glandular characteristics, or both. Most of the epithelia in the body contain glandular specialized cells that secrete substances into the ducts or cavities. This is the reason why carcinomas account for approximately 70-80% of all cancers. Common types of adenocarcinomas include breast cancer, colorectal cancer, lung cancer, stomach cancer, pancreatic cancer and prostate cancer.

- **Basal cell carcinoma:** it affects basal cells in the lower part of the epidermis, and therefore occurs predominantly in the skin. Basal cell carcinomas tend to grow slowly, and rarely spread to another part of the body.

- **Squamous cell carcinoma:** it is also known as epidermoid carcinoma and arises in the outer layer of the epidermis. These tumors arise from cells forming the protective layers of the body or to seal cavities. Common types of squamous cell carcinomas cause skin, lung, head and neck, esophageal, cervical or bladder cancer.

2) **Sarcomas:** originate from the connective or supportive tissue, such as bone, fat, cartilage or muscle. Sarcomas constitute only about 1 % of the diagnosed tumors and thus are considered rare tumors.

3) **Neural or brain tumors:** are formed by tumor cells of neuronal origin or contained within the brain. There are more than 120 different types of brain tumors, lesions and cysts, which are differentiated according to the cell of origin and the anatomical location. Malignant tumors of the brain are rare, accounting for approximately 2% of all cancers in adults.

4) Hematopoietic tumors: are derived from cells of the immune system. These tumors affect the blood, bone marrow, lymph, and lymphatic system. Common types of hematopoietic tumors include lymphomas, myelomas and leukemias.




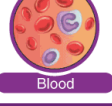
	NORMAL CELLS/TISSUES	BENIGN LESIONS	MALIGNANT LESIONS
 Epithelial tissue	Lining epithelium Glands and lobules	Papilloma Adenoma	Carcinoma Adenocarcinoma
 Connective tissue	Dense connective tissue Cartilage Bone Smooth muscle Skeletal muscle	Fibroma Chondroma Osteoma Leiomyoma Rhabdomyoma	Fibrosarcoma Chondrosarcoma Osteosarcoma Leiomyosarcoma Rhabdomyosarcoma
 Nervous tissue	Brain cells Meningeal cells	Neurofibroma Meningioma	Neuroblastoma Glioblastoma Astrocytoma Meningial carcinoma
 Blood	Blood Bone marrow	Myelodysplasia	Leukemia Lymphoma

Figure 1. Classification of benign and malignant lesions according to the cell and tissue of origin.

Prostate, lung and colorectal cancers account for almost one-half (48%) of all incident cases in men, and breast cancer, lung cancer and CRC account for 51% of all new diagnoses in women. The greatest number of deaths are from cancers of the lung, prostate, and colorectal in men; and of the lung, breast, and colorectal in women (Figure 2)¹.

Most cancers are preceded by cellular changes that are abnormal but not yet malignant. These precancerous or benign lesions consist of either hyperplastic or dysplastic cells. Hyperplasia is an increase in the number of cells in a particular tissue or organ, and as consequence is the result of the deregulation of processes controlling cell division. Dysplasia is defined as an abnormal change in the size, shape, or organization of cells or tissues. The main difference among both is that hyperplasia occurs in response to stimuli and thus, reverses when the stimuli disappear. Benign lesions are often encapsulated, localized and indolent, and the cells within the lesion highly resemble to the cells of origin. When these cells acquire molecular alterations leading to loss of normal cell architecture and unbalanced cell proliferation, premalignant lesions turn into malignant or fully blown tumors. The cells within malignant tumors are atypical of their tissue or cell of origin, lose the ability to perform their usual functions, and differently to those in the benign lesions, invade and destroy the surrounding tissue. Malignant tumors tend to spread from the primary tumor site to distant sites. This process of invasion is named metastasis. There are two main pathways leading to distant dissemination: hematogenous, when cells spread from the

site of origin to a secondary organ or tissue by means of the bloodstream; and lymphatic, when distant homing occurs through the lymphatic system.

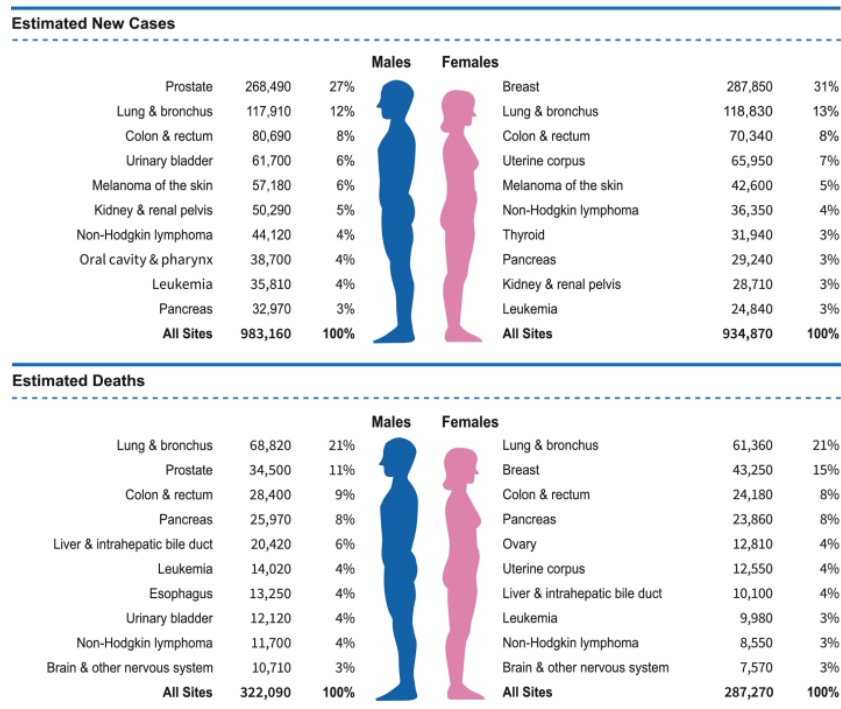


Figure 2. Incidence and mortality of the most common cancers. The ten most common cancers for men and women are depicted according to incidence and mortality (total number cases and percentage). Cancer cases shown correspond to the North America population/year¹.

The grade and the stage are important features of tumors. Tumor grade is the description of a tumor according to the examination of cells and tumor architecture under a microscope. Grade is a good predictor of proliferation and invasion. If the morphology of tumor cells and the organization of the tumor's tissue are similar to those of normal cells and tissue, the tumor is considered well-differentiated. Contrary, tumors containing abnormal cells leading to aberrant tissue structures are considered undifferentiated or poorly differentiated. The firsts tend to grow and disseminate at slower rates than the seconds².

The factors used to determine tumor grade vary between different types of cancer. However, in general tumors are graded with a numerical value ranging from 1 to 4, indicating the degree of abnormality. In Grade 1 tumors (well differentiated or low grade), the tumor cells and the organization of the tumor tissue appear close to normal. As mentioned, these tumors display a low proliferation rate and rarely spread to distant organs. Grade 2 tumors (moderately differentiated or intermediate grade), cells and tissue have already lost some features from the normal healthy tissue. In contrast, the cells and tissue of Grade 3 (poorly differentiated) and Grade 4 (undifferentiated) tumors neither cells, nor tissues look like normal. Grade 3 and Grade 4 are also known as high grade tumors and tend to grow and spread much more

rapidly than low or intermediate grade malignancies. Cells that divide rapidly and have poor or no resemblance to normal cells are also known as anaplastic cells (**Figure 3**).

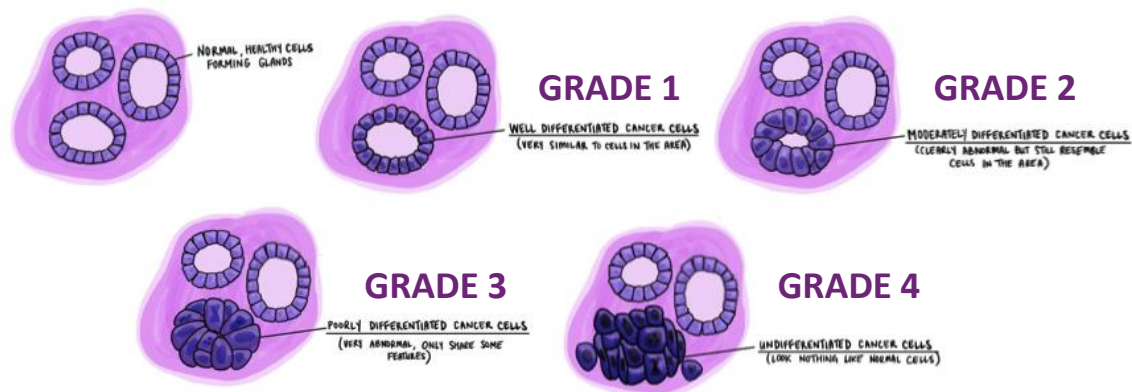


Figure 3. Classification of tumor lesions according to the grade of differentiation. (Modified from: <https://www.mypathologyreport.ca/definition-differentiated/>).

While a grade describes the appearance of cancer cells and tissue, the cancer's stage refers to the extent of a tumor, specifically how large the primary tumor is, and how far the cancer has spread in the patient's body². Stage has strong implications for cancer treatment.

There are several different staging systems. Some have been created for specific tumor types, while others can be used to describe several types of cancer. Most of the staging classifications include information about the size of the tumor, whether the cancer has spread to nearby lymph nodes, and whether the cancer has spread to a different part of the body. The most informative staging classifications also include information regarding where the tumor is located in the body, the cell type of origin and the tumor grade.

Traditionally, the stage has also been categorized with a numerical value ranging from 0 to IV. In stage 0 abnormal cells are present in the tissue but have not yet spread to nearby areas. Stage 0 is also named carcinoma *in situ*. In tumors in stage I, stage II and stage III, malignant cells have already spread. The higher the number, the larger the tumor and the more it has spread into nearby tissues, including the nearby lymph nodes. Stage I-II tumors are often described as localized tumors in which cancer cells are fairly limited to site of origin, while stage II-III are called either locally advanced or regional tumors since cancer cells have already spread to nearby tissues and lymph nodes. Finally, in stage IV the cancer has spread and colonized distant tissues and organs. These tumors are often referred to as advanced or distant tumors (**Figure 4**).

The current standard for cancer staging is the TMN system. The T stands for Tumor and refers to the size and extent of the primary tumor. The N stands for Node and refers to the number of nearby lymph nodes in which tumor cells have already homed. And the M stands for Metastasis and refers to whether the cancer has spread from the primary tumor to other parts of the body. A numerical value is given to each letter. The higher

the number, the higher the progression of the tumor, lymph nodes and metastasis. Tumor and lymph node values range from 1 to 4, while metastasis is only categorized as 0 if cancer has not spread to other parts of the body, and 1 if distant metastasis are already present (**Figure 4**).

Cancers are always referred to by the stage they were given at the time of diagnosis, even if they progress or relapse.

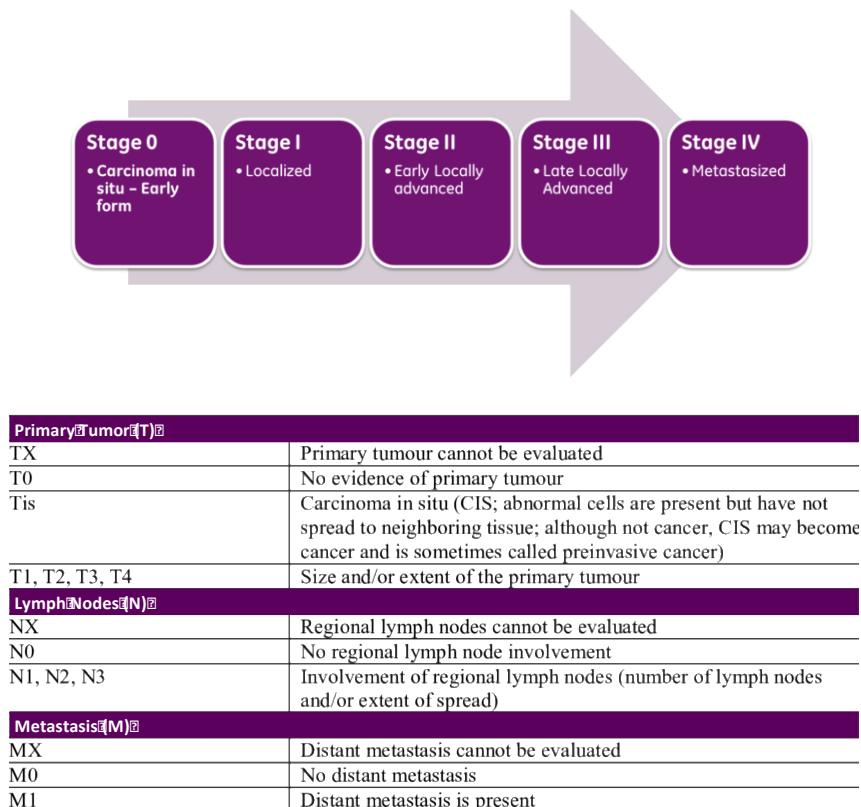


Figure 4. Classification of tumor lesions according to the stage. Upper panel shows the traditional stage classification and lower panel depicts the current stage classification based on the TNM system.

Tumorigenesis begins in somatic cells that acquire a driver mutation and that progressively gain new mutations that enhance distinctive and complementary functional capabilities. There are eight hallmarks that allow tumor cells to grow, survive and disseminate: sustained proliferative signaling, insensitivity to growth suppression signals, resistance to cell death, replicative immortality, enhanced angiogenesis, activation of invasion and metastasis programs, and very recently also phenotypic plasticity and disrupted differentiation^{3, 4}. Additional enabling characteristics that facilitate the acquisition of hallmark capabilities have been proposed, such as genome instability and high mutation rate accumulation, induction of tumor promoting inflammation, reprogramming of cellular energetics, activation of immune evasion mechanisms, non-mutational epigenetic reprogramming, induction of pro-tumorigenic senescence and polymorphic microbiomes (**Figure 5**)^{3, 5}

Genetic alterations normally occur in genes that can be classified in three categories according to its role in the tumorigenic process: oncogenes, tumor suppressor genes and DNA damage-repair genes. Oncogenes encode for proteins with the ability to transform cells in culture. Mutations and genomic rearrangements such as gene amplification in oncogenes lead to gain of function and thus to the induction of carcinogenesis. Contrary, tumor suppressor genes encode for proteins that act in safeguard mechanisms and thus inhibit aberrant cell proliferation or promote cell death. Mutations or deletions in tumor suppressor genes lead to loss of function sustaining increased proliferation or inhibition of cell death. Most tumor suppressor genes require inactivation of both alleles, in contrast to oncogenes, which can lead to a functional effect with only one of the two gene copies altered. In tumor suppressor genes, frequently, the first alteration occurs in one allele in the germline while a somatic mutation that inactivates the second allele occurs during cell division. This theory is called the “two-hit hypothesis”⁶. DNA damage-associated genes prevent the tumorigenesis preventing the accumulation of genetic alterations. This is the case of mismatch repair genes (MMR), base-excision repair (BER) genes and nucleotide-excision repair (NER) genes. Mutations in this group of factors produce an accumulation of aberrant mutations that can deregulate some of the hallmarks listed before⁷.

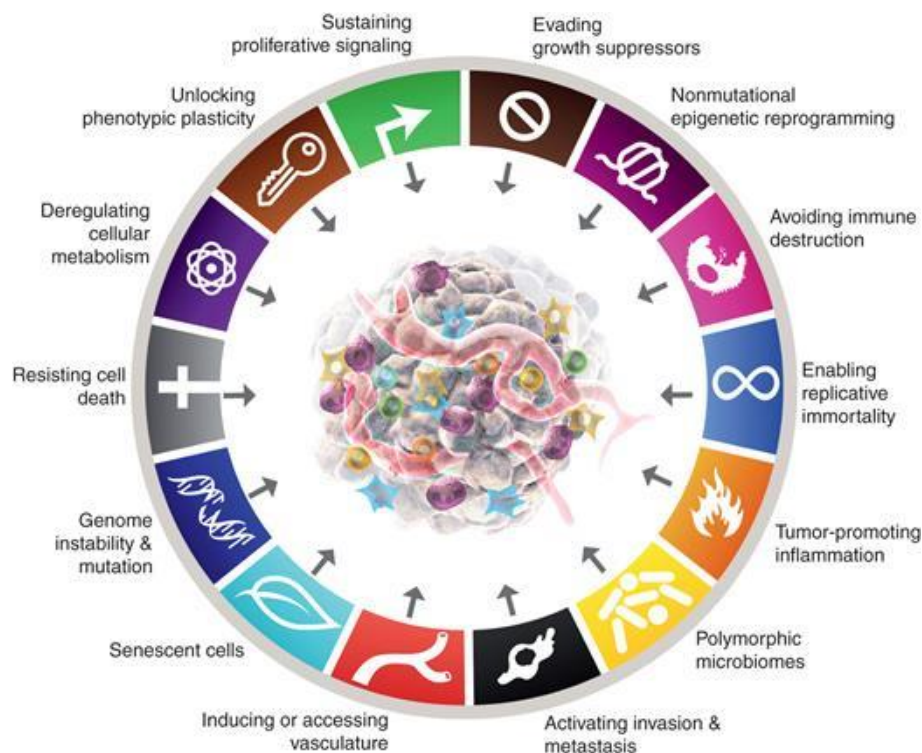


Figure 5. Hallmarks of cancer and enabling characteristics. Normal cells evolve progressively into a neoplastic state by acquiring a succession of hallmarks capabilities and enabling characteristics³.

2. Signaling pathways in cancer and contribution of small GTPases

The molecular alterations occurring sequentially in tumor cells lead to a full reprogramming of the signaling to enable and sustain cells to divide indefinitely, spread to different parts of the body, and acquire hallmark capabilities and enabling characteristics listed before. The principal molecular pathways underlying tumorigenesis are well known and shared by different tumor types. These pathways include the MAPK, PI3K, NF- κ B, Wnt, TGF- β , JAK/STAT and Notch signaling pathways (Figure 6). Small GTPases, which are the focus of the current thesis, strongly influence MAPK and PI3K signaling.

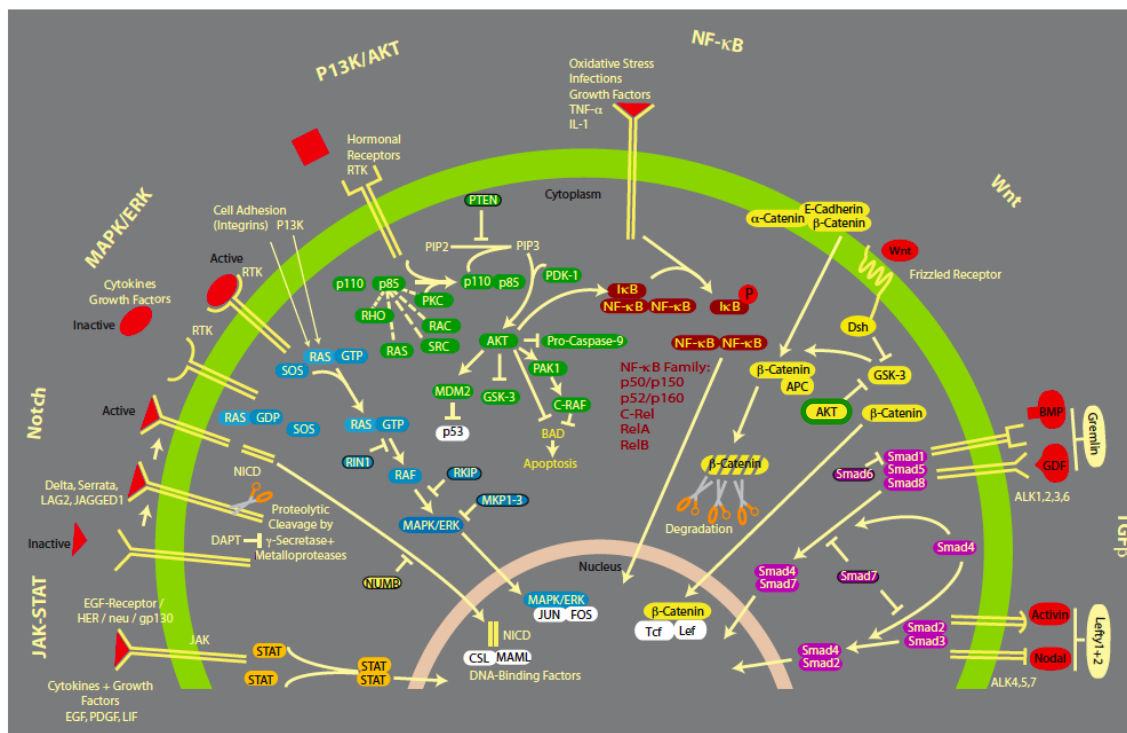


Figure 6. Principal signaling pathways driving tumorigenesis. Schematic representation of the seven most important signaling pathways in cancer onset and progression: JAK/STAT (orange), Notch, MAPK (blue), PI3K (green), NF κ B (red), Wnt (yellow), TGF- β (purple). All ligands are colored in red and transcription factors are colored in white. Factors that exert an inhibitory effect onto a particular pathway are framed with a black line. Lines with arrowheads indicate activation and lines with a block sign indicate inhibition⁸.

MAPK pathway

The mitogen-activated protein kinase (MAPK) pathway plays a central role in promoting cell proliferation, survival, adhesion and migration. The pathway is triggered by tyrosine kinase receptors such as growth factor and cytokine receptors, and to a lesser extent by some extracellular matrix molecules and changes in focal adhesion⁹. Upon ligand-induced receptor activation, phosphorylated residues act as

binding sites for proteins that contain Src homology 2 (SH2) or phosphotyrosine-binding (PTB) domains. These proteins in turn, recruit small GTPase proteins from the Ras or Rho family to the plasma membrane, that upon activation will ultimately stimulate and activate a three-tier serine/threonine kinase module in which a MAPK is activated upon phosphorylation by a mitogen-activated protein kinase kinase (MAPKK), which in turn is activated when phosphorylated by a MAPKKK (**Figure 7**). To date six distinct groups of MAPKs have been characterized in mammals; extracellular signal-regulated kinase (ERK)1/2, ERK3/4, ERK5, ERK7/8, Jun N-terminal kinase (JNK)1/2/3 and the p38 isoforms $\alpha/\beta/\gamma$ (ERK6)/ δ ¹⁰. Activated MAPK phosphorylate and activate a plethora of substrates and translocate to the nucleus to activate the Jun/Fos transcription factor.

Because of its central role in cell proliferation, the MAPK signaling cascade is deregulated in a broad spectrum of human tumors. Most of these alterations occur in RAS and RAF proteins, and result in a pathway activated regardless of the extracellular signals (constitute activation). The final output is the acquisition of a hyperproliferative state. Alterations in the pathway occur by gene amplifications at the level of receptor tyrosine kinases, and gain-of-function mutations in the GTPases and MAPKs. Overactivation of receptor tyrosine kinases has been found in a variety of human cancers such as lung, breast, gastric cancer, esophageal, glioblastoma, and thyroid cancer. In turn, RAS mutations are found in approximately 45% and 90% of colorectal and pancreatic cancers, and BRAF mutations in almost 65% of melanoma¹¹.

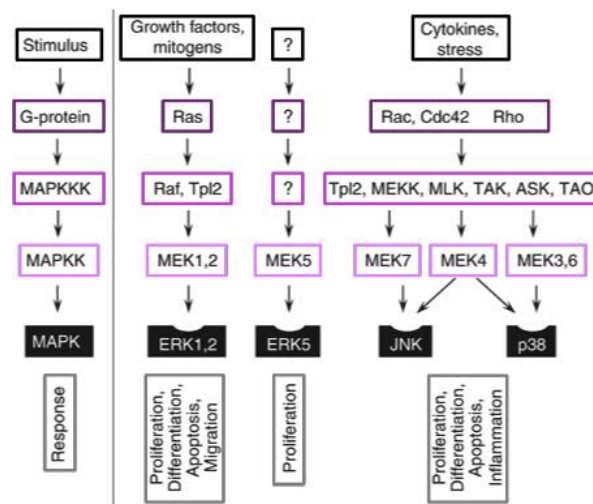


Figure 7. MAPK signaling pathway. The MAPK pathways mediate intracellular signaling triggered by extracellular stimuli such as growth factors and cytokines as well as by intracellular stimuli such as oxidative and endoplasmic reticulum stress. The MAPK signaling is hierarchically organized in a set of three serine/threonine kinase components: a MAPK kinase kinase (MAPKKK), a MAPK kinase (MAPKK), and a MAPK. MAPKKKs phosphorylate and activate MAPKKs, which then phosphorylate and activate MAPKs. The principal MAPK and their role within cells are shown.

PI3K pathway

The phosphatidylinositol 3-kinase (PI3K) pathway is critical in many aspects of cell growth, cell survival, cell metabolism and cytoskeletal rearrangements.

PI3Ks are a family of heterodimeric lipid kinases, which are grouped into class I (A and B), II and III according to the primary structure, regulation, and *in vitro* lipid substrate specificity. Class I PI3Ks are predominant in mammalian cells. Class IA subgroup is mainly activated by receptor tyrosine kinases and consists of a p110 catalytic subunit (p110 α , PIK3CA; p110 β , PIK3CB; p110 δ , PIK3CD) and one p85 regulatory subunit (p85 α , p55 α , p50 α , PIK3R1; p85 β , PIK3R2; p55 γ , PIK3R3). Accordingly, there is a strong crosstalk between MAPK and PI3K signaling pathways. Class IB subgroup is activated by G protein-coupled receptors and are composed of a catalytic subunit (p110 γ , PIK3CG) and regulatory subunit (p101, PIK3R5; p87, PIK3R6). Class II PI3Ks comprises PI3K-C2 α (PIK3C2A), β (PIK3C2B) and γ (PIK3C2G). And finally, the single class III PI3K described to date is hVPS34 (PIK3C3)¹².

Both, regulatory and catalytic subunits of PI3Ks need to be activated to be fully active. Active small GTPase proteins bind directly to p110 subunits, acting synergistically with the input from receptor tyrosine kinases and G-coupled receptors to optimally activate lipid kinase activity (**Figure 8**)¹³. Upon activation, PI3K catalytic subunits promote the conversion of phosphatidylinositol 4,5-bisphosphate (PI(4,5)P₂/PIP₂) to phosphatidylinositol 3,4,5-triphosphate (PIP(3,4,5)P₃/PIP₃). The major downstream mediators of PIP₃ in cells are Protein kinase B (PKB), also known as AKT, and Phosphoinositide Kinase 1 (PDK1). AKT regulates vital downstream effector molecules, such as mTOR, FOXO, GSK3-beta, and many other effectors through a phosphorylation cascade reaction to control cell growth, proliferation, survival, glucose metabolism, genome stability, and neovascularization¹⁴. Importantly, AKT directly activates MDM2, a negative regulator of p53 tumor suppressor. p53 is known as the guardian of the genome as tightly controls DNA damage surveillance. To so, p53 regulates the progression of cells through the cell cycle, activates DNA repair proteins and triggers an apoptotic response if the damage within a given cell proves to be irreparable¹⁵. Activated AKT inhibits apoptosis mediators such as BAD and pro-caspase 9, directly and indirectly through PAK1 and c-RAF, respectively¹⁶. Interestingly, AKT inhibits Glycogen Synthase Kinase-3 (GSK-3), a negative regulator of Wnt signaling; and PDK1 phosphorylates Inhibitor of Nuclear Factor Kappa B (IKK β), a negative regulator of NF- κ B signaling⁸. Accordingly, PI3K further stimulates cell proliferation by activation of the NF- κ B and Wnt signaling pathways that as described before, are essential in the onset and progression of tumorigenesis.

PI3K/AKT pathway is negatively regulated by phosphatase and tensin homolog deleted on chromosome 10 (PTEN). As a lipid phosphatase, PTEN directly suppresses the

activation of PI3K/AKT pathway converting the PIP3 generated by PI3K back to PIP2¹⁷ (Figure 8).

Deregulated PI3K signaling occurs in multiple cancer types. Activating mutations or gene amplification in PI3K, and inactivating mutations or gene loss in PTEN has been found in breast, colorectal, lung, melanoma, head and neck, glioblastoma, stomach and endometrial cancer^{18, 19}. In turn, AKT overexpression or overactivation is common in breast, ovarian and thyroid cancer²⁰.

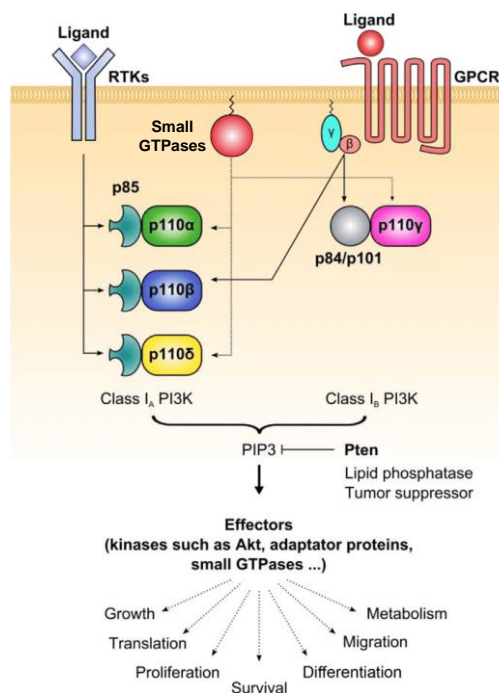


Figure 8. PI3K signaling pathway. PI3K pathway is activated by various receptor tyrosine kinases (RTKs) and G protein coupled receptors (GPCRs). PI3K proteins are recruited to the plasma membrane, leading to phosphorylation of phosphatidylinositol 4,5-bisphosphate (PIP2) to generate phosphatidylinositol 3,4,5-trisphosphate (PIP3). PIP3 recruits to the membrane the series of effectors triggering a plethora of cell functions. PTEN lipid phosphatase converts PIP3 back into PIP2 and thus antagonizes the role of PI3K. Modified from¹⁹.

3. RHO GTPases

The RAS (Rat sarcoma virus) superfamily is a protein superfamily of small GTPases. This superfamily consists of over 100 members that are divided into families and subfamilies according to their structure, sequence and function. The five main families are RAS, RHO, RAN, RAB and ARF GTPases. Members of the RAS family are highly involved in cell proliferation processes, RAN into the nuclear transport of proteins, RAB into membrane trafficking and ARF into vesicular transport. RHO GTPases, which are the focus of the current thesis, differ from other RAS-like GTPases by the presence of a Rho-specific insert domain. RHO family of GTPases includes both classical and non-

classical proteins. RHOA, RhoB, RhoC, Cdc42, Rac1 and Rac2 proteins are the principal classical Rho GTPases and contribute to the orchestration of the cytoskeletal rearrangement, cell morphology and cell motility and also participate in the activation of specific transcriptional pathways^{21, 22}. Deregulation of these processes trigger the development of different diseases, including cancer.

Structure

Classical RHO proteins display between 190 and 250 residues (20-30 kDa) and are made-up of various domains: an effector domain, two separate guanosine phosphate binding regions and a hypervariable region containing a CAAX box motif (**Figure 9**). The N-terminus region contains the effector domain and switch 1 and switch 2 regions, which oscillate between a GTP- and GDP-bound conformation.

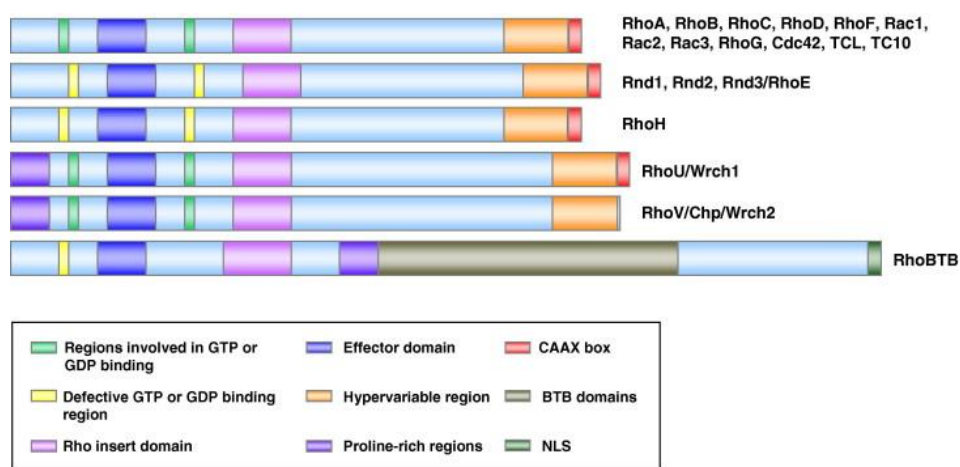


Figure 9. Domain organization of the Rho small GTPases. RHOA, RhoB, RhoC, Rac1, Rac2, Rac3, RhoG, RhoD, RhoF, Cdc42, TCL and TC10 are the canonical Rho small GTPases and they all share a very similar protein structure. The other members are atypical Rho proteins. RhoBTB (1 and 2) have the most divergent protein organization. Each domain or region is differently coloured²³.

The binding of RHO protein to downstream targets occurs when the GTPases are bound to GTP. Accordingly, the residues essential for the GDP-GTP binding are highly conserved among RHO family members. Specifically, Gly14, Thr19, Phe30 and Gln93 are required for GTP binding and hydrolysis. Modification of Gly14 to Val (G14V) and Gln63 to Leu (Q63L) result in activation of GTPase activity; alteration of Phe30 to Leu (F30L) increases the cycling of the GTPase, whereas mutation of Thr19 (T19N) inactivates RHO and is used as a dominant negative form (Figure 10). The hypervariable region in the C-terminus displays the highest diversity between individual RHO family members and contains sites for palmitoylation and a polybasic region influencing plasma membrane association. Specifically, for RHOA, the protein of study in this work, the C-terminus region is essential for correct localization of the protein. RHOA is post-translationally modified by prenylation in a conserved C-terminal cysteine, leading to methylation and proteolytic removal of the last three amino acids. The prenyl group (geranylgeranyl) anchors the GTPase into the plasma membrane. This

modification is essential for protein stability, cell growth, transformation, and cytoskeletal organization^{24, 25}.

Activity regulation

Like the classic monomeric RAS GTPases, Rho GTPases act as molecular switches by cycling between an active (GTP-bound) and an inactive (GDP-bound) conformation. This cycle is tightly regulated. Rho proteins are activated by incorporation of GTP, which is catalyzed by guanine nucleotide exchange factors (GEFs); and inactivation occurs through GTP hydrolysis. Small GTPases exhibit a very weak GTP hydrolysis and thus, this process is assisted by GTPase activating proteins (GAPs) (Figure 11). GEFs and GAPs proteins interact differentially with Rho family members adding an additional layer of regulation of GTPase proteins. GEFs and GAPs are themselves regulated by protein-protein interactions, post-translational modifications and subcellular localization.

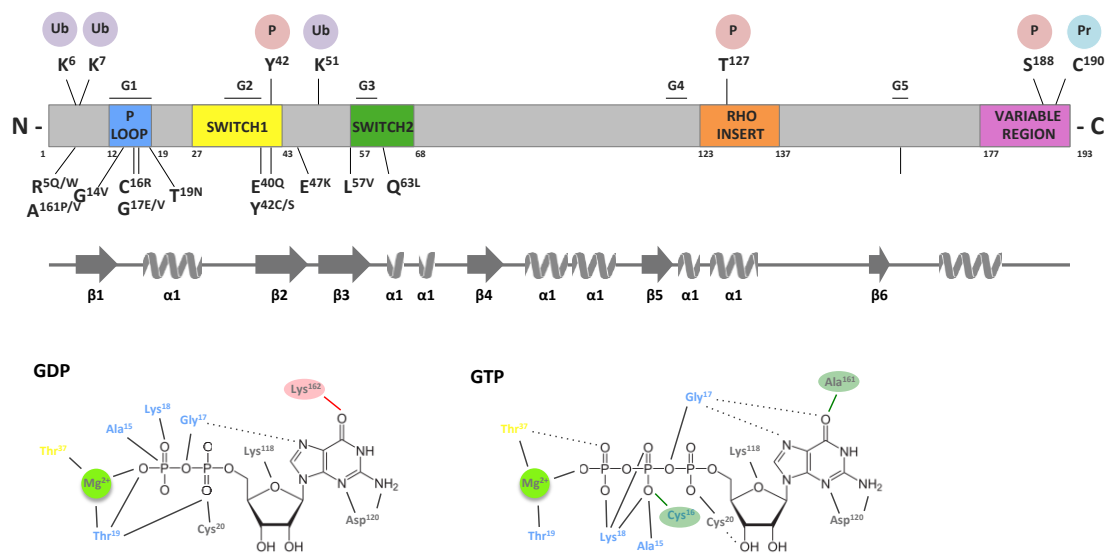


Figure 10. Structure of Rho GTPases. The structure of RHOA is depicted at different levels. The upper panel illustrates the domains of the protein (coloured boxes), regulatory amino acid residues (top) and frequently mutated residues in both solid and hematologic tumors (bottom). The secondary protein structure is also shown. The lower panels illustrate the tridimensional structure of GDP-bound RHOA (left) and the chemical structure of guanosine phosphates (GTP and GPD) (right). In both cases the magnesium ion required for GDP/GTP binding is shown. The residues found mutated in human cancers are shown. Residues involved exclusively in GTP (green background) or GDP (red background) binding have been highlighted. Ub: ubiquitinated residue, P: phosphorylated residue, Pr: prenylated residue.

Inactive GDP-bound Rho GTPases reside in the cytosol complexed with guanine nucleotide dissociation inhibitors (GDIs). GEFs cannot act directly on this complex to promote interconversion of GDP into GTP. The dissociation of Rho GTPases from GDI is executed by GDI displacement factors (GDFs). These proteins are also important for efficient ubiquitination of RHO proteins, which leads them to proteosomal degradation (Figure 11). Once Rho GTPases are GTP-bound, they are generally associated with the plasma membrane through its prenyl group²⁶.

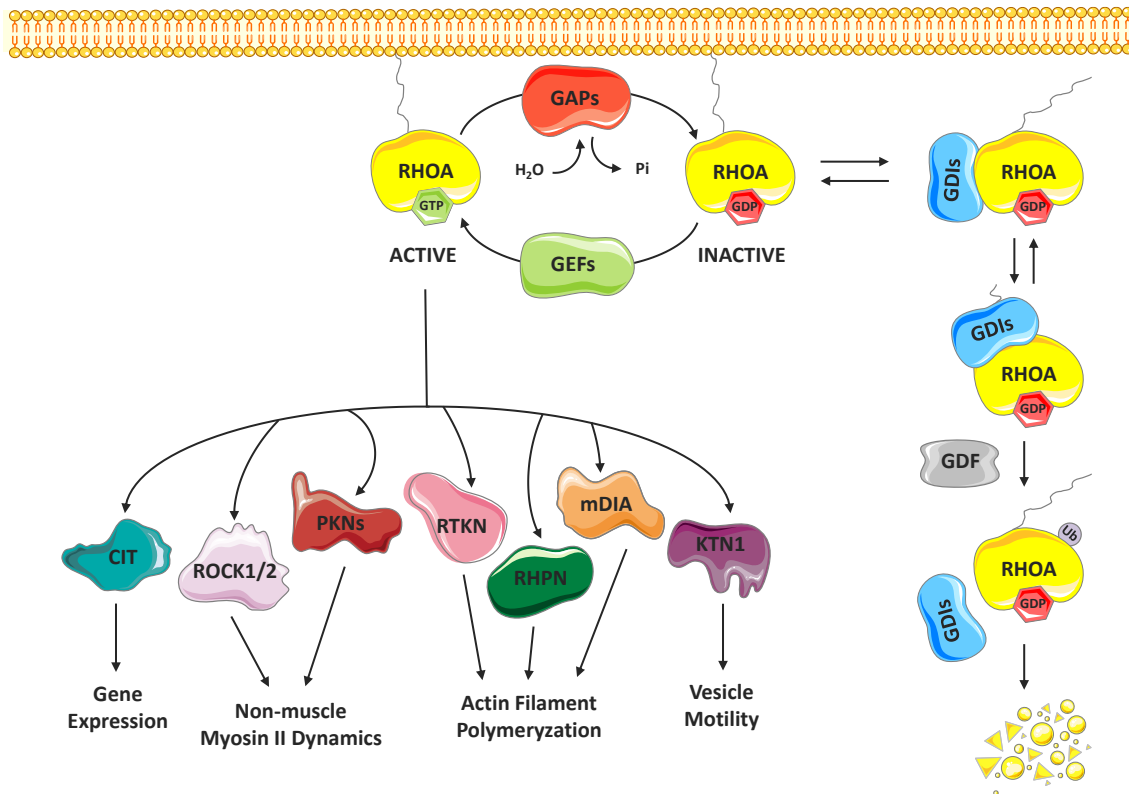


Figure 11. Rho GTPase cycle and its regulation. Rho GTPases cycle between an inactive GDP-bound form and an active GTP-bound form. Activation of Rho GTPases occurs by stimulation with a guanine exchange factor (GEF) that causes the release of GDP and the binding of GTP. In the GTP-bound form, Rho proteins interact with effector molecules initiating a downstream response. To exert their activity, Rho proteins require to be attached to membranes. As soon as the activated GTPase has initiated the cellular response, a GTPase activating protein (GAP), hydrolyzes GTP into GDP turning back Rho proteins to their GDP-bound state. This completes the cycle and terminates the signal transduction. Guanine dissociation inhibitor (GDI) proteins regulate Rho GTPases activity maintaining Rho proteins in the cytoplasm in an active form (bound to GDP), rather than associated to the plasma membrane. In turn, GDI displacement factors (GDF) catalyzes the dissociation of GDIs from Rho GTPases leading to ubiquitin targeting and degradation.

Rho GTPases undergo a series of post-translational modifications including phosphorylation, ubiquitination and AMPylation, which lead to changes in their function ²⁷ (**Figure 10**). For instance, it is well established that protein kinase A (PKA) phosphorylates RHOA Ser188 and increases its affinity towards GDI, resulting in RHOA inactivation ²⁸. Also, Tyr42 phosphorylation of RHOA is crucial for its activation in response to reactive oxygen species and promote to cell proliferation and tumorigenesis ²⁹.

Moreover, RHOA expression is tightly regulated. The Myc-Skp2-Miz p300 transcriptional complex binds to the RHOA promoter triggering its expression. Deficiency of this complex impairs RHOA expression, cell migration, invasion and metastasis in breast cancer cells. Also, overexpression of Myc-Skp2-Miz1 complex is observed in metastatic human cancers along with increased RHOA expression ³⁰. However, other studies have shown that RHOA activation is closely linked to increased

c-Myc expression through NF- κ B activation or increased β -catenin levels^{29, 31}. c-Myc expression is also dependent on RHOA, since overexpression of RHOA Q63L in fibroblasts induces increased expression of c-Myc³². But concomitant expression of c-Myc and RHOA Q63L decreased stress fiber formation, showing a negative feed-back loop that blocks the signaling of RHOA associated to the upregulation of Cdc42 and Pak1 and the repression of certain integrins^{22, 33}. HIF-1 binds to and activates directly the transcription of RHOA, and simultaneously elicits the expression of proteins activating MLC and FAK, leading to increased motility of breast cancer cells³⁴. Alike, P53 has also been involved in RHOA regulation, specifically modulating negatively its activation³⁵⁻³⁷. RHOA in turn regulates p53, promoting the stabilization of tumor-associated mutant p53³⁸. Other transcription factors such as STAT6 and NF κ B have been described as regulators of RHOA transcription³⁹.

RHOA is regulated also at the posttranslational level. While the cytosolic and inactive forms of RHOA are degraded through the proteasome, the membrane-associated and active pool of RHOA is degraded through the autophagy pathway^{40, 41}.

Cellular functions

Although Rho molecules were initially shown to have a role in cytoskeletal remodelling, it is now known that Rho GTPases are involved in several other cellular processes such as membrane trafficking and transcriptional activation.

Rho GTPases and cytoskeleton organization

Cells receive extracellular stimuli from soluble molecules (growth factors, cytokines and hormones) that interact with cell-surface receptors; from adhesive interactions with the extracellular matrix; and from cell-cell adhesions. All these stimuli act to generate changes in the actin cytoskeleton⁴². The actin cytoskeleton is composed not only by actin filaments, but specialized actin-binding proteins, as well. Its most characteristic feature is the reversibility: polymerization of globular actin monomers (G-actin) into filaments (F-actin) and the opposite phenomenon, occur constantly and simultaneously in living cells. Actin polymerization in eukaryotic cells occurs through the coordinated activity of filament severing and capping proteins and the two major actin polymerization factors ARP2/3 and Formin⁴³. Filamentous actin organizes into four different structures⁴⁴:

- Filopodia: finger-like protrusions that contain a tight bundle of long actin filaments in the direction of the protrusion. They are found primarily in motile cells and neurons.
- Lamellipodia: thin protrusive actin sheets at the edges of motile cells. Membrane ruffles result from lamellipodia, specifically upon lifting off the substrate and folding backward.

- Stress fibers: bundles of actin filaments traversing the cell. Stress fibers establish strong interactions with extracellular matrix component through focal adhesions. These are the regions where the cell adheres most tightly to the substrate. Focal adhesions include structural proteins such as α -actinin, vinculin, and talin and signaling and kinases, such as the focal adhesion kinase (FAK).

The direct evidence for the participation of Rho proteins in cytoskeleton dynamics was obtained from microinjection experiments using the constitutive active form of RHOA (G14V). Specifically, overexpression of this mutant form of RHOA in fibroblasts resulted in the induction of stress fibers and the appearance of focal adhesions⁴⁵. As described below, the identification of the downstream Rho signaling mediators linked the role of these small GTPase to both, the formation (actin polymerization) and the organization (filament bundling) of actin filaments²¹.

Rho GTPases in membrane trafficking

The transport of vesicles is essential for the biogenesis and maintenance of organelles integrity and for the trafficking of proteins, lipids and other mediators within the cell, as well as between neighbouring cells and the extracellular environment. Secretion, endocytosis and phagocytosis require the transport of intracellular vesicles. Multiple studies have demonstrated the importance of endosomal pool of Rho GTPases for actin-based endocytic uptake and vesicle movement⁴⁶. For instance, constitutive active Rho mutants have been shown to inhibit the formation of clathrin-coated vesicles and affect the receptor-mediated endocytosis⁴⁷. This is remarkable considering that termination of cell signaling initiated at the cell surface by transmembrane and GPI-linked receptors is often mediated by endocytosis.

Cytoskeleton rearrangement is intimately linked to vesicle trafficking. Actin filaments facilitate membrane deformation, formation of vesicles and contribute to vesicle movement and targeting within cells⁴⁸. The biochemical mechanisms that integrate these two cellular processes at the level of Rho GTPases are not fully understood, but it has been hypothesized that the effects of Rho GTPases on phospholipid metabolism might explain the coordinated control of membrane flow and cytoskeletal organization. Polyphosphoinositides are implicated in the regulation of vesicular traffic in a variety of systems, and the pool of membrane phospholipids within cells are modulated by Rho GTPases considering the crosstalk with PI3K pathway described before⁴⁹.

Normal temporal and spatial regulation of vesicular transport events is crucial not only to maintain cell homeostasis, but for cell proliferation and apoptosis, as well⁴⁴.

Rho GTPases in gene expression

Rho GTPases regulate several signal transduction pathways that lead to alterations in gene expression. In the cytosol, activated Rho GTPases induce transcriptional changes, both dependent and independent of filamentous actin⁵⁰. Rho proteins regulate the activity of several transcription regulators such as serum response factor (SRF)/MAL, AP-1, NF- κ B, YAP/TAZ, β -catenin, STAT3/5 and hypoxia inducible factor (HIF)-1 α ⁵¹. Of note, most of these transcription factors are strongly directly or indirectly related with the main cell signaling pathways governing tumorigenesis at the level of proliferation, migration and invasion of cancer cells (**Figure 6**).

Effector molecules

GTP-bound small RHO GTPases are able to perform their function through the interaction with a huge variety of effector proteins, including serine/threonine kinases, tyrosine kinases, lipid kinases, lipases, oxidases and scaffold proteins, among others (Table 1). Most of these effector proteins display a close inactive conformation, and an open active conformation. RHO GTPases promote the transition from the inactive to the active state⁵².

Most effectors identified display a kinase activity, and many of them actively participate in the cytoskeletal organization, specifically the actin cytoskeleton. The ability of these small GTPases to orchestrate cytoskeleton dynamics was discovered in the early 90s. But as RHO GTPases do not exhibit any domain that could directly interact with the cytoskeleton components, it was rapidly hypothesized that scaffold effector molecules might bridge Rho proteins with actin cytoskeleton. This led to the cloning of multiple Rho effectors, including Rhotekin, Rhophilin, PKN, Citron, ROCK and mDIA⁵³.

Effector	Upstream GTPase			Main biological function	Actin related
	RHO	RAC	CDC42		
RAC/CDC42 targets					
Non-kinases					
WASP		+		Cytoskeletal regulation via the Arp2/3 complex	+
COP4			+	G-protein coupled receptor of the visual transduction pathway	+
IQGAP1/2		+	+	GAP, cytoskeletal regulation (cell-cell contact)	+
P140Sra-1		+		Component of the WAVE regulatory complex, actin polymerization.	+
POR1		+		Porin in mitochondrial outer membrane permeability, membrane ruffling	+
POSH		+		Multidomain scaffold protein, apoptosis, calcium homeostasis, membrane trafficking	
P67 ^{PHOX}		+		Superoxide-generating NADPH oxidase activator activity	
MSE55		+	+	Actin cytoskeleton reorganization at the plasma membrane	+
Protein kinases					
P120 ^{ACK(pyK1)}			+	Cadherin trafficking	
ACK-2		+	+	Clathrin-mediated endocytosis	
PAK-family		+	+	Regulation of actin and microtubule networks	+
MRCK α,β			+	Cell contraction and F-actin turnover	+
MLK2, 3		+	+	Mitogen-activated protein kinase kinase kinase, activation JNK pathway	
MEKK1, 4	+	+	+	Mitogen-activated protein kinase kinase kinase, activation JNK pathway	
P70 ^{S6}		+	+	Ribosomal protein, regulate cell growth by inducing protein synthesis components	
Lipid kinases					
PI3K		+	+	Cell growth, proliferation, differentiation, motility, survival and intracellular trafficking	+
RHO TARGETS					
Non-kinases					
Rhopilin	+			Turn over of F-actin structures	+
Rhotekin	+			Cytoskeleton reorganization, cell differentiation, cell cycle progression, and cell migration	+
DIAPH1, 2	+	+		Formin, F-actin polymerization	+
kinectin	+	+	+	Kinesin-driven vesicle motility	
MBS	+			Myosin Phosphatase	
Protein kinases					
ROCK	+		+	Cytoskeleton regulation (cell shape, motility)	+
Citron	+	+	+	Cytokinesis control	+
PKN1	+			Cell cycle progression, actin cytoskeleton regulation, transcription activation	+
PKN2	+	+			+
Lipid kinases					
PI-4-P5K	+		+	Type I lipid kinase, actin organization	+
PLD	+	+	+	Protein trafficking, exocytosis, and vesicle coat recruitment	

Table 1. Main effectors of Rho GTPases. Adapted from Aspenström 1999⁵⁴; Bishop and Hall 2000⁵².

Briefly, effectors of Cdc42 and Rac1 mediate cell-cell adhesion and cell polarization through actin polymerization and cell protrusions, stabilization and capture of microtubules, and mediate the arrangement of the cytoskeleton and organelles such as the Golgi apparatus, the nucleus and the centrosomes. Processes that are regulated downstream of active RHOA signaling include the formation of actin stress fibers and focal adhesion complexes, transcription, cell transformation, cell cycle progression and cell migration. For example, the RHO-associated coiled-coil-containing protein kinases

(ROCK1/II) are RHOA effector kinases related with cell adhesion and migration through the regulation of acto-myosin-mediated contractility, inducing stress fiber formation and assembly of focal contacts. RHOA binding to the formin mammalian diaphanous 2 (mDIA2/DIAPH2) initiate the assembly of protein complexes required for actin polymerization. In turn, PKN family of proteins are serine/threonine kinases with a potential role in transcription regulation^{52, 54}.

It is known that effectors use distinct residues within the switch I and II regions of Rho proteins as major docking/recognition sites²² (Figure 10). A comparison of the RHOA-GDP and RHOA-GTP crystal structures reveals that the binding of GTP generates conformational changes that are restricted to the switch I and switch II regions. Hence, effectors must use these regions to discriminate between inactive and active Rho forms, though they also interact with other regions of the GTPase^{52, 55}. The interaction between the downstream effectors with Rho GTPases causes a conformational change from an auto-inhibitory state to a fully active conformation²². However, for certain effectors, the change at the structural level is not sufficient for the full activation and the cooperation of other signals are needed. For example, PKN proteins need not only RHOA binding, but lipid association and auto-phosphorylation as well to be fully activated^{56, 57}.

The final result of small GTPases binding to their effectors is the generation of a wide variety of signals that promote, among other responses, cytoskeletal rearrangements, regulation of cell morphology and motility along with transcription regulation.

4. RHOA GTPase in cancer

Both typical and atypical RHO GTPases contribute to cancer progression. In a few cancers, RHO GTPases are mutated, but in most cancers their expression levels and/or activity is altered. This is consistent with the role of RHO GTPases as signal transducers in the signaling pathways that regulate proliferation, survival, death and cell migration. Deregulation of RHOA appears to be involved in almost all stages of tumor progression and mutated at considerable high rates in certain types of malignancies. However, the way in which RHOA contributes to the tumor context is not simple since both tumor promoting and tumor suppressor roles have been attributed to the same protein. We have compiled bellow a systematic review of what is known about RHOA protein in the different tumor contexts in which it has been studied.

RHOA as oncogene

RHOA was postulated as an oncogene in 1989, due to the ability of amplified RHOA to induce tumorigenesis in fibroblasts⁵⁸. Upon this first study, many others followed explaining the pro-tumorigenic role of RHOA. The overexpression of the wild type form

(WT) of RHOA or the G14V mutant (constitutive active form of RHOA) was sufficient to confer anchorage- and serum-independent growth *in vitro*; and when cells were injected subcutaneously into nude mice were able to induce tumors^{59,60}. Interestingly, cells carrying the mutated version of RHOA were more efficient in inducing cellular transformation. Later in time, this effect was attributed to the ability of RHOA to regulate cell cycle progression, promoting G1-S transition by increasing CyclinD1 levels and reducing the expression of p21cip1 and p27kip1 cell cycle inhibitors⁶¹. Early data also evidenced an active role of RHOA in cell survival. RHOA increased apoptosis of erythroleukemic K562 cells through the production of ceramide and FasL⁶².

Next, most of studies concentrated on the role of RHOA as a regulator of the actin cytoskeleton and consequently, cell polarity, locomotion and cell shape through actin⁶³. RHOA and other Rho GTPases are strongly involved in angiogenesis, a physiological process indispensable for tumor formation *in vivo*. Specifically, RHOA was shown to play an important role in supporting the formation of new vessels leading to regulating proliferation, survival and migration of the endothelial cells⁶⁴.

Simultaneously to the description of the molecular pathways triggered by RHOA and the impact on cell fate, different tumor types were interrogated for the expression of this GTPase. High expression of RHOA was found in a plethora of tumor malignancies supporting the role of RHOA as an oncogene⁶⁵⁻⁷⁰.

Digestive tract cancer

RHOA transcripts levels were determined by quantitative real-time polymerase chain reaction (QRT-PCR) in colorectal cancer (CRC) patient samples and were found to correlate positively and significantly with the tumour grade⁷¹. And in an independent study, patients with higher RHOA expression had a significant poorer 5-year survival rate⁷². RHOA was found upregulated and associated to a TGF β signature in liver metastasis from CRC patients⁷³. When investigated using human cell lines and patient-derived colorectal cancer samples, RHOA was found highly expressed in CRC cell lines, especially those derived from metastatic sites, and *in vitro* downregulation strongly impaired migration and invasion⁷².

RHOA has been described to also have an important role in gastric cancer. The mRNA and protein expression levels of RHOA in tumors from gastric cancer patients and cell lines were significantly higher than in the adjacent non-tumorous tissues and non-tumoral cell lines^{69,74}. Furthermore, RHOA downregulation in gastric cells lines suppressed cell growth and increased chemosensitivity to chemotherapeutic agents⁷⁴. In addition, differences have been found between distinct types of gastric cancer, specifically between diffuse-type (DGC) and intestinal-type (IGC) gastric cancer. In patients with the DGC, high RHOA activity was associated with significant worse overall survival⁷⁵. The same association was not observed in IGC patients.

Fewer studies have been done in oesophageal squamous cell carcinoma (ESCC), but it has been demonstrated that patients with RHOA overexpression show a poorer prognosis compared. Additionally, RHOA expression was found to correlate with tumor differentiation status and ESCC progression ⁷⁶.

RHOA oncogenic role is not limited to squamous carcinomas. In hepatocellular carcinoma (HCC), RHOA overexpression correlates with venous invasion, cell differentiation, tumor progression and metastasis. Besides, higher expression indicates a poor prognosis in HCC patients ^{77, 78}. In pancreatic cancer, the cancer with worst prognosis worldwide, RHOA role seems to be restricted to motility and invasion promotion ⁷⁹. In this regard, a very interesting study inducing p53-null pancreatic ductal adenocarcinomas in mice showed high RHOA activity in the invasive front of the tumors ⁸⁰. The capability of pancreatic cancer to metastasize to the liver was attributed to RHOA activity and mediated by the sequestration of RhoGDIs proteins ⁸¹.

Lung cancer

RHOA has been studied in the respiratory tract. *In vitro* experiments have shown that the downregulation of RHOA in SPCA1 lung cancer cell line prevent proliferation and invasion ⁸². In the clinical setting, ERK/RHOA/FAK network has been found deregulated in high-grade lung tumors carrying mutant KRAS and CDKN2A, which are associated with an aggressive and therapy-resistant phenotype ⁸³.

HNSCC, melanoma and sarcoma

Elevated levels of RHOA have been found in head and neck squamous cancer (HNSCC) tumor cells compared with normal cells ^{67, 84}. Downregulation of RHOA cell lines derived from tongue tumors reduces cell migration, invasion and proliferation *in vitro*, and tumor growth and lymph node invasion in orthotopic xenografts in mice, indicating an oncogenic role of RHOA in this tumor type ⁸⁵. Most of the studies conducted in HNSCC are in tongue tumors or cell lines, but poor information is available regarding the role of RHOA in the other anatomical regions such as in larynx or pharynx tumors.

In melanoma, pharmacological inhibition of RHOA, assessed by the reduction of RHOA-GTP (active form of RHOA), leads to the reduction of stress fibers, lamellipodia protrusions and suppression cell motility and tumor growth *in vitro* ^{86, 87}.

RHOA has been involved in the progression of sarcoma cells. Specifically, using two amoeboid sarcoma cell lines overexpressing RHOA G14V and RHOA T19N forms, it was shown that ability of these cells to invade and metastasise *in vitro* and *in vivo* is dependent of RHOA activity ⁸⁸.

Urinary system cancer

RHOA has been demonstrated to contribute to the progression of cancers of the urinary system. RHOA expression is higher in pelvic, ureteric and bladder cancer tissues and metastatic lymph nodes compared with non-tumor tissues; and importantly, high RHOA level in these tumor contexts correlates with tumor stage and a reduced patient survival^{89,90}.

Cancer of the female and male genital tract

Vulvar squamous cell carcinoma (VSCC) is the fourth most common cancer of the female genital tract. It was shown that RHOA expression is higher in VSCC tissue than normal skin. Moreover, the downregulation of RHOA in VSCC cells results in G1 arrest, low proliferation and low migration⁹¹. In ovarian tumors, RHOA expression was also significantly upregulated in tumors compared to normal tissue^{68,92}. RHOA expression in the metastatic omentum was even higher and positively correlated with stage and degree of differentiation⁹². *In vitro* studies revealed that overexpression of RHOA in ovarian cancer cells did not change their proliferation rate but increased their invasiveness features. Consistently, mice injected in the abdominal cavity with cells overexpressing RHOA exhibited increased peritoneal invasion and the number of lesions were higher than the control mice⁹³. Conversely, RHOA downregulation reduced tumor cell viability, migration, invasion and adhesion abilities *in vitro*, and tumor formation in the abdominal cavity *in vivo*, further confirming the oncogenic role of RHOA in ovarian cancer⁹⁴.

Male genital tract cancer has been also related with RHOA. The constitutive active RHOA Q63L form in a murine prostate tumor cell line promotes its proliferation compared to wild-type RHOA and RHOA T19N dominant negative. This effect was attributed to the enhanced development of stress fibers and cell cycle progression⁹⁵. The later was shown to be mediated by RHOA signaling through PKCzeta⁹⁶. In tumor testis, RHOA and some of its effector proteins were shown to present higher expression in primary tumors than in non-tumor testis. And specifically for RHOA, the levels of expression of the protein correlated with tumor stage⁹⁷.

Breast cancer

RHOA act as an oncogene in breast cancer according to numerous and varied data. *In vitro*, RHOA has been shown to promote preneoplastic transformation of human mammary epithelial cells (hMEC)⁹⁸. Specifically, exogenous overexpression of RHOA wt and RHOA G14V is able to induce to immortalization and preneoplastic transformation of primary epithelial cells. As expected, RHOA T19N dominant negative did not retained this ability, whereas RHOA T37A which is unable to bind to many well-known effector proteins, *i.e.* ROCK, PKN, mDia1/2, surprisingly, led to epithelial immortalization. *In vitro* downregulation of RHOA in MDA-MB-231 breast cancer cells

inhibited cell proliferation and invasion; and intratumoral injection of an anti-RHOA siRNA in breast xenograft tumors, reduced tumor growth and angiogenesis⁹⁹. Same effects were observed *in vivo* when the anti-RHOA siRNA was encapsulated in nanoparticles and administered intravenously into mice ¹⁰⁰.

At the patient level, RHOA protein, but not mRNA, was increased in breast tumors when compared to paired normal tissue. Moreover, the amount of RHOA protein correlated with the histological grade ^{65, 101} and also tumor size ¹⁰¹.

RHOA as tumor suppressor

Despite the substantial experimental evidence that RHOA can function as an oncogene, a significant number of studies point out to an opposite role, as tumor suppressor gene.

Digestive system cancer

Using expression microarray experiments in Dukes' C colorectal cancer samples (that includes samples in which the cancer has spread to at least one lymph node in the area close to the bowel), RHOA was among the genes with lower expression levels in tumors from patients with poor prognosis compared with the ones with a good prognosis. Furthermore, analyzing survival curves upon determining RHOA protein levels by immunostaining in an independent set of samples, it was found that patients with patients with low levels of RHOA displayed worse overall and disease-free survival ¹⁰². It has been nicely shown that RHOA inactivation promotes cancer progression and metastasis through Wnt/ β -catenin pathway. In addition, using genetically modified or chemically-induced animal models of intestinal tumorigenesis, it was shown that targeted inactivation of RHOA in the intestine led to shorter survival of animals and higher tumor burden. Moreover, loss of RHOA led to increased development of lung metastasis ¹⁰³.

In the regulation of tumorigenesis, the crosstalk between RAS and RHOA has been largely studied in *in vitro* systems. Most of the studies suggest that RHOA enhances RAS-driven transformation. However, in a study done *in vivo* in zebrafish, RHOA T19N increased KRAS G12V-mediated liver growth, HCC development and cancer mortality, whereas RHOA G14V suppressed KRAS G12V-mediated liver growth, suggesting that active RHOA could have an inhibitory role in KRAS oncogenic signaling, inhibiting AKT activation and cyclin D1 expression ¹⁰⁴.

Immunohistochemical and clinical data analysis of samples from patients with pancreatic ductal adenocarcinoma (PDCA) showed a longer overall survival when the levels of RHOA were higher. In addition, RHOA expression together with tumor size and tumor stage resulted in a more reliable prediction of patient survival¹⁰⁵.

Lung cancer

In lung cancer, the role of RHOA in K-Ras-driven tumorigenesis *in vivo* seems to be of a tumor suppressor gene, because i) RHOA is not necessary for the normal lung function in mice, ii) K-Ras^{G12D}-induced adenomas can be formed in the absence of RHOA, and iii) an increase in the number of adenomas is found in a conditional RHOA knock-out mouse of sporadic lung tumor model ¹⁰⁶.

Breast cancer

Using a triple negative breast cancer (TNBC) mouse model, it has been demonstrated that reduced RHOA expression increases the colonization of lymph nodes and lung metastasis ¹⁰⁷. This tumor suppressive role of RHOA was suggested indirectly in previous studies, in which specific RhoGAPs were shown to be upregulated in basal-like breast cancer (BLBC) and TNBC ^{108, 109}.

Melanoma

The first work to demonstrate the clinical relevance of RHOA in skin melanoma described that the increased RHOA expression in primary tumors was associated with thin tumors, high infiltration of lymphocytes and lack of disease recurrence. Disease-free survival and overall survival of patients with high expression of RHOA within lesions were significantly prolonged ¹¹⁰. Previously, *in vitro* work with melanoma cell lines showed that pharmacological treatment with agents, such as histone deacetylase inhibitors (HDACi) or BRAF targeted therapies, this last already approved for melanoma treatment, led to a pro-invasive effect mediated by a decrease in RHOA signaling ^{111, 112}. In addition, loss of RHOA in keratinocytes *in vitro* and *in vivo* promotes tumor formation and invasion. Interestingly, in these model, the decrease in RHOA reduced RhoB degradation in autophagosomes, increased cell membrane localization and signaling, indicating a compensatory effect at the level of global Rho signaling in keratinocytes ¹¹³.

Brain tumors

Malignant brain and central nervous system (CNS) tumors are the 3rd most common cause of cancer mortality ¹¹⁴. In a study with glioma cells, overactivation of RHOA through oligodendrocyte lineage transcription factor 2 (OLIG2), led to decreased cell motility ¹¹⁵. Migration, and also anchorage-independent growth, was reduced in a likewise manner in an independent study with glioblastoma cell lines ¹¹⁶.

In the clinical setting, the expression of RHOA in astrocytic tumors showed an inverse correlation with grade ¹¹⁷.

Urinary system cancer

One of the first studies examining the expression of RHOA in normal kidney and renal cell carcinoma (RCC), revealed that RHOA expression was lower in tumors compared to normal tissue, although there was no correlation with the differentiation grade or TNM stage ¹¹⁸. Moreover, in a recent study, using serological identification of recombinant cDNA expression cloning (SEREX) and RCC cell line models, it was shown that a RhoGAP1 was upregulated and increased the proliferation and invasion of cells through inhibition of RHOA-ROCK signaling ¹¹⁹.

RHOA mutations in cancer

Rho GTPases were rarely reported to be mutated in cancer, until recently, when revolutionized sequencing technologies enabled unbiased analyses of cancer genomes and revealed frequent mutations in RHOA and related molecules in a wide variety of cancers. Some old studies tried to approach the mutational status of this protein, but failed not only due to the reduced number of samples tested, but to the low penetrance of RHOA mutations in the tumor types evaluated. For instance, in a study done with colorectal adenocarcinomas and breast cancer samples there were found no mutations in RHOA coding sequence ¹²⁰. Several groups identified RHOA mutations simultaneously in 2014, with the comprehensive molecular evaluation of large cohorts of primary gastric adenocarcinomas ¹²¹. At the same time, other groups found frequent RHOA mutations, specifically at the G17V position, in angioimmunoblastic T cell lymphoma (AITL) and peripheral T cell lymphomas (PTCL)¹²²⁻¹²⁴. Additional hotspot RHOA mutations were found in other tumor types (Figure 12). The role of these mutations along the tumor progression process, and their molecular characterization have been deeply studied by some groups. In this section we summarize information known to date about RHOA mutations in different tumor types.

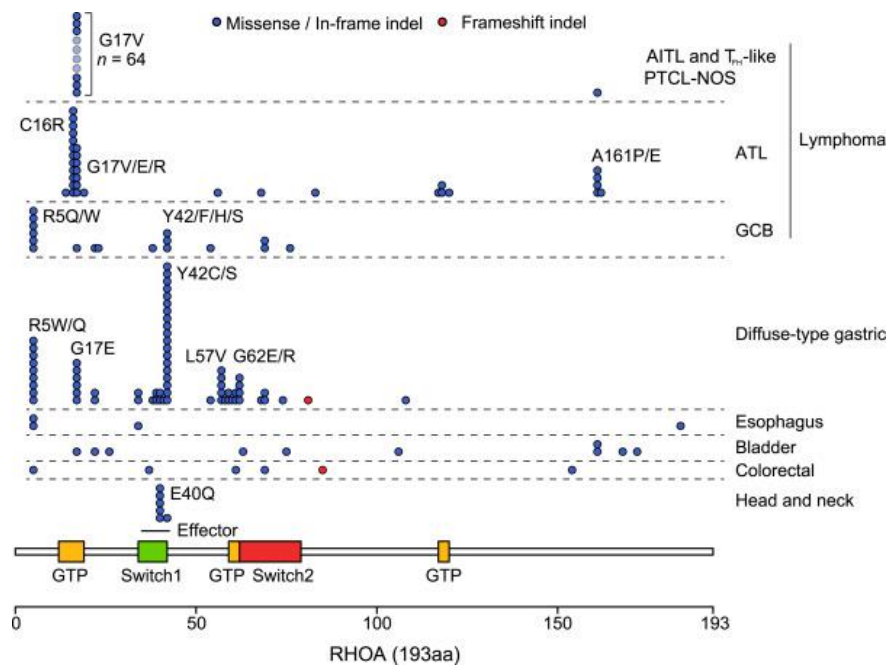


Figure 12. Distribution of *RHOA* mutations in human malignancies. Pattern of *RHOA* mutation in AITL, ATL, and GCB lymphomas (Germinal center B-cell lymphomas), as well as diffuse-type gastric (TCGA), oesophageal (ICGC and Broad), bladder (TCGA, BGI, and DFARBER_MSKCC), colorectal (TCGA and Genentech), and head and neck (TCGA and Broad) cancers¹²⁵.

Diffuse-type gastric cancer (DGC)

Gastric cancer is the third leading cause of cancer mortality worldwide and despite having a high heterogeneity, two subtypes well distinguished had been established and used to build Lauren classification of gastric adenocarcinomas: i) intestinal gastric cancer (IGC) and ii) diffuse gastric cancer (DGC). Poorly-differentiated or diffuse type gastric cancer (DGC) accounts for 30% of cases. From the histopathological point of view, a lack of intercellular adhesion, often observed with scattered signet-ring cell morphology, predisposes to a diffuse invasion growth pattern throughout the stroma¹²⁶. In 2014, The Cancer Genome Atlas (TCGA) proposed a molecular classification for gastric cancer based of four subtypes: Epstein-Barr virus positive tumors, microsatellite unstable tumors, genomically stable tumors, and chromosomally instable tumors. DGC are included mostly in the genomically stable tumors, in which a very high proportion of *RHOA* mutations or fusions involving *RHO*-family GTPase-activating proteins are observed. *RHOA* mutations were found in approximately 15% of the genomically stable tumors. The mutations found clustered in two independent but adjacent regions involved in the interaction of *RHOA* with some effectors, such as ROCK¹²⁷. This result was in concordance with a pair of studies published the same year describing for the first time novel recurrent mutations in *RHOA* in DGC patients^{128, 129}. Using whole-exome sequencing and targeted deep sequencing, *RHOA* mutation was observed in around 20% of the DGC cases analyzed^{128, 129}. Hotspot mutations in Tyr42 (effector-binding region), Arg5, Gly17 (GDP/GTP-binding region) and Lys57 residues were identified. Among all, Y42C was the most recurrent mutation. Interestingly, the

prevalence of RHOA hotspot mutants was skewed towards R5Q/W in Asiatic DGC¹³⁰. Furthermore, RHOA mutations occur at a significantly higher proportion in late-onset DGC patients (LODGC) compared with those with an early-onset (EODGC)¹³⁰. Intestinal-type adenocarcinomas with anastomosis glands, a rare histological subtype characterized by irregularly interconnected, also display a high RHOA mutation rate (around 50%). The more prevalent RHOA mutation in this type of tumors is G17E¹³¹.

Sample from peritoneal carcinomatosis, one of the major causes of death in advanced GC, have been analyzed by whole-exome sequencing. Several components of the Rho-ROCK signaling pathway accumulate mutations, and interestingly, 1 of the 7 malignant ascites from DGC patients, exhibited a RHOA L57V mutation absent in the primary tumor, suggesting a role of RHOA mutations in the promotion of DGC metastasis¹³². In concordance with these results, it has been described that RHOA mutations are more recurrent in N3 tumors compared to N0 tumors¹³³.

The first clinicopathological study with RHOA-mutant gastric cancer showed that most advanced tumors with RHOA mutations exhibited Borrmann type 3 lesions (81%). The Borrmann classification system divides gastric carcinomas into 4 different types according on macroscopic pathological assessments: polypoid carcinoma (type I), fungating carcinoma (type II), ulcerated carcinoma (type III), and diffusely infiltrative carcinoma (type IV)¹³⁴. So, RHOA mutation was linked with the development of ulcerated tumors. Moreover, although no associations were found between RHOA mutation presence and survival outcomes, RHOA-mutated tumors showed a predominant poorer cohesive histology, compared with RHOA wt tumors¹³⁵.

There are some studies about the molecular characterization and biological function of RHOA mutations found in DGC. RHOA effector-loop mutants (in codons F39, E40 and Y42) were tested for the binding capacity to downstream signaling effectors, stress fiber formation and activation of the serum response factor (SRF) pathway. It was shown that RHOA Y42C, the most recurrent mutation in DGC, impairs the binding to PKN but not to ROCK, mDIA2, Rho-philin, Kinectin, Citron and NET1. Assays in NIH3T3 cells revealed that RHOA Y42C maintains stress fiber formation and SRF activation¹³⁶.

The modulation of Y42S and G17E mutations expression in OE19 gastric cancer cells, BT474 breast cancer cells and SW948 colon cancer cells evidenced a role of these mutations in the promotion of cell proliferation. In a Rho binding domain assay, association of RHOA Y42C and L57V mutants to GTP was found to be lower than in WT and G14V forms using HEK293 cells¹²⁹. Further, RHOA G17E and Y42C/S mutations decreased stress fiber formation and intracellular adhesion in MKN74 cells, both key features in migrating cells; and in contrast with other reports^{130, 137}, overexpression of RHOA WT or G14V decreased migration capability, whereas overexpression of T19N led to its increase¹³⁸. The effect of RHOA R5W mutation, the most prevalent mutation in EODGC tumors, was assessed ectopically overexpressing it in 293FT cells. RHOA R5W

resulted in a decreased protein activation (GTP-bound levels) compared to RHOA WT. A decreased SRF activity and stress fiber formation were also observed with R5W. Downregulation of RHOA activity in DGC cells produced equivalent effects to overexpression of R5W mutation, *i.e.* increased β -catenin reporter activity and impaired aggregation of the cells¹³⁰. Interestingly, the effects of RHOA mutations seem to be mediated through ROCK inactivation. All these results would suggest that, in general, DGC RHOA mutants are oncogenes with a loss-of function activity. However, some discrepancies can be found in the literature. As an example, NIH3T3 cells expressing RHOA Y42C stimulated stress fiber formation, similarly to the constitutive active RHOA forms G14V and Q63L¹³⁸. Moreover, increased GAP-stimulated GTP hydrolysis activity, higher ROCK affinity and reduced Rhotekin binding were found in RHOA Y42C expressing cells¹³⁹. According to these studies, Y42C behaves as a gain-of-function mutation. Again, differences in the tumor context might influence the role of the mutations.

RHOA mutations RHOA Y42C/S are predominant in DGC. This has led to a deeper evaluation of this specific mutation in gastric tumor development. RHOA Y42C/S mutations have been studied in mice through the establishment of orthotopic gastric cancer tumors. MKN74 gastric cancer cells line grafted in the stomach of mice promoted poorly cohesive tumors both when wild-type for RHOA or mutant. However, RHOA mutant tumors contained smaller tumor nests, defined as clustered tumor cells surrounded by tumour stroma. This fact suggested that more factors apart from the presence of RHOA mutation are involved in this DGC histology. A deeper analysis indicated an higher number of blood vessel formation, and enhanced macrophage infiltration into the Y42 mutant tumors¹⁴⁰.

c-Met, is a tyrosine kinase receptor with an important role in promoting carcinogenic growth, angiogenesis, migration and invasion in gastric cancer¹⁴¹. This kinase phosphorylates RHOA at Tyr42 that, as result, undergoes to proteasome-mediated protein degradation. It has been observed that the proliferation and motility in gastric cancer cells induced by RHOA Y42C can be reduced by c-Met inhibitors, but not in cells expressing RHOA wt. So, c-Met inhibitors could be a good strategy against RHOA Y42C but not for RHOA wt tumors¹⁴². In addition, it has been demonstrated that the RHOA activation, through Y42C mutation, synergizes with the tumor suppressor Cdh1 (E-cadherin) to stimulate signaling networks that mediate transformation *in vivo* (peritoneal spread and ascites). Moreover, it was demonstrated that RHOA Y42C activates PI3K and YAP/TAZ pathways, suggesting that these could be the potential signaling pathways that enhance the survival and tumorigenicity of gastric tumor cells in this mutational context¹³⁹.

Mutations in other solid tumors: HNSCC, lung, breast, pancreas and colon

A large-scale genomic analysis across 21 tumor types, 4,000 human tumors, and their matched normal-tissue counterparts, aiming at identifying new somatic point mutations, identified six in HNSCC and 1 breast cancer tumor carrying mutations in the effector domain of RHOA. The predominant mutation was E40Q¹⁴³. ROCK1, the principal effector of RHOA, is often amplified in HNSCC, suggesting that RHOA E40Q could increase ROCK1 activation¹⁴⁴.

Data from public repositories shows that although in lung cancer RHOA is deleted in some cancers, in others the most frequent RHOA mutation is E47K.

RHOA mutations represent around 6 % of all cases in bladder cancer, being also E47K the predominant hotspot mutation.

In colon R5Q, C16S, A61V and L69P RHOA mutants have been identified in patient tumors. As data of interest, malignant pleural mesothelioma (MPM), an aggressive cancer relatively rare and linked to inhaling asbestos, presents RHOA mutations in three different codons (E32K, Y66N and A161V)¹⁴⁵. However, the molecular characterization of these mutations in all these different tumor contexts has not been studied yet.

Burkitt lymphoma

Burkitt lymphoma is the most common subtype of B-Cell non-Hodgkin's lymphoma (NHL) in pediatric and adolescent patients¹⁴⁶. IG-MYC translocation characterizes this lymphoma, but this genetic event is not sufficient for the malignant transformation of cells. When whole-genome sequencing was conducted on IG-MYC positive pediatric BL some genes were found to be recurrently mutated, and RHOA was among them¹⁴⁷. To study thoroughly RHOA in this cancer type, a big cohort of pediatric patients with mature aggressive B-cell lymphoma was analyzed. In 5 out of the 78 BL patients analyzed (6.41%) there was a RHOA mutation, being R5Q the most common¹⁴⁸. It has been hypothesized that this alteration might favour binding to GEFs¹⁴⁹. Indeed, this mutation was shown to decrease RHOA activity and to promote cancer progression. Moreover, analyzing SRF activity and stress fiber formation in HEK293 and MDCK cell lines, it was discovered that R5Q mutation impaired RHOA function compared with RHOA WT. In addition, mutations in Gα13 protein, an upstream regulator of RHOA, have been found in BL patients. This information suggests that R5Q mutation in BL might act as a loss-of-function mutation and that Gα13/RHOA axis in B cells is an important tumor suppressor¹⁵⁰.

Adult T-cell Leukemia/lymphoma (ATLL)

Adult T-cell leukemia/lymphoma (ATLL) is a subtype of peripheral T-cell lymphoma (PTCLs) caused by human T-lymphotropic virus type 1 (HTLV-1). This virus immortalizes T cells upon the infection, that occurs normally during the infancy and that has a latency period of 30 to 50 years. A cohort of 203 ATLL patients was subjected to targeted-deep sequencing to identify genetic changes involved in the development of this cancer. Approximately 15% of the patients harboured a RHOA mutation. Mutations concentrated in the GTP-binding pocket, with mutational hotspots at C16, G17 and A161 residues, being C16R substitution the most frequent alteration. Kinetics experiments revealed that C16R and A161P mutants function as fast-cycling mutants, showing an increased GDP/GTP exchange rate¹⁵¹. Contrary, G17V form was described as a dominant-negative mutation due to its incapability to bind to GTP^{122, 123, 152}. The biological effect of mutations found in ATLL patients was evaluated in HEK293 and NIH3T3 cells, obtaining a decreased activation of SRF and reduced stress fiber formation for G17V mutant, and the opposite results for C16R and A161V/P mutants. Altogether, RHOA mutants in ATLL exhibit a tumor promotion role when acting either as loss-of-function or gain-of-function. This counterintuitive effect is explained by the presence of the different mutations in different cellular contexts in ATLL. Specifically, C16R and A161P/V mutations occur predominantly in T-regulatory cells, whereas G17V mutations occur in memory T-cells¹⁵¹.

Angioimmunoblastic T-cell lymphoma (AITL)

Angioimmunoblastic T-cell lymphoma (AITL) is a common subtype of T cell lymphoma with poor prognosis. The molecular mechanisms behind this kind of lymphoma were unknown until recently. Using exome and transcriptome analysis of a large cohort of samples from lymphoma patients revealed that RHOA G17V mutation was found in a high percentage in patients with T cell lymphomas (53.3-70.8% in AITL and 17.2-18% in PTCL-NOS)^{122, 123, 152}, but absent in B cell lymphomas. G17V alteration occurs in the GTP-binding region of RHOA and impacts negatively on the GTPase resembling a dominant-negative form¹²³. This observation was in good concordance with the crystallographic structures of GDP- and GTP-bound RHOA G14V^{153, 154}. The oxygen atom in the main chain of G17 of RHOA WT should interact with the guanine base of GDP/GTP via water molecule, but when G17 is replaced by a valine, its voluminous side chain is predicted to impair GTP/GDP binding¹⁵⁵. When expressed in NIH3T3 cells, Rhotekin pull down assay showed the lower activation of the G17V mutant compared with the WT form. A161E, which is other mutation found in AITL showed as well an impaired binding capacity to GTP. The same results were observed upon analysis of SRF-dependent transcriptional activity and stress fiber formation, since both were diminished upon G17V mutation¹⁵². Similarly, in HeLa cells with RHOA G17V and T19N impaired the formation of stress fibers, while RHOA WT and RHOA Q63L boosted cytoskeleton reorganization. Additionally, Q63L overexpression in HEK293 cells

promoted round cell morphology, compared with the elongated morphology of the rest of the mutants tested (WT, G17V and T19N) ¹²². G17V overexpression in Jurkat T cells enhanced cell proliferating and invasion compared to RHOA WT and G14V ^{123, 152}.

Some groups have suggested that G17V locks RHOA GTPase in an inactive conformation. Indeed, G17A and G17A mutant interact with GEF with high affinity, but is resistant to GEF-induced GTP loading activation ¹⁵⁶. Interestingly, G17V mutation creates a binding site for Vav1 GEF protein. Binding of RHOA G17V to Vav1 increases phosphorylation at Tyr174 and consequently T-cell receptor (TCR) signaling ¹⁵⁷.

The biological relevance of RHOA G17V mutation in PTCL tumor has also been investigated. RHOA-G17V expression correlated with PD-1, nuclear pERK, p52, p38 PI3K and KRAS, NF- κ B and RAC1 ¹²⁴.

According to all the data summarized here, it is impossible to define which is the role of RHOA in cancer, because it varies from one tumor type to another. Furthermore, RHOA is involved in a great deal of signaling pathways, both oncogenic and tumor-suppressive. Interestingly, the different hotspot mutational profile in different cancers shows not only an exquisite tumor-type specificity, but selectivity as well, as each of the hotspot mutations activates or suppresses unique pathways to ultimately promote carcinogenesis.

Chapter I

Functional Characterization of RHOA hotspot mutations

AIMS OF THE STUDY

AIMS OF THE STUDY

The small GTPase RHOA has been widely described as an oncogene, displaying a key role in the carcinogenic process of several tumor types. Nevertheless, results from our group have shown that RHOA could act in a context-dependent manner, because it was found to have a tumor suppressive role in colon cancer¹⁰³ and in diffuse-gastric cancer (DGC). Recently, the use of high-throughput sequencing technologies has revealed that *RHOA* is frequently mutated in different liquid and solid tumor types, such as Burkitt lymphoma (BL), adult T-cell leukemia/lymphoma (ATLL), angioimmunoblastic T-cell lymphoma (AITL), diffuse gastric cancer (DGC) and head & neck squamous cell carcinoma (HNSCC)^{125, 127, 151, 158}. Intriguingly, these mutations are distributed along the *RHOA* coding sequence in a hotspot pattern; but, even more, the identity of the hotspot mutations in each tumor type is differential, suggesting a distinctive role of each mutant in the different tumor contexts.

Therefore, the specific aims of this thesis are:

1. To investigate the protein expression levels and the stability of the different RHOA mutants, as well as their cellular localization.
2. To investigate the functional relevance of the different RHOA mutations in the cytoskeletal dynamics through the study of F actin formation and adhesion properties.
3. To study the ability of RHOA mutants to activate the serum response factor (SRF) and NFκB signaling.
4. To evaluate the binding ability of RHOA hotspot mutants through two different assays:
 - a. A Rhotekin pull-down assay.
 - b. A yeast-two-hybrid approach to evaluate the binding capacity of DGC and HNSCC RHOA hotspot mutants to known effectors and regulators.

Chapter I

Functional Characterization of RHOA hotspot mutations

MATERIALS & METHODS

MATERIALS AND METHODS

The functional characterization of the *RHOA* hotspot mutations (C16R, G17V, R5Q, G17E, L57V, Y42C and E40Q) in comparison with the wild-type *RHOA* (*RHOA* WT), and the constitutive-active and dominant-negative control mutants, *RHOA* G14V and *RHOA* T19N, respectively, was approached systematically.

Cell lines

HEK293T (human embryonic kidney cells) and COS1 (green monkey kidney fibroblast-like cell line) cell lines were used to perform all the experiments. Both cell lines were maintained on Dubelco's Modified Eagle's Medium (DMEM; SIGMA) containing 10% fetal bovine serum (Sigma) under a 37°C and 5% CO₂ atmosphere. Cells were routinely tested for mycoplasma contamination using PCR Mycoplasma Detection Set (TaKaRa Bio, Inc. Kusatsu, Japan).

Plasmids

pINDUCER20-GFP-RHOA for RHOA expression in mammalian cells: lentiviral pINDUCER20 vector was used to transiently transfect cell lines, leading to inducible GFP-RHOA overexpression systems. This plasmid is a tet-on system, in which the rtTA (reverse tetracycline-controlled transactivator) protein binds the operator TRE (tetracycline response element) only if bound to tetracyclines. So, the culture of cells in the presence of doxycycline (dox) initiates the transcription of the inducible cassette, in this case the green fluorescent protein (GFP) alone of fused to the N-terminal end of *RHOA* open reading frame (**Figure13**). The different pINDUCER20-GFP-RHOA vectors (one for each mutant tested) were created using Gateway technology and pDONR221 encoding GFP-RHOA as donor. *RHOA* mutant forms in pDONOR221 were generated using QuikChange mutagenesis kit (Agilent Technologies Inc.) according to manufacturer's specifications and transferred to pINDUCER20 using LR Clonase (Life technologies, USA).

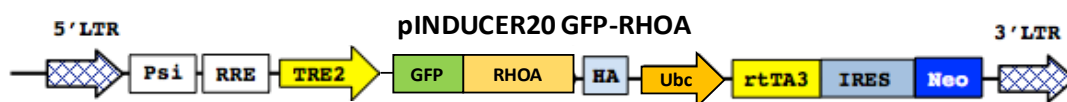


Figure 13. pINDUCER20-GFP-RHOA plasmids. LTR: Long terminal repeat; Psi: Retroviral Psi packaging element; RRE: Rev Response Element; TRE2: Tetracycline response element; GFP: Green fluorescent protein; Ubc: Ubiquitin C promoter; rtTA3: Reverse tetracycline-controlled transactivator; IRES: internal ribosome entry site; Neo: Neomycin resistance gene.

Sequencing: The presence of the desired mutations in the pDONR221-GFP-RHOA constructions and the transfer to pINDUCER20 destination vector was confirmed through Sanger sequencing (Macrogen Inc) using the primers detailed in **Table 2**.

1. RHOA expression

HEK293T and COS1 cells were transiently transfected with the different pINDUCER20-GFP-RHOA constructs. Specifically, 2 million of cells were seeded on 10-cm plates to achieve about 60% confluence on the following day. Twenty-four hours after seeding, cells were transfected with 7 µg of the corresponding lentiviral vector (pINDUCER20-GFP-RHOA). PEI (1 mg/mL) was used in a 4:1 ratio to DNA in the transfection. Six-hour post-transfection, cell medium was renewed and supplemented with doxycycline at 1 µg/ml (Sigma-Aldrich). Forty-eight hours post-induction cells were harvested for analysis of RHOA expression at protein, mRNA and/or DNA level.

RHOA protein expression

Protein extracts were obtained using Small GTPase lysis buffer (25 mM Hepes pH 7.5, 150 mM NaCl, 5 mM MgCl₂, 1% NP-40, 1mM DTT, 10% Glycerol) supplemented with protease inhibitors (Complete™, Mini, EDTA-free Protease Inhibitor Cocktail, Roche). Cell pellets were resuspended in the lysis buffer and incubated on ice for 5 minutes. Then, the lysate was centrifuged for 10 min, at 12,000 rpm and 4°C, and the supernatant was transferred into a new microtube and stored at -80°C until used. Total protein concentration was determined using a BCA™ Protein Assay Kit (Thermo Scientific). Briefly, 2 µl of the test sample diluted in distilled water (final volume 25 µl) were mixed with 200 µl of BCA reagent mixture in a 96 well-plate. A series of bovine serum albumin (BSA) protein standards diluted in distilled water was run alongside with the protein lysates to establish a protein standard curve. The plate was incubated in the dark at 37 °C for 30 minutes prior to absorbance measurement at 595 nm in a plate reader (Sunrise™ model, TECAN Group Ltd.). Protein concentrations were inferred using the BSA standard curve.

Western blot (WB): Gel electrophoresis: Separation of proteins was performed by one-dimensional SDS-PAGE (Sodium dodecyl sulfate - polyacrylamide gel electrophoresis) assay as follows. Proteins were thawed on ice and 30 µg of protein were mixed with Laemlli buffer 4X (250 mM Tris pH 6.8, 4.2% SDS, 20% Glycerol, 0.008% bromophenol blue, 10% 2-mercaptoethanol) and denatured at 95°C for 5 min. Then, proteins were separated by SDS-PAGE electrophoresis in polyacrylamide gels (4% acrylamide stacking gel; 10% acrylamide separating gel). The electrophoresis chamber was filled with running buffer (0.25 M Tris, 1.92 M Glycine and 34.6 mM SDS) and the current was set to 120 V, allowing the proteins to run and separate until the loading dye went out from

the gel. **Protein transfer to filters:** Proteins were electrophoretically transferred from the gel to polyvinylidene fluoride (PVDF; Amersham – GE Healthcare Life Sciences) filters. For this, the membrane and gel were set up in a “sandwich configuration” together with filter papers and sponges in the following order: sponge, Whatman filter, gel, membrane, Whatman filter and sponge. The transfer was carried out in a tank containing ice-cold transfer buffer (0.23 M Tris and 1.92 M Glycine). The proteins were allowed to transfer for 90-120 min at 110 V and 4°C. **Blocking and antibody blotting:** The membrane with the transferred proteins was blocked with 5% skim milk or BSA in PBS-0.1% Tween, according to the antibody manufacturer’s specifications, for 1 hour at room temperature in order to prevent unspecific binding of the antibodies. Next, the membrane was incubated overnight at 4°C with primary antibodies diluted in fresh blocking buffer (**Table 2**). The following day, membranes were washed 3 times for 10 min with PBS-0.1% Tween under agitation to remove unbound primary antibodies. Membranes were then incubated with secondary antibodies conjugated with horseradish peroxidase (Anti-mouse 1:5,000; Anti-rabbit 1:5,000; **Table 2**) for 1 h at room temperature and washed again with PBS-0.1% Tween 3 times for 10 min. **Detection:** Finally, proteins were detected using ‘Enhanced chemiluminescence system’ kit (ECL – GE Healthcare) and blue-light sensitive autoradiography films (AGFA (CP-BU)) or ChemiDoc XRS+ system (Bio-Rad). Specifically, membranes were incubated with 1:1 mixture of detection reagent A and reagent B (which contain a light-emitting non-radioactive substrate for horseradish peroxidase) for 1 min. When autoradiography was used, AGFA films were placed on the top of membranes in a dark room to detect the chemiluminescent signal, followed by an automated film development (Curix 60 – AGFA healthcare). When digital chemiluminescence was used, ChemiDoc system and Image Lab software were programmed to acquire images at the desired time points. Quantification of band intensity was performed using ImageJ program (NIH-National Institutes of Health).

Table 2. Antibodies used in this study.

Antibody	Source	Reference	Host	Application (dilution)
RhoA (67B9)	Cell Signaling	2117	Rabbit, monoclonal	WB (1:1,000)
Vinculin	Sigma-Aldrich	V4505	Mouse, monoclonal	WB (1:1,000)
Polyclonal Swine Anti-Mouse Immunoglobulins/HRP	Dako	P0447	Goat	WB (1:10,000)
Polyclonal Swine Anti-Rabbit Immunoglobulins/HRP	Dako	P0217	Goat	WB (1:5,000)

WB: Western blot

Flow cytometry analysis: GFP expression in HEK293T and COS1 cells overexpressing GFP-RHOA (wt or mutants) or GFP alone was analyzed by flow cytometry using FACScalibur instrument and Cell Quest Software (Becton-Dickinson). Propidium iodide

(PI, Sigma-Aldrich) staining (40 µg/ml) was used for exclusion of dead cells in the analysis.

RHOA mRNA expression

RNA extraction and quantitative real-time PCR (qPCR). Total RNA from cells was extracted with TRIZOL[®] reagent (Invitrogen) according to the instructions of the manufacturer. Retrotranscription was performed using 1 µg of total RNA and High Capacity cDNA Reverse Transcription kit (Applied Biosystems) following the vendor's guidelines. Relative mRNA levels for every RHOA mutant were assessed by Real Time Polymerase Chain reaction (RT-PCR) using SYBR Green Master Mix (Applied Biosystems). Transcript normalization was conducted by assessing 18S rRNA (Taqman Fast Advanced Master Mix, Applied Biosystems). RT-PCR reactions were run under standard conditions in a 7500 Fast Real-Time PCR System (Applied Biosystem). *RHOA* and *neomycin* resistance cassette contained in the pINDUCER20 vector were amplified using the primers described in **Table 2**. Relative *RHOA* and *Neomycin* resistant gene expression levels were determined with the $\Delta\Delta CT$ method using 18S as a housekeeping standard control, as previously described¹⁰².

DNA extraction and genomic qPCR: DNAzol[®] reagent (Invitrogen) was used to extract DNA from HEK293T and COS1 cells according to manufacturer's instructions. Then, genomic qPCR was performed to calculate the number of GFP-*RHOA* transgene copies present into the transfected cells using SYBR Green Master Mix (Applied Biosystems). The normalization control was performed with GAPDH. qPCR reactions were run under standard conditions in a 7500 Fast Real-Time PCR System (Applied Biosystem). Genomic *GFP-RHOA* and *GAPDH* DNA levels were amplified using the primers described in **Table 3**. *GAPDH* species sensitive primers were used for HEK293T (human) and COS1 (monkey) cells. Eventually, *GFP-RHOA* DNA relative levels were quantified following the $\Delta\Delta CT$ method using *GAPDH* as a housekeeping standard control, as previously described¹⁰².

Table 3. Oligos used in this study.

Primer name	Sequence (5' to 3')	Application	
RHOA G14V (F)	ggtgattgttggtgatgtagcctgtggaagacat	Site-directed mutagenesis	
RHOA G14V (R)	atgtctttccacaggctacatcaccaacaatcacc		
RHOA T19N (F)	ggtgatggagcctgtggaagaactgcttgc tcatagtc		
RHOA T19N (R)	gactatgagcaagcagttctttccacaggctccatcacc		
RHOA C16R (F)	caagcatgtctttccacgggctccatcaccaaca		
RHOA C16R (R)	ttgttggtgatggagcccgaggaaagacatgcttg		
RHOA G17V (F)	ggtgatggagcctgtgtaagaacatgcttgctc		
RHOA G17V (R)	gagcaagcatgtctttacacaggctccatcacc		
RHOA R5Q (F)	caatcaccagtttcttctggatggcagccatgaat		
RHOA R5Q (R)	attcatggctgccatccagaagaactggtgattg		
RHOA G17E (F)	gagcaagcatgtctttccacaggctccatcacc		
RHOA G17E (R)	ggtgatggagcctgtgaaagaacatgcttgc tc		
RHOA L57V (F)	ctgtgtccacacagccaactctacctgctttcca		
RHOA L57V (R)	tggaaagcaggtagagtggctgtgtgggacacag		
RHOA Y42C (F)	gatatctgccacacagttctcaaacactgtgggcac		
RHOA Y42C (R)	gtgccacagtggtttagaactgtgtggcagatc		
RHOA E40Q (F)	gccacatagttctgaaacactgtgggcacatacacc		
RHOA E40Q (R)	ggtgtatgtgccacagtggttcagaaacta gttggc		
pDONR221 (F)	gtaaacgacggccag		Sequencing
pINDUCER20 (R)	ggacgtcgtatgggtatt		
RHOA qPCR (F)	ctcatagtctcagcaaggaccagtt	qPCR (RNA)	
RHOA qPCR (R)	atcattccgaagatccttcttatt		
Neomycin qPCR (F)	cgttgctaccctgatatt		
Neomycin qPCR (R)	ctcgtcaagaaggcagatagaag		
18s human qPCR (F)	agtccctgccctttgtacaca		
18s human qPCR (R)	gatccgagggcctcactaac		
18S Taqman Probe	FAM-6cgccctgcgctactaccgattgg0-TAMRA		
GFP- RHOA genomic qPCR (F)	acatggctcctgctggagttc	qPCR (DNA)	
GFP- RHOA genomic qPCR (R)	acctctgggaactggtcctt		
GAPDH human - genomic qPCR (F)	acaccactctccaccttt		
GAPDH human - genomic qPCR (R)	ctgagccagccaccagag		
GAPDH monkey - genomic qPCR (F)	acaccactctccaccttc		
GAPDH monkey - genomic qPCR (R)	ctgagccagtcaccagag		

(F): forward; (R): reverse

RHOA protein stability

Protein half-life of the different GFP-RHOA forms used in this study was evaluated in HEK293T cells as follows. First, cells seeded on the previous day on 10-cm plates were transiently transfected with 7 µg of the corresponding pINDUCER20-GFP-RHOA lentiviral plasmid and polyethylenimine reagent. Six hours post-transfection, cells were exposed to 1 µg/ml dox to promote the expression of GFP-RHOA. Forty-eight hours after, cells were harvested with trypsin and washed three times with sterile PBS by centrifugation for doxycycline withdrawal. Then 2.5×10^5 cells were seeded onto 6 well-plates. Finally, cells were harvested at different time points (0, 6 and 24 hours) for evaluating GFP fluorescence. Paraformaldehyde (PFA) fixation was used to preserve

cells fluorescence along the time-course assay before analyzing GFP expression by cytometry as described above. Specifically, cells were trypsinized, PBS washed incubated with 4% PFA solution at room temperature and orbital rotation. Then, cells were pelleted by centrifugation and washed once with PBS. Finally, fixed cells were resuspended in PBS and stored at 4°C until collection of all the samples in the time course and analyzed by cytometry. FlowJo X software was used for data analysis and plotting of the results. Median fluorescent intensity was the parameter used to determine differences in protein half-life using GraphPad Prism (phase decay non-linear regression).

2. RHOA subcellular localization

To address the subcellular localization of the different RHOA hotspot mutants, HEK293T cells were transiently transfected with the different *GFP-RHOA* lentiviral constructs, as described before. The determination of the subcellular localization of GFP-RHOA was determined using two different approaches (**Figure 14**):

Co-localization studies in fluorescent confocal microscopy: HEK293T cells seeded at low confluence on glass coverslips (2×10^4 cells in 24 well-plates) were transiently transfected with 0.5 µg of pINDUCER20-*GFP-RHOA* constructs and polyethylenimine reagent. GFP-RHOA expression was induced with 1 µg/ml dox for 48 hours. Then, cells were stained. For that, coverslips were fixed in 4% PFA (Sigma-Aldrich), permeabilized with 0.1% Triton X-100 and stained with Rhodamin-phalloidin (0.1 µM; Cytoskeleton) for 30 min into a dark humid chamber. Later, upon three PBS washes, coverslips were stained for 1 min with 0.1 µM of 4',6-diamidino-2-phenylindol (DAPI, ThermoFisher). Finally, coverslips were mounted with ProLong® Gold antifade reagent (Life technologies). Protein localization was scored using images taken under a confocal fluorescence microscopy (60X, Olympus FV1000 spectral confocal microscope). At least 20 transfected cells (green)/mutant were scored in each of the three independent experiments conducted. Nuclear localization percentage was obtained using the ImageJ plugin JACoP to quantify the overlap of the blue (nuclei) and green (GFP-RHOA) signals. Mander's Overlap Coefficient was used to plot the results.

GFP nuclear signal of isolated nuclei through flow cytometry analysis: transiently transfected HEK293T cells were treated with 1 µg/ml dox for forty-eight hours to induce GFP-RHOA overexpression. Then, cells were trypsinized and divided in two samples upon a PBS wash. Half of cells were kept on PBS until analysis and the other half were processed for nuclei isolation as follows. Cells were centrifuged at 1,500 rpm for 10 min at 4°C and resuspended in 3 ml of ice-cold hypotonic buffer N (10 mM Hepes pH 7.5, 2 mM MgCl₂, 25 mM KCl, 250 mM Sucrose), supplemented with protease inhibitors cocktail (Complete™, Mini, EDTA-free Protease Inhibitor Cocktail, Roche). Cells were centrifuged and resuspended again in 15 volumes of supplemented

ice-cold hypotonic buffer N and incubated on ice for 40 minutes. Next, cells were homogenized with a glass Dounce pestle B on ice (20 strokes). Once cells were lysed, 125 μ l of sucrose solution per ml of lysate was added and mixture was homogenized by inversion 5 times. Later, cells were centrifuged at 1,000 rpm in 15 ml conical tubes for 10 min at 4°C in swinging bucket rotor; and the supernatant was decanted. The pellet (isolated nuclei) was resuspended in 5 ml of ice-cold buffer N. Finally, after repeating the previous centrifugation step, supernatant was decanted again, and nuclei were resuspended in PBS. Both, whole cells and nuclei were analyzed using a FACScalibur instrument and Cell Quest Software (Becton-Dickinson). The relative mean fluorescent intensity (MFI) of nuclear GFP was calculated by normalizing data with the MFI of the whole cells.

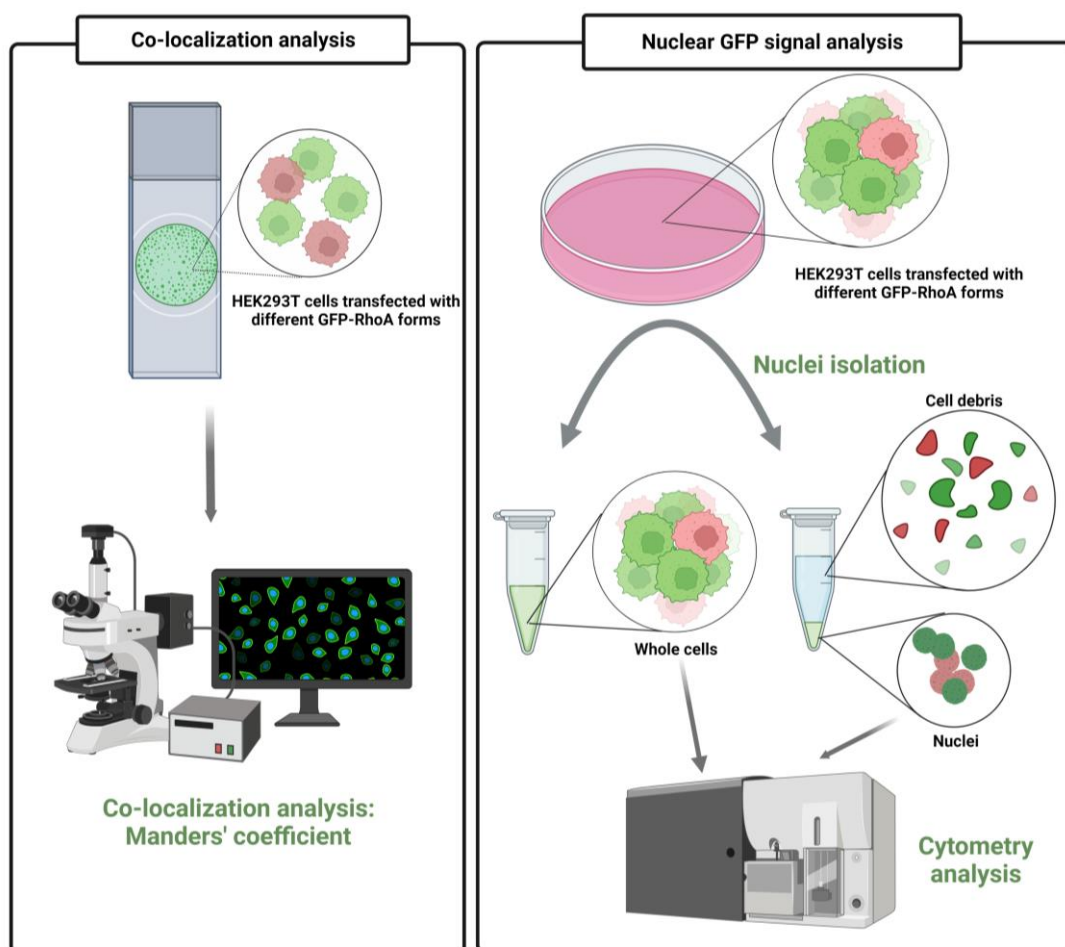


Figure 14. Assessment of RHOA subcellular localization. GFP-RHOA subcellular localization in transiently transfected HEK293T cells was assessed through two different approaches: Co-localization in confocal microscopy analysis, measuring the overlap between blue (nucleus) and green (GFP-RHOA forms) signals (left); and quantification of the relative nuclear GFP signal through cytometry analysis. Created in BioRender.com

3. Analysis of RHOA cytoskeleton regulation

Two different assays were performed to characterize the cytoskeleton rearrangements dependent on the different RHOA mutants: F actin formation and cell adhesion properties.

F actin formation: COS1 cells were used for these experiments. Visualization of F actin under the microscope was enhanced in COS1 cells over HEK293T cells. Thereby, 2×10^4 cells were seeded on poly-L-lysine coated glass coverslips in 24 well-plates. The day after, cells were transfected with 0.5 μg of the different pINDUCER20-GFP-RHOA forms and polyethylenimine reagent. Upon 48 h of treatment with 1 $\mu\text{g}/\text{ml}$ of doxycycline to induce RHOA expression, cells were fixed and stained as previously described in 'RHOA subcellular localization' section. Images (60X) were acquired using confocal fluorescence microscopy (Olympus FV1000 spectral confocal microscope). The intensity in the red channel (phalloidin, F actin) was scored in at least 20 transfected cells (green)/coverslip using ImageJ software. Data from three independent experiments was averaged.

Cell adhesion assay: HEK293T cells were used to study the adhesion properties of the cells after being transiently transfected with pINDUCER20 lentiviral vectors expressing the different GFP-RHOA mutants. Cells were seeded in 10-cm plates and transfected as described above. Upon 48 h of treatment with 1 $\mu\text{g}/\text{ml}$ of doxycycline to allow the expression of GFP-RHOA, GFP signal was observed under an inverted microscope (Nikon ECLIPSE Ts2R coupled to a Nikon INTENSILIGHT C-HGFI fluorescence illuminator); and pictures at 10X were taken to evidence differences in cell morphology and confluence. Next, cells were used to assess cell adhesion under centrifuge forces. Briefly, 1×10^5 cells were seeded in two independent 96 well-plates (12 wells/RHOA form), after being harvested from the original 10-cm plate with accutase (Corning). One plate served as control and the other was subjected to centrifugation after 20 min of incubation at $37^\circ\text{C}/5\% \text{CO}_2$ to allow cell re-attachment. For plate centrifugation, the plate lid was discarded and substituted by an adhesive sealing tape, and the plate was centrifuged upside down at 1,500 rpm for 5 min to remove loosely adherent cells. At this point, both plates, control and assayed, were fixed and stained as follows. First, medium from wells was carefully aspirated and cells that remained attached were fixed for 20 min at RT adding 100 μl of the fixation solution (75% methanol, 25% glacial acetic acid). Next, wells were washed thrice with 100 μl of water and stained with 1% (w/v) crystal violet (Fisher Scientific) in 25% methanol solution for 1 h at RT. Three additional washes with water were performed. Finally, the dye was solubilized with 100 μl of 10% (v/v) acetic acid solution and placed on a shaker at 150 rpm for 5 min at RT. Absorbance at 570 nm was measured using a microplate reader (Epoch –

BioTek Instruments). OD was used to calculate the relative percentage of attached and detached cells over the control plate.

4. Analysis of the RHOA-dependent SRF and NFκB transcriptional regulation

The activation of serum response factor (SRF) and nuclear factor kappa-light-chain-enhancer of activated B cells (NFκB) signaling by the different RHOA hotspot mutants was studied using luciferase reporter assays.

The luciferase reporter plasmid for SRF activity, namely pGL4.34[luc2P/SRF-RE/Hygro], was obtained from Addgene. Its homologue for NFκB, pGL4.32[luc2P/NF-κB-RE/Hygro], was a kind gift from Dr. Sayós (Vall Hebron Institute of Research). Both reporter plasmids contain five tandem copies of SRF and NFκB response elements, respectively, upstream of a minimal SV40 promoter driving firefly luciferase gene expression. pRL-SV40 expressing Renilla luciferase, obtained from Promega, was used to normalize luciferase signal according to cell viability and transfection efficiency.

3×10^4 HEK293T cells were seeded 24 hours prior to transfection in 96 well-plate (6 replicates per RHOA variant). The day after, cells were transfected with 10 ng of Renilla luciferase plasmid, 40 ng of the SRF-luciferase or NFκB-luciferase plasmid and 150 ng of each one of the pINDUCER20 plasmids expressing GFP-RHOA variants. PEI (1 mg/mL) was used in a 4:1 ratio to DNA in the transfection. After 7 hours, cells were treated for 48 hours with 1 μg/ml of doxycycline to induce GFP-RHOA expression. Then, cells were lysed for 20 minutes at room temperature with Passive Lysis Buffer (25 mM Tris-phosphate pH 7.8, 2 mM DTT, 2 mM 1,2 diaminocyclohexane- N,N,N,N -tetraacetic acid, 10% glycerol, 1% Triton X-100). Firefly and Renilla luciferase activity were measured using a non-commercial Dual luciferase assay. 15 μl of A reactive (25 mM glycylglycine, 15 mM KPO4 pH 8.0, 4 mM 25 EGTA, 2 mM ATP, 1 mM DTT, 15 mM MgSO4, 0.1 mM CoA, 75 μM luciferin, final pH adjusted to 8.0) were used to measure firefly luciferase activity; and 15 μl of B+C reactive (B: 1.1 M NaCl, 2.2 mM Na EDTA, 0.22 M KPO4 pH 5.1, 0.44 mg/mL BSA, 1.3 mM NaN3; C: 1.43 μM coelenterazine Promega, final pH adjusted to 5.0) were used to measure Renilla activity with a FB-12 tube luminometer (Berthold). Promoter activity (luciferase relative levels) was calculated dividing the luciferase relative light units (RLU) for SRF or NFκB by the renilla RLU in the same sample.

5. RHOA known interactome analysis

Differences in the binding capacity of the different RHOA mutants were assessed through two different approaches. A Rhotekin pull-down assay was used to evaluate the binding to the known effector Rhotekin, whereas a Yeast-Two-Hybrid assay was performed to screen RHOA interaction with ROCK, DIAPH/mDIA, PKN1 and Kinectin effector proteins, and NET1 RhoGEF protein.

RHOA binding capacity to Rhotekin through a pull-down assay

Pull-down assay was selected to compare the ability of RHOA mutants expressed in HEK293T to bind Rhotekin. Specifically, the assay uses the Rho binding domain (RBD) of the Rho effector protein, Rhotekin.

GST-Rhotekin-RBD purification: pGEX-Rhotekin-GST was transformed by heat-shock into BL21 E. coli. Transformed cells were grown in 250 mL of liquid LB medium (1% Tryptone, 0.5% yeast extract, 1% NaCl) supplemented with 100 µg/mL ampicillin at 37 °C, 250 rpm, until OD₆₀₀ reached 0.5. Rhotekin-GST expression was induced with 0.5 mM IPTG at 30 °C until reaching OD₆₀₀ = 1 (3 h approximately). Then, bacteria were harvested by centrifugation at 4,000 xg, 20 min, and resuspended in 10 mL of buffer A [50 mM Tris-HCl pH 7.5, 1% Triton X-100, 150 mM NaCl, 5 mM MgCl₂, 1 mM 1,4-Dithiothreitol (DTT), 0.1 µg/mL aprotinin, 1 mM phenylmethylsulfonyl fluoride (PMSF), 200 µg/mL lysozyme (USB, Chicken egg white)] and incubated for 20 min on ice. The cells were disrupted by sonication on ice with a Fisher Sonic Dismembrator Model 100 (30 seconds constant duty cycle, output 4 and 1 min on ice, 4 cycles). Cell debris and high molecular weight DNA were removed by centrifugation, at 10,000 xg for 30 minutes and the supernatant was recovered. 200 µL of Glutathione sepharose beads slurry (GSH-sepharose) were equilibrated by washing them twice with 400 µL of buffer A without lysozyme, and resuspended in 200 µL complete buffer A. Then, the already equilibrated glutathione sepharose beads were added to the bacterial lysate and incubated in rotation for 2 h at 4 °C. Next, the beads were centrifuged at 300 xg for 2 min at 4 °C, the supernatant was discarded, and the beads were washed with 400 µL buffer B (50mM Tris pH 7.5, 0.5% triton X-100, 150 mM NaCl, 5 mM MgCl₂, 1 mM DTT) 3 times. Finally, the beads were resuspended in 300 µL buffer C (50 mM Tris HCl pH 7.2, 150 mM NaCl, 5 mM MgCl₂, 1 mM DTT, 10% glycerol) and protein concentration was quantified using BCA™ Protein Assay Kit (Thermo Scientific), as described before.

Rhotekin Pull-down: 20 µg of recombinant GST-Rhotekin-RBD beads were incubated for 2 h at 4 °C in constant orbital rotation with and 0.3 mg of fresh protein lysate obtained from HEK293T cells transiently transfected with the different pINDUCER20-GFP-RHOA vectors and cultured in the presence of doxycycline for 48 h. The beads were then pelleted by centrifugation, the supernatant discarded, and the beads were washed thrice with 1 mL of protein extraction buffer. Finally, the beads were

resuspended in 2x Laemmli buffer and incubated at 95 °C for 5 minutes. Finally, the proteins were resolved by 10% SDS-PAGE, transferred to PVDF filters and probed with anti-RHOA antibody (**Table 2**) to detect active (pulldown) and total (INPUT) GTPases by Western blot. Band intensity was analyzed using ImageJ software. Relative active-RHOA levels were obtained normalizing the band intensity from the pull-down with vinculin housekeeping protein in the INPUT.

Analysis of RHOA binding to known effectors and regulatory proteins through a Yeast-Two-Hybrid Assay

Yeast two-Hybrid (Y2H) assay is a molecular biology approach used to discover and measure the strength of direct protein–protein interactions. Proteins of interest are fused to the DNA-binding domain (BD) or activation domain (AD) of GAL4 transcription factor, henceforth named as ‘bait’ and ‘prey’, respectively. If the hybrid proteins bind to each other, the BD and AD are brought together within the cell nucleus and lead the expression of specific reporter genes ¹⁵⁹ (**Figure 15**).

We conducted MATCHMAKER Two-Hybrid system 2 (CLONTECH®) according to the manufacturer’s specifications to screen the interaction of RHOA wild type and the most common RHOA mutants in diffuse gastric cancer (DGC) and head & neck squamous cell cancer (HNSCC), with bona fide RHOA effectors and interacting molecules.

Bait constructions containing the DGC mutant forms of RHOA (R5Q, L57V, Y42C or G17E) and HNSCC mutant RHOA E40Q were generated. Specifically, *RHOA* open reading frame contained in the pDONR221 vector was PCR amplified and cloned in frame with the yeast GAL4 transcription factor DNA-binding domain into the vector, that allows yeast to grow efficiently in leucine (Leu)-deficient substrates. pGTB9 RHOA construct was subjected to site-directed mutagenesis using QuikChange mutagenesis kit (Agilent Technologies Inc.) to introduce the desired mutations in *RHOA*. The DNA oligos used for mutagenesis are shown in **Table 3**.

pGAD424 prey DNA constructs encoded a fusion protein consisting on the GAL4 activation domain fused to well known RHOA effector proteins (ROCK1, DIAPH2, PKN1 and Kinetin) or the guanine nucleotide exchange factor (GEF) NET1. This vector confers efficient growth of yeast in tryptophan (Trp)-deficient substrates. All these constructions were a kind gift from Dr. Erik Sahai (Tumor Cell Biology Laboratory, Francis Crick Institute, London, UK). The pGTB9-RHOA wild type or RHOA mutants and pGAD424 constructs were co-transformed into the *Saccharomyces cerevisiae* yeast strain GC-1945. Following bait-prey mating, the culture was plated onto primary selection Synthetic Defined media lacking leucine and tryptophan (SD/-Leu, -Trp), allowing yeast growth only if efficiently transformed with pGTB9 and pGAD424 constructions.

Yeast were grown until colonies were visible (5-7 days). To assess the interaction between bait/prey proteins and the strength of the interaction, two colonies for each transformation were inoculated into SD/-Leu, -Trp medium and grown until reaching an OD₆₀₀ of 0.5. Serial dilutions of yeast cultures were performed (10^{-1} , 10^{-2} and 10^{-3}) and plated onto SD/-Leu, -Trp, -His supplemented or not with 3-amino-1,2,4 triazole (3-AT) at 1, and 5 mM. 3-AT is a competitive inhibitor of the product encoded by the HIS3 reporter gene, which is only expressed upon direct binding of bait and prey proteins. Accordingly, 3-AT is used to score the strength of the interaction. Plates were incubated at 30 °C until colonies were visible (**Figure 15**).

Summarizing, the presence of growth in mediums lacking leucine, tryptophan and histidine (SD/LTH) indicates a positive direct interaction between bait and prey proteins. And the ability to grow with increasing concentrations of 3-AT illustrates the strength of the interaction. The presence/absence of interactions and their strength was scored as follows: '+++' when robust growth was observed with 0 mM, 1 mM and 5 mM of 3-AT; '++' when robust growth was observed with 0 mM and 1 mM of 3-AT; '+' when robust growth was observed only in the absence of 3-AT; and '-' when no growth was observed, regardless of 3-AT.

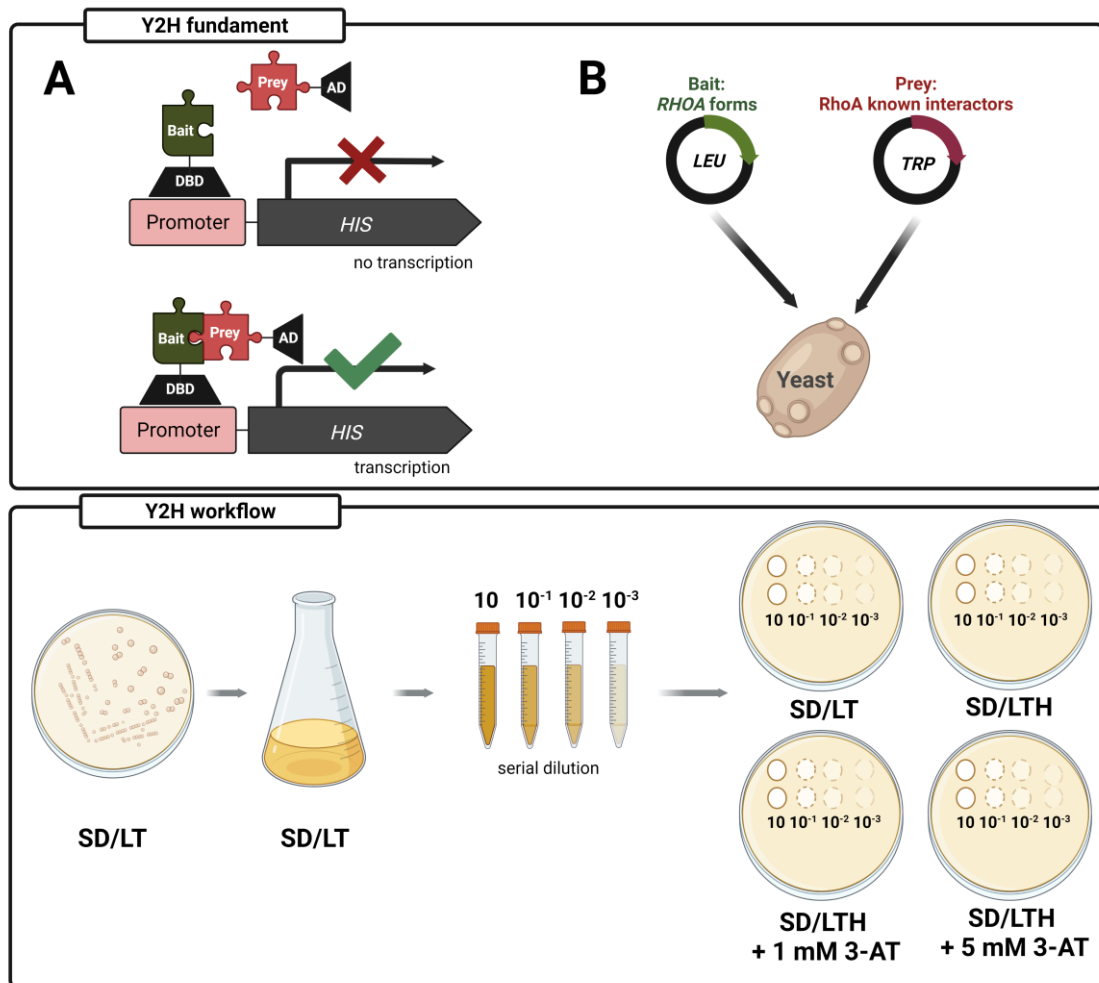


Figure 15. Yeast-Two-Hybrid spot assay: fundamentals and workflow. (A) The coding sequence of *RHOA* was fused to the GAL4-DNA BD (bait) and the coding sequence of the known *RHOA* interactor/regulator proteins was fused to the GAL4-AD (prey). Only if bait and prey interact, the activity of the transcription factor is reconstituted, and leading the transcription of an autotrophic reporter gene (*HIS*, histidine), and the yeast to growth in mediums lacking histidine (SD/LTH). Recombinant vectors were co-transformed into *Saccharomyces cerevisiae* yeast strain GC-1945 (B). The Y2H assay workflow is represented: after transformation with bait and prey constructions, yeast were grown into plates lacking leucine and tryptophan (SD/LT). Then, two colonies were culture in liquid SD/LT medium, serially diluted and spotted (10 μ l) in plates lacking leucine and tryptophan (SD/LT); leucine, tryptophan and histidine (SD/LTH); and SD/LTH containing 3-amino-1,2,4 triazole (3-AT) at 1 mM and 5 mM. AD: activation domain; DBD: DNA binding domain; *HIS*: histidine; LEU: leucine; TRP: tryptophan; SD: Synthetic Defined media.

Statistical analysis. Student's test was used to determine statistical difference between groups. GraphPad Prism 8 was used to analyze data. A p value <0.05 was considered significant. *<0.05; **<0.01; ***<0.001; ****<0.0001.

Chapter I

Functional Characterization of RHOA hotspot mutations

RESULTS

RESULTS

RHOA GTPase has been widely investigated due to its role as an oncogene in the process of malignant transformation of cells^{58, 65-70}. However, our laboratory described that this protein acts as tumour suppressor in colorectal cancer^{102, 103}, suggesting that the role of this GTPase could be context-dependent.

The use of high-throughput sequencing platforms has revolutionized the molecular characterization of tumours. Exome sequencing of large cohorts of patients samples evidence frequent *RHOA* mutations in a wide variety of human cancers, both solid cancers, *i.e.* diffuse-gastric cancer (DGC) and head & neck cancer (HNSCC); and haematological malignancies, such as Burkitt lymphoma (BL), adult T-cell lymphoma/leukaemia (ATLL) and angioimmunoblastic T-cell lymphoma(AITL)¹⁵¹. *RHOA* mutations are not randomly distributed along the coding sequence of the gene, but instead are enriched in specific and recurrent hotspots which, interestingly, are different for each tumour type (FIGURE?). This suggests that, although all these mutations are likely oncogenic, must have different biological effects into the cells affected. Intrigued by this observation, we aimed to characterize the most predominant *RHOA* mutations in human tumours to identify the distinctive functional and biological properties contributing to tumorigenesis. Accordingly, in this chapter we summarize the work conducted to functionally characterize the following *RHOA* mutations: C16R (ATLL); G17V (AITL), R5Q (BL and DGC); G17E, L57V, Y42C (DGC); and E40Q (HNSCC). Two additional *RHOA* mutants were included in our study: G14V and T19N. These mutations are not found in tumours but constitute excellent models for comparison purposes. Specifically, G14V and T19N have been widely characterized as constitutive-active and dominant-negative forms of RHOA, respectively.

1. Protein expression of RHOA hotspot mutants

To dissect the effect of the different *RHOA* mutations in the cell signalling pathways and cellular processes controlled by RHOA, we first selected the cellular model in which performing the experiments. Considering the diversity of tumour contexts in which RHOA is mutated, the number of mutants to be compared and the cellular processes to be explored, we selected HEK293T cell line. HEK293T cell line is a well-known and widely used derivative of the HEK293 parental cell line (human embryonic kidney cells), obtained by transduction with the SV40 large T antigen (SV40 T) to achieve cell immortalization. HEK293T cells are easily maintained in conventional cell

culture conditions, display a reliable and consistent cell growth, and exhibit high transfection rates with exogenous DNA and high protein synthesis. Accordingly, HEK293T was an excellent model to transduce with mammalian expressing vectors encoding the wild-type (wt) or mutant forms of human RHOA fused to the fluorescent protein GFP at the N-terminal end (GFP-*RHOA*), or GFP alone as a control. We selected pINDUCER20tetraacycline-inducible vector (doxycycline) to overexpress the different GFP-*RHOA* forms within cells. The use of an inducible system was motivated to avoid cell death events, since it has been reported that *RHOA* overexpression at high levels promotes apoptosis in fibroblastic-like cells^{62, 160, 161}. In this way, we could manipulate not only the time in which transgene expression would be switched on, but also the expression levels of GFP-*RHOA* proteins.

First, protein levels of the different *RHOA* forms were interrogated. Upon transient transfection of HEK293T with the vectors containing GFP-*RHOA* wt or mutants, and 48 hours of induction with 1 µg/mL of doxycycline (Dox), the levels of exogenous *RHOA* were assessed by Western blot. We observed a consistent and significant decrease in the levels of G17 mutants compared to *RHOA* wt (**Figure 16 A-B**). Equivalent results were obtained when the mean fluorescence intensity of GFP was analysed through flow cytometry (**Figure 16 C**). Importantly, all HEK293T cells exhibited a similar proportion of GFP positive cells, ruling out a reduced cell transfection efficiency of *RHOA* G17 mutants (**Figure 16 D**).

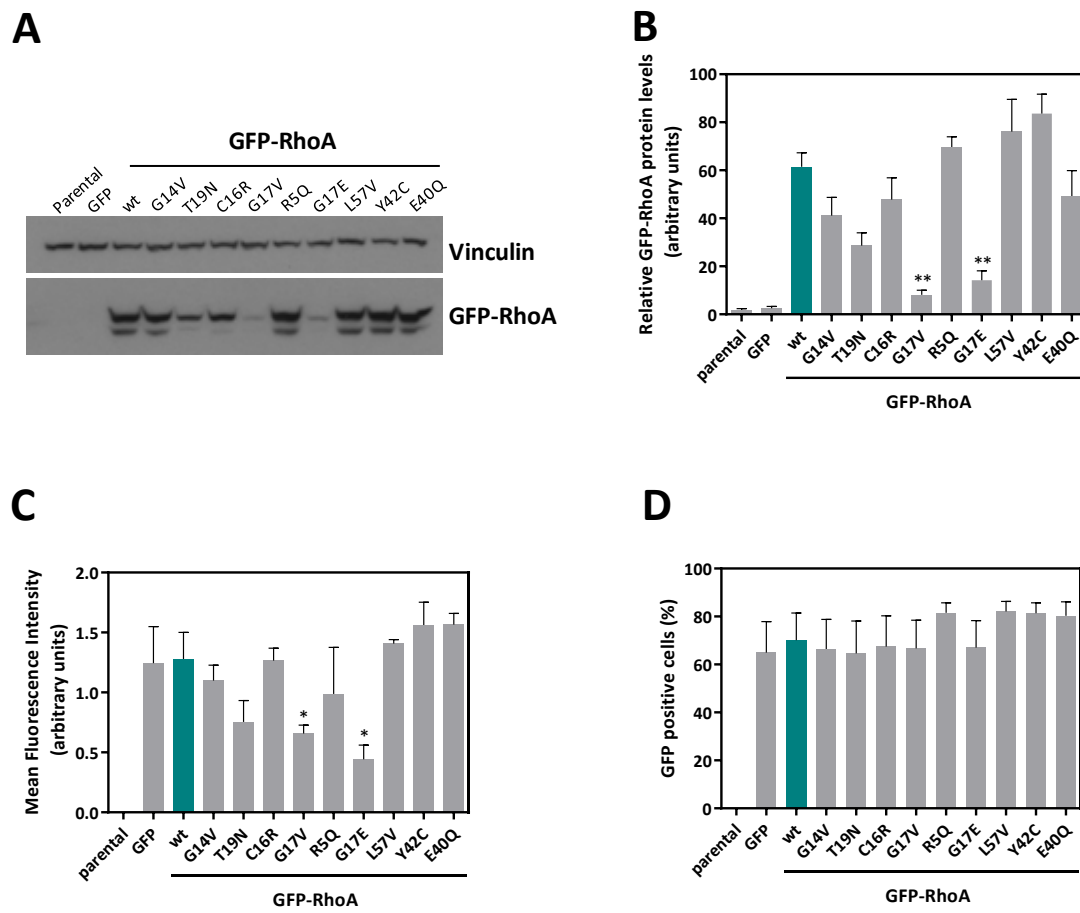


Figure 16 Protein expression of GFP-RHOA wt and GFP-RHOA mutants in HEK293T cells. GFP-RHOA levels after treatment with 1 μ g/mL Dox for forty-eight hours in transiently transfected HEK293T cells were assessed by Western blot analysis (A-B) and flow cytometry (C-D). The intensity of the bands was quantified with ImageJ to obtain RHOA protein levels normalised to the vinculin protein (B). Flow cytometry analysis to determine the mean fluorescence intensity (MFI) of GFP positive cells (C) and the percentage of GFP-positive cells (D). The average of three independent experiments (\pm SEM) in panels B-D is shown. *Student's t-test $p < 0.05$, ** $p < 0.001$; comparing each condition to GFP-RHOA wt.

We wondered whether the differences in the expression of RHOA G17 mutants were specific of the HEK293T cellular system chosen to overexpress this GTPase, or alternatively was a widespread phenomenon. COS1 is an African green monkey kidney fibroblast-like cell line also very suitable for transfection and protein production. These cells were subjected to the same transient transfection and analyses described before. Interestingly, the reduced protein levels in G17 mutants observed in HEK293T cells was also reproduced in the COS1 cell line system (Figure 17).

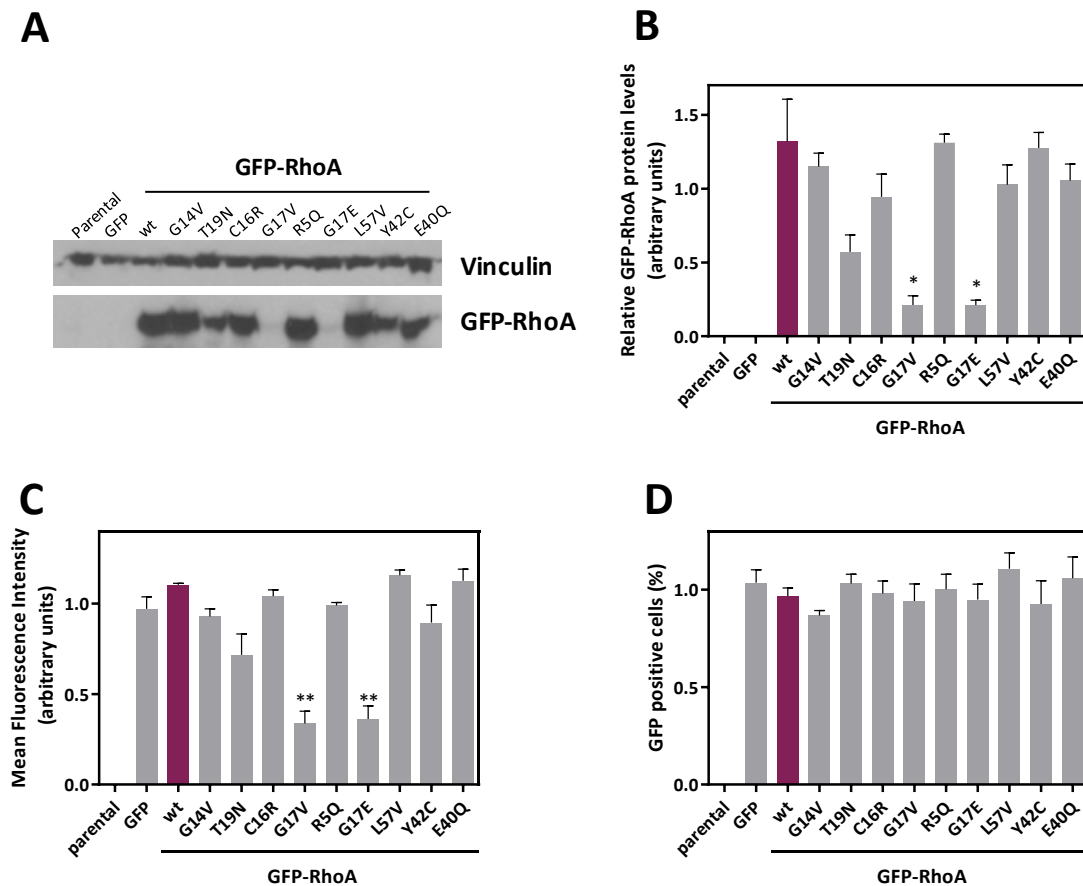


Figure 17. Protein expression of GFP-RHOA wt and GFP-RHOA mutants in COS1 cells. GFP-RHOA levels after treatment with 1 $\mu\text{g}/\text{mL}$ Dox for forty-eight hours in transiently transfected COS1 cells were assessed by Western blot analysis (**A-B**) and flow cytometry (**C-D**). The intensity of the bands was quantified with ImageJ to obtain RHOA protein levels normalised to the vinculin protein (**B**). Flow cytometry analysis to determine the mean fluorescence intensity (MFI) of GFP positive cells (**C**) and the percentage of GFP-positive cells (**D**). The average of three independent experiments (\pm SEM) is shown.

Next, we wondered whether the differential protein expression observed for RHOA G17 mutants occurred in the cellular tumour context in which these mutations are found. To this aim, the GFP-RHOA G17E mutant occurring in DGC was transfected into MKN45 cell line (diffuse gastric type cancer cell line), and the GFP-RHOA G17V mutant, which constitutes the hotspot mutation in AITL, was transfected into Jurkat cells (immortalized T lymphocytes). Cytometry analysis interrogating GFP fluorescence as a surrogate marker of RHOA protein levels showed significantly lower mean fluorescent intensity of GFP of both G17V mutants compared to RHOA wt (**Figure 18 A-B**). Thus, G17 mutants showed reduced RHOA expression regardless of cellular context.

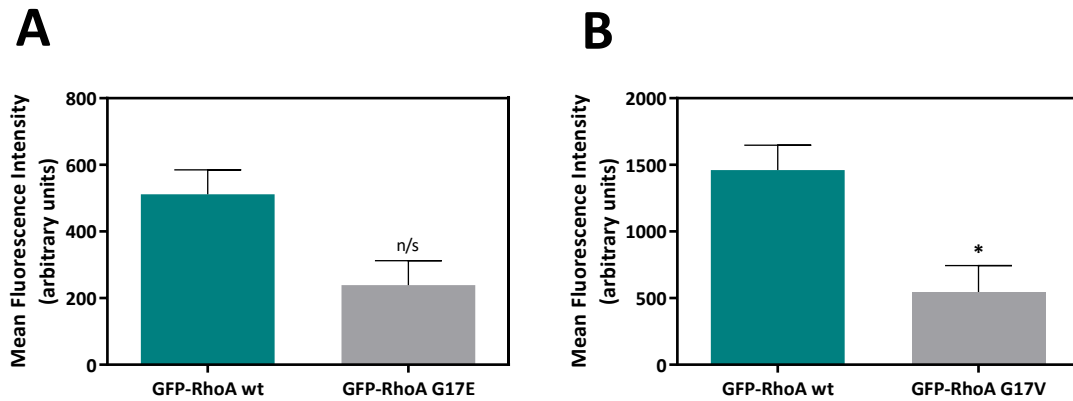


Figure 18. Protein expression of GFP-RHOA G17E and G17V in MKN45 and Jurkat cells. GFP Mean Fluorescence Intensity (MFI) after treatment with 1 μ g/mL Dox for forty-eight hours upon transient transfection of GFP-RHOA G17E in MKN45 (A) and GFP-RHOA G17V in Jurkat cells (B). The average of three independent experiments (\pm SEM) is shown. *Student's t-test $p < 0.05$.

Altogether, the results obtained suggested the existence of post-transcriptional and/or post-translational mechanisms regulating the expression of RHOA G17 mutant forms. To gain a greater insight into the regulation of RHOA expression, HEK293T cells transiently transfected with vectors encoding for GFP alone or GFP-RHOA wt/mutants were further analysed. Quantitative real-time PCR (qPCR) on total DNA was conducted to determine the number of GFP-RHOA transgene copies present in HEK293T cells (Figure 19 A). As no differences were observed at the DNA level, we then explored post-transcriptional events in the HEK293T cell line system. Reverse-transcription quantitative PCRs (RT-qPCR) on total RNA was conducted to assess the transcript levels of GFP-RHOA (Figure 19 B) and the neomycin 3'-glycosylphosphotransferase as a control (Figure 19 C). Both transgenes are encoded in the same expression vector used to transfect HEK293T cells. No significant differences were observed at the RNA level between the different RHOA mutant forms. Pearson's correlation analysis demonstrated lack of association between GFP-RHOA protein levels (from Western blot analysis) and DNA or RNA levels of GFP-RHOA (from qPCRs) (Figure 19 D-E).

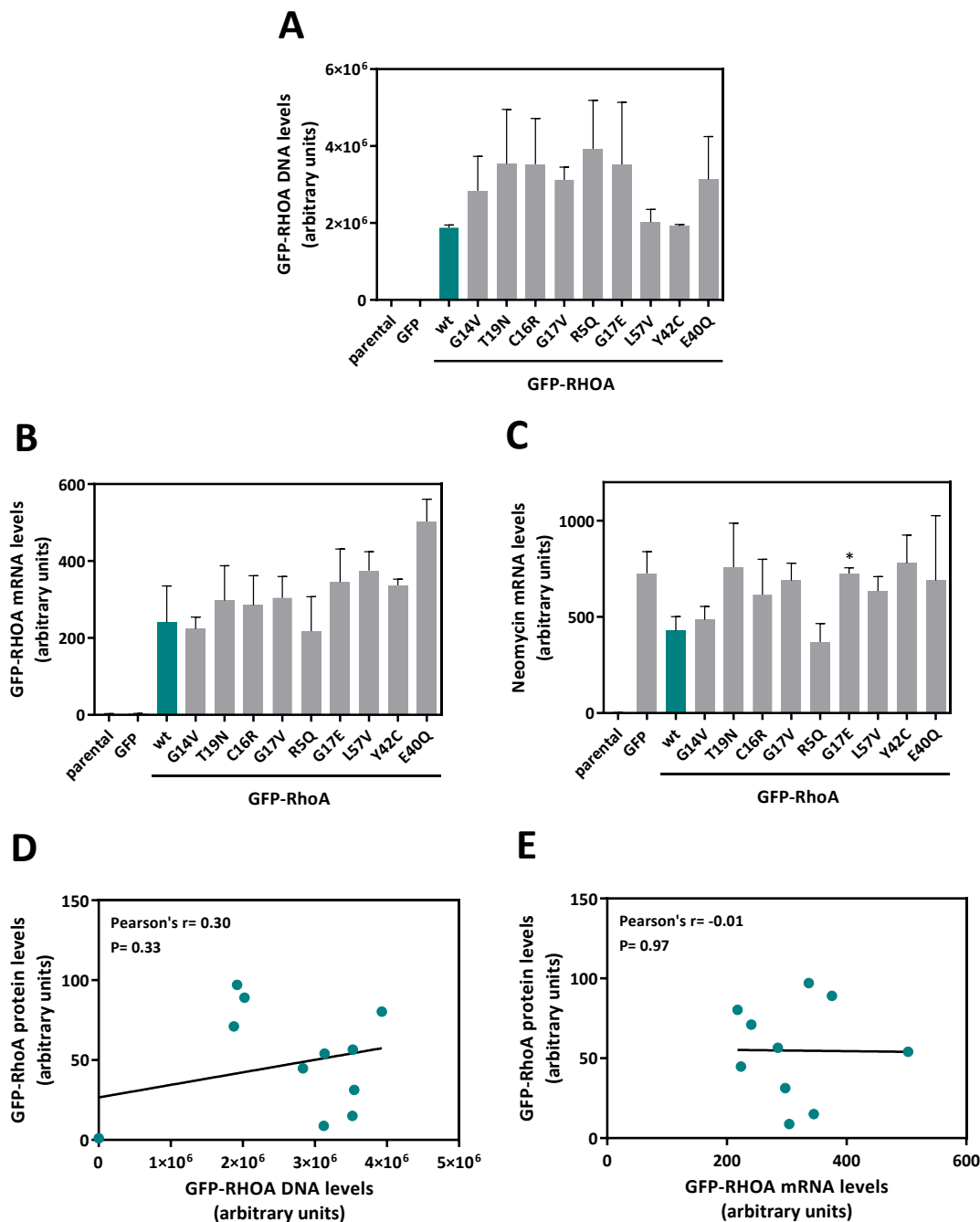


Figure 19. GFP-RHOA mutants DNA and RNA levels in HEK293T cells. GFP-RHOA DNA levels were assessed by quantitative real-time PCR (qPCR) upon transient transfection of cells with the indicated plasmids and transcript induction with 1 μ g/mL Dox for forty-eight hours (**A**). GFP-RHOA and Neomycin, the resistance gene, mRNA expression levels were assessed through reverse-transcription quantitative PCRs (RT-qPCR) under the same conditions (**B-C**). GFP-RHOA protein levels were correlated with GFP-RHOA DNA levels (**D**) and with GFP-RHOA RNA levels (**E**). The average of three independent experiments (\pm SEM) is shown. *Student's t-test $p < 0.05$; comparing each condition to GFP-RHOA wt.

The same experimental approach was carried out in COS1 cells, yielding equivalent results regarding the expression of RHOA G17 mutants (**Figure 20**). A significant reduction at the mRNA level, compared with RHOA wt, for both, GFP-RHOA and the

neomycin resistant cassette, was observed in COS1 when transfecting cells with Y42C mutant. However, this lower expression did not have an impact at the protein level (Figure 20 A-B).

Collectively, these results point out to a post-translational regulation of RHOA G17 mutant forms in the cell line systems used in the study.

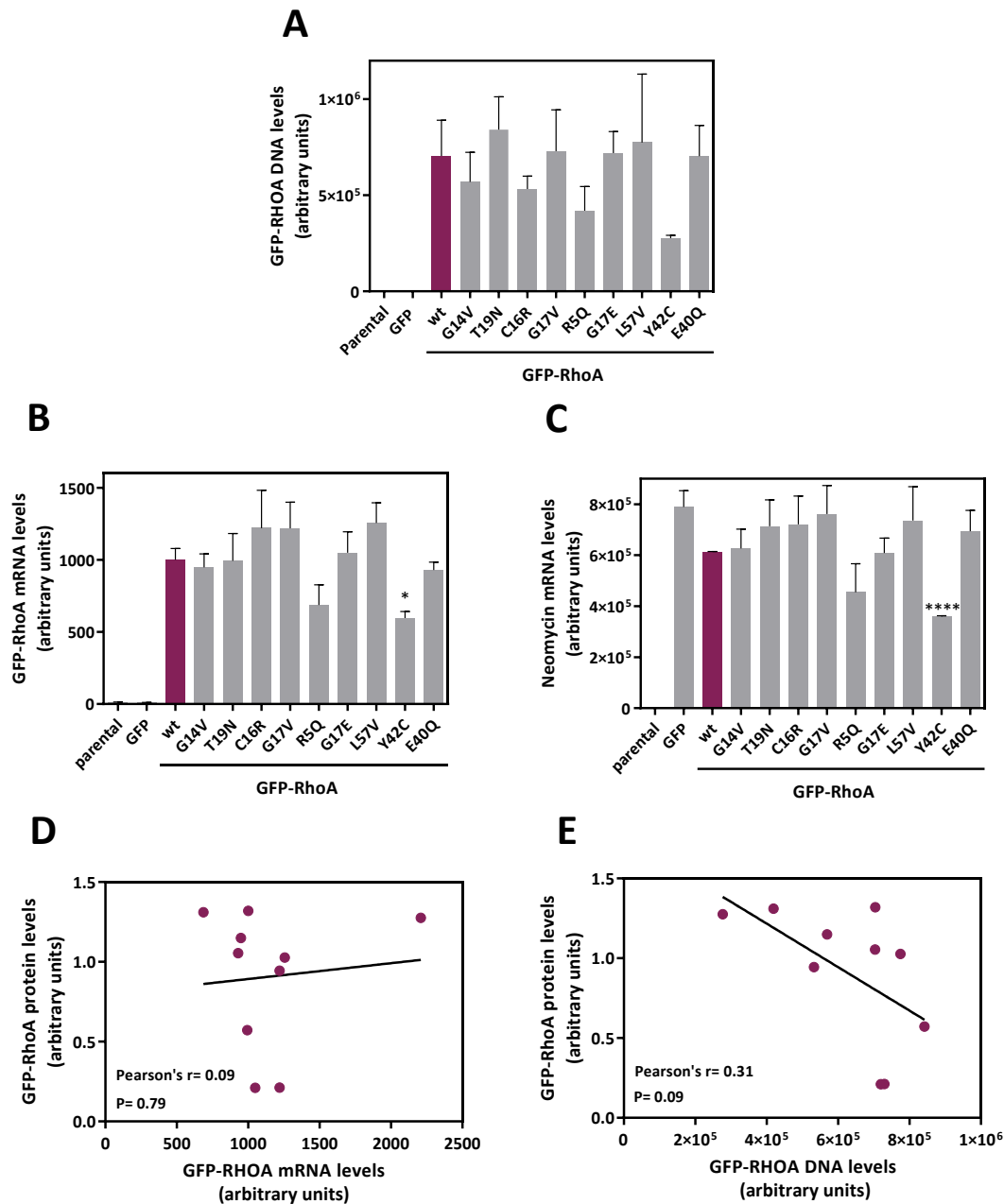


Figure 20. GFP-RHOA mutants DNA and RNA levels in COS1 cells. GFP-RHOA DNA levels were assessed by quantitative real-time PCR (qPCR) upon transient transfection of cells with the indicated plasmids and transcript induction with 1 μ g/mL Dox for forty-eight hours (A). GFP-RHOA and Neomycin mRNA levels were assessed through reverse-transcription quantitative PCRs (RT-qPCR) under the same conditions (B-C). GFP-RHOA protein levels were correlated with GFP-RHOA DNA levels (D) and with GFP-RHOA RNA levels (E). The average of three independent experiments (\pm SEM) is shown. *Student's t-test $p < 0.05$, **** $p < 0.0001$; comparing each condition versus GFP-RHOA wt.

Proteins regulate nearly every cellular event. The protein pool within cells is tightly controlled from synthesis to degradation. Determining the stability of a protein is one of the first steps towards understanding their cellular turnover and abundance. Protein half-life, defined as the time required to reduce by 50% the protein level at the beginning of a chase, is an important feature of protein homeostasis (proteostasis). HEK293T cells were transiently transfected with GFP-*RHOA* wt and G17E/V mutants. After 48 hours of doxycycline induction, cells were trypsinized and subjected to extensive wash cycles for elimination of doxycycline and interruption of transcript production. Cells were paraformaldehyde-fixed at different time points (0, 6 and 24 hours) and median fluorescence intensity of GFP was determined by flow cytometry. Results indicated that GFP-*RHOA* G17 mutants exhibit a reduced half-life compared with GFP-*RHOA* wt (**Figure 21 A**). GFP signal in cells transfected with *RHOA* G17 mutants was significantly reduced (over 50%) at the six-hour time point, whilst the fluorescence of *RHOA* wt cells levels were almost unaffected under the same experimental conditions (**Figure 21 B**). According to these results, *RHOA* G17E and G17V mutations might affect *RHOA* protein stability, decreasing the amount of *RHOA* protein present into a given cell.

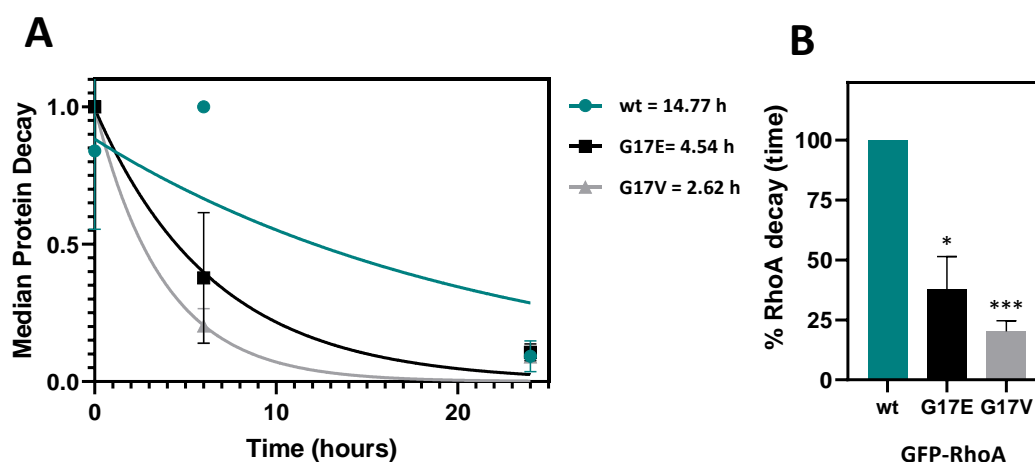


Figure 21. Half-life determination of *RHOA* G17E and G17V proteins in HEK293T cells. Median fluorescence intensity of transiently transfected HEK293T cells with GFP-*RHOA* was determined by cytometry analysis. *RHOA* half-life was calculated using GraphPad Prism (phase decay non-linear regression). Protein half-life time of the GFP-*RHOA* tested is indicated in the figure (**A**). Differences in the percentage of *RHOA* decay at time point 6 were investigated by unpaired, two-tail Student's t test (**B**). p values are indicated for statistically different means: * <0.05 ; *** ≤ 0.001 . The average of three independent experiments (\pm SEM) is shown.

2. Protein localization of RHOA hotspot mutants

Subcellular localization strongly influences protein function by controlling access to and availability of all types of molecular interaction partners. Thus, knowledge of protein localization plays a significant role in characterizing the cellular function of proteins.

RHOA localizes mainly in the cytosol and is translocated to the inner leaflet of the plasmatic membrane when activated¹⁶²⁻¹⁶⁵. However RHOA has been found into the nucleus as well^{166, 167}. Little is known about the role of RHOA into the nucleus. However, this GTPase has been involved in the DNA damage response (DDR) upon genotoxic stress to contribute to the cell cycle arrest. p38 MAPK and the ROCK RHOA effector protein, seem to mediate the cell arrest required for DNA repair, and as consequence cell survival¹⁶⁸.

To investigate differences in the cytoplasmic and nuclear localization of the different RHOA mutants in the study, HEK293T cells were transiently transfected with the vectors expressing GFP-RHOA wt or RHOA mutant forms and analysed using two different experimental approaches: confocal microscopy and flow cytometry.

To determine the amount of RHOA present in the nucleus using the first approach, HEK293T cells transiently transfected with GFP-RHOA wt and mutants were seeded on glass coverslips, fixed, permeabilized and stained with DAPI (blue) and Rhodamine-phalloidin (red) for nuclei and F-actin visualization, respectively. Confocal images were taken and co-localization of GFP-RHOA and DAPI was calculated. The ImageJ plugin JACoP was used to calculate the Mander's Overlap Coefficient. This coefficient is based on the Pearson's correlation of the fraction of co-localizing objects in each component of a confocal dual-colour images¹⁶⁹. Results vary from 0 to 1, being 0 non-overlapping images and 1, 100% co-localization between the channels tested.

Confocal observation of HEK293T transfected with GFP-RHOA wt and some GFP-RHOA mutant vectors, such as G17E, evidenced clear differences in the proportion of nuclear RHOA protein (**Figure 22 A**). Mander's coefficient for the different RHOA forms confirmed the visual observation, since a higher proportion of nuclear RHOA protein was obtained for GFP-RHOA G17 mutants compared to GFP-RHOA wt (**Figure 22 B**). Flow cytometry-assisted analysis further supported these results. Nuclei from HEK293T expressing GFP-RHOA wt/mutants were isolated, and GFP mean fluorescence intensity was analyzed separately and compared to whole cell GFP intensity (**Figure 22 C**). Results from this approach confirmed the predominant localization of RHOA G17 mutants into the cell nucleus. Furthermore, the expression of the constitutive-active form RHOA G14V revealed a significant increase in nuclear localization by the cytometry analysis, suggesting that activation of RHOA could foster nuclear

translocation. Pearson's correlation analysis revealed a strong association between the results obtained from both, confocal microscopy and flow cytometry (**Figure 22 D**; Pearson's $r = 0.41$ and $P = 0.02$).

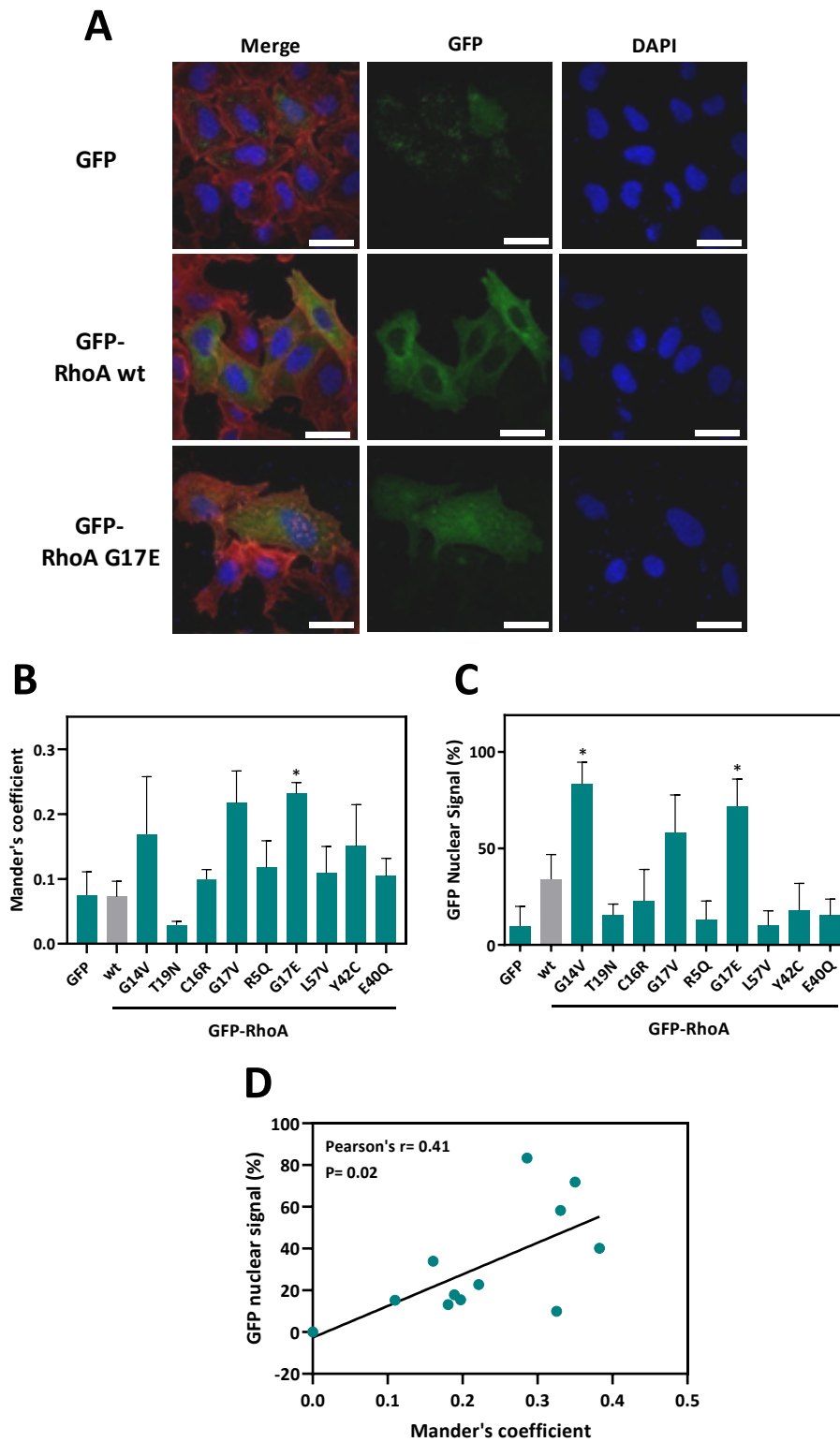


Figure 22. RHOA wt and mutants' nuclear localization in HEK293T cells. Cells were transiently transfected with GFP-RHOA wt or mutant forms and cultured in the presence of 1 $\mu\text{g}/\text{mL}$ of Dox for forty-eight hours. Cells seeded on glass coverslips were stained for F-actin (Phalloidin, red) and nuclei (DAPI, blue) and three representative confocal images of different fields were taken after staining for each GFP-RHOA form. Representative confocal images of HEK293T cells expressing GFP-RHOA wt and G17E forms are shown **(A)**. The average Manders' overlap coefficient was determined for green (GFP) and blue (DAPI) co-localization using ImageJ JaCoP plugin **(B)**. Alternatively, mean fluorescence intensity of whole cell and isolated nuclei were analysed through cytometry analysis. The percentage of GFP nuclear signal is represented **(C)**. The average of three independent experiments (\pm SEM) is shown **(B-C)**. Correlation of GFP nuclear signal in B and C **(D)**. *Student's t-test $p < 0.05$; comparing each condition to GFP-RHOA wt. Scale bars: 50 μm .

These results clearly demonstrate that some RHOA mutants display enhanced nuclear localization. This could provide novel insights in the deregulation of cellular functions key for the carcinogenic process in which RHOA actively participates, and more importantly, explain the selection of certain hotspot RHOA mutations in specific tumor types. Nevertheless, additional experiments and analysis are needed to fully elucidate the role of RHOA and the mutant forms into the nucleus.

3. Cytoskeleton regulation of RHOA hotspot mutants

During the oncogenic process, tumour cells undergo a series of changes associated with cytoskeletal rearrangements, as well as alterations in cell-cell and cell-matrix adhesion, allowing cells to detach from the bulk tumour, invade into the surrounding tissues and, ultimately, metastasize to distant organs¹⁷⁰.

Cytoskeleton organization is one of the best-known functions of the Rho family of small GTPases. Different Rho members are involved in the formation of different cytoskeletal structures. For instance, Cdc42 activation is required for cytoskeletal changes associated to filopodia formation in fibroblasts, whereas the activation of Rac is needed for lamellipodia formation and membrane ruffling; and the activation of RHOA is essential for the formation of stress fibers and focal adhesions¹⁷¹⁻¹⁷³. Specifically, RHOA orchestrates the formation of F-actin filaments leading to changes in cell morphology and adhesion through binding to ROCK and mDIA effector proteins¹⁷⁴.

To study the assembly of F-actin, COS1 cells were transiently transfected with the constructs encoding GFP-RHOA wt/mutants, exposed to doxycycline for protein expression and stained with phalloidin to visualize F-actin filaments. As reported previously¹³⁶, overexpression of RHOA wt and the constitutive-active form RHOA G14V increased F-actin formation within cells **(Figure 23 A-B)**. Conversely, RHOA T19N, the dominant-negative form of the GTPase impaired F-actin formation **(Figure 23 B)**. Interestingly, all the additional RHOA forms tested but C16R showed a significant downregulation in the F-actin formation.

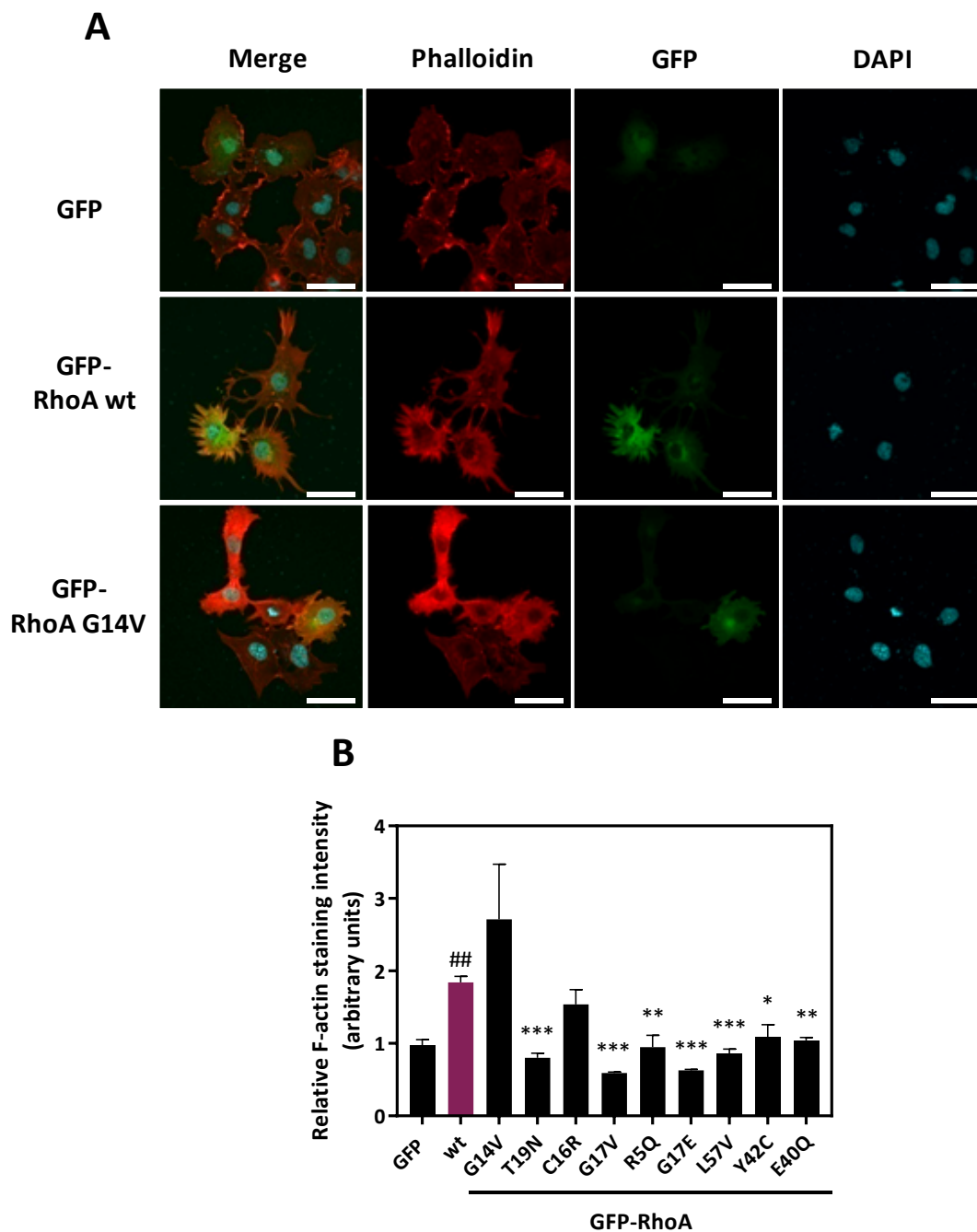


Figure 23 RHOA hotspot mutants downregulate F-actin formation in COS1 cells. Cells were transiently transfected with GFP-RHOA wt or the indicated RHOA mutant forms and cultured in the presence of 1 $\mu\text{g}/\text{mL}$ of Dox for forty-eight hours. Cells seeded on glass coverslips were fixed and stained with Rhodamine-phalloidin to monitor F-actin formation and DAPI to visualize nuclei. Representative confocal images of COS1 cells expressing GFP-RHOA wt, GFP-RHOA G14V and control GFP are shown (A). Quantitation of F-actin formation of GFP expressing cells determining phalloidin intensity in individual cells with ImageJ (20 GFP⁺ cells per condition and experimental replicate) (B). The average of three independent experiments (\pm SEM) is shown. *Student's t-test $p < 0.05$, ** $p < 0.01$, *** $p < 0.001$; comparing each condition to RHOA wt. ## Student's t-test $p < 0.01$, when compared GFP-RHOA wt with GFP. Scale bars: 50 μm .

Cell adhesion to the extracellular matrix strongly influences cellular morphology and migration, among others cell functions^{175, 176}. We wondered if the differences in the F-actin assembly exhibited by some of the RHOA mutants studied (**Figure 22**) led to changes in cell adhesion. Indeed, both the morphology and adhesion of HEK293T was noted different depending on the GFP-RHOA form used for overexpression when cells were visual inspected through a microscope. While RHOA wt and the constitutive-active RHOA G14V form promoted cell roundness compared with parental cells, moderate cell detachment from cell culture plates and lower cell confluence was observed in most mutants, as RHOA G17V, maintained the HEK293T fibroblastic-like morphology and displaying higher cell confluence (**Figure 24 A**).

Most cellular adhesion assays measure the relative ability of adherent cells to remain attached to the surface after a specific time of incubation and washing of non-adherent cells. But this kind of assay lacks sensitivity and reproducibility. This limitation can be solved using specific and well-calibrated detachment forces, such as centrifugation¹⁷⁷.

For this assay, transiently transfected HEK293T cells with expressing GFP-RHOA wt or RHOA mutants and Dox induction for 48 hours were used. The number of cells for each RHOA form that remained attached to the plate after 48 hours of ectopic RHOA expression induction is shown as reference of attachment capability. Obtained results demonstrated a significant increase of most of RHOA mutants' adhesion capability, except for C16R and L57V forms when compared with RHOA wt (**Figure 24 B**). Then, to preserve the adhesion proteins present in the membrane of the cells already expressing RHOA wt/mutants, accutase was used instead of trypsin for the detachment of the cells. This enzymatic mixture is considered less damaging and performs exceptionally well in detaching cells while maintaining intact most cell surface proteins. The same number of cells was plated for each RHOA protein and, upon 15 minutes in culture to allow cell attachment, cells were subjected to a centrifugal detachment force. Results were obtained after fixing and staining with crystal violet the cells that remained attached (**Figure 24 C**). Interestingly, the constitutive-active RHOA G14V form showed a significant reduction in the adhesion capability to the substrate, whereas most of the mutants exhibited the opposite effect, higher attachment ability (**Figure 24 C**).

Cytoskeletal arrangement alterations are important traits for tumor progression, as are directly related with migration and invasion promotion. Therefore, the differences observed in F-actin formation and adhesion, provide remarkable information about the involvement of specific RHOA mutants in the tumor aggressiveness process.

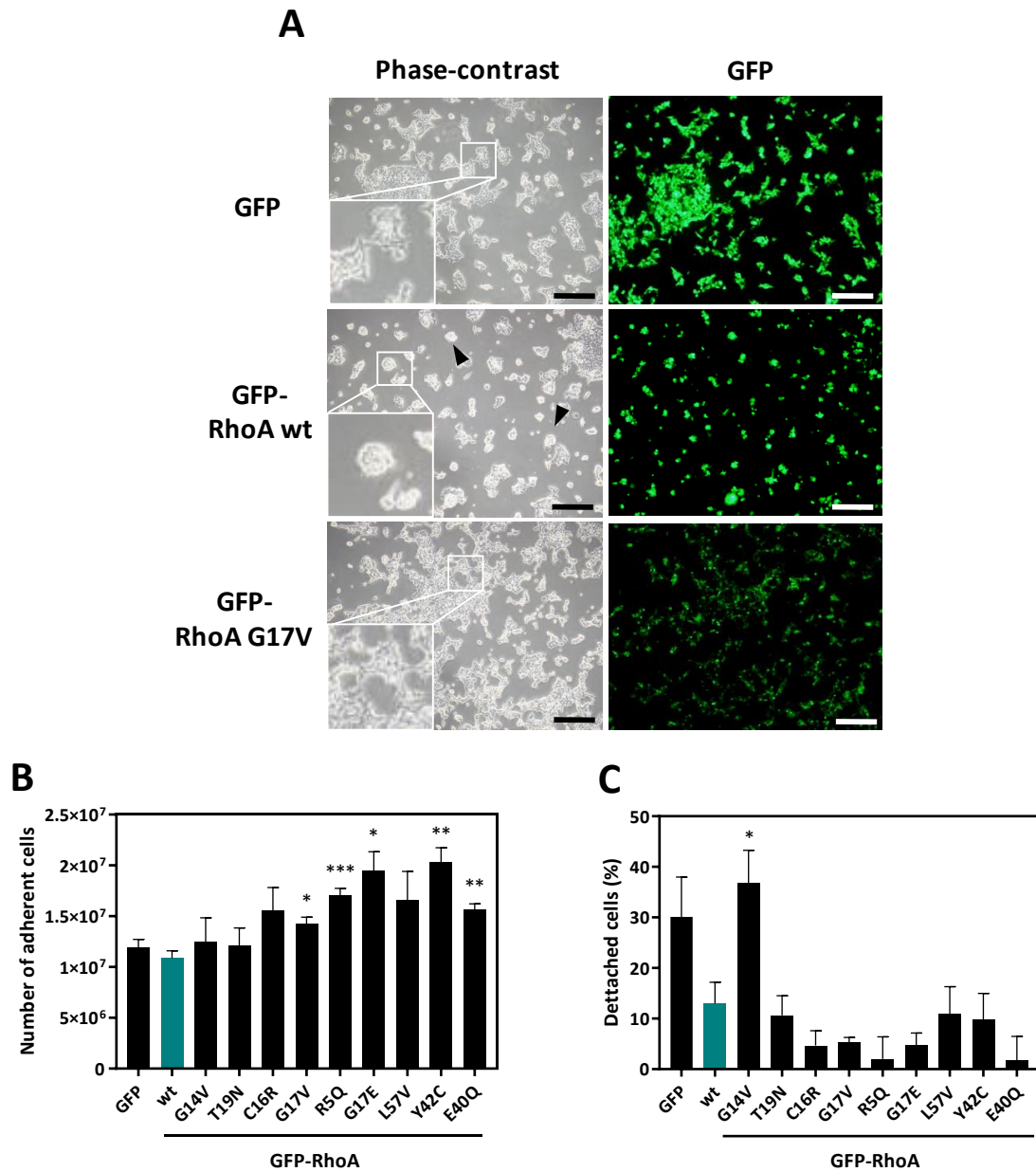


Figure 24. HEK293T cell morphology and adhesion upon expression of GFP-RHOA wt and GFP-RHOA mutants. HEK293T cells were transiently transfected with vectors expressing GFP-RHOA wt or RHOA mutants. Upon forty-eight hours of induction with 1 $\mu\text{g}/\text{mL}$ of Dox, cells were imaged with an inverted microscope (**A**, left: phase contrast, right: fluorescence) and were counted as reference of cell attachment (**B**, number of cells). Then, cells were subjected to adhesion assay through a centrifugation approach¹⁷⁷. Percentage of detached cells after analysis of adhesion assay (15 min cell adhesion, 100 g centrifugation for 5 min) is shown (**C**). Data are mean \pm SEM of three independent experiments. *Student's t-test $p < 0.05$, ** $p < 0.01$, *** $p < 0.001$; comparing each condition *versus* RHOA wt. Scale bars: 200 μm . Arrow heads indicate roundness morphology (non-adherent phenotype).

4. Transcriptional regulation of SRF and NFκB by RHOA hotspot mutants

Among the wide variety of the cell functions regulated by small GTPases, transcriptional activity is of great importance. There are several transcription factors whose activity is regulated by RHOA, for example serum response factor (SRF) and nuclear factor kappa-light-chain-enhancer of activated B cells (NFκB).

Serum response factor (SRF) is involved in the transduction of mechanical signals from the cytoplasmic actin and the extracellular environment to the cell nucleus. Several studies have shown a correlation between elevated levels of SRF and human cancer¹⁷⁸⁻¹⁸¹. SRF activity is controlled through its association with two families of regulatory cofactors. The first is the ternary complex factor (TCF) family of Ets proteins (SAP-1, Elk-1 and Net), which are controlled by phosphorylation of their C-terminal activation domains by MAP kinases. And the second are the members of the myocardin related transcription (MRTF) family (MRTF-A/MAL/MKL1, MRTF-B/MKL2 and myocardin) which are regulated through Rho GTPase signalling. MRTFs when bound to globular actin (G-actin) remain inactive in the cytoplasm. Rho GTPases promote the incorporation of G-actin into fibrous actin (F-actin), leading to free MRTFs, which can then shuttle into the nucleus to bind and activate SRF^{26, 182}.

In turn, the NFκB pathway is a conserved signalling cascade extensively implicated in cancer development and progression. NFκB control the expression of genes mediating tumour cell proliferation, survival and angiogenesis, such as TNFA, IL6 and BCL2¹⁸³. RHOA participates in regulating the ubiquitylation and degradation of phosphorylated IκB, facilitating NFκB translocation and engagement of transcriptional programs.

Considering the role of RHOA in the signalling of SRF and NFκB transcription factors, the capability of the different RHOA mutants to activate both transcription factors was investigated.

RHOA-dependent SRF and NFκB transcriptional activity was measured co-transfecting GFP-RHOA expressing vectors with a reporter assay containing serum or NFκB response elements binding sites upstream of a firefly luciferase reporter gene. A wild-type *Renilla* luciferase control reporter vector was used for transfection efficiency normalization.

As expected, overexpression of wt and constitutive active GFP-RHOA G14V increased the activity of both, SRF and NFκB reporter systems¹³⁶ (**Figure 25 A-B**). SRF luciferase relative levels of all GFP-RHOA mutants tested, except GFP-RHOA C16R, significantly decreased when compared with GFP-RHOA wt (**Figure 25 A**). Similarly, NFκB

transcriptional activity was decreased when all RHOA mutated forms were expressed (**Figure 25 B**).

Importantly, a significant correlation was observed between F-actin formation and SRF activity (Pearson's $r=0.92$ and $p<0.0001$, **Figure 25 C**), further confirming the downregulation of the RHOA-actin-SRF pathway upon RHOA mutation in the hotspots tested.

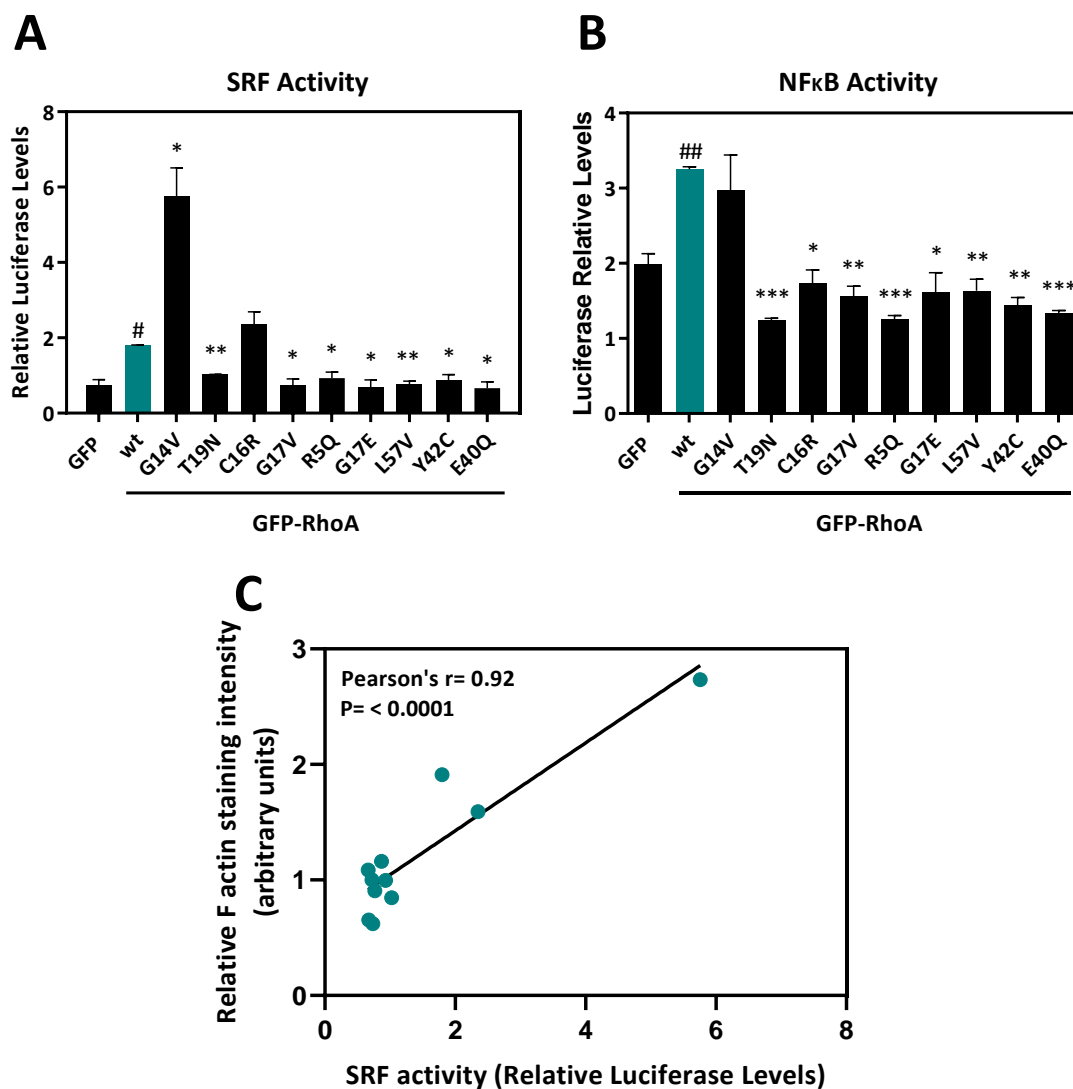


Figure 25. Effects of GFP-RHOA mutants on SRF and NFκB transcriptional activity. HEK293T cells were seeded in 96-well plates and transiently co-transfected with GFP-RHOA expressing vectors and a luciferase expression vector driven by a SRF responsive element (pGL4.34[luc2P/SRF-RE/Hygro) (**A**), or NFκB (2xNFκB-LUC) (**B**) that drive the transcription of a firefly luciferase reporter gene. A vector constitutively expressing Renilla (pRL-SV40) was used for transfection efficiency normalization. Luciferase and Renilla activity were measured forty-eight hours after transfection and induction of GFP-RHOA with 1μg/mL Dox. The average fold differences in luciferase activity of three independent experiments run in quintuplicate are shown (±SEM). *Student's t-test $p<0.05$, ** $p<0.01$, *** $p<0.001$; comparing each condition *versus* RHOA wt. # Student's t-test $p<0.05$, ## $p<0.01$ when compared GFP-RHOA wt with GFP. F-actin staining intensity in Figure 7 B, were correlated with SRF activity (**C**).

5. RHOA hotspot mutant interactome

Mutations within a protein can affect its interactome. To study the impact of the hotspot *RHOA* mutations in the binding capability to known RHOA effectors, a Rhotekin pull-down and a yeast two-hybrid assays were performed.

Rhotekin binding capacity of RHOA hotspot mutants

RHOA GTPase acts as a molecular switch cycling between an active GTP-bound, and an inactive GDP-bound state. In the GTP-bound state, RHOA interacts with effector or target molecules to initiate downstream responses. The return of the proteins to the GDP-bound state completes the cycle and terminates signal transduction²⁶.

As depicted in **Figure 12**, *RHOA* mutations under study are distributed in a hotspot pattern along the coding the sequence, and some of them occur in the GDP/GTP binding region or close to it, whereas others are allocated in the effector binding domains. Hence, we hypothesized that certain mutations could impact on the GTP binding and subsequently RHOA activation and others to the effector binding domain, affecting to the downstream signaling.

Rhotekin pull-down assay is a common approach used in research to determine the proportion of GTP-bound GTPase, and consequently, its activity. Since we do not know to what extent *RHOA* hotspot mutations could be affecting GDP/GTP or effector binding domains, we used this assay to study the Rhotekin binding capacity. This pull down uses as bait the Rho binding domain (RBD) of the Rho effector protein Rhotekin, which recognizes the GTP-bound active form of RHOA, but not the inactive (GDP-bound form). Protein lysates from HEK293T cells transiently transfected with GFP-*RHOA* wt and the different RHOA mutants were subjected to Western blot analysis after pulling-down active RHOA with Rhotekin-RBD beads (**Figure 26 A**). The band intensity was quantified with ImageJ and used to calculate the active RHOA levels normalised to vinculin control protein (**Figure 26 B**). The assay revealed no differences in the Rhotekin-bound levels between the different RHOA forms studied, except for G17E and G17V mutants. However, this result must be interpreted with caution since the lower activity may be due to the reduced expression of these mutants. Unexpectedly, the constitutive-active RHOA G14V form was not found to be more active than RHOA wt. The dominant-negative RHOA T19N mutant showed a significant reduction in its Rhotekin binding ability.

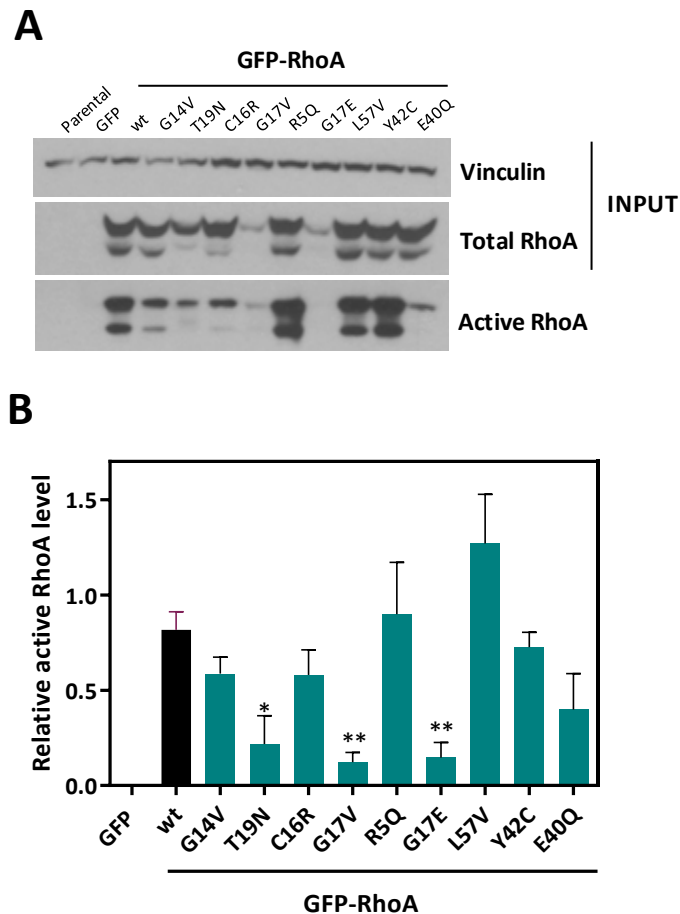


Figure 26. Rhotekin binding of RHOA wt and mutants in HEK293T. Cells were transiently transfected with GFP-RHOA wt or mutant forms, cultured in the presence of 1 $\mu\text{g}/\text{mL}$ of Dox for forty-eight hours. Cell lysates were obtained and subjected to pull-down with RBD Rhotekin beads and analysed by Western blot (**A**). Active RHOA levels in the Western blot were quantified, normalised both to vinculin control protein and RHOA wt (**B**). The average of three independent experiments (\pm SEM) is shown. *Student's t-test $p < 0.05$, ** $p < 0.01$; comparing each condition to GFP-RHOA wt.

Yeast two-hybrid screening of effectors binding to wild type and DGC and HNSCC hotspot RHOA mutants

This approach is a powerful method to identify and map direct protein-protein interactions¹⁸⁴. The principle is based on the reconstitution of the activity of Gal4 transcription factor to enable the proliferation of yeast under amino acid restrictive growth conditions and the expression of reporter genes. To this aim, fusion proteins ('hybrids') are constructed. Specifically, one protein of interest is fused to the Gal4 DNA Binding Domain (BD), and the other to the Gal4 activation Domain (AD). The protein fused to the BD is referred to as the 'bait', and the protein fused to the AD as the 'prey'. Yeast cells are co-transfected with hybrids and plated in amino acid deprived growth mediums. Yeasts incorporating bait and prey hybrids grow in leucine (*LEU*) and tryptophan (*TRP*) deficient substrates, respectively. If bait and prey interact, Gal4 BD and AD are brought together within the cell nucleus and lead the expression of

additional autotrophic factors such as histidine (*HIS*) allowing further selection and growth of the yeast transformants. Contrary, in the absence of interaction between the bait and the prey proteins, Gal4 BD and AD stay apart and the *HIS* autotrophic reporter gene is not expressed and, therefore yeast are unable to grow in HIS-deficient medium. The strength of the interaction between bait and prey proteins can be determined if 3-amino-1,2,4-triazole (3-AT) is incorporated to the solid substrates. 3-AT is a competitive inhibitor of the product of the *HIS* reporter gene. The stronger the interaction between the bait and the prey proteins, the higher the ability of yeast to grow in the presence of 3-AT (**Figure 15**).

For the generation of bait proteins (RHOA mutants), first G14V and I90S mutations were introduced in the coding sequence of RHOA. These mutations allow RHOA protein to be active and impair membrane-anchorage and facilitate nuclear shuttling of the bait proteins, respectively¹³⁶. The RHOA bait protein carrying these two mutations (G14V and I90S) is hereafter referred to as RHOA wt. Next, R5Q, G17E, L57V, Y42C or E40Q mutations were individually introduced into *RHOA* sequence. Prey constructs encoded for the best-characterized RHOA binding, effector and regulatory proteins, *i.e.* ROCK, DIAPH/mDIA, PKN1, Kinectin and NET1. Yeast cells were co-transfected with RHOA and RHOA-interacting proteins and plated onto growth mediums deprived of leucine, tryptophan and histidine, and containing increasing concentrations of 3-AT (0mM, 1mM and 5mM). The presence/absence of interactions and their strength was scored as follows: '+++′ when robust growth was observed with 0mM, 1mM and 5mM of 3-AT; '++′ when robust growth was observed with 0mM and 1mM of 3-AT; '+′ when robust growth was observed only in the absence of 3-AT; and '-′ when no growth was observed, regardless of 3-AT (**Figure 27**).

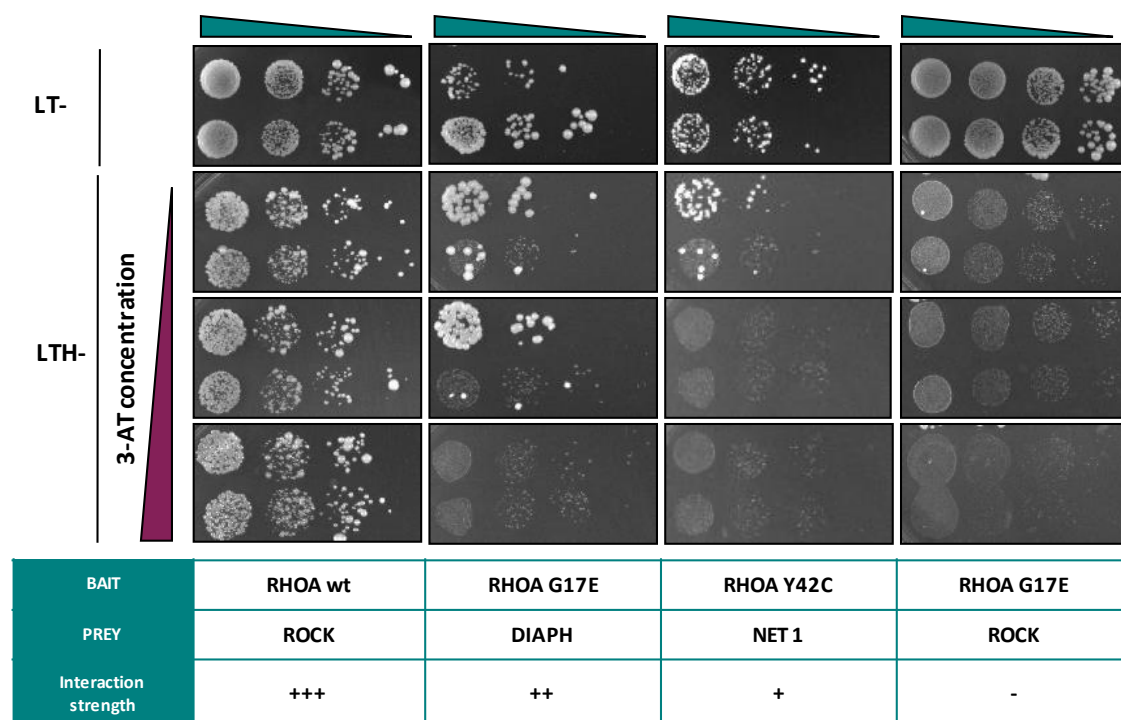


Figure 27. Yeast-Two-Hybrid assay for testing protein-protein interactions between *RHOA* wild type and *RHOA* mutants to different binders. A yeast two-hybrid system was performed to evaluate the interaction of the most frequent *RHOA* mutations in DGC and HNSCC to the well-known *RHOA* binders PKN1, ROCK, DIAPH2, NET1 and Kinectin. After co-transfection of yeast with bait and prey expressing vectors, cells were plated onto primary selection Synthetic Defined (SD) media lacking amino acids Leu and Trp (LT-). Upon growth, two independent colonies were dissolved in sterile water and then diluted from 1 to 10^{-3} (green triangle, from the left to the right), and seeded onto primary selection Synthetic Defined (SD) media lacking amino acids Leu, Trp, His (LTH-). To measure the strength of the interactions, three different 3-amino-1,2,4-triazole (3-AT) concentrations were added to the growth plates (purple triangle; 0, 1 and 5 mM, from the top to the bottom, respectively). Interactions were classified as follows: +++ Robust growth in 0mM, 1mM and 5mM 3-AT; ++ Robust growth in 0mM and 1mM 3-AT; + Robust growth only in the absence of 3-AT; - No growth with or without 3-AT. Representative images for the co-transfection and growth of *RHOA* wt-ROCK (+++), *RHOA* G17E-DIAPH (++) , *RHOA* Y42C-NET1(+) and *RHOA* G17E-PKN1 (-) are shown.

As expected, *RHOA* strongly interacted with all the selected binding molecules (**Table 4**). Among the diffuse gastric cancer *RHOA* hotspot mutants, *RHOA* R5Q retained the ability to interact with all the binding proteins tested. Contrary, *RHOA* G17E was least able to bind the interacting proteins tested, as no binding was detected with ROCK, PKN1 and Kinectin. *RHOA* L57V and Y42C mutations only abrogated the interaction with PKN1 (**Table 4**).

Interestingly, the *RHOA* E40Q hotspot mutation found in head and neck cancer, unlike the diffuse gastric cancer *RHOA* hotspot mutants, retained a moderate PKN1 interaction. Moreover, ROCK and DIAPH interactions were unaffected. Also, contrary to the DGC mutants, *RHOA* E40Q lost its binding capacity to the GEF protein NET1, and Kinectin effector protein (**Table 4**).

Collectively, these results demonstrate that different *RHOA* mutations affect differentially to the binding of RHOA to key effectors and/or regulators of the GTPase activity. Further assays and analysis should be performed to investigate the biological effect of these mutations in the loss of interaction with specific effectors.

Table 4. Interaction of *RHOA* mutants with canonical binders in the yeast two hybrid assay.

Bait Prey	DGC					HNSCC
	RHOA WT	RHOA R5Q	RHOA G17E	RHOA L57V	RHOA Y42C	RHOA E40Q
ROCK	+++	+++	-	+++	+++	+++
DIAPH	+++	+++	++	+++	+++	+++
PKN1	++	++	-	-	-	++
Kinectin	+++	+++	-	+++	+++	-
NET1	++	++	++	++	+	-

+++ : Robust growth at 0mM, 1mM and 5mM 3-amino-1,2,4-triazole (3-AT), a competitive inhibitor of the product of the *HIS3* gene. ++ : Robust growth at 0mM and 1mM 3-AT. + Robust growth only in the absence of 3-AT. - : No growth, with or without 3-AT.

Chapter II

RHOA in head & neck cancer

ABSTRACT

Head & neck cancer squamous cell carcinoma (HNSCC) is the seventh most common type of cancer. It comprises a heterogeneous collection of malignancies of the upper aerodigestive tract, salivary glands and thyroid. Approximately 950,000 cases arise every year worldwide, but only 40–50% of patients with HNSCC survive after 5 years of the diagnosis. Tobacco consumption, alcohol consumption and HPV infection are the main risk factors involved in the development of HNSCC. Despite targeted drugs have been approved for the treatment of HNSCC patients, the survival has not markedly improved because patients frequently recur. The limited information available on the molecular carcinogenesis of HNSCC, and the genetic and biological heterogeneity of the disease has hindered the development of new and more effective therapies.

RHOA is one of the most extensively investigated member of the Rho GTPase family. It has long been involved in the malignant transformation of cells, as well as in tumor invasion and metastasis. The use of highthrough put sequencing platforms have revealed frequent *RHOA* mutations distributed as hotspots in a wide variety of human cancers, including angio-immunoblastic T-cell lymphoma, adult T-cell leukemia/lymphoma, diffuse-type gastric cancer and HNSCC, among others. Only around of 1.5% of HNSCC patients display *RHOA* mutations, but surprisingly, when present more than 60% of the cases occur in codon E40Q. Therefore, the selection of this specific mutation in HNSCC tumors predicts a key role in the tumorigenic process. In order to study the impact of RHOA E40Q in HNSCC, first we studied and characterized the role of RHOA wild-type (wt) in this particular tumor type. Using tissue microarray data of paired tumor and normal surrounding tissue, we observed that RHOA expression is reduced in tumors compared to normal epithelial cells. Moreover, our data using tissue microarrays for big cohorts of HNSCC samples derived from different anatomical regions (oral cavity, oropharynx and larynx) indicates that RHOA protein expression is not associated globally with the survival outcomes of the disease. However, RHOA expression is associated with shorter overall survival in patients with tumors allocated specifically in the larynx. This association was further validated using data from the The Cancer Genome Atlas (TCGA).

To study the possible role of RHOA in HNSCC cancer, we engineered isogenic cell line systems with doxycycline-inducible RHOA overexpression, and constitutive downregulation with shRNAs against RHOA (shRHOA). Surprisingly, although the downregulation significantly impaired cell growth and colony formation ability in cells derived from tongue tumors, the same phenotype was observed upon RHOA was overexpressed. Strikingly, doxycycline-inducible overexpression of RHOA in the RHOA knock-down (shRHOA) cells exhibited equivalent results.

In larynx-derived tumor cells, we were able to show for the first time that RHOA depletion by CRISPR/Cas9 (RHOA knock-out, KO) impairs cell growth, colony formation and migration. Reintroduction of RHOA wt or RHOA E40Q expression in these cell line systems did not modify the tumorigenic behavior of cells.

Collectively, our results indicate that RHOA provides a significant growth advantage to HNSCC cancer cells, indicating a possible oncogenic role of RHOA in this tumor type. However, the controversial and unexpected results obtained when RHOA was exogenously expressed will need further analysis.

Chapter I

RHOA in head & neck cancer

INTRODUCTION

INTRODUCTION

Head and neck squamous cell carcinoma (HNSCC) is the most common malignancy developed in the head and neck region. It emerges principally from the mucosal epithelium of the upper aerodigestive tract, *i.e.*, oral cavity, nasopharynx, oropharynx, hypopharynx, larynx, paranasal sinuses and salivary glands (**Figure 28**). Among all, cancer in the oral cavity and oropharynx are the most prevalent. From the histological point of view, squamous cell carcinoma is the most common tumor type and accounts for approximately 90% of all malignancies¹⁸⁵. Despite most cancers originate in the squamous cells that line the mucosal surfaces of the head and neck, the disease is highly heterogeneous. Heterogeneity accounts for anatomical location, aetiology and molecular features driving HNSCC tumorigenesis.

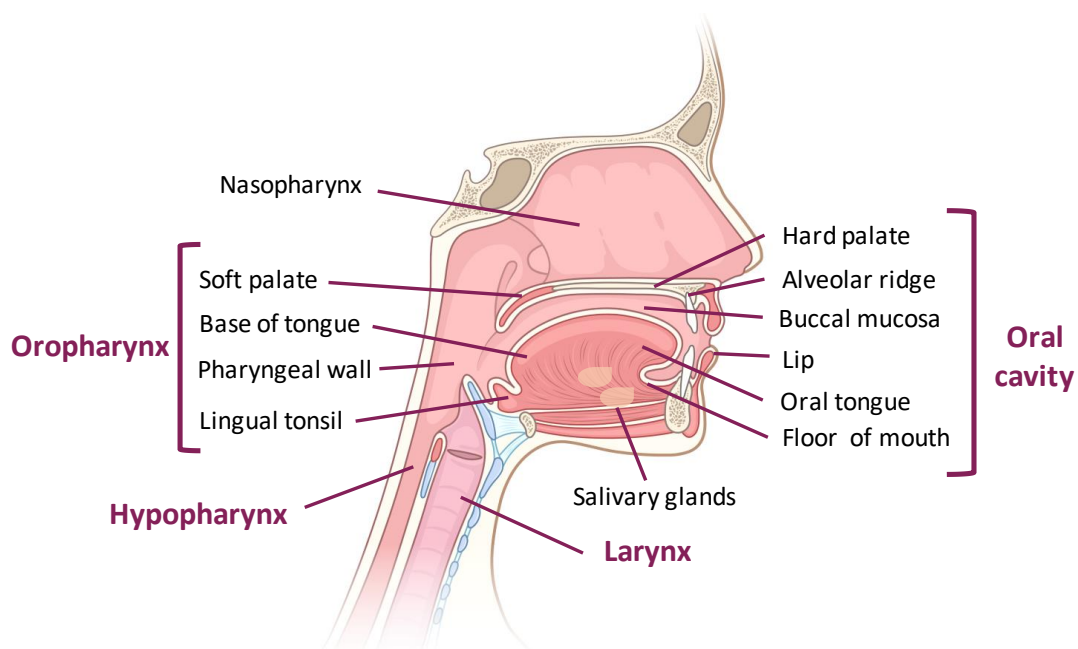


Figure 28. Anatomical sites of HNSCC development. Head and neck squamous cell carcinoma (HNSCC) emerges from the mucosal epithelium of the oral cavity (lips, buccal mucosa, hard palate, alveolar ridge, oral tongue and floor of mouth), nasopharynx, oropharynx (tonsils, base of tongue, soft palate and posterior pharyngeal wall), hypopharynx and larynx. Created with BioRender.

1. Epidemiology

HNSCC represents the sixth most common cancer worldwide, with 931,931 estimated new cases and 467,125 estimated deaths only in 2020 (GLOBOCAN)¹⁸⁶. Risk factors associated to the development of HNSCC include age, tobacco consumption, alcohol consumption, environmental pollution and infection with the human papillomavirus

(HPV) and Epstein-Barr virus (EBV) viral agents. The relative prevalence of these risk factors explains the geographical distribution of HNSCC (**Figure 29**). Tobacco and alcohol consumptions are the highest risk factors and are distributed globally at the geographical level. Contrary, other extremely prevalent risk factors are highly restricted to certain geographical regions. This is the case of India, in which oral cavity malignancies represents the first most common cancer in men and the fourth in women, and is directly associated with the consumption of areca nut, the seed of the areca palm (*Areca catechu*). Gender is also associated with the development of HNSCC. Men are at 2-4-fold higher risk than women of developing HNSCC. This difference is in turn strongly influenced by sex differences in risk-taking behaviours.

Risk factors also determine the anatomical site where primary tumors develop. For instance, HPV-associated HNSCCs arise primarily in the palatine and lingual tonsils of the oropharynx; while tobacco-associated HNSCCs arise primarily in the oral cavity, hypopharynx and larynx.

It is well accepted to classify oropharyngeal HNSCCs into HPV-negative (HPV-ve) and HPV-positive (HPV+ve), as tumors between these two subgroups are clearly different regarding prognosis and socioeconomic and molecular profiles ¹⁸⁷. (HPV)-associated oropharyngeal cancer cases are caused predominantly by HPV type 16. These cases are worryingly increasing among younger people, particularly in the Western world ¹⁸⁸. Generally, the prognosis for HPV+ve patients is more favorable because of the higher fitness and the higher response rate to treatment of patients compared to HPV-ve patients, who are often physically compromised by chronic tobacco and alcohol consumption ¹⁸⁹.

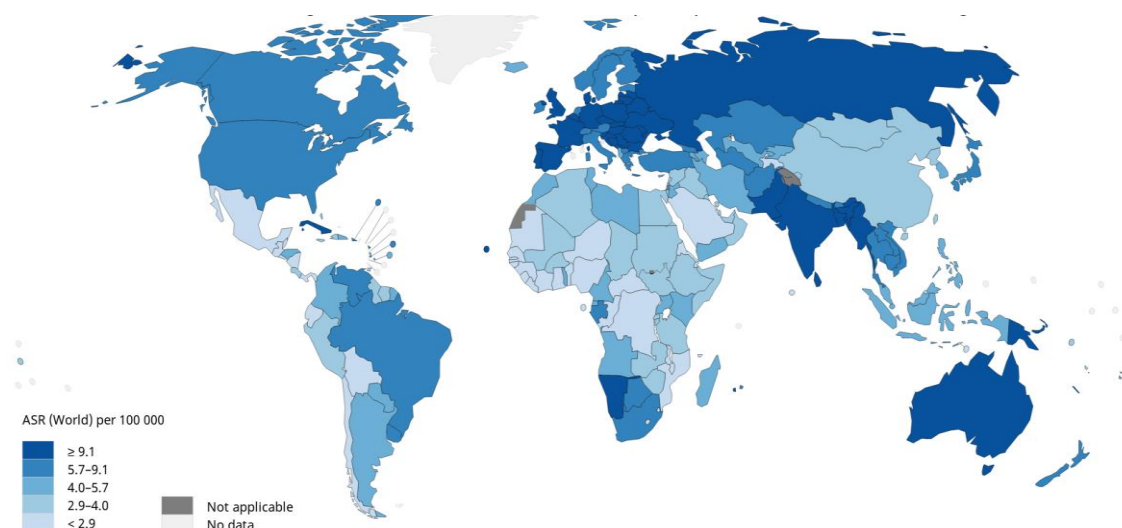


Figure 29. Worldwide age-standardized incidence of HNSCC in 2020. Estimated age-standardized incidence rates (ASR) worldwide are shown. Data from GLOBOCAN, 2020 ¹⁸⁶. Map was generated using the GLOBOCAN website mapping tool, by grouping 'lip, oral cavity', 'nasopharynx', 'oropharynx', 'hypopharynx' and 'larynx' cancer cases.

2. Histopathology

The head and neck lining epithelium is stratified in a multilayer fashion in which the topmost layer is made up of flattened and scale-like epithelial cells, and the deeper layer display cuboidal or columnar cells (**Figure 30**). Typically, three layers of cells with different differentiation status are distinguished: a single basal layer containing stem cells, 2-3 layers of proliferative and intermediate basaloid cells, and a layer towards the surface heavily keratinized. The thickness and keratinization degree of the outer layer highly depends on the exposure to mastication forces.

The epithelium is delimited by a lamina propria that regulates the differentiation and migration of epithelial cells, and at the same time acts as a barrier to stromal invasion in the tumorigenic process. Interestingly, the tonsil epithelium is highly specialized and formed by a reticulated squamous epithelium that is interrupted by non-epithelial cells, including lymphocytes and antigen-presenting cells that constitute the first line of defense against external insults. The loss of structural integrity of this tissue, due to an incomplete basal cell layer and porous basement membrane, causes the exposure of the basement membrane to viral particles. This fact explains why oropharynx tumors are highly associated with HPV infection¹⁹⁰.

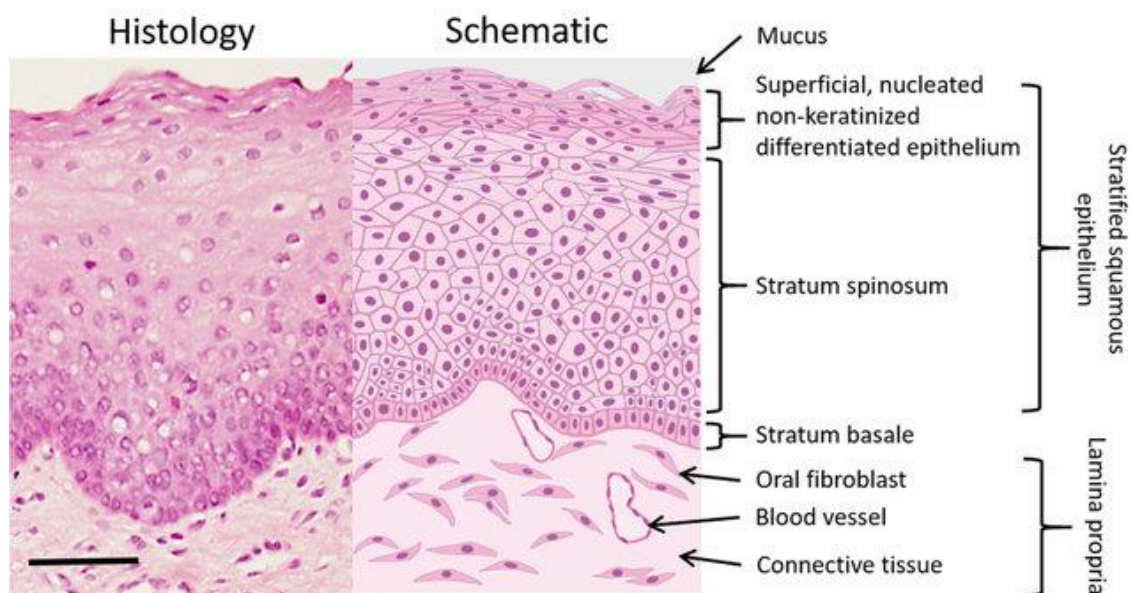


Figure 30. Histology of the buccal oral mucosa. Histological (left) and schematic (right) images of the buccal oral mucosa. Scale bar= 100 μm ¹⁹¹.

In the carcinogenic process, before cancer cells accumulate in tissues, the cells undergo a series of abnormal changes called dysplasia. In head & neck cancer, squamous dysplasia refers to the abnormal cellular organization, nuclear enlargement, pleiomorphism and increased mitotic activity in the epithelium, but in the absence of invasion of the subepithelial connective tissue. These alterations are graded according to the severity of the atypia, which corresponds to the extension of affected

epithelium: mild atypia, moderate atypia and dysplasia/carcinoma *in situ*. If tumor progresses, then it breaks the basement membrane and infiltrates the sub-epithelial connective tissue and finally, invades the muscle, bone and facial skin.

Regarding head & neck cancer histopathology, the most common and prototypic HNSCC is the moderately differentiated tumor, histologically characterized by nests of squamous cells with pink cytoplasm, intracellular bridges and keratin pearl formation in a background of stromal fibrosis. Nevertheless, other HNSCC subtypes comprise spindle-cell variant (proliferation of non-cohesive spindle cells; resembles a sarcoma), verrucous carcinoma (exophytic mass with papillary surface and thickened epithelium; no potential to metastasize), papillary variant (exophytic papillary growth), and basaloid variant (basaloid morphology and aggressive behavior) ¹⁹⁰.

Pathogenesis of HNSCC

Most HNSCCs originate from the mucosal epithelial cells that line in the oral cavity, pharynx and larynx. Histologically, the progression towards an invasive HNSCC is a stepwise process that initiates with an epithelial cell hyperplasia, followed by dysplasia, carcinoma *in situ* and, ultimately, an invasive carcinoma. Specific molecular events associate to each of these steps. Of note, HNSCC formation is driven by the inactivation of tumor suppressor genes rather than the activation of oncogenes. Inactivation of *CDKN2A* and *TP53* are essential in the early stages of HNSCC, while *PTEN* loss occurs at later stages (**Figure 31**).

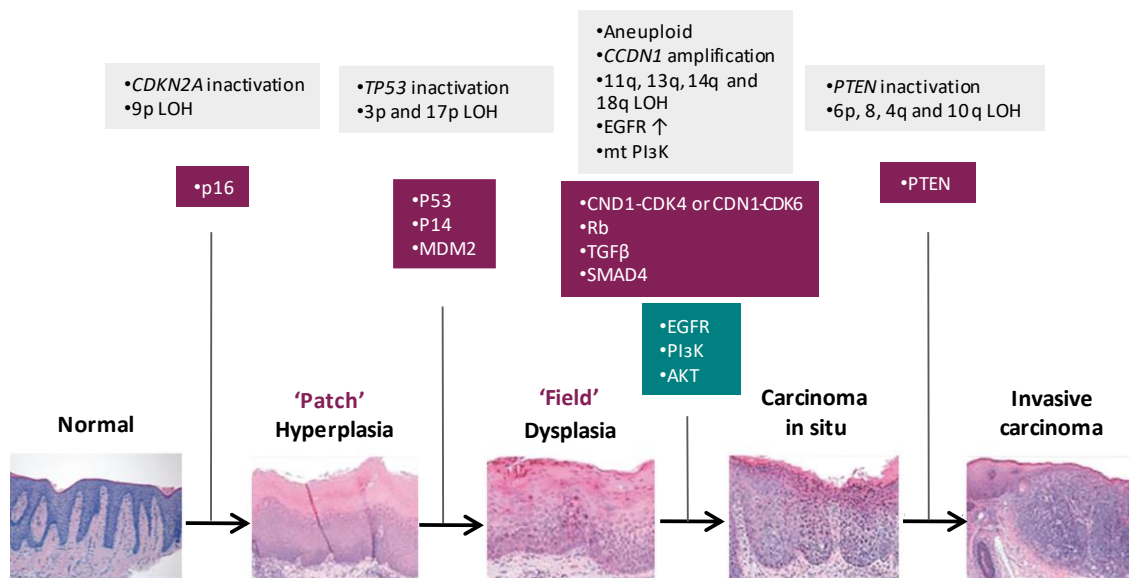


Figure 31 Molecular carcinogenesis in HNSCC. Model of the chronologic genetic events occurring during the HNSCC carcinogenic process. Global alterations are indicated in grey boxes, tumour-suppressive pathways are shown in the red boxes, and oncogenic pathways are depicted in the green box. Histopathology images are reprinted from ¹⁹².

HNSCC lacks a cytological or gross precursor lesion. Oral leukoplakia, a white lesion in the mucosa of the oral cavity, is the most frequent precursor lesion known to date.

However, it shows a very low prevalence (ranging from 0.1% to 0.5%) when considering all HNSCCs^{193, 194}. The presence and number of cancer-associated genetic events in these lesions serves for their classification into low and high-risk leukoplaquias^{193, 195, 196}.

Leukoplaquia precursor lesions are clearly visible by eye, but other changes in the mucosa already predicting malignancy may go unnoticed. There has been a great effort to investigate whether there is a link between dysplastic changes in the mucosa surrounding the tumors, henceforth named as 'field'¹⁹⁷, that remain in the patient after tumor excision, and local recurrence and multiple primary tumors. One of the first changes described in the fields was the loss of heterozygosity at chromosome level. Specifically, 3p, 9p and 17p occur in these dysplastic areas, whereas changes at chromosomes 11q, 4q and 8 are related with carcinomas¹⁹⁸. Relevant tumor suppressor genes and oncogenes are found in specific genetically altered chromosomal regions, including p16 in 9p21, p53 in 17p13, and cyclin D1 in 11q13.

The clonal relationship between the genetic profile of carcinomas and their surrounding fields strongly supports the hypothesis that the fields precede the development of invasive carcinoma. The studies that have tried to elucidate the entity preceding the 'field' have reported p53-positive focal patches in tumor-adjacent areas. Then, a more complete model for HNSCC development is the patch-field-tumor-metastasis model¹⁹⁹.

3. Molecular heterogeneity of HNSCC

More than 90% of head and neck cancers are squamous cell carcinomas. This high percentage could give us the wrong impression of HNSCC as a relatively homogeneous disease when compared to other tumor types. HNSCC is a very heterogeneous cancer that hinders accurate prognosis, treatment and the identification of the key cancer genes involved in the onset and progression of this tumor type.

As described before, HNSCC can be stratified in several histological subtypes. But RNA and DNA profiling studies have evidenced a high diversity and heterogeneity of this disease also at the molecular level.

Several laboratories have addressed the molecular classification of HNSCC. Chung et al. defined up to four different HNSCC subgroups with different clinical outcomes²⁰⁰. Group 1 is characterized by high expression of TGF α , activation of EGFR pathway and association with poor prognosis. Group 2 shows a clear mesenchymal cell signature with high fibroblast expression-based features. Group 3 is defined by tumors with normal tonsil epithelium and positives for cytokeratin 15. And finally, Group 4 contains

tumors showing expression patterns very similar to the ones observed upon exposure to tobacco smoke and exhibiting high transcript levels for antioxidants and detoxification enzymes.

Walter et al. defined also four groups based on gene-expression, namely basal (Group 1), mesenchymal (Group 2), atypical (Group 3) and classical (Group 4)²⁰¹. Although other studies have reported five²⁰² and even six molecular subtypes using metanalysis of gene-expression data-sets in public repositories²⁰³, most studies converge in the existence of four molecular subgroups.

The Atlas Cancer Genome consortium refined the molecular classification of HNSCC using a comprehensive multi-platform analysis including copy number alterations, somatic mutations, gene expression and DNA promoter methylation in a high number of HNSCC tumor samples²⁰⁴. Interestingly, the list of frequently mutated genes in HNSCC is dominated by tumor suppressors, including *TP53*, *CDKN2A*, *FAT1*, *NOTCH1*, *KMT2D*, *NSD1* and *TGFBR2*. *PIK3CA* is the single oncogene recurrently mutated in HNSCC. So, in contrast to many other solid tumors that are frequently driven by mutations in *RAS*, *BRAF*, *EGFR*, *HER2*, β -catenin, among others, HNSCC seems to be driven main by loss of tumor suppressors, for which unfortunately, either no therapies have been developed, or those that exist are ineffective. Results from TCGA evidenced a widespread prevalence of loss-of-function mutations in *TP53* and *CDKN2A* in HPV-ve tumors, and the presence of point mutations in *TRAF3*, *PIK3CA* and *E2F1* in HPV+ve HNSCC tumors.

From the therapeutic point of view, PI3K pathway and cyclin-dependent kinases (CDKs) 4/6 are the most promising actionable targets in HNSCC defined by TCGA (**Figure 32**).

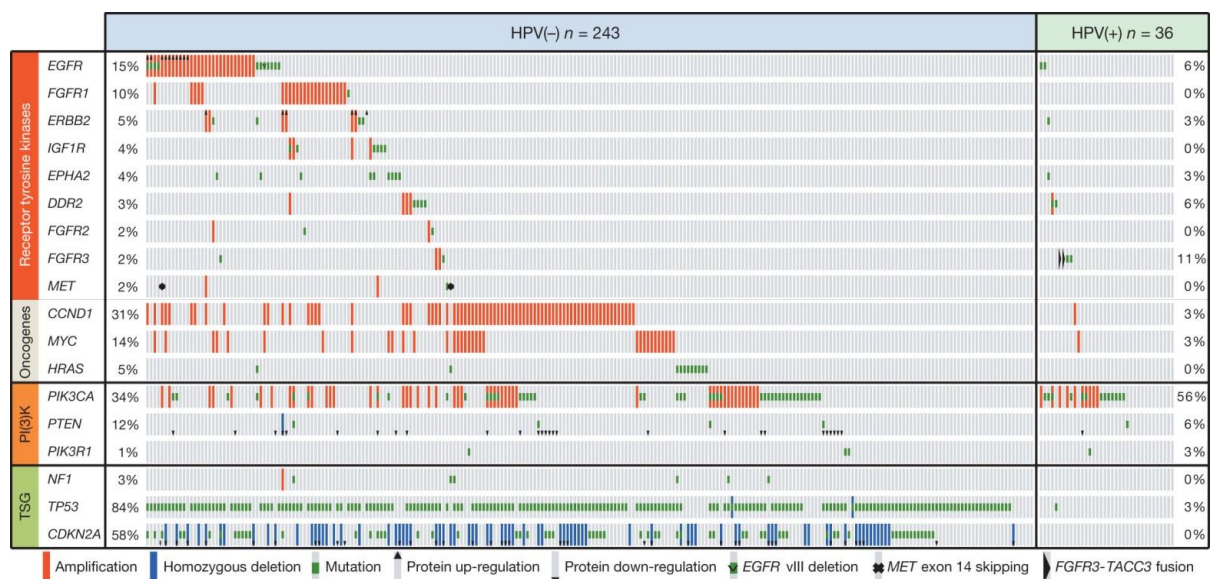
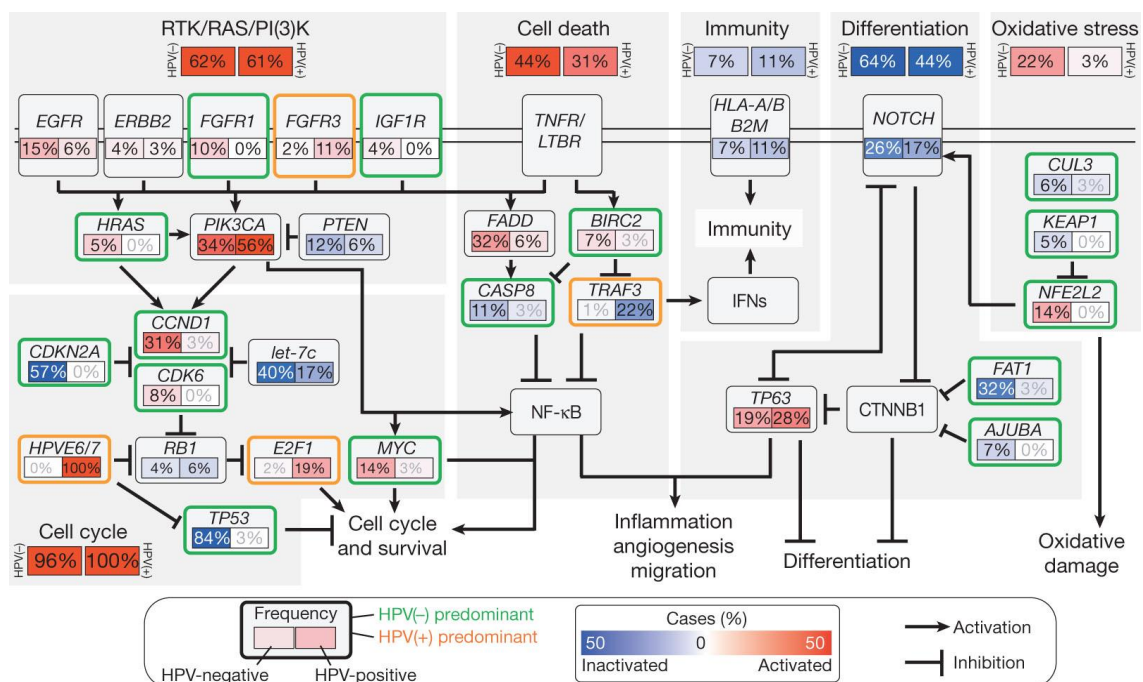


Figure 32. Candidate therapeutic targets and driver oncogenic events in HNSCC according to TCGA.

The genes listed reflect somatic alterations and changes in protein expression identified and have been proposed as putative therapeutic targets in HNSCC tumors. The frequency of genetic alterations is shown. TSG, tumour suppressor gene²⁰⁴.

Alternative studies have classified HNSCC tumors based on the risk of patient recurrence. Patients with high and low risk of recurrence were differentiated using gene expression profiling. Specifically, tumors with high-risk of relapse display a strong signature of genes related to epithelial to mesenchymal transition (EMT) and activation of NF- κ B signaling²⁰⁵.

Nevertheless, the most outstanding classification of HNSCC tumors is based on HPV infection status. Indeed, there is a strong consensus in the field to consider HPV+ve HNSCC tumors a specific subgroup within HNSCCs²⁰⁶. Seminal studies have demonstrated that the different aetiology of HPV+ve and HPV-ve tumors strongly influences the differences found at the genetic level in HNSCC tumors (**Figure 33**)²⁰⁴.



carcinogenesis. Although there are more than 100 different HPV subtypes, two of them, HPV-16 and HPV-18, cause the majority of HPV-related cancers. HPV-16 is predominant in HNSCC, especially in oropharyngeal tumors (>90%). Curiously, HPV infection is associated with a better prognosis in HNSCC ²⁰⁸.

At the molecular level, HPV+ve tumors are typically *TP53* wild-type. The presence and type of mutations within *TP53* display an intrinsic prognostic value, since *TP53* truncating mutations are associated with reduced patient survival outcomes²⁰⁹. Indeed, it is difficult to determine whether the better prognosis of HPV-positive tumors is due to HPV infection or *TP53* wild-type status.

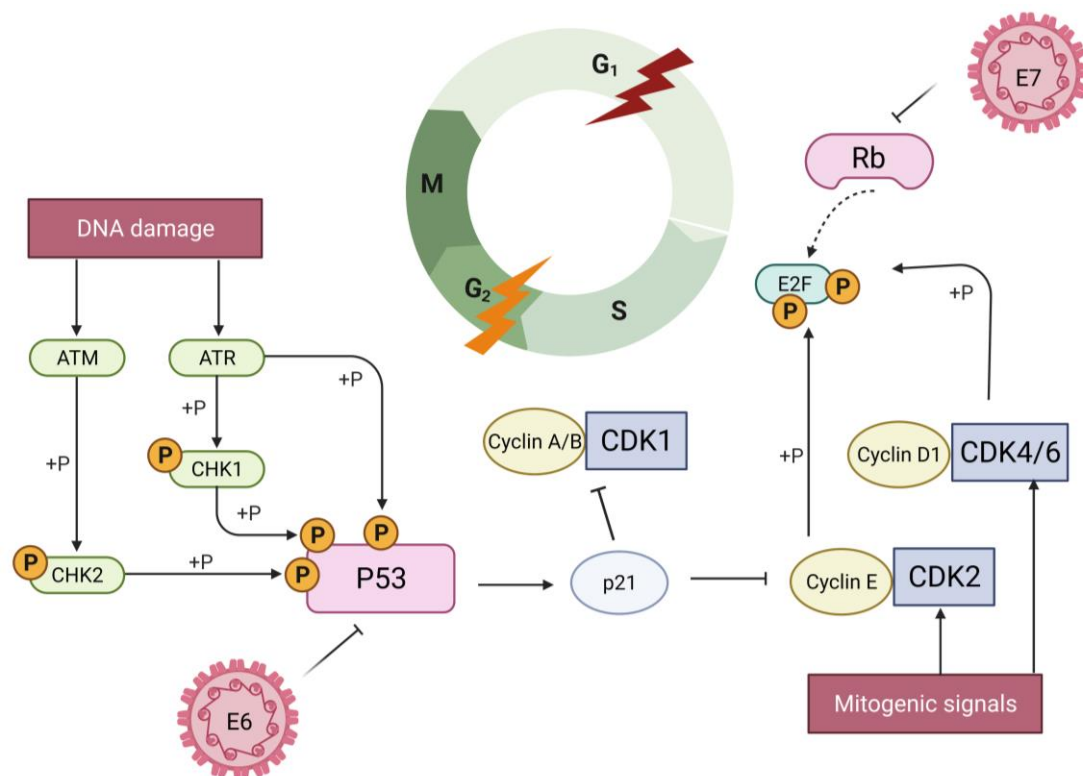


Figure 34. Deregulation of the cell cycle by HPV. The cell cycle is tightly regulated by complexes of cyclins and cyclin-dependent kinases (CDKs). To guarantee the integrity of cells along cell cycle, cells encounter G₁ checkpoint (red lightning) that is controlled by retinoblastoma pocket proteins (Rb). These proteins bind and inactivate E2F transcription factors, which induce the expression of S phase genes. In response to mitogenic signals, the cyclin D1–CDK4/6 and cyclin E–CDK2 complexes are activated. These complexes phosphorylate Rb pocket proteins leading to the release and activation of E2Fs and, subsequently, the transition of cells into S phase. The interplay between cyclins, CDKs and their regulatory proteins determines the transition along the checkpoint. A second important cell cycle checkpoint occurs in the G₂ phase (yellow lightning). Cells encounter this checkpoint upon completion of DNA replication and serves for the repair of errors occurring during the process. p53 is a key protein in the response to replication errors and DNA damage. DNA-damage sensors, including ataxia-telangiectasia (ATM) and ataxia-telangiectasia and Rad3-related (ATR), phosphorylate the checkpoint kinases CHK1 and CHK2, leading to increased p53 activity by phosphorylation of various downstream molecules, including p53 itself. p53 induces the expression of p21, which inhibits several cyclin–CDK complexes leading to interruption of the cell cycle for DNA repair. The human papillomavirus (HPV) genome contains various early and late open reading frames and encodes two viral oncoproteins,

namely E6 and E7. E6 protein binds p53 and targets the protein for degradation, whereas the E7 protein binds to and inactivates Rb proteins, promoting cells to resume the cell cycle and block p53-mediated apoptosis. Both events allow the virus to actively replicate into infected cells. Viral infection and replication in the intermediate and superficial layers of the epithelium poses no risk of malignization of the whole tissue. As a consequence of the rapid turnover of the epithelium in the head and neck region (3-6 days), infected cells are shed and eliminated by the immune system. However, if viral infection reaches the stem cells in the basal layer the whole tissue becomes transformed, as these cells fuel tissue homeostasis and regeneration ¹⁹⁹. Created with BioRender.com.

HPV-ve HNSCC

Tobacco consumption is the primary risk factor for the development of HPV-ve HNSCC tumors. Chemicals contained within tobacco, such as polycyclic aromatic hydrocarbons and nitrosamines, are well known carcinogens. During the detoxifying and excretion processes of these compounds, highly reactive metabolites with the ability to form covalent DNA adducts are generated. If not repaired, these adducts led to mutations and other genetic abnormalities. The accumulation of alterations in key tumor suppressor genes (*TP53* and *CDKN2A*) or deregulation of cell signaling pathways such as PI3K-AKT-mTOR and RAS-MAPK are associated with the onset and progression of HPV-ve HNSCC ¹⁹².

4. Hallmarks of HNSCC

In 2000, Hanahan and Weinberg compiled the first collection of cancer-related phenotypes ⁴. This collection included six hallmarks of cancer, namely limitless replicative potential, self-sufficiency in growth signals, insensitivity to growth suppressor signals, ability to evade apoptosis, sustained angiogenesis and tissue invasion and metastasis. Along time, additional hallmarks and enabling characteristics such as genome instability and mutation, deregulation of cellular metabolism, tumor promoting inflammation, immune evasion, phenotypic plasticity and disrupted differentiation, non-mutational epigenetic reprogramming, cellular senescence and polymorphic microbiomes have been incorporated ^{3, 5}. The most important molecular and cellular processes underlying the hallmarks of cancer in HNSCC are summarized below.

Limitless replicative potential

The regulation of the cell cycle is often lost in cancer. p53 and Rb pathways are the main tumor-suppressor pathways controlling cell responses to potentially oncogenic stimuli and cell cycle transition in HNSCC. As described before, both, p53 and Rb proteins are frequently mutated or alternatively, inactivated by HPV-16 *E6* and *E7* oncogenes in HPV+ve tumors.

TP53 mutations occur in 60% of HNSCC cases. Specifically for HPV-ve tumors, *TP53* is the most commonly mutated tumor suppressor gene (75% to 85%)^{204, 210, 211}. HNSCC tumors arising in the larynx and hypopharynx display higher *TP53* mutation rates compared to oropharynx and oral cavity tumors²¹². Indeed, it has been shown that overexpression of a dominant-negative mutant form of p53 (p53^{R172H}) together with TERT (telomerase reverse transcriptase) and a cyclinD1/cyclin-dependent kinase 4 (CDK4) mutant is sufficient to trigger immortalization of keratinocytes *in vitro*^{213, 214}. An independent study has shown that the lifespan of keratinocytes can be extended *in vitro* inactivating p53, either with a short hairpin RNA (shRNA) against p53, by expressing the p53^{R172H} mutant or by transducing cells with the E6 HPV oncoprotein²¹⁵. All these effects were dependent on TERT overexpression.

Similarly, the p16^{INK4A}–cyclinD1–CDK4–RB and p16^{INK4A}–cyclinD1–CDK6–RB axis are altered in the vast majority of HNSCC. p16^{INK4A} is the protein encoded by *CDKN2A* gene, which is frequently inactivated in this tumor type either by homozygous deletion, or chromosomal loss in combination with mutation or promoter methylation²¹⁶. In turn, *CCND1*, the gene that encodes cyclinD1, is amplified in around 80% of the HPV-ve HNSCC²¹⁷.

The cellular phenotype associated with alterations in the p53 and Rb pathways is cell immortalization. This event coincides with the onset of the carcinogenesis process. Indeed, the loss of chromosome 9p21 (*CDKN2A*) and the inactivating *TP53* mutations are already present in most HNSCC premalignant lesions¹⁹⁹. If 60% of HNSCCs display inactivating *TP53* mutations, and about 20% of the tumors are positive for HPV infection which in turn leads to efficient inactivation of *TP53* protein, then, only 20% of tumors harbor a functional p53²¹⁸. The progression of these tumors has been hypothesized to be p53-independent, or alternatively driven by genes other than p53 but within the same pathway²¹⁹.

Collectively, the unlimited growth potential in HPV-ve HNSCC is attributed to *TP53*, *CCND1* and *CDKN2A* alterations, while changes in *TP53* and Rb family genes, such as *RB1*, *RBL1* and *RBL2*, account this phenotype in HPV+ve tumors.

Self-sufficiency in growth signals

Normal and healthy cells require growth factors, hormones and other molecules in the extracellular media to engage growth and cell division. Nevertheless, cancer cells have the ability to grow independently to external signals. Overactivation of signalling pathways controlling cell growth is common in HNSCC.

EGFR pathway

EGFR is a tyrosine kinase receptor that belongs to the ErbB family. The activation of ErbB receptors and, as consequence, the initiation of signaling cascades, occurs upon the homo- or heterodimerization triggered by ligand binding. In squamous cells, EGFR

downstream signaling is controlled by RAS-MAPK, PI3K-PTEN-AKT and phospholipase C pathways²²⁰. Moreover, EGFR bound to its ligands is able to translocate to the nucleus to act as a transcription factor and co-activate other transcription factors, such as STAT (signal transducer and activator of transcription) proteins, or even induce the expression of *CCND1*, that as described before, promotes progression through the G1-S in the cell cycle^{221, 222}.

Overexpression of EGFR protein in HNSCC has been reported and confirmed in several studies^{223, 224}. This data is relevant from the clinical point of view, as HNSCC patients with EGFR overexpression exhibit a better response to radiotherapy when a concomitant combination with EGFR blocking antibodies is prescribed²²⁵. *EGFR* gene amplification has been observed in approximately 10-30% of the patients with EGFR overexpression^{226, 227}.

Overactivation of the EGFR pathway does not only occur as consequence of EGFR overexpression. EGFR has multiple tyrosine phosphorylation sites (at least 13) that mediate interaction with downstream effector proteins. Activating point mutation occurring at these phosphorylation sites have been observed in HNSCC tumors²²⁸. Additionally, an oncogenic EGFR mutant form devoid of amino acids 6 to 273 in the extracellular region (EGFRvIII) has been identified in the 42% of HNSCC cases. This isoform is caused by an in-frame deletion of EGFR exons 2–7 and confers enhanced proliferation and reduced response to anti-EGFR treatment²²⁹.

TGFβ pathway

Transforming growth factor beta (TGFβ) is a multifunctional cytokine belonging to the transforming growth factor superfamily. TGFβ binds to specific receptors in the cell surface of cells resulting in the phosphorylation of receptor-regulated Smad2/3 proteins and association with Smad4. This complex translocates to the nucleus and regulates the transcription of target genes involved in cell growth, differentiation, migration, apoptosis and extracellular matrix production (**Figure 35**). TGFβ acts as a tumor suppressor or an oncogene depending on the context. On one hand, TGFβ is able to inhibit the growth of epithelial cells and promote apoptosis, whereas on the other, induces the transcriptional reprogramming of epithelial to mesenchymal cells (EMT) and, consequently boosts migration and invasion^{230, 231}.

There are several studies that link TGFβ pathway with the HNSCC carcinogenesis process. An overall downregulation of TGFβ receptors is often found in HNSCC tumors^{232, 233}. Also, a frequent loss of chromosome 18q, which encodes *SMAD2*, *SMAD3*, *SMAD4* and *TGBRII* (TGFβ receptor II) genes, and mutations in *SMAD2* and *SMAD4* genes have been reported in HNSCC²³⁴. Remarkably, the conditional knock-out of *SMAD4* in the oral mucosa of mice causes HNSCC²³⁵.

RHOA and *CDC42* are among the genes transcriptionally regulated by the canonical TGFβ pathway. *RHOA* is also a key player in the non-canonical (Smad-independent)

TGF β signaling (**Figure 8**). The activity of RHOA in epithelial cells is regulated by TGF β in two different and opposing ways. During the early stimulation phase, TGF β induces Smad-mediated expression of NET1, a RHOA-specific guanine exchange factor that mediates RHOA activation²³⁶. At later time points, TGF β promotes RHOA degradation specifically at cellular protrusions that allow the disassembly of tight junctions, an essential event in epithelial-mesenchymal transition²³⁷.

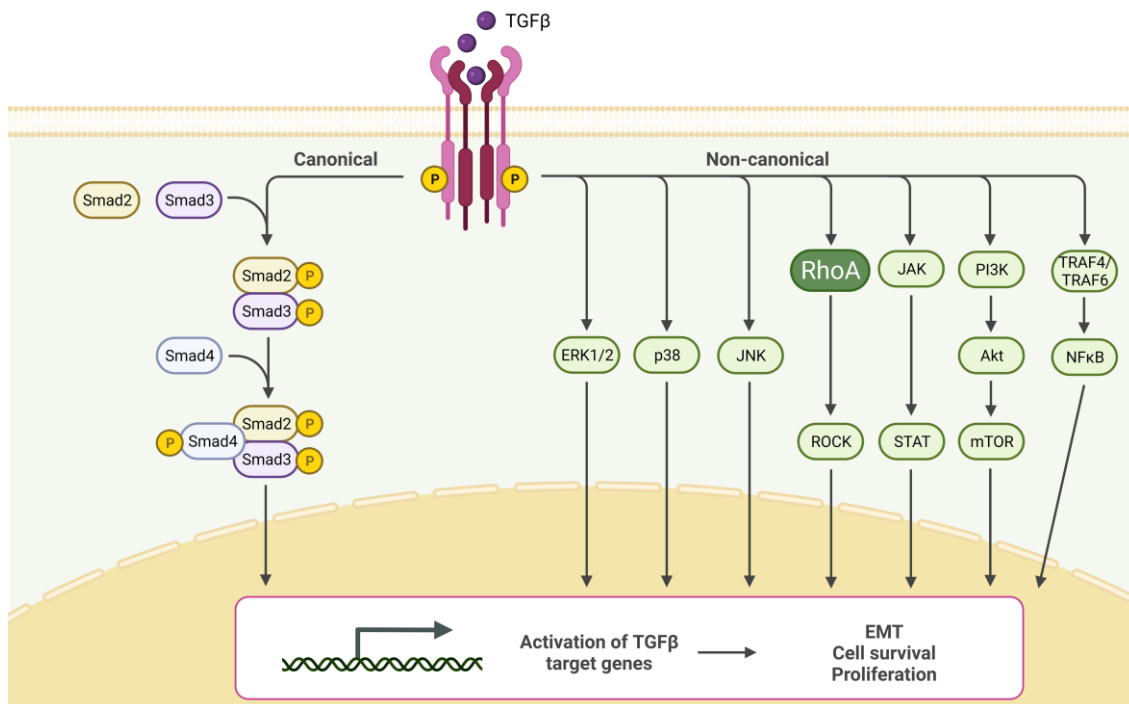


Figure 35. Canonical and non-canonical TGF β signaling pathways. In the canonical signaling pathway, biologically active TGF β ligands binds to TGF β RII, which in turn activates TGF β RI. TGF β R serine/threonine receptor complex promote phosphorylation of Smad2/3 proteins which form a complex with Smad4. Upon Smad4 phosphorylation, the complex shuttles to the nucleus and initiates several biological processes through transcriptional regulation of target genes. In the non-canonical TGF β signaling, the TGF β receptor complex engages a downstream signaling through the mitogen-activated protein kinases (MAPKs), phosphatidylinositide 3-kinase (PI3K), TNF receptor-associated factor 4/6 (TRAF4/6) and Rho family of small GTPases. These pathways promote transcriptional regulation, either through direct interaction with the nuclear Smad protein complex or alternative downstream proteins. Activation of the canonical and non-canonical TGF β signaling promotes epithelial to mesenchymal transition (EMT), cell survival and proliferation. Created with BioRender.com.

Evading programmed cell-death

Apoptosis is a form of programmed cell death. Together with senescence, apoptosis restricts the proliferation of cells if their DNA becomes damaged. Cancer cells bypass this tumor suppressor mechanism in different ways.

PI3K-PTEN-AKT pathway

PI3K-PTEN-AKT is an important signaling pathway that regulates biological processes such as apoptosis, metabolism and cell growth, among others.

Class I PI3Ks catalyze the conversion of phosphatidylinositol (4,5)-bisphosphate (PI(4,5)P₂, PIP₂) into phosphatidylinositol (3,4,5)-trisphosphate (PI(3,4,5)P₃, PIP₃). PIP₃ promotes the recruitment to cellular membranes of a variety of signaling proteins, containing PX domains, pleckstrin homology domains (PH domains), FYVE domains and other phosphoinositide-binding domains. One of these proteins is protein kinase B (PKB/AKT). This is a very well-known protein activated as a result of its translocation to the cell membrane, where it is then phosphorylated and activated by phosphoinositide dependent kinase 1 (PDK1). The phosphorylation of AKT leads to the activation of the TSC/mTOR pathway, which plays an important role in regulating cell growth, survival and migration.

Phosphatase and tensin homolog (PTEN) is a dual protein/lipid phosphatase whose main substrate is PIP₃. PTEN specifically catalyzes the dephosphorylation of PIP₃. This dephosphorylation is important because it results in inhibition of the AKT signaling pathway.

Class Ia PI3Ks are heterodimers coupled to receptor tyrosine kinases such as EGFR or adaptor molecules that will be active upon receptor phosphorylation. The catalytic unit of this receptor is encoded by *PIK3CA*, located in chromosome 3q26, which is often amplified in HNSCC. Additionally, somatic activating mutations in the *PIK3CA* gene have been described in about 10-20% of HNSCC patients^{238, 239}. These mutations have been shown to promote cell migration and invasion, both *in vitro* and *in vivo*. Furthermore, inactivating mutations or homozygous deletions of *PTEN* gene have been reported in about 10% of HNSCCs²⁴⁰. *PI3K* and *PTEN* alterations, both ultimately resulting in activation of AKT, are mutual exclusive not only in HNSCC but also in other tumor types. Globally, the PI3K/AKT/mTOR pathway is upregulated in over 90% HNSCC carcinomas, both, HPV+ve and HPV-ve²⁴¹. Hyperactivation of this pathway is associated to resistance to radiotherapy and cytotoxic drugs²⁴². The use of inhibitors against PI3K, AKT and mammalian target of rapamycin (mTOR) have shown remarkable effects inhibiting tumor cell proliferation and sensitizing HNSCC tumor cell cultures and mouse models of tumorigenesis to radiotherapy. Nevertheless, compensatory feedback mechanisms are rapidly acquired limiting their therapeutic effect^{243, 244}.

Phenotypic plasticity

Epithelial cells are highly differentiated cells. Acquisition of cellular differentiation often results in an anti-proliferative phenotype. Differentiated cells originate from immature cells undergoing programmed gene expression patterns for the acquisition of highly specialized functions. Differentiated cells are terminally committed with a functional phenotype, and thus restricted in plasticity. There is increasing evidence that unlocking the normally restricted capability for phenotypic plasticity is a critical component of cancer pathogenesis as it facilitates evasion from the state of terminal differentiation³.

NOTCH1 belongs to the NOTCH family of receptors (NOTCH1-4), which regulate essential cellular functions, including proliferation, differentiation, apoptosis and stem cell renewal. After ligand binding, the γ -secretase complex releases the NOTCH intracellular domain (NICD), which translocates to the nucleus, resulting in the transcriptional activation of NOTCH target genes, such as *HES* and *HEY* family of transcriptional repressors²⁴⁵. Comprehensive genomic analysis performed in HNSCC revealed *NOTCH1* gene as the second most mutated gene after *TP53*²⁰⁴. The vast majority of *NOTCH1* mutations are considered inactivating and associated with a worse patient prognosis. However, certain HNSCC patients display activating *NOTCH1* mutations, suggesting a bimodal role and signaling of this protein in HNSCC^{245, 246}.

Tissue invasion and metastasis

HNSCC tumors progress similarly to most of tumors, metastasizing first to lymph nodes and to distant organs at later stages. Both, the number of lymph nodes affected and the extranodal extension, known as the growth of cancer cells beyond the confines of the capsule of a lymph node into adjacent tissues, predict distant metastasis and survival in patients. Degradation of the extracellular matrix (ECM), epithelial-to-mesenchymal transition (EMT) and detachment from bulk tumors are processes required by tumor cells to obtain an invasive phenotype.

Degradation of ECM is one of the first steps in the metastatic process. Matrix metalloproteinases (MMPs) have an integral role in degrading and remodeling ECM and thus promoting cell invasion. High levels of MMP2, MMP9 and MMP13 in HNSCC are associated with invasion, metastasis and poor patient prognosis²⁴⁷⁻²⁴⁹. Furthermore, the CD44 HNSCC cancer stem cell marker, a cell surface receptor that binds to and activates MMP9, co-localizes with MMP9 in the invasive front of HNSCC tumors. CD44 levels of expression in HNSCC also correlate with metastasis^{250, 251}.

The epithelial-to-mesenchymal transition (EMT) is a process by which epithelial cells lose their cell polarity and cell-cell adhesion, to become mesenchymal cells and gain migratory and invasive properties. EMT-associated changes in E-cadherin (downregulation) and vimentin (upregulation) correlated with increased metastasis in HNSCC^{252, 253}. TWIST, SNAIL and SLUG are the transcription factors mediating the downregulation of E-cadherin during EMT process²⁵⁴. Furthermore, hypoxic conditions in the tumor microenvironment contribute to EMT, since the alpha subunit of the HIF1 transcription factor, induces vimentin, TWIST and SNAIL expression^{252, 255}.

Detachment from the basement membrane and extracellular matrix components, and survival under non-adherent conditions is also necessary to metastasize. In other words, tumors cells need to acquire resistance to anoikis, the programmed cell death that occurs in anchorage-dependent cells upon loss of cell adhesion. The cell survival in non-adherent conditions is driven by RAS-MAPK, PI3K-AKT-mTOR and STAT3 signaling pathways^{192, 256}.

Sustained angiogenesis

Tumors need blood supply to support continuous growth. The formation of new vessels is essential in the carcinogenic process. Solid tumors induce neo-angiogenesis by producing pro-angiogenic factors. The vascular endothelial growth factor (VEGF) is a well-known inducer of angiogenesis and several studies have associated the high expression in HNSCC tumors with a worst patient prognosis ²⁵⁷. Interestingly, VEGF expression is triggered under hypoxic conditions and thus dependent on HIF1 α ²⁵⁸.

Evasion of immune destruction

Tumor cells undergo a profound reprogramming to thrive in a chronically inflamed microenvironment, evade immune recognition and suppress immune reactivity.

Immune cells in the HNSCC tumor microenvironment contain tumor-infiltrating lymphocytes (including T cells, B cells and natural killer cells); and myeloid-derived cells such macrophages, neutrophils, dendritic cells and myeloid-derived suppressor cells. The extent and composition of the immune infiltrate varies according to the anatomical region and HPV status. The identification of different immune phenotypes has allowed a better classification of HNSCC tumors, providing a powerful tool to predict patient's response to treatment with immuncheckpoint inhibitors.

High levels of tumor-infiltrating lymphocytes are associated with a better patient prognosis, although if immunosuppressed by inhibitory signals triggered by the tumors, the prognostic value of the infiltrate is lost. HPV+ve tumors display increased numbers of neoantigens as consequence of the viral infection, leading to a concomitant increase in the immune infiltrate and better survival outcomes.

HNSCC tumors use different mechanisms to evade immune surveillance. HNSCC tumor microenvironment is enriched in immunosuppressive growth factors and cytokines that promote the recruitment or activity of myeloid-derived suppressor cells, regulatory T cells and M2-skewed macrophages. All these cells block the anti-tumour activity of effector T cells (both, T helper and T cytotoxic) and NK cells. Moreover, genetic and epigenetic alterations resulting in decreased levels of human leukocyte antigen (HLA) or defects in the processing of tumor antigens, lead to decreased immune recognition and cytolysis of tumour cells. In addition, HNSCC tumors, specially late-stage tumors, exhibit upregulation of PD-L1, which attenuates the cytolytic activity of T cells ¹⁹².

5. Head and neck cancer treatment

The mainstay treatment of head and neck cancer patient is still nowadays radiation and surgery. Head and neck cancers involve critical structures associated with speaking, swallowing and appearance. Removal of part or all of these structures, including the tongue, upper and lower jawbones, nose, larynx (voice box), salivary glands, and skin of the face and neck, may result in difficulty in speaking and swallowing, and disfigurement. Modern anesthesia, reconstruction surgery and medical integral care have led to fewer surgery-associated deaths and an increase the life quality of HNSCC patients. Nevertheless, the overall survival rate of the disease is about 50% and has not improved significantly in the last 60 years¹⁸⁵. Consequently, active research on the molecular mechanisms leading to the development of HNSCC, and the identification of new therapeutic targets is crucial for improving patient survival.

HNSCC treatment differs according to the stage of disease, anatomical site and surgical accessibility. Generally, a multispecialty team decides the treatment for each HNSCC patient, not only to reduce the risk of relapse with the use of surgery, radiotherapy and chemotherapy, but to preserve patients' life at the dental, nutritional, speech and language and auditory level as well^{189, 259}.

Treatment in HPV-associated tumors

As described above, HPV infection has a causal role in the development of HNSCC, especially in oropharynx tumors²⁶⁰. The epidemiology, pathophysiology and response to treatment of HPV+ve tumors differ from HPV-ve HNSCC malignancies^{188, 261}.

Patients with an HPV-associated HNSCC typically present a small primary lesion and cervical lymphadenopathy. Despite the high frequency of spreading to the lymph nodes, HPV+ve HNSCC patients display better prognosis and survival outcomes^{262, 263}. As consequence of the improved prognosis for this subgroup of patients, The American Joint Committee on Cancer (AJCC) and the Union for International Cancer Control (UICC) decided to include HPV status in the staging system for HNSCC (**Table 5**). Nevertheless, this change resulted in the downstaging of more than 90% of HPV+ve patients compared with previous staging systems, increasing the proportion of patients in stage I. Patients with a prognostic stage I receiving therapy based exclusively in radiotherapy or chemotherapy show inferior therapeutic benefit and survival outcomes^{189, 264, 265}. Accordingly, surgery is mandatory except for surgically inaccessible tumors and/or patients with a very low performance.

Table 5. HNSCC stages according to the TNM classification.

Stage	HPV-Positive Oropharyngeal Cancer			HPV-Negative Oropharyngeal Cancer		
	Tumor	Node	Metastasis	Tumor	Node	Metastasis
0	Tis	N0	M0	Tis	N0	M0
I	T0, T1, or T2	N0 or N1	M0	T1	N0	M0
II	T0, T1, or T2	N2	M0	T2	N0	M0
	T3	N0, N1, or N2	M0			
III	T0, T1, T2, T3, or T4	N3	M0	T1, T2, or T3	N1	M0
	T4	N0, N1, N2, or N3	M0			
IV	Any T	Any N	M1			
IVA				T4a	N0 or N1	M0
				T1, T2, T3, or T4a	N2	M0
IVB				Any T	N3	M0
				T4b	Any N	M0
IVC				Any T	Any N	M1

HNSCC staging system by the American Joint Commission on Cancer and the Union for International Cancer Control, 8th edition ²⁶⁶. Tis denotes tumor in situ.

Treatment in early-stage disease

It comprises patients in stage I or II of the disease (approximately 30 to 40%). These patients are cured with surgery or definitive radiotherapy alone. The choice depends on the anatomical accessibility of tumor lesions. Seventy to 90% of early-stage patients display long-term survival ²⁶⁷.

Treatment in locally-advanced disease

More than 60% of the HNSCC patients are diagnosed at stage III or IV disease, namely tumors with marked local invasion, metastases to regional lymph nodes, both, and eventually distant metastasis (stage IV). These patients have higher risk of recurrence and poor prognosis. The treatment for these patients is individualized and depends on tumor size, tumor localization in the head and neck region, stage of disease (III vs IV), age and performance status of the patient. Resection surgery is the gold-standard treatment for accessible tumors, such as those in the oral cavity. Adjuvant radiotherapy or chemoradiotherapy are recommended depending on the assessment of high-risk features. Contrary, when lesions cannot be surgically resected, or when the surgery might lead to a drastic reduction in the wellness of the patient, chemoradiotherapy becomes the first therapeutic option ²⁶⁸.

Definitive concurrent chemoradiotherapy

The standard adjuvant therapy for high-risk patients is the concurrent chemoradiotherapy (CCRT). Three chemotherapeutic agents are approved for combination therapy. Cisplatin is the chemotherapeutic agent used as first option, but substituted by carboplatin, although with inferior therapeutic benefit, in patients with reduced performance status due to its high toxicity ²⁶⁹. The third agent is Cetuximab, a blocking antibody against epidermal growth factor receptor (EGFR). Cetuximab was

approved as standard therapy in 2006 but displays limiting survival outcomes compared to cisplatin²²⁵.

Recurrent or metastatic disease

Depending on initial therapy and extent of disease, recurrent HNSCC may occasionally be treated surgery, radiation or a combination of both ²⁷⁰. But all too often, recurrent disease (like metastatic HNSCC) is incurable. Recurrent or metastatic disease occurs in 65% of patients with HNSCC. These patients have a fatal prognosis (6 to 9 months survival in the absence of treatment). The administration of platinum-based agents, taxanes, antifolates or Cetuximab is used for palliation therapy in recurrent and metastatic patients ²⁷¹. Radiotherapy is not recommended in these patients due to the low performance and the painful and long-term side effects occurring at the therapeutic doses.

Targeted therapies and immuncheckpoint inhibitors

Although, new-targeted therapies have been tested in the context of HNSCC none of them has reach significant improvement over the standard care.

The fact that modulating the immune system could promote regression of solid tumors has revolutionized the comprehension and treatment of cancer. Pembrolizumab and nivolumab, monoclonal antibodies targeting PD-1, an inhibitory receptor on the surface of cytotoxic effector T cells, showed improved response rates and patient survival in the clinical trials in recurrent or metastatic HNSCC platinum-treated patients. Accordingly, these agents were approved by the Food and Drug Administration (FDA) in 2016 ²⁷²⁻²⁷⁴, and by The European Medicines Agency (EMA) in 2019 ^{275, 276}. Pembrolizumab has been also approved for first-line treatment of metastatic HNSCC patients as monotherapy or in combination with platinum and 5-fluorouracil (5-FU) ²⁷⁷. Unfortunately, about 85 to 95% of patients with recurrent or metastatic HNSCC relapse upon treatment with immuncheckpoint inhibitors or display primary therapeutic resistance. Unresponsiveness to anti-PD-1 is usually multifactorial, highly individualized, and evolves over time during treatment. Broadly, the pathogenesis of acquired resistance to anti-PD-1 therapy includes loss of T cell function, disruption of antigen presentation, and acquired resistance of interferon-induced T cells ^{273, 278, 279}.

6. RHO signaling in HNSCC

Several studies have reported associations between the levels of expression of different small GTPases and HNSCC carcinogenesis. Some of these studies are controversial. On the one hand, RHOA, Rac2 and Cdc42 are shown to be increased in

dysplastic and fully malignant cell lines compared to normal keratinocytes. Indeed, based on immunohistochemistry analysis, RHOA was appointed as a promising biomarker for malignancy in HNSCC^{67, 280}. But on the other hand, a study evaluating the activity of small GTPases in HNSCC cell lines showed that whereas Rac1 was active in most of them, RHOA and Cdc42 were active only in a subgroup^{280, 281}.

It has been described that increased levels of PKC ϵ in HNSCC, an isoform of the PKC family of protein kinases, are associated with high disease recurrence and decreased overall survival in patients. Interestingly, this protein promotes migration and invasion in a RHOA and RhoC-dependent manner^{280, 282}.

Elevated RhoC levels in patients are also associated with advanced-stage, lymph node metastasis and aggressive tumor behavior²⁸³. This is not surprising considering that RhoC downregulation in HNSCC cell lines using lentiviral small hairpin RNAs (shRNAs) resulted in diminished migration and invasion *in vitro* and *in vivo*²⁸⁴. Elevated RhoC levels in HNSCC can be explained by reduced expression of miR-138. This microRNA targeting RhoC is downregulated in HNSCC, and reported to have an important role in EMT, cell migration and invasion²⁸⁵.

Rac1 has been also related with head and neck carcinomas, specifically in the cell invasion processes mediated by the EGFR/Vav2/Rac1 signaling axis²⁸¹. High expression, activity and nuclear localization of Rac1 has been associated with chemoradiotherapy resistance and, subsequently, with tumor recurrence in HNSCC^{286, 287}.

Rho downstream signaling proteins have also been linked to HNSCC. α -catulin is a cytoskeletal protein that acts as scaffold protein for Lbc Rho guanine nucleotide exchange factor (ARHGEF1) and supports serum response factor activation¹²¹. The overexpression of this protein in HNSCC results in faster proliferation, migration and invasion, enhanced EMT and reduced apoptosis *in vitro*. Conversely, α -catulin when downregulated leads to a decreased invasive and metastatic potential both *in vitro* and *in vivo*²⁸⁸. Moreover, its expression is higher in HNSCC patient samples than in normal tissues²⁸⁹. Another Rho downstream signaling molecule associated with HNSCC carcinogenesis is CD44. In HNSCC, CD44 physically associates in a multimolecular complex with LARG, a RhoGEF, inducing RHOA signaling, ROCK activation and subsequently tumor progression²⁹⁰⁻²⁹².

Regarding RHOA, the focus of study of this doctoral thesis, it has been shown that its expression is higher in HNSCC cells compared to normal cells^{67, 84}. The role of RHOA has been recently studied in tongue cancer cell lines and pointed out as an oncogene in this tumor context. Specifically, the downregulation of RHOA in tongue tumor cells reduces cell migration, invasion and proliferation *in vitro*; and tumor growth and lymph node colonization in orthotopic xenografts in mice⁸⁵. However, there are not enough studies to confirm the role of this GTPase in HNSCC tumorigenesis and, in addition,

poor information is available regarding the function of *RHOA* in head and neck anatomical regions such as larynx or pharynx.

Interestingly, the massive use of sequencing technologies has provided a huge amount of information regarding the genetic alterations undergoing in tumors. The analysis of somatic point mutations from large-scale genomic screenings across 21 tumor types and more than 4,000 human cancers (and their matched normal-tissue samples) has allowed the identification of genes significantly mutated in cancer that were previously unnoticed. *RHOA* turned out to be one of these genes. When interrogating the mutations occurring specifically in the effector domain of *RHOA* the prevalence was low, but interestingly six out of the seven tumors identified occurred in the head and neck region ²⁹³. *RHOA* E40Q mutation was markedly predominant. In an alternative and similar study, a higher percentage of *RHOA* mutations was found (<5%). *RHOA* mutations in human tumors were described at codons R5, E40 and Y42, but E40Q. As observed before, the most frequent mutation in HNSCC ²⁹⁴.

Chapter II

RHOA in head & neck cancer

AIMS OF THE STUDY

AIMS OF THE STUDY

RHOA has been widely described as an oncogene. However, recent results from our group have shown that RHOA has a tumor suppressive role in colon cancer¹⁰³ and in diffuse-gastric cancer (unpublished data). Head & neck cancer (HNSCC) groups very heterogeneous tumors. The lack of improvement in the survival of patients and the low rate of personalized treatments have promoted the active research into the molecular mechanisms of HNSCC. Recently, it has been reported that *RHOA* is frequently mutated in HNSCC. This is observed in specific types such as diffuse gastric cancer, angio-immunoblastic T-cell lymphoma, adult T-cell leukemia/lymphoma and Burkitt lymphoma. Interestingly, these mutations are distributed in hotspots and differ from one tumor type to another. In HNSCC, *RHOA* is mutated only in around of 1.5% of the cases, but more than 60% of these mutations involve E40Q. In this thesis we focused to get a better understanding of the role of RHOA in HNSCC tumorigenesis, and particularly to unveil whether RHOA E40Q mutation in HNSCC tumors exhibits a relevant role in the carcinogenic process.

Therefore, the specific aims of this thesis are:

7. To evaluate the association between RHOA expression in primary tumors and the clinicopathological features of HNSCC cancer patients.
8. To investigate *in vitro* and *in vivo* the role of RHOA in a) cell growth, b) colony formation ability, c) migration and d) invasion potential of HNSCC cells genetically modified for the downregulation of the protein.
9. To investigate *in vitro* the effects of the hotspot RHOA mutation observed in HNSCC (RHOA-E40Q) in pharynx, tongue and larynx engineered cell systems.

Chapter II

RHOA in head & neck cancer

MATERIALS & METHODS

MATERIALS AND METHODS

1. Study of RHOA in HNSCC patient samples

Tissue microarray (TMA) analysis

Clinical samples: A total of 360 samples from primary tumors of HNSCC patients and their respective clinical data were analyzed. Patients samples were obtained at Hospital Univertitari Vall d'Hebron (HUVH) and Hospital Universitario Central de Asturias (HUCA). Informed consent for genetic analysis of the tumor was obtained from every patient, according to protocols approved by the 'Human Investigations and Ethical Committee' in both institutions. All patients were diagnosed with a single primary tumor, underwent surgically treated, and received no additional treatment prior to surgery. All samples were formalin-fixed, paraffin-embedded, arrayed into a tissue microarray (TMA) and used for immunohistochemical assessment of RHOA. For tissue microarray preparation, areas containing a high proportion of tumor cells were selected after histological examination of hematoxylin and eosin-stained tumor sections. Triplicate 0.6mm cores from every sample were arrayed in a fresh paraffin block using a Beecher Instrument tissue arrayer (Silver Spring, MD). Unstained four- μ m sections from the tissue microarray were mounted on slides coated with Poly-L-lysine solution (Sigma-Aldrich). For immunohistochemical analysis, the commercial NovoLink polymer detection system (Novocastra Laboratories) was used according to the instructions of the manufacturer. Finally, anti-RHOA rabbit monoclonal antibody was used at 1:1000 dilution (2117 – Cell Signaling) for protein detection (**Table 8**).

RHOA expression levels were scored using a semiquantitative scale ranging from 0 (absence of RHOA immunostaining) to 3 (highest RHOA immunostaining). The investigator was blinded for both, sample identity and patient clinical data; and the average of signal of the three spots for every patient was calculated. Next, patients were dichotomized as high or low RHOA according to the levels of protein expression in the primary tumor. The cutoff value for patient dichotomization was determined using X-tile tool²⁹⁵. Differences in survival outcomes were represented in Kaplan-Meier plots as a function of tumor RHOA protein expression. The association of RHOA protein expression levels with clinicopathological features other than survival was also analyzed.

TCGA RNA sequencing data analysis

Clinical data and RHOA mRNA expression in primary tumors, expressed as mRNA z-score, from 528 HNSCC patients were downloaded from 'The Cancer Genome Atlas' (TCGA) database: "Head and Neck Squamous Cell Carcinoma - TCGA, Firehouse Legacy" study. Patients were dichotomized as high or low RHOA based on the mRNA

expression of RHOA within tumors. Selection of the cutoff value was calculated through X-tile software²⁹⁵.

2. Study of RHOA in HNSCC cell lines

Human HNSCC cancer cell lines: A total of 12 HNSCC cancer cell lines were used: FaDu, Detroit 562, 92VU040, 92VU041, 92VU078, 92VU08, 92VU094, 92VU120, SCC25, JHU029, JHU011 and JHU012 (**Table 6**). FaDu, Detroit 562 and SCC25 cell lines were purchased from ATCC bank (<https://www.atcc.org/>). 92VU040, 92VU041, 92VU078, 92VU08, 92VU094 and 92VU120 cell lines were kindly provided by Dr. Martin Rooimans, Free University Medical Centre, Amsterdam, the Netherlands; and JHU029, JHU011 and JHU012 by Dr. Mariana Brait, Johns Hopkins University School of Medicine, Baltimore, Maryland, United States. All cell lines were maintained on Roswell Park Memorial Institute (RPMI) 1640 Dubelco's Modified Eagle's Medium (RPMI; Life technologies) containing 10% fetal bovine serum (Sigma) at 37°C and 5% CO₂. All the cell lines were tested to be negative for mycoplasma contamination by PCR Mycoplasma Detection Set (TaKaRa Bio, Inc. Kusatsu, Japan) every time before use.

Table 6. General information of cell lines used in the study.

Cell Line	Primary site	RhoA mutation	HPV infection
FaDu	Hypopharynx	-	-
Detroit 562	Nasopharynx*	-	-
92VU040	Oral cavity (tongue)	-	-
92VU041	Oral cavity (floor of mouth)	-	-
92VU078	Oral cavity (tongue)	-	-
92VU080	Oropharynx (base of the tongue)	-	-
92VU094	Oral cavity (tongue)	-	-
92VU120	Oral cavity (tongue)	-	-
SCC25	Oral cavity (tongue)	-	-
JHU029	Larynx	A61V	-
JHU011	Larynx	-	-
JHU012	Larynx	-	-

*derived from pleural effusion. (-) no mutation or HPV infection

Lentiviral vectors: pLKO-shRHOA pLKO.1 Puro containing 3 different shRNAs against RHOA (TRCN0000047710, TRCN0000047711 and TRCN0000047712 hereafter named sh10, sh11 and sh12, respectively) or a control shRNRA (hereafter named shNT) were

obtained for Sigma-Aldrich. pLKO.1 Puro vectors were used to generate HNSCC cell lines with stable downregulation of RHOA protein.

pINDUCER20 vector was used to generate HNSCC cell lines with inducible RHOA overexpression. This plasmid is a Tet-on system, in which the rtTA (reverse tetracycline-controlled transactivator) protein binds and activates the operator TRE (tetracycline response element) only if bound by tetracyclines. Thus, doxycycline initiates the transcription of the cassette, either the green fluorescent protein (GFP) fused to the coding sequence of RHOA (wild-type, wt; or E40Q mutant), or RHOA alone (again wt or E40Q mutant) flanked by the 5' and 3' UTRs (**Figure 13**). All pINDUCER20-RHOA containing vectors were created by gateway LR recombination (Life technologies) using either pDONOR221 (GFP-RHOA tagged proteins) or pENTR4 (RHOA^{UTRs}). The mutant form RHOA E40Q was generated entry gateway vectors using QuikChange mutagenesis kit (Agilent Technologies Inc.) according to manufacturer's specifications. The presence of the mutation was confirmed with Sanger sequencing. The concentration of doxycycline (Dox) (Doxycycline hyclate – Sigma-Aldrich) used to activate the expression of the transgenes *in vitro*, was determined experimentally by exposing transiently transfected cells to increasing concentrations of doxycycline for 48 hours, and determination of protein levels by Western blot (WB).

Generation of isogenic HNSCC cell lines

RHOA downregulation: SCC25 were stably transduced with lentiviral vectors containing short-hairpin RNAs (MISSION shRNA Vectors TRCN0000047710 (sh10), TRCN0000047711 (sh11) and TRCN0000047712 (sh12); Sigma) as described before. Subsequently, cells were selected with puromycin at 1 µg/ml. After antibiotic selection, knockdown was confirmed by Western blot.

Knockout cell line model: For this purpose, CRISPR/Cas9 technology was used. A sgRNA sequence targeting RHOA exon 3 was designed using CRISPR design tool (<http://crispr.mit.edu>). The sgRNA was selected according to its on-target score and low probability of off-targets. The predicted sequence (5' ATCAGTATAACATCGGTATC 3') was cloned into pSpCas9(BB)-2A-GFP (pX458, Addgene #48138) following the protocol described by Zhang's Lab ²⁹⁶. SCC25 and JHU012 cells were transfected with pX458 vector using Human Keratinocyte Nucleofactor™ Kit (Lonza) and The Nucleofactor™ 2b Device (Lonza). GFP positive cells (Cas9 expressing cells) were sorted and seeded at low density 0.5 cells/well in a 96 well-plate to isolate individual clones. Genomic DNA was obtained, and the region targeted by sgRNA interrogated by Sanger Sequencing. RHOA knockout (KO) at the DNA level were further evaluated by Western blot. RHOA KO clones at the protein level were expanded and used in the experiments. Moreover, KO clones were mixed, when corresponded, to generate

polyclonal knockout populations. Cells with low passage were used for all the experiments.

RHOA overexpression: SCC25 and JHU012 cells were stably transduced with pINDUCER20-GFP-RHOA or pINDUCER20-GFP-RHOA-sh12-resistant (wt or E40Q mutants), and the corresponding control vectors by lentiviral infection. Briefly: the first day, TLA-HEK293T cells were plated in a 10-cm plate (3×10^6 cells/plate) to achieve about 80% confluence on the following day. Twenty-four hours after seeding, TLA-HEK293T cells were transfected with 10 μ g of the corresponding lentiviral vector; and 3.5 μ g and 2.75 μ g of the viral packaging vectors pMD.G2 and psPAX2 respectively, using PEI (4 μ g PEI: 1 μ g total DNA). The following day, around sixteen hours after transfection, the media was replaced with 7 ml of 5% FBS DMEM media containing 5 mM sodium butyrate. From this point on, biosecurity level-2 conditions were applied. On the fourth and fifth day, supernatants containing the viral particles were collected and filtered with 0.45 μ m PVDF filters (Millipore).

The day before the infection, HNSCC cells were seeded in 6 well-plates to reach around 40% confluence on the following day. Target cell lines were infected for 10 hours with the lentiviral particles in the presence of 4 μ g/mL polybrene (Sigma-Aldrich). Finally, medium was replaced by fresh complete RPMI medium, and the cells were grown for seventy-two hours. Then, antibiotic-containing selective medium was added and renewed every two days until selection finished. Stably transduced cells were selected with G418 at the following concentrations: 0.7 mg/mL and 1 mg/ml for SCC25 and JHU012, respectively; Life Technologies. Antibiotic-resistant cells were sorted to enrich the GFP-positive population upon culture with doxycycline. RHOA overexpression was confirmed by Western blot.

Sequencing: RHOA mutations in HNSCC cell lines was determined by Sanger sequencing of PCR-amplified genomic DNA. DNA from cell lines was extracted using DNAzol[®] (Invitrogen) according to manufacturer's instructions. PCR amplifications were carried out with primers detailed in **Table 7**. Taq-polymerase (Bio-Taq – Ecogen) was used for all the PCRs. Residual primers and nucleotides were removed from 4 μ l of PCR product by adding 2 μ l of ExoSAP mix (0.1U Exonuclease I, Fermentas and 0.056 U Shrimp Alkaline Phosphatase, Roche). Samples were then subjected to Sanger Sequencing (Macrogen).

Table 7. Sequences of the primers used in this study

Primer name	Sequence (5' to 3')	Application
RHOA exon 2 (F)	gaggttatgccccatggtt	PCR amplification & sequencing
RHOA exon 2 (R)	ctgaagaggcaaaaagctctaa	
RHOA exon 3 (F)	tgtttagaccgtctgccatt	
RHOA exon 3 (R)	tgcttttcagccacttgatg	
RHOA exon 4 (F)	gcatttttctgaagccacaa	
RHOA exon 4 (R)	aaacaacctggcctgtgaag	
RHOA exon 5 (F)	Accgacgagcaaaaactgtct	
RHOA exon 5 (R)	tgaaaaaggccagtaatacata	
RHOA E40Q (F)	gccacatagtctgaaacactgtgggcacatacacc	Site-directed mutagenesis
RHOA E40Q (R)	ggtgatgtgccacagtgttcagaactatgtggc	

(F): forward; (R): reverse

Western blot analysis: Cell protein extraction and quantification: To obtain whole protein cell lysates, cell cultures were washed with ice-cold PBS (Phosphate buffered saline solution – Fisher Scientific) and harvested mechanically with a sterile rubber scraper, using Small GTPase lysis buffer (25 mM Hepes pH 7.5, 150 mM NaCl, 5 mM MgCl₂, 1% NP-40, 1mM DTT, 10% Glycerol) supplemented with protease inhibitors cocktail (Complete™, Mini, EDTA-free Protease Inhibitor Cocktail, Roche). Cell pellets were transferred to Eppendorf microtubes and incubated on ice for 5 minutes. Eventually, the lysate was centrifuged for 10 min, at 12000 rpm and 4°C, and the protein lysate was transferred into a new microtube and stored at -80°C. Protein concentration was quantified with BCA™ Protein Assay Kit (Thermo Scientific). Briefly, 2µl of test sample diluted in distilled water (final volume 25 µl) were mixed with 200 µl of BCA mixture in a 96 well-plate. A series of BSA protein standards diluted in distilled water were prepared alongside with the protein lysates to establish a protein standard curve. The plate was incubated in the dark at 37°C for 30 minutes. Next, absorbance at 595 nm was determined on a plate reader (Sunrise™ model, TECAN Group Ltd.). Protein concentrations were determined by comparison to BSA in the standard curve.

Western blot (WB): Gel electrophoresis: Separation of proteins was performed by one-dimensional SDS-PAGE (Sodium dodecyl sulfate - polyacrylamide gel electrophoresis) assay as follows. Proteins were thawed on ice and thirty µg of protein, upon protein concentration determination, were mixed with loading dye (Laemlli buffer 4X: 250 mM Tris pH 6.8 (Sigma-Aldrich), 4.2% SDS (Sigma-Aldrich), 20% Glycerol (Sigma-Aldrich), 0.008% bromophenol blue (Sigma-Aldrich), 10% 2-mercaptoethanol (Sigma-Aldrich)) and denatured at 95°C for 5 min. Then, proteins were separated by SDS-PAGE electrophoresis in polyacrylamide gels (4% acrylamide stacking gel; 10% acrylamide running gel; Acrylamide – Fisher Scientific). The electrophoresis chamber was filled with running buffer (0.25 M Tris, 1.92 M Glycine (Fisher Scientific) and 34.6 mM SDS (Sigma-Aldrich)) and the current was set to 120 V, allowing the proteins to run and separate until the loading dye went out from the gel. **Protein transfer to filters:** Proteins were electrophoretically transferred from the gel to a polyvinylidene fluoride (PVDF; Amersham – GE Healthcare Life Sciences) membrane. For this, the membrane

and gel were set up as a “sandwich configuration” together with filter papers and sponges in the following order: sponge, Whatman filter (VWR), gel, membrane, Whatman filter and sponge. The transfer was carried out in a tank containing ice-cold transfer buffer (0.23 M Tris and 1.92 M Glycine). The proteins were allowed to transfer for 90-120 min at 110 V and 4°C. Blocking and blotting: The membrane with the transferred proteins was blocked with 5% skim milk or BSA, according to antibody manufacturer’s specifications in PBS-0.1% Tween (Sigma-Aldrich) for 1 hour at room temperature in order to prevent unspecific binding of the antibodies. Next, the membrane was incubated overnight at 4°C with primary antibodies diluted in fresh blocking buffer (**Table 8**). The following day, membranes were washed 3 times for 10 min with PBS-0.1% Tween under agitation to remove unbound primary antibodies. Membranes were then incubated with secondary antibodies conjugated with horseradish peroxidase (Anti-mouse 1:5,000; Anti-rabbit 1:5,000; **Table 8**) for 1 h at room temperature and washed again with PBS-0.1% Tween 3 times for 10 min. Detection: Finally, proteins were detected using ‘Enhanced chemiluminescence system’ kit (ECL – GE Healthcare) blue-light sensitive autoradiography films (AGFA (CP-BU)) or ChemiDoc XRS+ system (Bio-Rad). Specifically, membranes were incubated with 1:1 mixture of detection reagent A and reagent B (which contain a light-emitting non-radioactive substrate for horseradish peroxidase) for 1 min. When autoradiography was used, AGFA films were placed on the top of membranes in a dark room to detect the chemiluminescent signal and followed by an automated film development (Curix 60 – AGFA healthcare). When digital chemiluminescence was used, ChemiDoc system and Image Lab software were programmed to acquire pictures at the desired time points. Quantification of band intensity was performed using ImageJ program (NIH-National Institutes of Health).

Table 8. Antibodies used in the study.

Antibody	Source	Reference	Host	Application (dilution)
RhoA (67B9)	Cell Signaling	2117	Rabbit, monoclonal	WB & IHC (1:1,000)
GFP	Hybridome	RCB2309 : JFP-J1	Rat, monoclonal	WB (1:10)
Vinculin	Sigma-Aldrich	V4505	Mouse, monoclonal	WB (1:1,000)
β-Tubulin	Sigma-Aldrich	T4026	Mouse, monoclonal	WB (1:10,000)
GAPDH	Cusabio	CSB-MA000071M0m	Mouse, monoclonal	WB (1:1,000)
PKN (49)	Santa Cruz	sc-136037	Mouse, monoclonal	WB (1:1,000)
PKN2	Atlas Antibodies	HPA034861	Rabbit, polyclonal	WB (1:1,000)
Polyclonal Swine Anti-Mouse Immunoglobulins/HRP	Dako	P0447	Goat	WB (1:10,000)
Polyclonal Swine Anti-Rabbit Immunoglobulins/HRP	Dako	P0217	Goat	WB (1:5,000)

WB: Western Blot; IHC: Immunohistochemistry. Antibodies for WB were diluted in '5% skim milk or BSA - PBS-0.1% Tween'. Antibodies for IHC were diluted in PBS.

Flow cytometry analysis: GFP expression in HNSCC cell systems overexpressing GFP-RHOA (wt or E40Q) or GFP alone was analyzed by flow cytometry using FACScalibur instrument and Cell Quest Software (Becton-Dickinson). Propidium iodide (PI, Sigma-Aldrich) staining (40 μ g/ml) was used for exclusion of dead cells in the analysis. When necessary, GFP expressing cells were enriched using a FACS Aria sorter and FACSDiva Software (Becton-Dickinson). FlowJo X software was used for data analysis and plot the results.

In vitro cell growth

Cell counting: Cells (RHOA wt or E40Q; fused or not to GFP and the corresponding negative controls) were treated or not with the corresponding doxycycline concentration (see 'Results' section) for forty-eight hours to induce transgene overexpression. Next, cells were seeded in triplicates in 24 well-plates with medium containing or not doxycycline, accordingly (SCC25: 3×10^4 ; JHU012: 5×10^4). For direct cell counting, cells were trypsinized and stained with trypan blue (Serva). Viable cells were counted using a Neubauer hemocytometer at different time points. The average number of cells of three independent experiments run in triplicates is shown.

Sulforhodamine B (SRB) staining: SRB dye stains cell protein, so the absorbance measurement at 595 nm was used as a surrogate marker of cell density²⁹⁷. Cells (RHOA wt or E40Q; fused or not to GFP, and the corresponding negative controls) were treated or not with the corresponding doxycycline concentration (see 'Results' section) for forty-eight hours to induce transgene overexpression. Next, cells were seeded in 96 well-plates (6 replicates per cell line and condition) with medium containing or not doxycycline, accordingly (; SCC25: 3×10^4 ; JHU012: 5×10^4). At the indicated days (see

'Results' section) cells were fixed with 50 μ L of 50% trichloroacetic acid (w/v) (TCA – Fisher Scientific) for 1 h at room temperature (RT), washed with tap water and air-dried. Then, plates were stained with 50 μ L of 0.4% (w/v) sulforhodamine B (SRB – Sigma-Aldrich) in 1% acetic acid (VWR) for 30 min at RT, washed with 1% acetic acid to remove excess of SRB and air-dried. Finally, SRB dye was solubilized with 200 μ L of 10 mM Tris buffer (pH 10) (Fisher Scientific) and absorbance at 595 nm was determined using a microplate reader (Epoch – BioTek Instruments). Absorbance was plotted versus time and used to assess the proliferation of each cell system tested. The averaged absorbance of three independent experiments is shown.

Clonogenicity assay

Cells were seeded in 6 well-plates in triplicate (SCC25: 1.0×10^3 ; JHU012: 1.0×10^3) and allowed to attach and grow as individual colonies. Medium was renewed every week. Once colonies were visible, cells were fixed with methanol-acetic acid solution (3:1 v/v) (Methanol – Fisher scientific; Acetic acid – VWR) for 5 min and stained with 1% crystal violet in methanol (Crystal violet – Fisher Scientific) for 10 min. Dye excess was removed by extensive wash of plates with tap water. The number of macroscopically visible colonies was scored manually and/or using ImageJ software (NIH-National Institutes of Health) on scanned images of plates. Three independent experiments were carried out in triplicate.

Migration (Wound-healing assay)

SCC25 and JHU012 KO RHOA cells in which RHOA wt or E40Q was reintroduced (fused or not to GFP) and the corresponding controls, were treated for forty-eight hours with or without doxycycline at the appropriate concentration to induce the expression of transgenes. Cells (4×10^5) were seeded in triplicates onto 6 well-plates in the presence of two different concentrations of doxycycline (10 and 100 ng/ml) or the absence of the antibiotic. Cells achieved about 90% confluence on the following day. The cell monolayer was then scratched with a sterile micropipette tip, washed with PBS to eliminate scratched floating cells and feed with RPMI-1% FBS medium. The area free of cells was allowed to repopulate the wound by cell migration. The area that remained clear of cells after 4, 8, and 12 hours was quantified using ImageJ software (NIH-National Institutes of Health) and compared with the scratched area at time zero. The averages of three independent experiments in triplicate are shown.

Matrigel invasion assay

The ability of cells to invade through matrigel-coated filters was determined using a 24 well-plate Boyden chamber (Beckton Dickinson; 8 μ m pore size). SCC25 KO RHOA cells in which RHOA wt or E40Q was reintroduced (fused to GFP) and the corresponding GFP control, were treated for forty-eight hours with or without doxycycline at the appropriate concentration to induce the expression of transgenes. Then, 10^5 cells were resuspended in 100 μ L of RPMI-1% FBS in 50% of Matrigel (Corning) and seeded onto

the membrane of Boyden Chambers. The Matrigel was allowed to solidify at 37°C for 20 min. Then, the upper compartment of the transwell was filled with 100 μ L of RPMI-1% FBS and the lower compartment with 600 μ L of RPMI-10% FBS, containing or not doxycycline, generating an FBS-based chemoattraction. Cells were allowed to invade for 48 h and the invading cells were fixed with cold 100% methanol (Fisher Scientific) for 5 min and stained with 1% crystal violet in methanol (Crystal violet – Fisher Scientific) for 10 minutes. Excess of crystal violet was washed out with distilled water. The non-invading cells were removed from the upper part of the chamber with cotton swabs. The total number of invading cells was scored after imaging filters with an inverted microscope (Eclipse TE2000-S – Nikon) at 20X magnification. The number of colonies in three independent microscope fields was scored (**Figure 36**). The averages of three independent experiments in duplicate are shown.

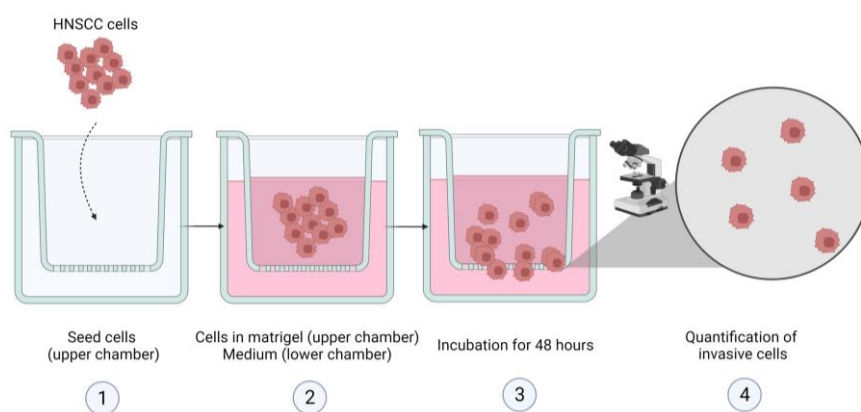


Figure 36. Matrigel invasion assay workflow. (1) HNSCC cells in a 1:1 medium (1% FBS): Matrigel were seeded into the upper part of the Boyden chamber. (2) After Matrigel solidification, medium was added to both upper and lower part of the chamber creating an FBS gradient (top and bottom compartments at 1% and 10%, respectively). (3) Cells were incubated for 48 hours. (5) Upon staining of the cells in the chamber with crystal violet, invading cells were imaged with an inverted microscope and quantified. Created in BioRender.com

In vivo cell growth in subcutaneous xenografts

10 NOD/SCID (Charles River Laboratories) 7-16 weeks old female mice were subcutaneously injected with 1×10^6 SCC25 shNT and SCC25 shRHOA cells into left and right flanks. Specifically, cells were resuspended in 100 μ L of cold PBS: Matrigel (1:1) and injected in the rear flanks of mice under mild anesthesia. The tumor size was measured twice per week for a total of 10 weeks. Tumor volume was calculated based on tumor dimensions, measured using calipers, and expressed in cubic millimeters according to the formula: $V = 0.5a \times b^2$, where 'a' and 'b' are the long and short diameters of the tumor, respectively. At the end of the experiment, animals were euthanized, and the tumors were surgically excised and weighted. Finally, xenograft tumor samples were formalin-fixed (10% neutral buffered formalin – DiaPath), and

paraffin-embedded (Klinipath) for immunohistochemical analysis. The average tumor size and tumor volume are shown.

Study of RHOA interactome by shotgun proteomics

To characterize the effectors proteins and regulators binding to RHOA wt and RHOA E40Q in HNSCC in an unbiased and high-throughput manner we conducted liquid chromatography coupled to mass spectrometry (LC-MS) studies, which has been successfully used before for the identification of GAPs and GEFs associated GTPase proteins¹⁵⁶. Recombinant RHOA wt and RHOA E40Q fused to GST was produced in bacteria cells, purified and used in a pull-down assay with protein cell lysates from a broad collection of HNSCC (**Table 6**). RHOA-bound proteins were analyzed by LC-MS. The full procedure is described as follows.

pGEX-4T-RHOA WT/E40Q vector generation: RHOA open reading frame coupled to EcoRI and BamHI restriction sites was cloned into pGEX-4T vector leading to the expression of a GST-RHOA fusion protein under the control of an inducible lactose promoter. Isopropyl β -D-1-thiogalactopyranoside (IPTG) lactose analog was used for transgene expression. pGEX-4T-RHOA WT construction was used to introduce RHOA E40Q mutation with QuikChange mutagenesis kit (Agilent Technologies Inc.) according to manufacturer's specifications. All plasmids were confirmed by Sanger sequencing.

Expression and purification of GST-fusion proteins: The control empty vector pGEX-4T-GST and pGEX-4T-GST-RHOA constructs (wt and E40Q) were transformed by heat-sock into *E. coli* BL21. Transformed cells were grown in 250 ml of liquid LB medium (1%Tryptone, 0.5%yeast extract, 1%NaCl) supplemented with 100 μ g/mL ampicillin at 37°C, 250 rpm, until OD₆₀₀ reached 0.5. The GST, GST-RHOA wt and GST-RHOA E40Q expression was induced with 0.5 mM IPTG at 30°C until OD₆₀₀ = 1 (3h approximately). Then, bacteria were harvested by centrifugation at 4000 xg, 20 min, and resuspended in 10 mL of buffer A [50 mM Tris-HCl pH 7.5, 1% Triton X-100, 150 mM NaCl, 5 mM MgCl₂, 1 mM 1,4-Dithiothreitol (DTT), 0.1 μ g/mL aprotinin, 1 mM phenylmethylsulfonyl fluoride (PMSF), 200 μ g/mL lysozyme (USB, Chicken egg white)] and incubated for 20 min on ice. The cells were disrupted by sonication on ice with a Fisher Sonic Dismembrator Model 100 (30 seconds constant duty cycle, output 4 and 1 min on ice, 4 cycles). Cell debris and high molecular weight DNA were removed by centrifugation, at 10,000 xg for 30 minutes and the supernatant was recovered. 200 μ L of Glutathione sepharose beads (GSH-sepharose) were equilibrated washing them twice with 400 μ L of buffer A without lysozyme and finally resuspended in 200 μ L complete buffer A. Then, 100 μ L of already equilibrated glutathione sepharose beads was added to the bacterial lysates and incubated in rotation for 2 h at 4°C. Next, the beads were centrifuged at 300 xg for 2 min at 4°C, the supernatant was discarded, and the beads were washed with 400 μ L buffer B (50mM Tris pH 7.5, 0.5% triton X-100, 150mM NaCl, 5mM MgCl₂, 1mM DTT) 3 times. Finally, the beads were resuspended in

300 μ L buffer C (50mM Tris HCl pH 7.2, 150mM NaCl, 5mM MgCl₂, 1mM DTT, 10% glycerol) and protein concentration was quantified using BCA™ Protein Assay Kit (Thermo Scientific), as described before.

Pull-down: 20 μ g of recombinant GST, GST-RHOA wt and GST-RHOA E40Q were incubated for 3 h at 4°C in constant rotation with 2 mg of freshly isolated protein lysate for 10 HNSCC cell lines. Specifically, equivalent amounts of total protein lysate from FaDu, Detroit562, 92VU040, 92VU041, 92VU078, 92VU080, 92VU094, 92VU120, JHU029 and SCC25 HNSCC cells were mixed. The beads were centrifuged at 300 xg for 2 min at 4°C, the supernatant was discarded, and the beads were washed with at 1 mL of protein extraction buffer. Finally, the beads were resuspended in 100 μ L of 50 μ M Tris pH 7.5 and 10 μ M DTT as reducing agent. The eluate was processed for Liquid Chromatography/Mass Spectrometric analysis (LC-MS) as was described before ²⁹⁸.

LC-MS: Sample preparation and trypsin digestion: Protein eluates were concentrated and buffer exchanged to 6 M Urea 50mM ammonium bicarbonate (AB) using 0.5 mL 3KDa cut-off Amicon Ultra ultrafiltration devices (Merck-Millipore). Total protein content was quantified using RCDC kit (Bio-Rad). Eight μ g of protein were reduced with DTT to a final concentration of 10 mM, for 1 h at RT, and then alkylated with 20 mM of iodoacetamide (IAA) for 30 min at RT in the dark. Carbamidomethylation reaction was quenched by addition of N-acetyl-L-cysteine to final concentration of 35 mM followed by incubation for 15 min at RT in the dark. Samples were diluted with 50 mM AB to a final concentration of 1 M Urea, and then modified porcine trypsin (Promega Gold) was added in a ratio of 1:20 (w/w), and the mixture was incubated overnight at 37°C. The reaction was stopped with formic acid (FA) to a final concentration of 0.5%, and the digest was kept at -20°C until further analysis.

Liquid chromatography-Mass spectrometry analysis (LC-MS): Tryptic peptides from RPHP-LC fractions were analyzed on a LTQ Velos-Orbitrap mass spectrometer (ThermoFisher Scientific, Bremen, Germany) coupled to a nano-HPLC system (Proxeon Biosystems, Thermo Fisher Scientific, Bremen). Instrument control was performed using Xcalibur software package, version 2.2.0 (Thermo Fisher Scientific, Bremen, Germany). Peptide mixtures were initially concentrated on an EASY-column, 2 cm long, 100 μ m internal diameter (id), and packed with ReproSil C18, 5 μ m particle size (Proxeon, Thermo Fisher Scientific), and subsequently chromatographed on an EASY-column, 75 μ m id, 10 cm long, and packed with ReproSil-Pur C18-AQ, 3 μ m particle size (Proxeon, Thermo Fisher Scientific). An ACN gradient (5–35% ACN/0.1% formic acid in water, in 120 min, flow rate of 300 nL/min) was used to elute the peptides through a stainless steel nanobore emitter (Proxeon, Thermo Fisher Scientific) onto the nano spray ionization source of the LTQ Velos Orbitrap mass spectrometer. MS/MS fragmentation spectra (200 ms, 100–2800 m/z) of 20 of the most intense ions, as detected from a 500 ms MS survey scan (300–1500 m/z), were acquired using a dynamic exclusion time of 20 s for

precursor selection and excluding single charged ions. Precursor scans were acquired in the Orbitrap analyzer at a mass resolution of 30,000. MS/MS spectra were acquired at the LTQ Velos analyzer using normalized collision energy of 35%. An intensity threshold of 1,000 counts was set for precursor selection. Orbitrap measurements were performed enabling the lock mass option (m/z 445.120024) for survey scans to improve mass accuracy. **Peptide mapping and protein identification:** LC-MS/MS data were analyzed using the Proteome Discoverer software (Thermo Fisher Scientific) to generate mgf files. Processed runs were loaded to ProteinScape software (Bruker Daltonics, Bremen, Germany) and peptides were identified using Mascot (Matrix Science, London UK) to search the SwissProt 20160108 database, restricting taxonomy to human proteins (20171 sequences). MS/MS spectra were searched with a precursor mass tolerance of 10 ppm, fragment tolerance of 0.8 Da, trypsin specificity with a maximum of 2 missed cleavages, cysteine carbamidomethylation set as fixed modification and methionine oxidation as variable modification. Significance threshold for the identifications was set to $p < 0.05$ for the probability-based Mascot score, minimum ions score of 20, and the identification results were filtered to 1% FDR at peptide level, based on searches against a Decoy database (**Figure 37**). The total number of spectra identified for a protein has used as a quantitative measure of protein abundance. LC-MS analysis was carried out at the Proteomics Core Facility, Vall d'Hebron Institut of Oncology (VHIO).

Analysis of spectral count data: To identify and remove background contaminant proteins and in specific interactors, CRAPome (Contaminant Repository for Affinity Purification Mass Spectrometry Data) database was used (crapome.org). This database aggregates negative controls from multiple MS studies and is a valuable tool to identify common contaminants across multiple experiments and eliminate them from data analysis. CRAPome tool calculates SAINT (Significance Analysis of INteractome) Fold change (FC-A and FC-B) scores to determine both, enrichment and specificity. Proteins with SAINT score lower than 0.9 and FC-A and FC-B lower than 3.5 and 2.5, respectively, were excluded. Proteins binding to GST alone were used for further filtering and refinement of the results.

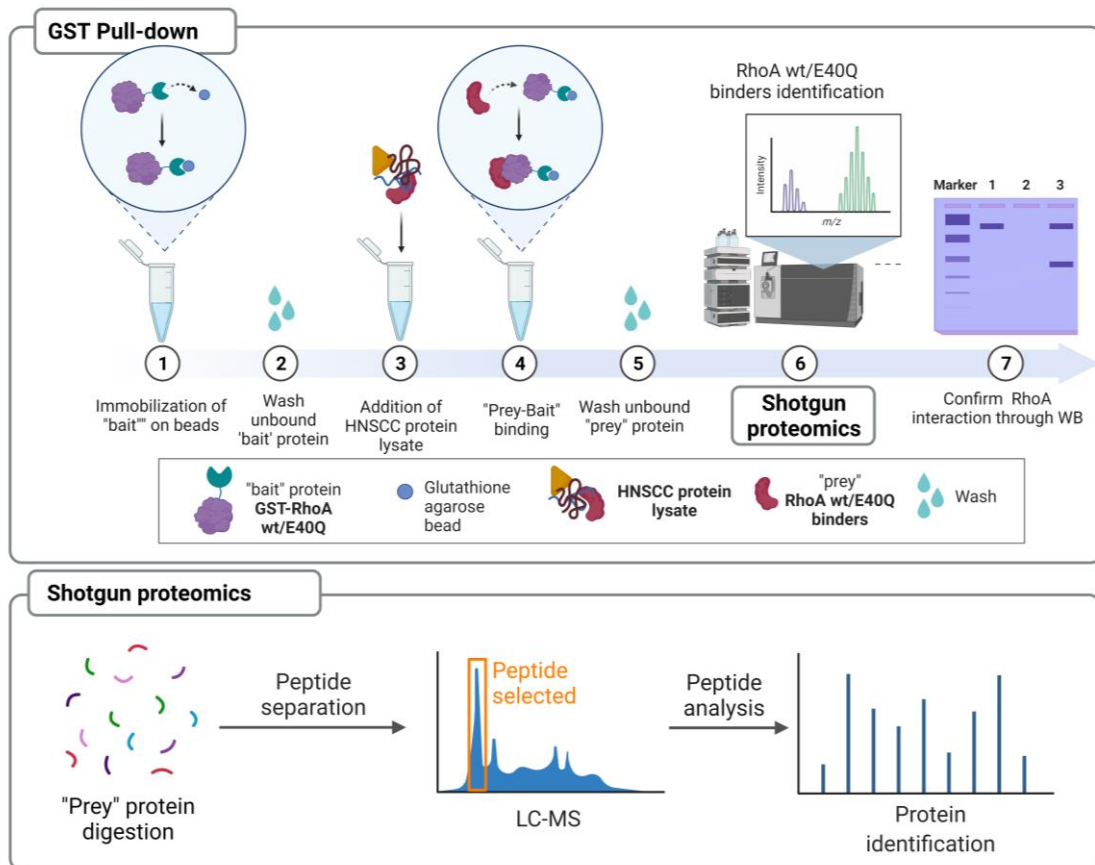


Figure 37. Workflow for the identification of RHOA wt and RHOA E40Q interactors in HNSCC cell lines. GST alone, GST-RHOA wt and GST-RHOA E40Q beads were used to pull-down RHOA interactors from the protein extracts of 10 HNSCC cell lines. The pull-down eluate were subjected to shotgun proteomics for protein identification and quantitation. Created in BioRender.com

Chapter II

RHOA in head & neck cancer

RESULTS

RESULTS

An association between RHOA expression levels and tumorigenesis has been widely studied in different tumor types. Positive correlations between RHOA expression and cancer development and progression had been found in gastric cancer⁶⁹, hepatocellular carcinoma⁷⁸, urinary tract tumors⁸⁹ and breast cancer⁶⁵. But in 2005, we reported for colorectal cancer, that lower RHOA expression in patient tumors associated with poor prognosis¹⁰², suggesting that the role of RHOA in cancer might be context-dependent.

More recently, in 2014, recurrent hotspot RHOA mutations were identified using high throughput genome sequencing, both in hematological malignancies and solid tumor types^{125, 299}. Specifically for head and neck squamous cell carcinoma (HNSCC), RHOA is mutated in approximately 2% of the patients. This is a low percentage compared to other tumor types in which RHOA accumulates mutations, but interestingly E40Q substitutions present in more than 60% of the tumors of this subset of patients, suggesting that RHOA E40Q might elicit a relevant role in the HNSCC tumorigenesis.

That was the reason why we found interesting to know which is the role of RHOA and its hotspot mutant E40Q in this tumor type.

1. Role of RHOA in HNSCC tumors

First, we investigated the role of wild type RHOA in human HNSCC. For this purpose, the study was addressed using both, tumor samples and clinical data from HNSCC patients and HNSCC cell lines.

Study of RHOA in HNSCC patient samples

RHOA expression and patient survival:

Two tissue microarrays (TMA), containing triplicate tumor samples from a total of 360 HNSCC patients, were used to investigate possible associations between RHOA tumor protein expression and clinicopathological features, as well as patient survival. The first TMA contained 95 larynx tumor specimens from patients diagnosed and treated at Hospital Univertari Vall d'Hebron (HUVH) in Barcelona. The second TMA contained 271 surgical tissue specimens from patients diagnosed with HNSCC arising in the oropharynx, hypopharynx and larynx at Hospital Universitario Central de Asturias (HUCA). All samples were retrospectively collected in accordance with the Institutional

Ethics Committee of the HUVH and HUCA. Informed consent was obtained from all the patients. All patients were surgically treated, displayed a single primary tumor and received no chemotherapeutic treatment prior to surgery (neoadjuvant treatment).

RHOA protein expression in tumor samples was determined by immunohistochemistry using a commercially available monoclonal antibody that specifically recognizes RHOA. The specificity of the antibody on formalin-fixed, paraffin-embedded samples was verified by immunostaining in MKN45 diffuse gastric cancer cells which express RHOA at high levels, and a RHOA CRISPR/Cas9 knockout engineered cell system grown subcutaneously in immunodeficient NOD SCID mice (**Figure 38 A**). The relative intensity of RHOA immunostaining in each sample of the tissue microarrays was assessed by an experienced pathologists using a semiquantitative scale ranging from 0 (no staining) to 3 (high staining) and blinded from the clinical data of the patients (**Figure 38 B**).

To interrogate differences in patient survival dependent on RHOA protein expression, tumors were dichotomized into high and low RHOA expression. X-Tile software was used to identify the cutoff staining level maximizing the differences in survival between patients with high and low RHOA expression within the tumor. This software is a tool for the assessment of biological relationships between a biomarker and a clinical outcome²⁹⁵. We evaluated disease-specific (DSS) and disease-free survival (DFS) as clinical survival outcomes. The first refers to the period between the date of diagnosis of the patient, until the date of the last follow up (when the patient is alive) or the date death (when the patient is deceased). Only cancer-associated deaths are considered. Disease-free survival measures the time from surgery until disease relapse, or the last follow up.

Survival analyses were performed using a cutoff RHOA staining value of 1.08 to assort HNSCC patient samples (**Figure 38 C-D**). Therefore, patient samples with staining values of 1.08 or lower were considered as low RHOA tumors (280 of 360 tumors, 77.7%), and those displaying a staining intensity higher than 1.08 were considered as high RHOA (80 of 360 tumors, 22.3%). No differences neither in disease-specific nor disease-free survival were found (Log-rank test $p=0.89$ and $p=0.71$, respectively; **Figure 38 C-D**). Hence, RHOA expression is not a good prognostic biomarker for HNSCC patient survival.

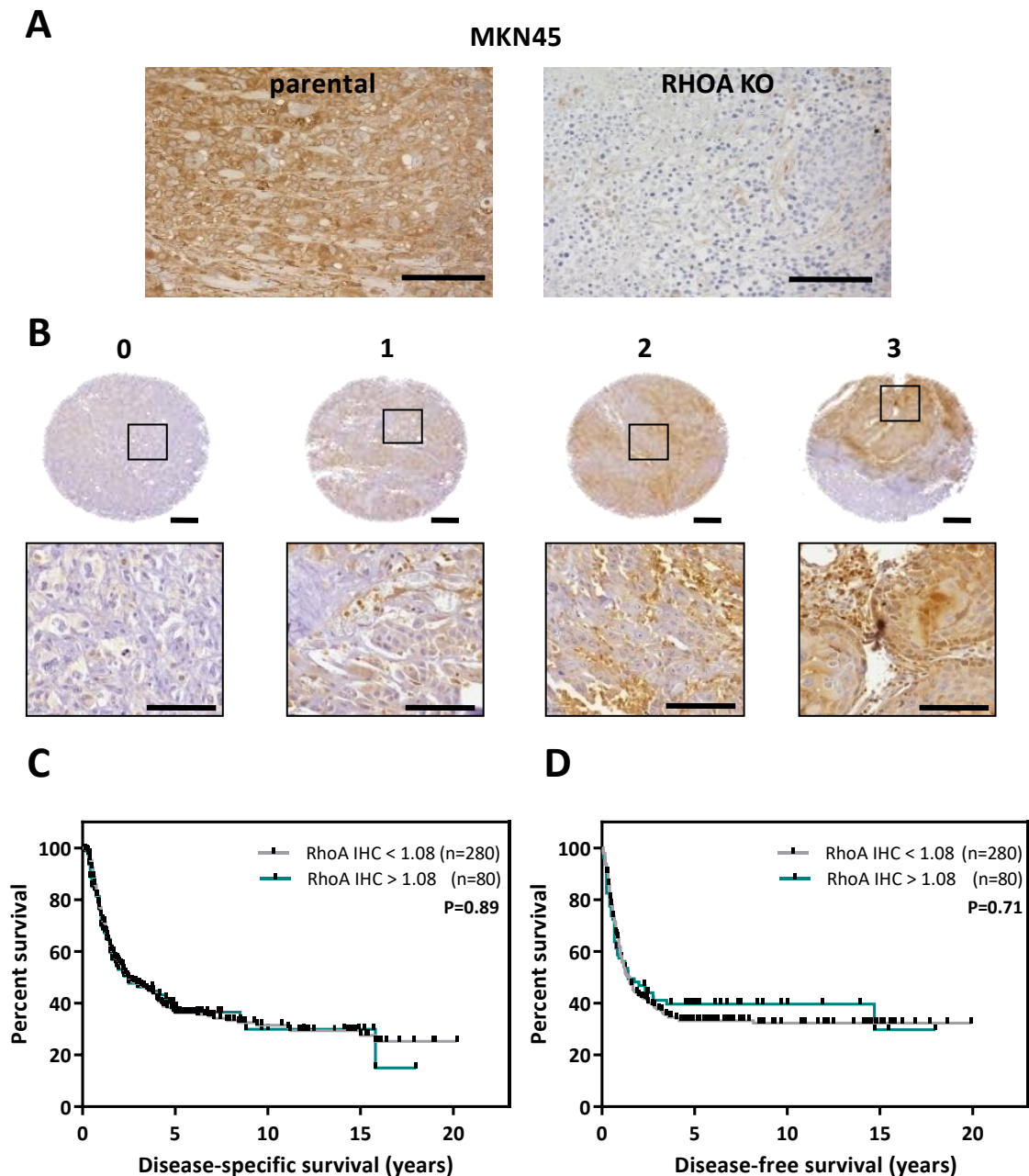


Figure 38. Survival of HNSCC patients with low and high tumor RHOA protein expression. (A) Validation of the antibody specificity against RHOA by immunostaining in formalin-fixed, paraffin-embedded MKN45 parental and RHOA KO cells grown as subcutaneous xenografts in NOD/SCID immunodeficient mice. **(B)** Expression of RHOA was assessed by immunohistochemistry in a cohort of 360HNSCC tumor samples. Representative images of the different RHOA staining scores are shown: 0: no staining; 1: low staining; 2: moderate staining; 3: high staining. Higher magnification images of the boxed regions are shown. **(C-D)** Kaplan-Meier plots showing **(C)** disease-specific and **(D)** disease-free survival of the 360HNSCC cancer patients, as a function of RHOA levels. Cutoff value: 1.08. n: number of patients. Log-rank test p values (P) are shown. Scale bar: 100 μ m.

Associations between RHOA expression and other clinicopathological variables, such as sex, age of diagnostic, degree of differentiation, tumor stage, tobacco and alcohol consumption, among others, were also explored (**Table 9**).

Table 9 Clinicopathological features of the 360 HNSCC patients in the TMAs.

	Total	High RHOA	Low RHOA	p value
Sex, n (%)				
Female	9	4 (5.0)	5 (1.8)	0.11 ^a
Male	351	76 (95.0)	275 (98.2)	
Age at diagnosis (years), mean±SD	58.1 ± 10.0	57.3 ± 10.3	58.3 ± 9.9	0.52 ^b
Degree of differentiation, n (%)				
Good	161	30 (38.5)	131 (47.6)	0.00001 ^a
Moderate	119	17 (21.8)	102 (37.1)	
Poor	73	31 (39.7)	42 (15.3)	
Mean follow up (years), mean±SD	4.0 ± 4.4	3.9 ± 4.2	4.0 ± 4.5	0.46 ^b
Five-year survival				
Alive	58	11 (19.0)	47 (22.2)	0.72 ^a
Dead	212	47 (81.0)	165 (77.8)	
Adjuvant treatment, n (%)				
Yes	248	60 (77.9)	188 (70.4)	0.25 ^a
No	96	17 (22.1)	79 (29.6)	
Stages, n (%)				
1	14	3 (3.8)	11 (4.0)	0.76 ^a
2	31	7 (8.7)	24 (8.6)	
3	62	17 (21.3)	45 (16.2)	
4	251	53 (66.2)	198 (71.2)	
1,2,3	107	27 (37.8)	80 (28.8)	0.41 ^a
4	251	53 (66.2)	198 (71.2)	
Recidiva, n (%)				
Yes	227	48 (60.0)	179 (63.9)	0.51 ^a
No	133	32 (40.0)	101 (36.1)	
Distant metastasis, n (%)				
Yes	129	33 (41.2)	96 (34.3)	0.29 ^a
No	231	47 (58.3)	184 (65.7)	
Tobacco consumption, n (%)				
>50 PA	117	26 (36.6)	91 (34.7)	0.78 ^a
<50 PA	216	45 (63.4)	171 (65.3)	
Alcohol consumption, n (%)				
Yes	291	62 (91.2)	229 (90.2)	1 ^a
No	31	6 (8.8)	25 (9.8)	

^aFisher's exact test; ^bMann-Whitney test; ^cChi-square test.

Interestingly, RHOA expression was associated with the degree of tumor differentiation (grade) (Fisher test = 10^{-5}). Specifically, tumors classified as 'poorly differentiated' exhibited higher levels of RHOA expression (**Figure 39 A**). Interestingly, disease-specific survival (DSS) and disease-free survival (DFS) outcomes of poorly differentiated tumor patients were significantly reduced when compared with 'good differentiated' and 'moderate differentiated' tumor patients (**Figure 39 B-C**). No significant associations were observed between RHOA protein expression and the rest of the clinicopathological variables studied.

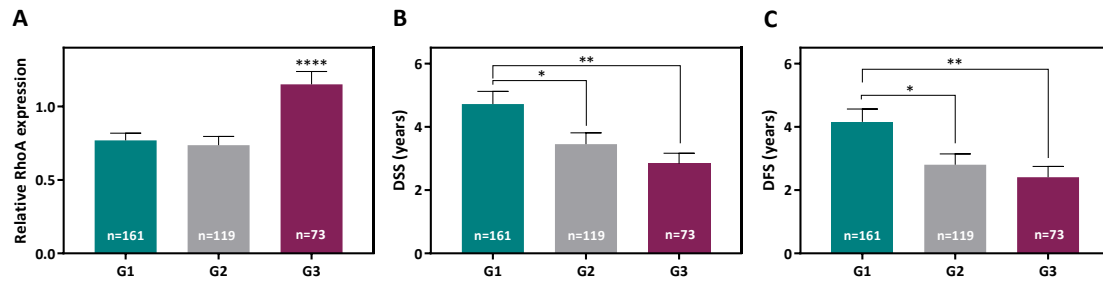


Figure 39. RHOA tumor expression and survival outcomes according to the grade of differentiation of primary HNSCC tumors. The levels of RHOA immunostaining in tissue microarrays containing triplicate tumor samples from 360 patients with head and neck squamous cell carcinoma (HNSCC) were quantified blinded from the clinical patient data. **(A)** The histogram shows the average intensity (\pm SEM) of RHOA immunostaining in HNSCC tumors according to the degree of differentiation (grade). **(B-C)** The average of the disease-specific (DSS)**(B)** and disease-free (DFS)**(C)** survival outcomes expressed in years was calculated for HNSCC tumours according the degree of differentiation (grade). *Student's t-test $p < 0.05$; ** $p < 0.01$; **** $p < 0.0001$. G1: well differentiated, G2: moderately differentiated, G3: poorly differentiated.

It is well known that HNSCC is a very heterogeneous cancer type that comprises different organs (**Figure 28**). The TMAs used in this study contained tumor tissues from oropharynx ($n=182$), hypopharynx ($n=49$) and larynx ($n=129$). We wondered whether RHOA expression level was similar in all tumor sites or conversely the tumor location strongly influenced RHOA expression. RHOA protein expression was found to be significantly higher in hypopharynx and larynx compared with oropharynx (**Figure 40 A**). Hence, we decided to reanalyze patient survival separately for tumor location at the time of diagnosis. Tumors were classified as oropharynx, hypopharynx and larynx location and analyzed separately. RHOA tumor protein expression was dichotomized in two groups (high and low RHOA) as previously described (**Figure 40 B-D**).

No associations between RHOA protein levels and survival were found in oropharynx and hypopharynx head and neck patients (**Figure 40 B-C**). However, a significant association between RHOA levels and disease-specific survival was observed in larynx tumor patients (cutoff value 1.08; Logrank test $p=0.02$; **Figure 40 D, left**). Consistently, a clear trend and close to statistical significance, was also observed between RHOA levels and with disease-free survival in this cohort of patients (cutoff value 1.08; Logrank test $p=0.06$; **Figure 40 D, right**).

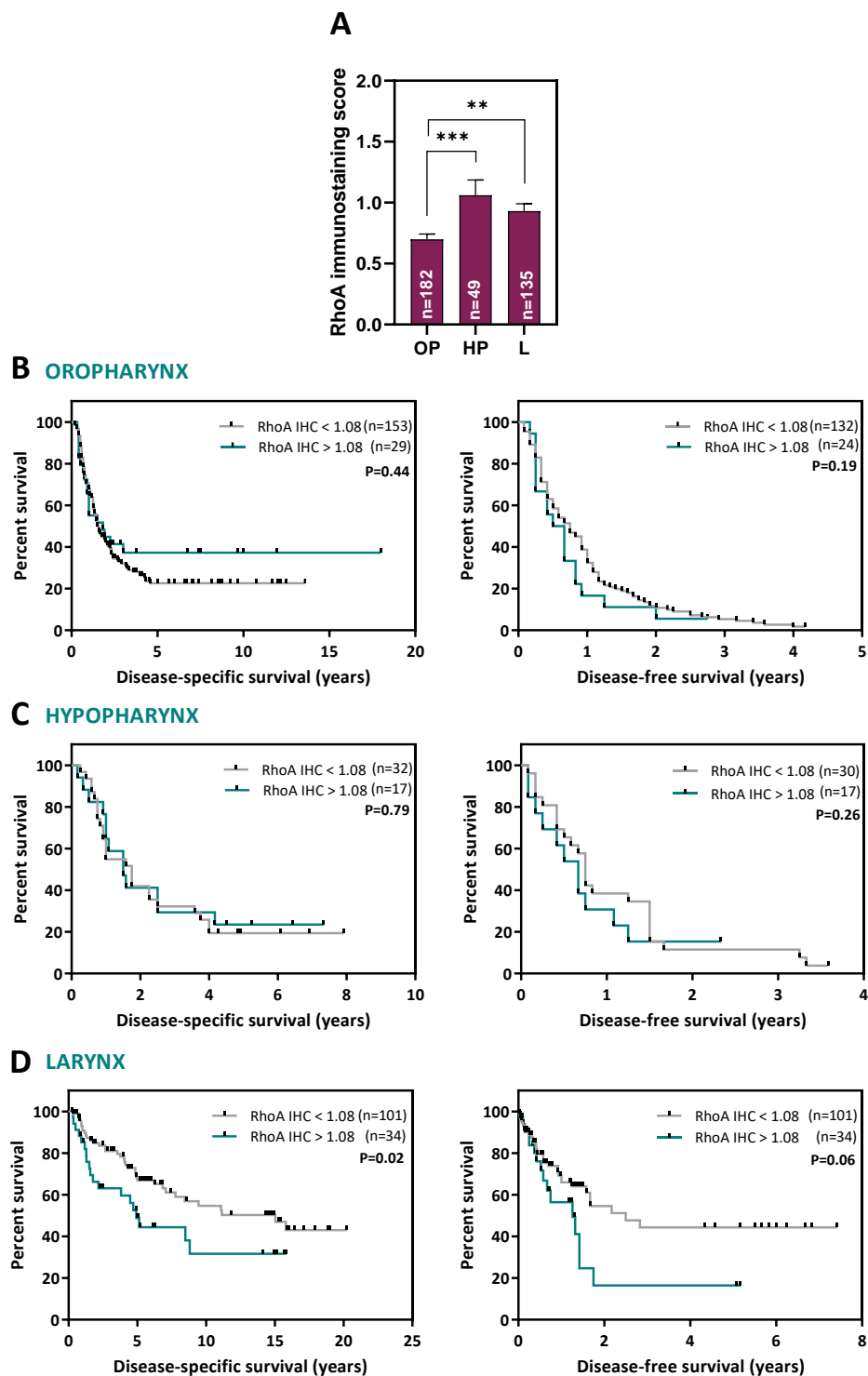


Figure 40. Survival of oropharynx, hypopharynx and larynx tumor patients with low and high RHOA protein expression. (A) RHOA tumor protein expression in patients affected by head and neck tumors in different anatomical regions. Average (\pm SEM) of RHOA protein immunostaining levels (score) in oropharynx (OP), hypopharynx (HP) and larynx (L) cancer patients. n: number of samples. **Student's t-test $p < 0.01$, * $p < 0.001$. (B-D) Kaplan-Meier plots showing disease-specific and disease-free survival of 182 oropharynx (B), 49 hypopharynx (C) and 135 larynx (D) cancer patients, as a function of RHOA protein levels. Cutoff value: 1.08. n: number of patients. Log-rank test p values (P) are shown.**

We also repeated the association analysis between RHOA protein expression and the main clinicopathological features. RHOA expression was associated with the degree of tumor differentiation (grade) in oropharynx (Fisher test = 0.01, **Supplementary Table 1, Supplementary Figure 1**) and hypopharynx (Fisher test= 0.01, **Supplementary Table2, Supplementary Figure 2**) tumors, whereas this association was not observed in larynx (Fisher test= 0.1, **Table 10**). No other associations were observed between RHOA protein expression and the clinicopathological variables studied.

Table 10. Clinicopathological features of the 135 larynx cancer patients in the HUCA/HUVH cohort and associations with RHOA protein expression.

	Total	High RHOA	Low RHOA	p value
Sex, n (%)				
Female	3	2 (5.9)	1 (1.1)	0.17 ^a
Male	132	32 (94.1)	94 (98.9)	
Age at diagnosis (years), mean±SD	59.3 ± 10.2	56.5 ± 9.4	60.3 ± 10.4	0.93 ^b
Degree of differentiation, n (%)				
Good	66	15 (46.9)	51 (56.7)	0.1 ^a
Moderate	39	9 (28.1)	30 (33.3)	
Poor	17	8 (25.0)	9 (10.0)	
Mean follow up (years), mean±SD	1.5 ± 1.9	1.1 ± 1.4	1.6 ± 2.0	0.86 ^b
Five-year survival				
Alive	60	12 (37.5)	48 (57.1)	0.06 ^a
Dead	56	20 (62.5)	36 (42.9)	
Adjuvant treatment, n (%)				
Yes	82	23 (74.2)	59 (71.1)	0.81 ^a
No	32	8 (25.8)	24 (28.9)	
Stages, n (%)				
1	11	2 (5.9)	9 (9.7)	0.60 ^a
2	16	6 (17.6)	10 (10.8)	
3	29	9 (26.5)	20 (21.5)	
4	71	17 (50.0)	54 (58.0)	
1,2,3	56	17 (50.0)	39 (42.0)	0.40 ^a
4	71	17 (50.0)	54 (58.0)	
Recidiva, n (%)				
Yes	49	16 (47.1)	33 (34.7)	0.22 ^a
No	80	18 (52.9)	62 (65.3)	
Distant metastasis, n (%)				
Yes	16	6 (17.6)	10 (10.5)	0.36 ^a
No	113	28 (82.4)	85 (89.5)	
Tobacco consumption, n (%)				
>50 PA	23	8 (29.6)	15 (19.2)	0.28 ^a
<50 PA	82	19 (70.4)	63 (80.8)	
Alcohol consumption, n (%)				
Yes	72	20 (83.3)	52 (74.3)	0.42 ^a
No	22	4 (16.7)	18 (25.7)	

^aFisher's exact test; ^bMann-Whitney test; ^cChi-square test.

Collectively, RHOA protein expression in HNSCC as a single disease does not associate with patient survival but could constitute a good marker for tumor differentiation grade. However, if patient survival is analyzed stratifying patients according to anatomical localization of the tumors (oropharynx, hypopharynx or larynx), there is a significant association between RHOA expression and the survival of patients with larynx cancer. Strikingly, the RHOA association found with the degree of differentiation in oropharynx and hypopharynx tumors was not observed in larynx tumors.

To confirm the associations regarding patient survival and clinicopathological features in the TMAs from the HUCA/HUVH, we conducted additional analysis using the data available at The Cancer Genome Atlas (TCGA). Specifically, we used the cohort of patient samples from “Head and Neck Squamous Cell Carcinoma - TCGA, Firehose Legacy” dataset, which contains mRNA expression levels obtained through RNA sequencing for 528 HNSCC patients. RNA levels in the dataset are expressed as z-scores. This value computes the relative expression of an individual gene and tumor to the gene's expression distribution in a reference population. That reference population is either all diploid tumors for the target gene or, when available, normal adjacent tissue. In the HNSCC Legacy dataset z-score is defined as the number of standard deviations by which a given transcript in a given sample is above or below the mean of expression across all tumor samples in the dataset. Specifically, for RHOA a positive z-score in a tumor sample indicates RHOA expression above the average of all tumor samples, whereas a negative z-score indicates lower expression compared to the mean.

To investigate survival differences associated with the expression of RHOA mRNA within the tumor, patients were divided into two groups (low and high RHOA expression) as described above using X-Tile software. Patients with RHOA mRNA z-score expression below -1.800 were classified in the low RHOA mRNA group, whereas patients with z-score higher than -1.800, were classified in the high RHOA mRNA group.

When the association of RHOA expression with survival (both, disease-specific and disease-free types) was studied considering all patients in the TCGA dataset, no significant differences were obtained between high and low RHOA groups (**Figure 51**).

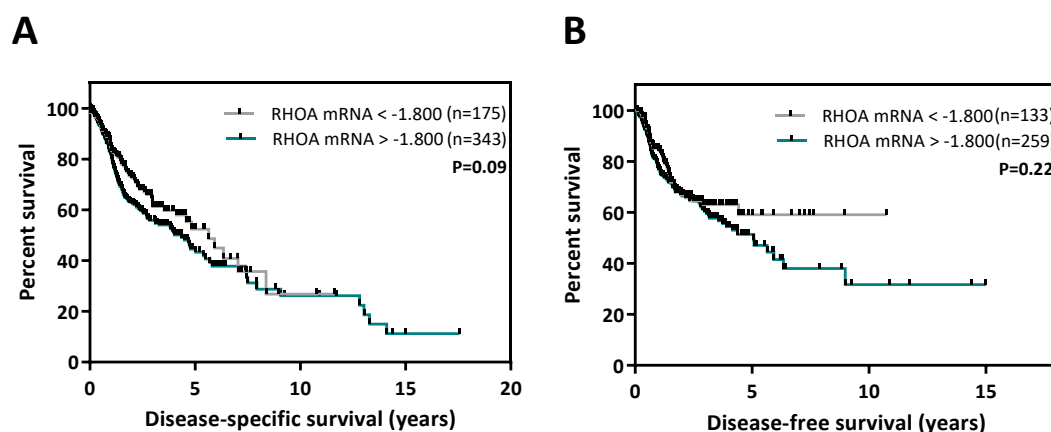


Figure 41. Survival of HNSCC patients as a function of RHOA mRNA expression. Kaplan-Meier plots showing **A)** disease-specific and **B)** disease-free survival of 518 and 392 HNSCC cancer patients, respectively, as a function of RHOA tumor mRNA expression (RNA-sequencing, z-score). Cutoff value: -1.800. n: number of patients. Log-rank test p values (P) are shown.

No significant associations were found either between RHOA transcript expression and patient/tumor clinicopathological features. Only patient sex showed a significant association, specifically, tumors from female patients displayed high levels of RHOA (Table 11).

Table 11. Clinicopathological features of 520 HNSCC cancer patients from TCGA and association with RHOA transcript expression.

	Total	High RHOA	Low RHOA	p value
Sex, n (%)				
Female	136	106 (30.7)	30 (17.1)	0.001 ^a
Male	384	239 (69.3)	145 (82.9)	
Age at diagnosis (years), mean±SD	60.9 ± 11.9	60.9 ± 12.9	60.8 ± 9.6	0.97 ^b
Degree of differentiation, n (%)				
Good	62	42 (12.8)	20 (11.7)	0.67 ^a
Moderate	304	195 (59.6)	109 (63.4)	
Poor	132	90 (27.5)	42 (24.6)	
Mean follow up (years), mean±SD	2.52 ± 2.38	2.51 ± 2.54	2.53 ± 2.02	0.61 ^b
Five-year survival				
Alive	265	165 (53.7)	100 (63.3)	0.06 ^a
Dead	200	142 (46.3)	58 (36.7)	
Adjuvant treatment, n (%)				
Yes	120	83 (66.4)	37 (64.9)	0.87 ^a
No	62	42 (33.6)	20 (35.1)	
Stages, n (%)				
1	27	19 (6.5)	8 (5.3)	0.53 ^a
2	71	52 (17.6)	19 (12.7)	
3	81	52 (17.6)	29 (19.3)	
4	266	172 (58.3)	94 (62.7)	
1,2,3	179	123 (41.7)	56 (37.3)	0.41 ^a
4	266	172 (58.3)	94 (62.7)	
Recidiva, n (%)				
Yes	48	36 (27.7)	12 (19.7)	0.28 ^a
No	143	94 (72.3)	49 (80.3)	
Distant metastasis, n (%)				
Yes	6	3 (0.9)	3 (0.6)	0.40 ^a
No	489	328 (99.1)	161 (99.4)	
Tobacco consumption, n (%)				
>50 PA	105	61 (32.6)	44 (40.4)	0.21 ^a
<50 PA	191	126 (67.4)	65 (59.6)	
Alcohol consumption, n (%)				
Yes	166	107 (75.4)	59 (75.6)	1 ^a
No	54	35 (24.6)	19 (24.4)	

^aFisher's exact test; ^bMann-Whitney test; ^cChi-square test.

We also analyzed TCGA data stratifying HNSCC patients according to the anatomical location of the tumor. This time fourth anatomical regions were defined: oral cavity (OC), oropharynx (OP), hypopharynx (HP) and larynx (L). The oral cavity group was formed by tumors occurring at the oral tongue, floor mouth, hard palate, buccal

mucosa, alveolar ridge, lips and oral cavity as generic label. The oropharynx tumors contained malignancies arising in the base of tongue, tonsils and oropharynx. Hypopharynx and larynx groups were not further subdivided. As observed for RHOA protein, RHOA mRNA expression was dependent on the anatomical location. Significant differences in expression were observed when comparing oral cavity and oropharynx tumors with larynx tumors, which turned out to display the highest RHOA transcript levels (**Figure 42 A**).

We conducted correlation studies to identify association of RHOA mRNA levels with patient survival in all the different HNSCC anatomical locations except for hypopharynx tumors. The small number of tumors in this location (n= 10) prevented a reliable analysis. Patients exhibiting tumors in oral cavity (OC), oropharynx (OP) and larynx were dichotomized into two groups: low and high RHOA mRNA using the z-score cutoff used before for the entire cohort of HNSCC samples (-1.800). The results in patient survival obtained with RHOA mRNA mimicked the results with RHOA protein levels in the TMA (**Figure 42 B-D**). Briefly, high RHOA mRNA levels in larynx patients were associated with lower disease-specific and disease-free survival (**Figure 42 D**), whereas no associations in the survival outcomes studied were found for OC and OP tumor patients (**Figure 42 B-C**).

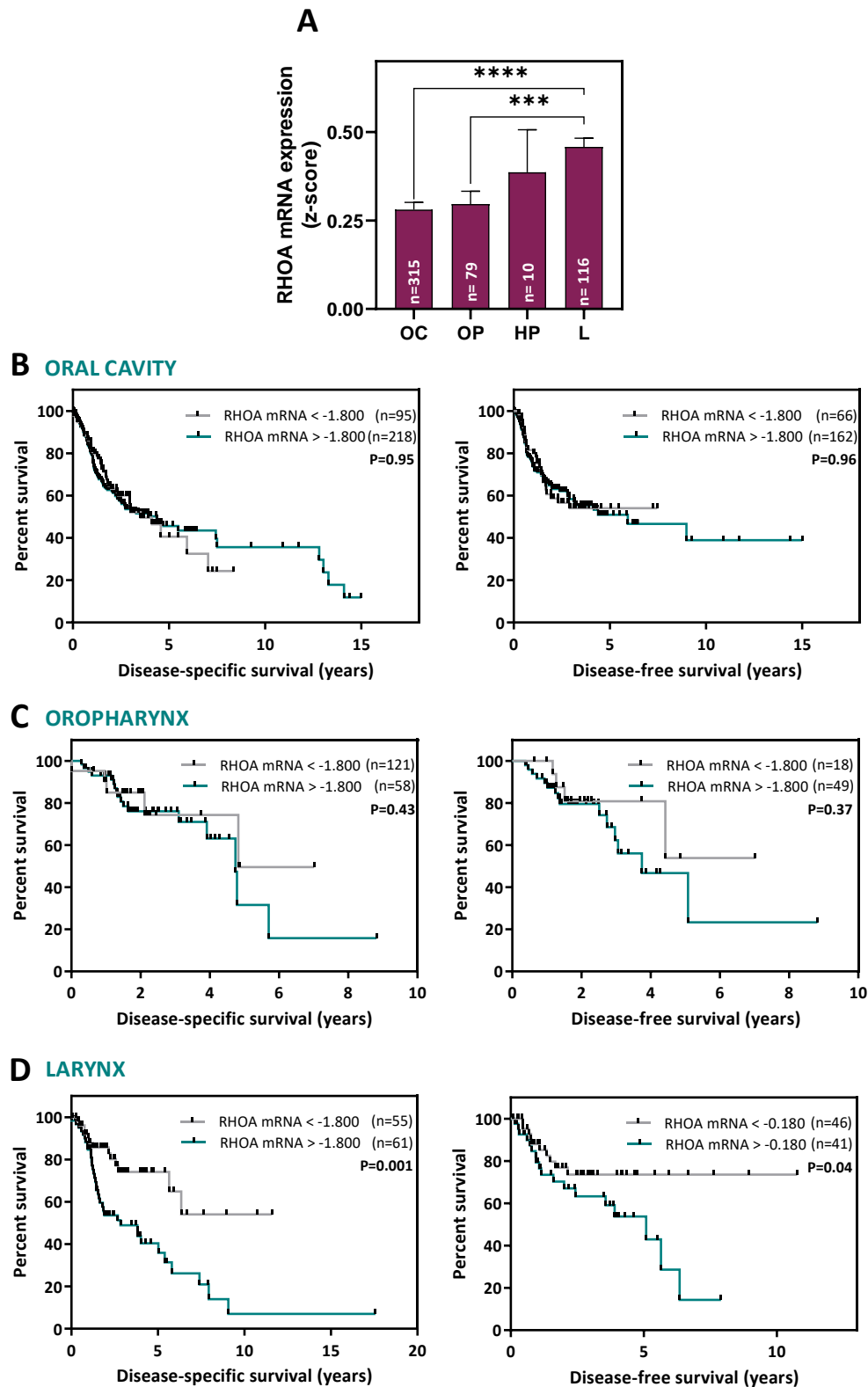


Figure 42. Survival of oral cavity, oropharynx and larynx cancer patients from the TCGA with low and high RHOA mRNA levels. (A) RHOA mRNA levels in different head and neck localizations. Average (\pm SEM) of RHOA mRNA expression (z-score values) in oral cavity (OC), oropharynx (OP), hypopharynx (HP) and larynx (L) samples. n: number of samples. ***Student's t-test $p < 0.001$, **** $p < 0.0001$. **(B-D)** Kaplan-Meier plots showing disease-specific and disease-free survival of 315 oral cavity **(B)**, 79 oropharynx **(C)** and 116 larynx **(D)** cancer patients, as a function of RHOA mRNA levels. Cutoff value: -1.800. n: number of patients. Log-rank test p values (P) are shown.

Potential associations between RHOA transcript expression and clinicopathological features were evaluated individually for each anatomical region. The higher RHOA mRNA expression in female patients observed when analyzing the entire cohort of HNSCC patients was maintained in oral cavity tumors but lost in oropharynx and larynx tumor samples (**Supplementary Table 3-4 and Table 12**). No additional associations were found. The correlation of RHOA levels with tumor differentiation evidenced when analyzing RHOA protein expression in the HUCA/HUVH TMAs, was not observed when addressing the same analysis at the mRNA level in TCGA dataset. RHOA protein expression in the HUCA/HUVH cohort was assessed exclusively in the epithelial compartment of the tumors, while RNA sequencing data was generated using bulk tumors, which additionally to epithelial cells can contain activated fibroblasts, endothelial cells and immune cells infiltrate. Considering that RHOA is a ubiquitous protein, the mixed cellular composition in the RNA sequencing might influence some of the results obtained.

Collectively, our analyses indicate that RHOA expression is a prognosis factor in HNSCC patients affected by larynx tumors. Specifically, high expression of the GTPase associate with poor disease-specific and disease-free survival. And also, reinforce the idea that the role of RHOA in the oncogenic process is highly dependent on the tumor context.

Table 12. Clinicopathological features of 116 larynx cancer patients from TCGA and association with RHOA transcript expression.

	Total	High RHOA	Low RHOA	p value
Sex, n (%)				
Female	20	12 (60)	8 (40)	0.62 ^a
Male	96	49 (51.04)	47 (48.96)	
Age at diagnosis (years), mean±SD	60.93±11.94	60.30±12.24	61.91±11.44	0.67 ^b
Degree of differentiation, n (%)				
Good	8	5 (62.50)	3 (37.50)	0.77 ^a
Moderate	71	37 (52.11)	34 (47.89)	
Poor	33	16 (48.48)	17 (51.52)	
Mean follow up (years), mean±SD	2.49±2.35	2.46±2.26	2.57±2.50	0.42 ^b
Five-year survival				
Alive	57	22 (42.3)	35 (76.1)	0,001 ^a
Dead	41	30 (57.7)	11 (23.9)	
Adjuvant treatment, n (%)				
Yes	27	15 (55.56)	12 (44.44)	1 ^a
No	4	2 (50.00)	2 (50.00)	
Stages, n (%)				
1	2	0 (0.00)	2 (100.00)	N.A.
2	9	6 (66.67)	3 (33.33)	
3	14	7 (50.00)	7 (50.00)	
4	74	40 (54.05)	34 (45.95)	
1,2,3	25	13 (52.00)	10 (48.00)	0.83 ^a
4	74	40 (54.05)	34 (45.95)	
Recidiva, n (%)				
Yes	3	3 (100.00)	0 (0.00)	0.22 ^a
No	28	13 (46.43)	15 (53.57)	
Distant metastasis, n (%)				
Yes	1	0	1 (6.7)	0.36 ^a
No	40	26 (100)	14 (93.3)	
Tobacco consumption, n (%)				
>50 PA	107	54 (50.47)	53 (49.53)	0.21 ^a
<50 PA	6	5 (83.33)	1 (16.67)	
Alcohol consumption, n (%)				
Yes	38	15 (83.3)	23 (85.2)	1 ^a
No	7	3 (16.7)	4 (14.8)	

^aFisher's exact test; ^bMann-Whitney test; ^cChi-square test; N.A.: not applicable.

Study of the role of RHOA in the oncogenic process of HNSCC using cell lines

As shown in the previous section, RHOA protein expression levels are associated with HNSCC patient survival, specifically in larynx-affected cancer patients; and also with cell differentiation, which has a profound impact on tumor progression and has very recently incorporated as an emerging enabling cancer characteristic in the hallmarks of cancer³. To investigate the role of RHOA in HNSCC, we generated isogenic cell line

downregulating this GTPase to further address a functional characterization of this GTPase *in vitro* and *in vivo*.

Generation of isogenic HNSCC cell systems downregulating RHOA expression. We engineered two independent HNSCC cell line systems in which we downregulate or eliminate RHOA expression. The first consisted in a constitute RHOA knockdown (KD) using pLKO lentiviral vectors for the expression of shRNAs against *RHOA* (Sigma Mission clones TRCN0000047710 (sh10), TRCN0000047711 (sh11) and TRCN0000047712 (sh12)). The second was based on RHOA knocked-out using a CRISPR/Cas9 approach.

To select the cell line models for the modulation of RHOA expression, first the genomic sequence of RHOA was analyzed in a panel of 12 HNSCC cell lines available. RHOA DNA was analyzed through Sanger capillary electrophoresis sequencing to determine RHOA mutational status. Only JHU029 larynx cell line was shown to have a RHOA mutation (change A61V) (data not shown). Next, the expression of RHOA protein was assessed by Western blotting and moderate differences were found among the HNSCC cell lines tested (**Figure 43**).

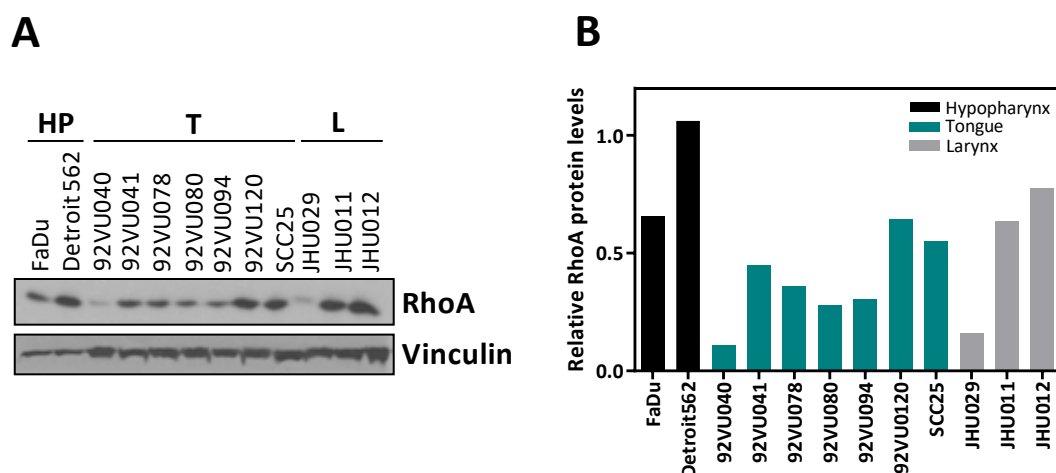


Figure 43. RHOA expression in HNSCC cell lines. (A) RHOA protein expression was assessed by Western blot in a panel of 12 HNSCC cell lines. Vinculin expression is shown as loading control. HP: hypopharynx, T: tongue; L: larynx. (B) The intensity of RHOA signaling (A) was quantified using ImageJ and normalized to the vinculin protein.

Based on RHOA expression results, SCC25 and JHU012 cells lines isolated from oral cavity (tongue) and larynx cancers, respectively, and with moderate levels of RHOA protein expression, were selected for the downregulation of RHOA.

Constitutive overexpression of three independent shRNAs targeting RHOA was used to generate SCC25 RHOA downregulation (RHOA KD) cell systems. After lentiviral transduction and puromycin selection, RHOA downregulation was confirmed by western blot (**Figure 43 A**).

As an alternative approach, the wild type RHOA in SCC25 and JHU012 cells was knocked out using a CRISPR/Cas9 approach. We co-transfected these cell lines with vectors containing a gRNA targeting RHOA exon 3 and the Cas9 endonuclease fused to the GFP fluorescent reporter protein. GFP-positive cells were then sorted, seeded at low density, and allowed to grow as individual clones.

A total of 35 single cell clones for the SCC25 cell sand 60 clones for the JHU012 cells were picked, amplified and analyzed by Sanger sequencing. Low genome editing rate was achieved in both cell line models, with only two clones for SCC25 (clones KO4 and KO31) (5.7%) and five clones for JHU012 (8.3%; clones KO1, KO39, KO40, KO57 and KO87) displaying RHOA mutations after gRNA targeting of exon 3 (**Figure 44 B**). Both SCC25 clones (KO4 and KO31), and KO39 and KO40JHU012 clones showed RHOA frameshift mutations, whereas KO1, KO57 and KO87 JHU012 clones displayed truncating mutations. These last 3 clones were chosen to characterize the RHOA expression loss in JHU012 cells in further analysis. The absence of RHOA protein expression in the clones bearing frameshift and truncating mutations in the RHOA coding sequence was confirmed by Western blot (**Figure 44 C-D**).

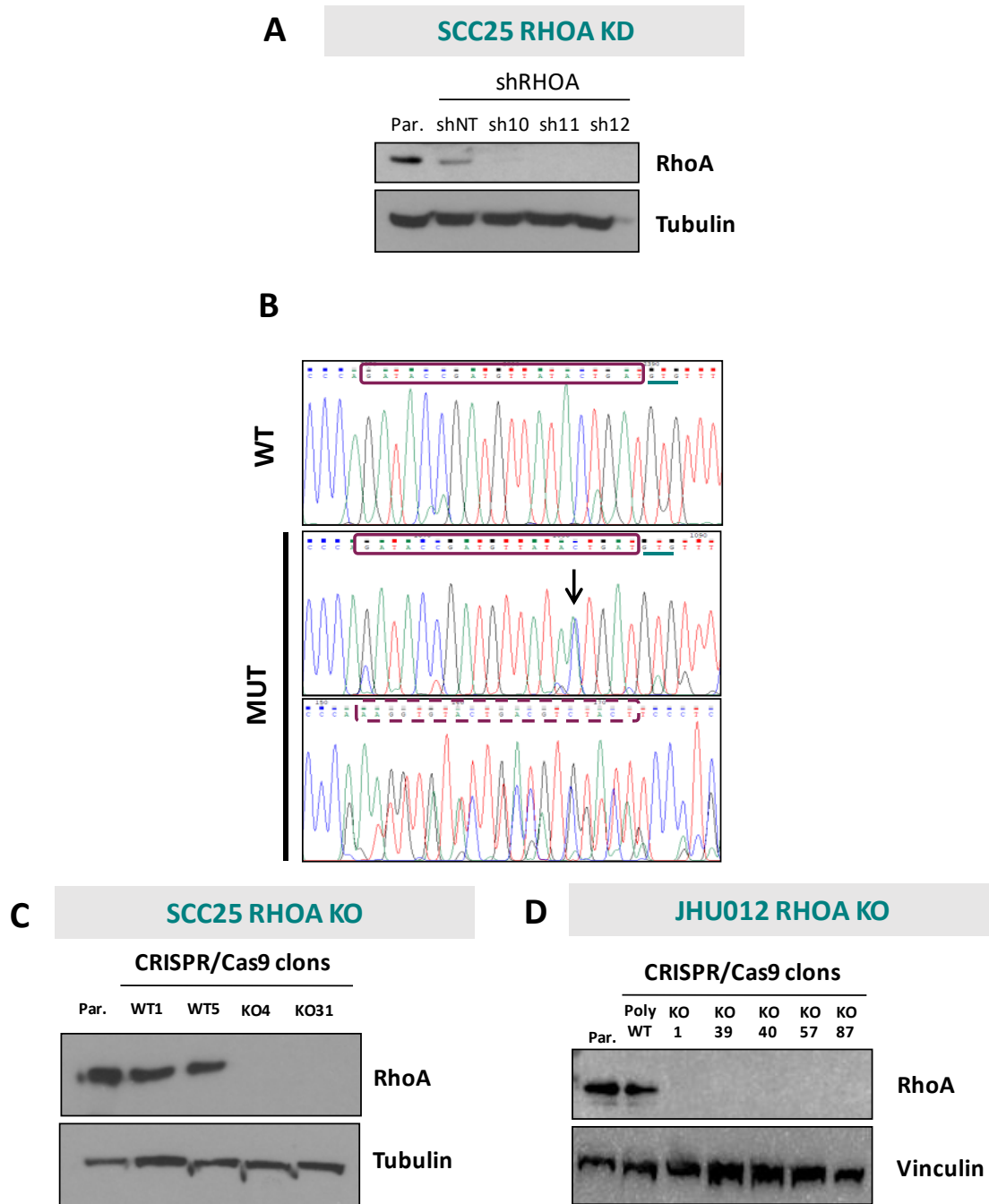


Figure 44. Validation of SCC25RHOA KD, and SCC25 and JHU012 isogenic cell line models with targeted inactivation of RHOA by CRISPR/Cas9 technology. **(A)** Western blot showing the levels of RHOA expression after stable RHOA downregulation (RHOA KD) with targeting shRNAs (sh10, sh11 and sh12) in the tongue cancer cell line SCC25. Tubulin was used as loading control. Par.: parental cell line, shNT: non-targeting shRNA. **(B)** Four-colour DNA chromatogram showing the results of RHOA exon3 sequencing in a parental cell line (WT) and two mutant clones (MUT). A representative example of a point mutation (black arrow) and a frameshift mutation (dashed rectangle) is shown. sgRNA (purple rectangle) and PAM sequences (green line) are indicated in the figure. **(C)** RHOA protein expression in SCC25 parental (Par.), a wild type clon (WT1) and RHOA knockout clones (KO4 and KO31). Tubulin levels are shown as a loading control. **(D)** RHOA protein expression in JHU012 parental (Par.), a pool of three RHOA WT clones (PolyWT) and RHOA knockout (RHOA KO) clones (KO1, KO39, KO40, KO57 and KO87). Tubulin and vinculin levels are shown as a loading control.

RHOA downregulation reduced HNSCC cell growth and migration *in vitro* and *in vivo*. Unlimited proliferation is one of the most important abilities acquired by tumoral cells in the first steps of carcinogenesis. Indeed, the sustained proliferative signaling is one of the eight hallmarks of cancer established by Hanahan and Weinberg⁵. Therefore, the engineered cell line systems were used to study the possible role of RHOA on the growth of HNSCC cells *in vitro*.

Cell growth in SCC25 RHOA KD cell systems was determined by directly counting the number of cells over time, and by sulforhodamine B (SRB) staining of cellular protein content as a surrogate marker of cell density. Despite not reaching statistical significance, RHOA downregulation led to a reproducible reduction in cell growth (**Figure 45 A-B**). This trend was specially observed with the sh12 targeting RHOA.

The ability of a single cell to form a colony is also an important feature of tumorigenesis. This capacity to sustain long-term proliferation was tested in the engineered SCC25 RHOA KD cells growing on a solid substrate and resulted in a significant colony formation reduction on solid substrate compared with the corresponding non targeting control (**Figure 45 C**).

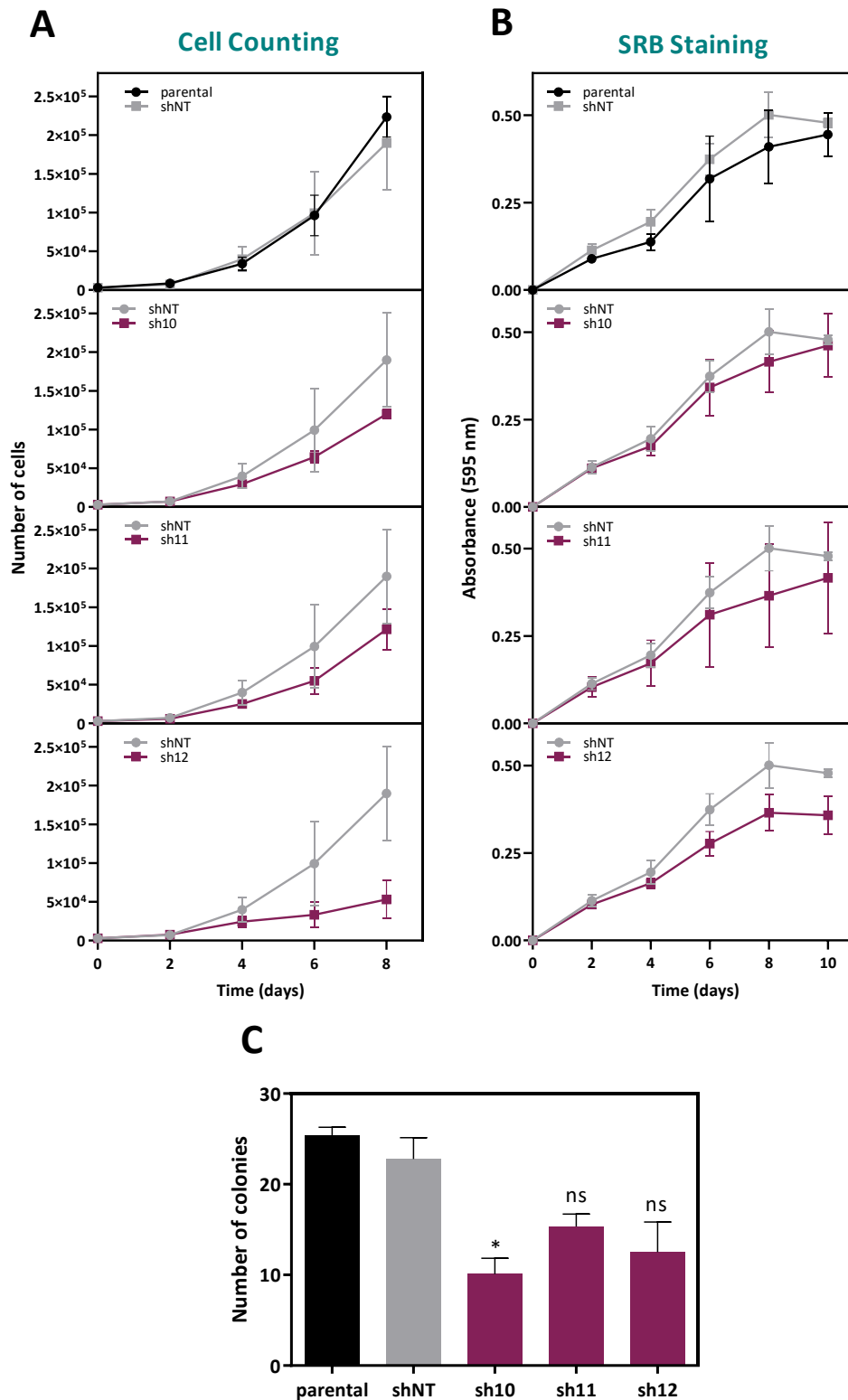


Figure 45. Effects of RHOA expression downregulation through shRNA in cell growth and colony formation ability of SCC25 tongue cancer cells. (A-B) The effects of RHOA downregulation with shRNAs targeting RHOA -sh10, sh11 and sh12- or the corresponding non-targeting control on the growth of SCC25 tongue cancer cells was assessed by cell counting **(A)** and SRB staining **(B)**. **(C)** Changes in the colony formation ability on solid substrate. ns: no significant; *Student's t-test $p < 0.05$, comparing *versus* shNT.

The effect of RHOA downregulation in tumor growth was also investigated *in vivo*. SCC25 cells stably expressing sh12 against RHOA (shRHOA) or the control non-targeted RNA (shNT) were subcutaneously injected in the rear flanks of immunodeficient NOD/SCID mice. A noticeable decrease in growth was observed for RHOA-deficient tumors compared to RHOA shNT tumors, when monitoring the volume of the formed tumors along time (**Figure 46 A**). However, the differences did not reach statistical significance. No significant differences were found either when the weight of tumors was analyzed at endpoint (**Figure 46 B**).

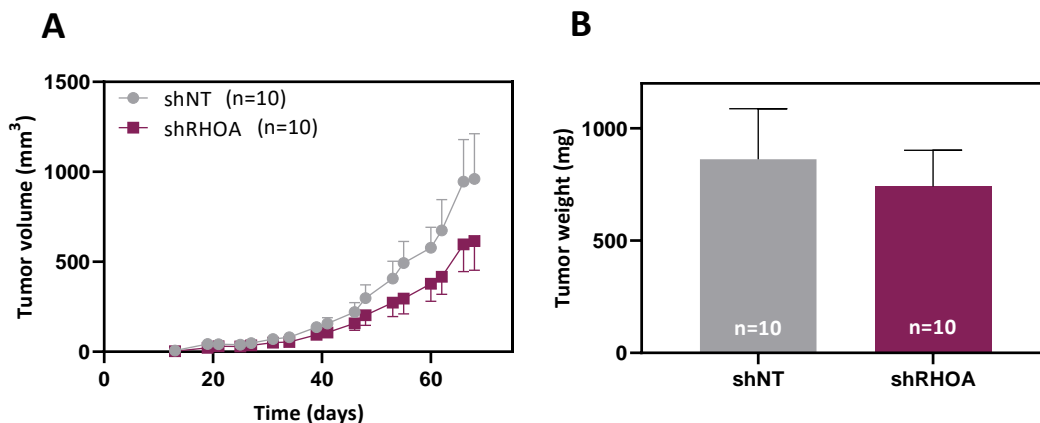


Figure 46. Effect of RHOA downregulation in the growth of SCC25 tongue cancer cells *in vivo*. (A-B) Effects of RHOA downregulation on the growth of SCC25 shRHOA and the corresponding controls shRNA, by measuring tumor volume overtime upon injecting the cells subcutaneously in NOD/SCID animals **A**) and by determining tumor weigh at the endpoint **(B)**. The averages of tumor volume and tumor weigh (\pm SEM) are shown. n indicates number of animals per group.

To further confirm the results obtained with SCC25 RHOA KD cells, namely, a potential oncogenic role of RHOA in HNSCC, the functional characterization of this GTPase was approached as well with the generated RHOA KO cell systems in SCC25 and JHU012 cells through CRISPR/Cas9 technology. The growth of SCC25 KO4 and KO31 clones were assessed by direct cell counting to confirm the phenotype observed in our engineered cell line systems in which RHOA was downregulated using shRNAs. Accordingly, RHOA KO clones exhibited a marked and significant reduction in cell growth compared with parental cells, thus confirming and extending the results obtained with the shRNA approach (**Figure 47**).

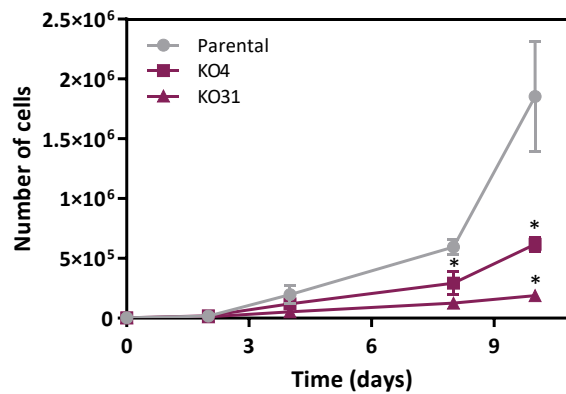


Figure 47. Effect of knocking out RHOA on the growth of SCC25 cells. The effect of knocking out RHOA on cell growth was assessed in SCC25 cells by direct cell counting. Averaged number of cells (\pm SEM) of three independent experiments is represented. *Student's t-test $p < 0.05$.

The functional role of RHOA have not been previously investigated in larynx cancer cells. Therefore, we not only studied cell growth (through cell count and SRB staining) and colony formation ability on solid substrate for JHU012 RHOA KO cells, but also extended the study to possible changes in their motility using a wound healing assay. Three RHOA KO clones (KO1, KO57 and KO87) and three RHOA WT clones (WT15, WT18 and WT25) were pooled together to generate polyKO and polyWT cell line systems. JHU012 polyKO showed a significant reduction in cell growth compared to JHU012 polyWT when growth was assessed through direct cell counting, but not when assessed with SRB staining (**Figure 48 A**). Colony formation ability and migration of JHU012 cells were also impaired when RHOA was knocked out (**Figure 48 B-D**).

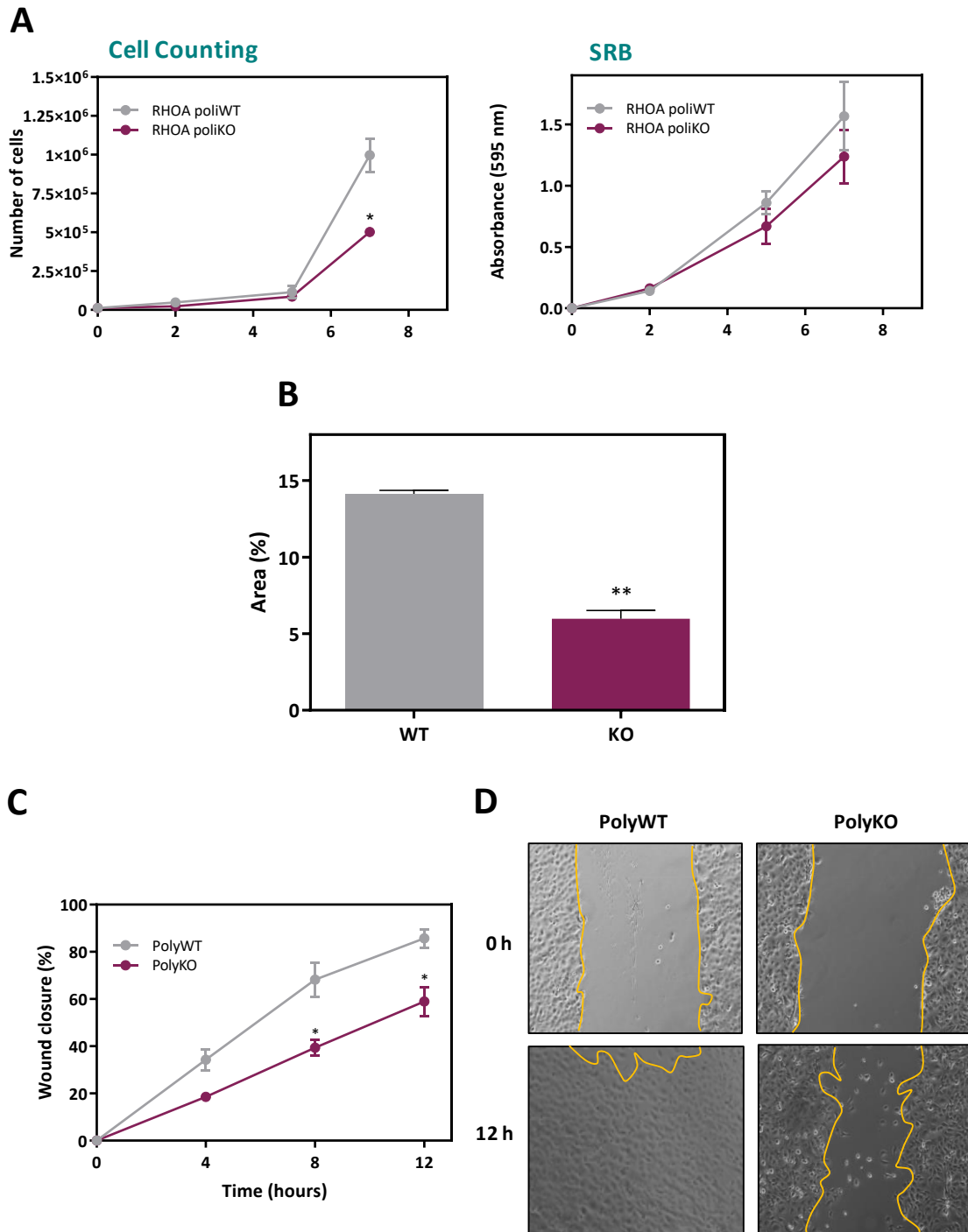


Figure 48. Effect of RHOA KO in cell growth, colony formation on solid substrate and cell migration in JHU012 larynx tumor cells. (A) The growth of JHU012 RHOA KO cells was assessed by direct cell counting and SRB staining. A pool of three RHOA KO clones (KO1, KO57 and KO87 clones, PolyKO) was compared to a pool of three RHOA WT clones (KO15, KO18 and WT25, PolyWT). **(B)** Colony formation ability of cells on solid substrate (data represent a representative experiment performed in duplicate of three independent experiments), and **(C)** cell motility measured by wound-healing of JHU012 PolyKO and PolyWT cell systems. **(D)** Representative pictures of cells at 0- and 12-hour time-point in the wound-healing are shown. The mean (\pm SEM) of three independent experiments carried out in triplicates is shown. *Student's t-test $p < 0.05$.

The results obtained by RHOA downregulation through shRNAs and targeted inactivation through CRISPR/Cas9 in SCC25 cells, are consistent with an oncogenic function in tongue cancer, and this is in good agreement with previous studies³⁰⁰. Moreover, the results obtained by knocking out RHOA in JHU012 cells demonstrate for the first time that RHOA might act also as an oncogene in the tumorigenic process in larynx tumors.

2. RHOA mutations in HNSCC:

As mentioned above, recurrent RHOA mutations are observed in HNSCC, but the biological significance of these mutations has not been investigated. Here, we first analysed the genetic data available at public repositories, and then engineered isogenic cell line systems with RHOA manipulations to directly investigate the functional role of E40Q mutations.

RHOA mutation profile in HNSCC patient tumors

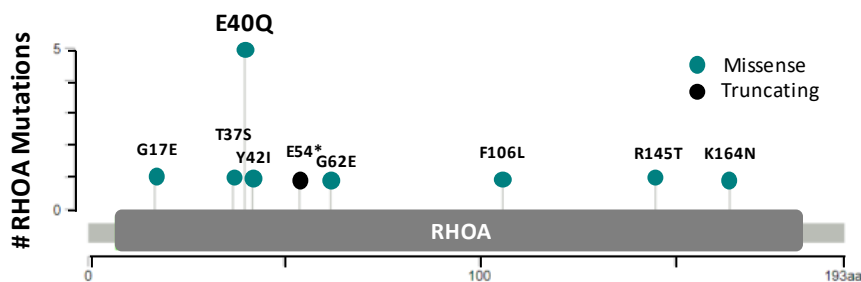
RHOA mutation profile was studied using a cohort of 827 Stage HNSCC patients available at The Cancer Genome Atlas (TCGA) program. Patient samples were collected from 5 different studies^{301,210,211,302} (**Table 13**).

Table 13. Studies used to evaluate the mutational profile of RHOA in HNSCC

Study	Number of cases	Reference
Head and Neck Squamous Cell Carcinoma (TCGA, Firehose Legacy)	530	Broad GDAC Firehose 20160128 run
Recurrent and Metastatic Head & Neck Cancer (MSKCC, JAMA Oncol. 2016)	151	301
Head and Neck Squamous Cell Carcinoma (Johns Hopkins, Science 2011)	32	210
Head and Neck Squamous Cells Carcinoma (Broad, Science 2011)	74	211
Oral Squamous Cell Carcinoma (MD, Anderson, Cancer Discov. 2013)	40	302

Twelve mutations affecting RHOA were identified in these studies, representing a 1.57% mutation rate in the full cohort of 825 HNSCC patients included in this study. Among the 12 mutations identified, 11 mutations were missense and 1 was a truncating mutation (**Figure 49**).

Mutations at codon 40 of RHOA (E40Q) comprised the 45.5% of missense RHOA mutations (5 out of the 11 missense mutations). Regarding the anatomical location of the primary tumors containing RHOA E40Q mutations, we observed that this change was predominant in the oral cavity (4 out of 5 RHOA E40Q mutant tumors), although also detected in larynx malignancies (1 out of 5 RHOA E40Q mutant tumors). No hypopharynx tumors containing E40Q RHOA hotspot mutation were found (**Figure 49**).



Patients with RHOA E40Q mutation (TCGA)		
Patient	Study of Origin	Primary Tumor Site
TCGA-DQ-5625-01	TCGA, Firehouse Legacy	Oral cavity (tongue)
TCGA-CN-6998-01	TCGA, Firehouse Legacy	Oral cavity (tongue)
TCGA-CV-7102-01	TCGA, Firehouse Legacy	Oral cavity (floor of mouth)
TCGA-CV-7410-01	TCGA, Firehouse Legacy	Larynx (glottis)
HN_00313	Broad, Science 2011	Oral cavity

Figure 49. *RHOA* E40Q mutation in HNSCC patients from TCGA. *RHOA* was mutated in almost 2% of HNSCC patients investigated from TCGA^{210, 211, 301, 302}. *RHOA* E40Q mutation represents more than 45% of these mutations. *RHOA* mutation mapper and details of the HNSCC patients with *RHOA* E40Q mutation are shown.

The role of *RHOA* E40Q in HNSCC cell lines

As shown before, *RHOA* is expressed at different levels in the different anatomical locations classified as HNSCC (**Figure 40 and 42**). Moreover, the mutation data in patient samples indicated that *RHOA* E40Q mutations are not restricted to a specific head and neck region. Hence, we decided to investigate the role of *RHOA* E40Q *in vitro* using the *RHOA* KO cell systems generated with SCC25 and JHU012 cell lines, which were derived from tongue and larynx tumors, respectively.

SCC25 KO4 (SCC25 *RHOA* KO) and JHU012 KO1 (JHU012 *RHOA* KO) clones were stably transduced with lentiviral particles containing a pINDUCER20 vector expressing human wild-type *RHOA* or the hotspot mutant *RHOA* E40Q fused to GFP in the N-terminal end (GFP-*RHOA* wt and GFP-*RHOA* E40Q, respectively), or the corresponding empty vector control (GFP). After neomycin selection and FACS/sorting for enrichment in GFP-positive cells, cell lines were analyzed by flow cytometry. GFP-positive cells ranged between 84.7% and 95.3 % upon induction for 48 h of the corresponding transgenes (**Figure 50 A-B**). In addition, doxycycline-dependent expression of *RHOA* was assessed by Western blot using several concentrations of the antibiotic. Because supraphysiological expression of a small GTPase can indirectly affect the stability of other GTPases through the competition for binding to GDP-

dissociation inhibitor such as GDI1^{303, 304}, doxycycline concentration was adjusted in order to re-express RHOA (GFP-RHOA wt or GFP-RHOA E40Q) at levels close to the physiological ones in the parental SCC25 and JHU012 cells. A moderate expression of GFP-RHOA was observed upon 48 hours of induction at concentrations of doxycycline in the ng/ml range in both HNSCC cell line models (**Figure 50 C**). We selected two different concentrations of doxycycline to conduct the subsequent functional analysis: one concentration leading to a physiological RHOA protein expression (10 ng/mL Dox) and thus able to avoid a misbalance between Rho GTPases and the engagement of the crosstalk described above; and another one leading to RHOA protein titers higher than the endogenous (100 ng/mL Dox).

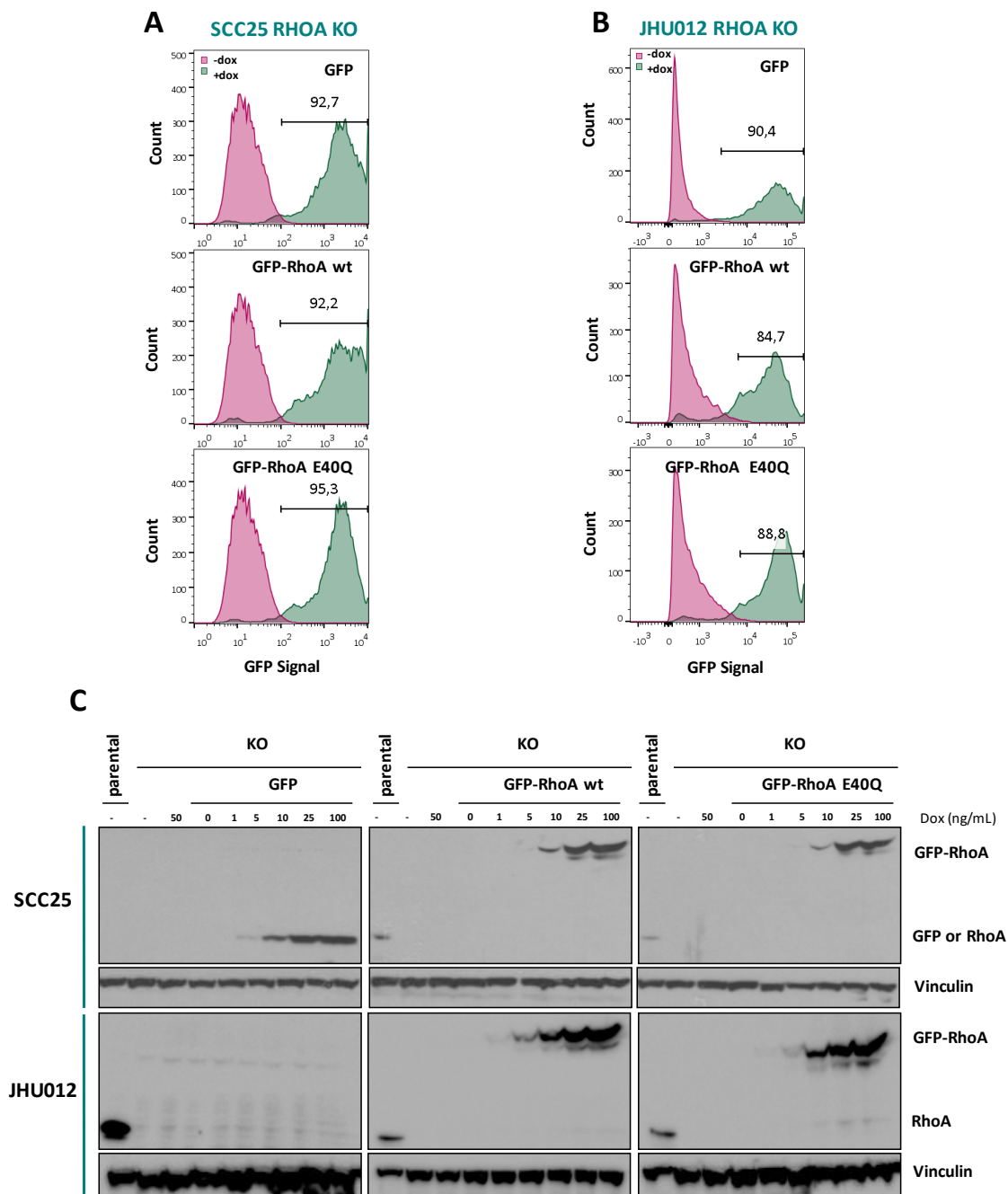


Figure 50. RHOA WT or E40Q mutant reintroduction in HNSCC RHOA KO cell lines. (A-B) Flow cytometry analysis of SCC25 **A**) and JHU012 **B**) engineered cell lines. The percentage of GFP-positive cells is indicated. **(C)** Western blot showing GFP alone and/or GFP-RHOA wt/E40Q expression after 48h treatment with increasing concentrations of doxycycline (ng/mL). Vinculin levels are shown as loading control. GFP in SSC25 (upper left panel) was detected using an antibody against GFP. GFP-RHOA was detected in the rest of panels using an antibody against RHOA.

Differences in cell growth, migration and invasion were assessed in the SCC25 newly engineered cell line systems. Cell growth was assessed as described previously, through direct cell counting and SRB staining. Reintroduction of GFP-RHOA wt would be expected to rescue the growth reduction caused by knocking out RHOA. However,

no differences were found when GFP-RHOA wt or GFP-RHOA E40Q expression were re-expressed, at physiological or supra-physiological levels (**Figure 51 A**).

The formation of distant metastasis is the main cause of cancer death. Changes in the actin cytoskeleton assembly are essential in the migration and invasion of tumor cells, and Rho GTPases are well known for orchestrating cytoskeletal rearrangements and thus contribute to the metastatic process¹⁷¹⁻¹⁷⁴. Next, the effect of RHOA reintroduction on the capacity of SCC25 cells to migrate/invade was assessed. The migration and invasion capacity of the SCC25 RHOA KO isogenic models in which GFP-RHOA wt or GFP-RHOAE40Q were reintroduced was studied using a wound-healing assay and a Boyden chamber Matrigel invasion assay, respectively. In the wound healing assay, the motility of the cells is evaluated by their capacity to close a wound made on a confluent monolayer of cells. In the Boyden chamber Matrigel invasion assay, the invasive capacity of the cells is measured by their capacity to degrade and migrate through a complex extracellular matrix, mimicking the basement membrane components, in response to chemo-attractants. The motility of SCC25 RHOA KO cells was not affected upon GFP-RHOA wt or GFP-RHOA E40Q doxycycline-induced overexpression (**Figure 51 B**). Likewise, no differences were detected in the Matrigel transwell invasion capacity of SCC25 RHOA KO cells after reintroduction of wild type or E40Q RHOA (**Figure 51 C**).

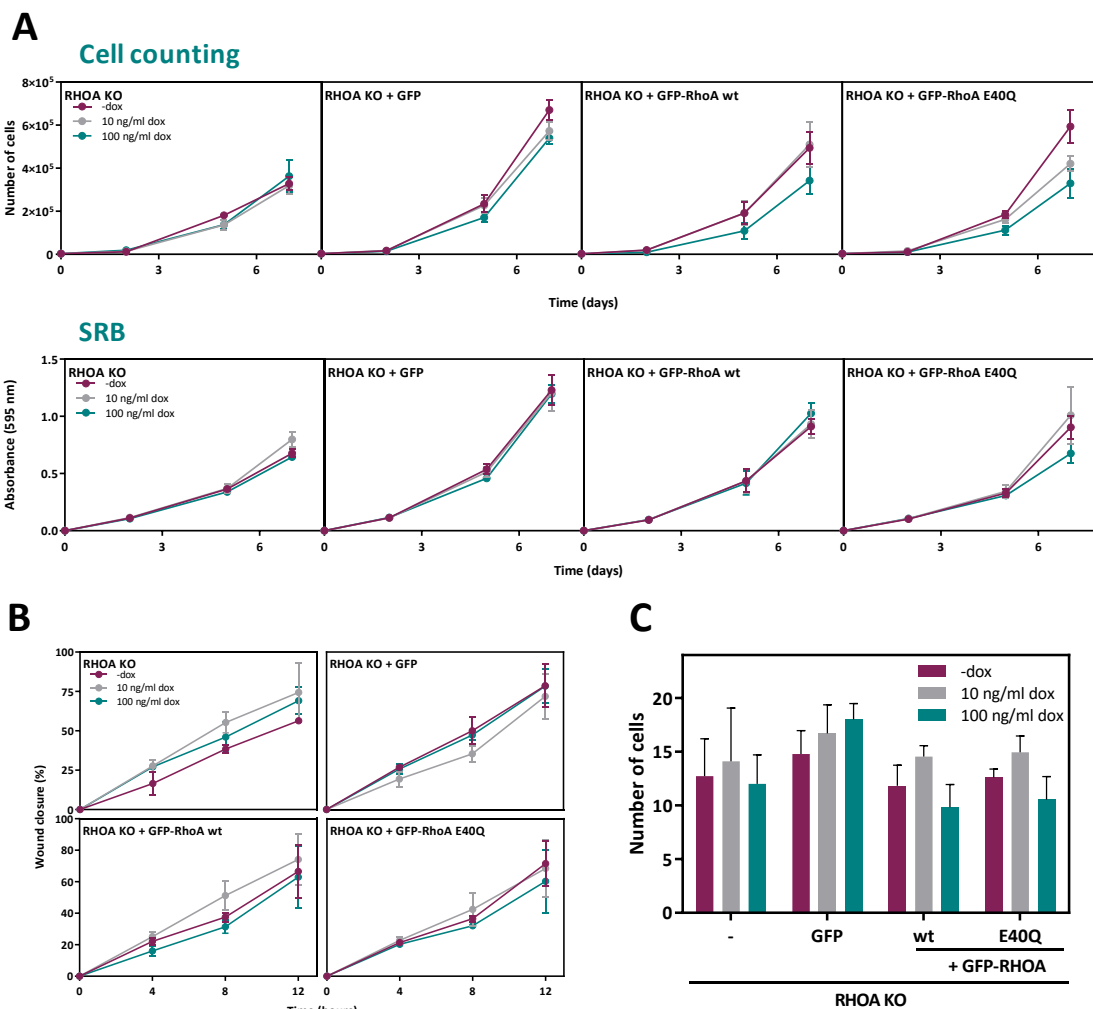


Figure 51. Effect of GFP-RHOA wt and GFP-RHOA E40Q reintroduction in the SCC25 RHOA KO cell line model. (A) Cell growth of SCC25 RHOA KO with doxycycline-inducible (10 and 100 ng/ml) overexpression of GFP-RHOA wt or E40Q measured by direct cell counting and SRB staining approaches. **(B)** Motility of cells in **(A)** measured by wound-healing assay. **(C)** Invasion capacity of cells in **(A)** measured as the number of cells reaching the lower chamber in a Matrigel transwell invasion assay. Cells overexpressing GFP in a doxycycline-dependent manner were used as control in all the assays. The mean (\pm SEM) of three independent experiments carried out in triplicates is shown.

We also assessed cell growth in the JHU012 RHOA KO isogenic models in which GFP-RHOA wt or GFP-RHOAE40Q was reintroduced. Similarly, to the results observed in SCC25 cells, no differences were found in the number of cells or SRB staining upon GFP-RHOA wt or E40Q doxycycline-dependent expression (**Figure 52**). Accordingly, these intriguing results observed in tongue and larynx HNSCC cell lines were not cell type dependent.

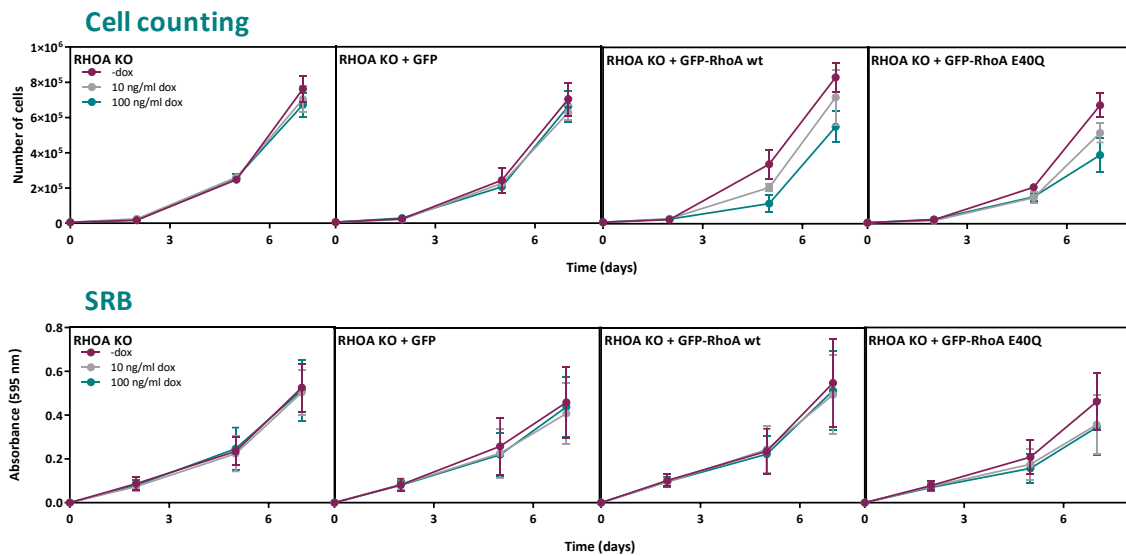


Figure 52. Effects of RHOA wt and RHOA E40Q reintroduction in JHU012 RHOA KO cell model. Cell growth of JHU012 cancer cells RHOA KO after induction of GFP-RHOA wt or E40Q overexpression (10 and 100 ng/ml Dox) and using GFP overexpression as control, measured through cell counting and SRB staining approaches. Overexpression of GFP was used as control in every assay. The mean (\pm SEM) of three independent experiments carried out in triplicates is shown.

We were highly intrigued by the fact that RHOA re-expression in RHOA-deficient models was unable to restore the cellular features altered by the later.

Analysis of the human genome with high-throughput technologies has revealed that only about 1.5% of the genetic material encodes for proteins. Indeed, most genomic DNA participates in the regulation of gene expression at the transcriptional or post-transcriptional level. In eukaryotic cells, mature mRNAs contain untranslated regions in the 3' and 5' end of the coding region (3'-UTR and 5'-UTR, respectively). UTRs are instrumental in the post-transcriptional regulation of gene expression, being highly involved in the transport of mRNAs out of the nucleus, the subcellular localization and stability, and in the control of the translation efficiency³⁰⁵. The lentiviral vectors used for the reintroduction of GFP-RHOA wt and GFP-RHOA E40Q in the SCC25 and JHU012 HNSCC RHOA KO cell line systems, contained exclusively the RHOA protein coding sequencing, namely open reading frame. We wondered whether the inability of exogenous GFP-RHOA to restore RHOA-deficiency could be related to the lack of regulatory sequences such as UTRs in the new source of RHOA within cells. In addition, it has been reported that GFP and other tags, such as His-tag might affect the bioactivity of the protein to which it is bound^{306, 307}. Although GFP did not impair RHOA function in other cell line models such as colorectal or gastric cancer, but we could not rule out that key binding or catalytic sites in HNSCC would be masked by fusion and folding of GFP reporter fluorescent protein. Accordingly, we build a pINDUCER20 lentiviral vector containing RHOA wt and RHOA E40Q lacking GFP tag in the coding sequencing and containing the full length 5'- and 3'-UTRs.

We generated SCC25 RHOA polyKO and JHU012 RHOA polyKO cell systems by pooling together the clones KO4 and KO31 for SCC25; and clones KO1, KO57 and KO87, for JHU012. Next, RHOA polyKO cell line systems were stably transduced with the newly generated constructs encoding RHOA wt or RHOA E40Q (henceforth called RHOA wt^{UTRs} and RHOA E40Q^{UTRs}). After neomycin selection and forty-eight hours of induction with doxycycline, the expression of RHOA was assessed by Western blot to confirm efficient transgene expression. Results showed that RHOA wt^{UTRs} and RHOA E40Q^{UTRs} were expressed in both SCC25 and JHU012 RHOA polyKO (**Figure 53 A**).

Then, changes in growth and cell migration were investigated in SCC25 and JHU012 after RHOA reintroduction. Reintroduction of RHOA wt^{UTRs} or RHOA E40Q^{UTRs} expression in the SCC25 and JHU012 with targeted inactivation of RHOA is cause statistically significant changes in growth or cell motility (**Figure 53 B-C**).

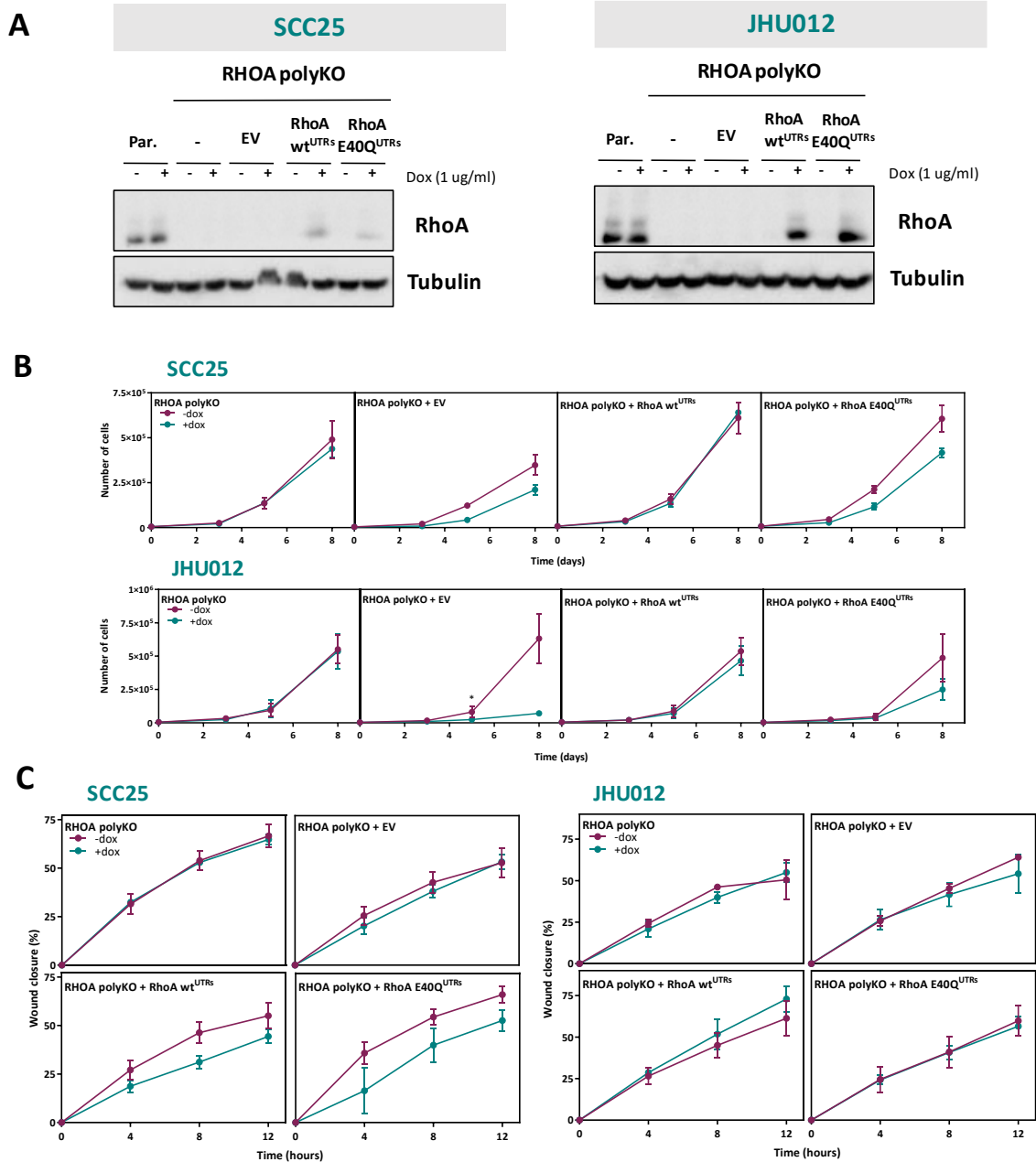


Figure 53. Functional analysis of the reintroduction of RHOA wt^{UTRs} and RHOA E40Q^{UTRs} in SCC25 and JHU012 RHOA polyKO cell line models. (A) Western blot showing RHOA wt^{UTRs}/E40Q^{UTRs} expression upon cell culture of cells with 1 μ g/ml Dox for forty-eight hours. Tubulin levels are shown as a loading control. Par: parental. **(B)** Cell growth by direct cell counting of RHOA polyKO cells after induction of RHOA wt^{UTRs} or E40Q^{UTRs} overexpression (1 μ g/ml Dox). **(C)** Motility of RHOA polyKO cells after induction of RHOA wt^{UTRs} or E40Q^{UTRs} overexpression (1 μ g/ml Dox) measured by wound-healing assay. Cells transduced with an empty-vector (EV) were used as control. The mean (\pm SEM) of three independent experiments carried out in triplicate is shown. * Student's t-test $p < 0.05$.

3. Characterization of the interactome of RHOA wt and RHOA E40Q in HNSCC cell lines

RHOA is an important molecular switch that acts through binding and activating several downstream effectors⁵². Interestingly, when *RHOA* is mutated in this tumor type, most of the mutations, around 60% of them, are E40Q¹²⁵ (**Figure 49**). However, the effects of this mutation have not been studied in detail. In 'Chapter I' of this thesis, it has been demonstrated through a Yeast-Two-Hybrid (Y2H) approach that RHOA E40Q fails to bind to kinectin, a microtubule-associated protein required for the transport of the cellular organelles and vesicles, and NET1, a RHOA-specific guanine exchange factor (GEF) that mediates RHOA activation by Smad-mediated transcription. Therefore, the interactome of RHOA wt and RHOA E40Q in HNSCC cell lines was investigated here more in detail using an unbiased method.

Shotgun proteomics refers to the use of bottom-up proteomic techniques in identifying proteins using a combination of high-performance liquid chromatography combined with mass spectrometry (LC/MS). To assess this, a pulldown assay was coupled to (LC/MS) analysis. RHOA wt or the RHOA E40Q mutant were produced in bacteria as a fusion protein with GST. These proteins were purified and used as 'bait' to identify binding proteins in a protein lysate obtained from mixing equal amounts of total protein extracted from 10 HNSCC cell lines (FaDu, Detroit562, 92VU040, 92VU041, 92VU078, 92VU080, 92VU094, 92VU120, JHU029 and SCC25), used here as a protein lysate representative of human HNSCC tumors. RHOA and interacting proteins were pulled down with glutathione sepharose beads; and binding proteins were eluted and identified using LC/MS after being previously digested (**Figure 37**).

As expected, RHOA wt was found to bind to proteins that are known RHOA interactors, including some effectors (DIAPH1, RTKN, PKN1, PKN3) and regulators of RHOA activity (data not shown). Interestingly, there were some notable absences on the list of known RHOA binders, such as ROCK which are among the best known RHOA effectors. This issue might be due to these proteins not being expressed at significant levels in HNSCC cell lines, or the many settings and parameters used in LC/MS to detect the interactome. Further analysis needs to be done to address this question.

The Contaminant Repository for Affinity Purification (CRAPome)³⁰⁸ was used to find only the *bona fide* interactors, binding proteins that did not pass stringent filtering criteria (Saint score greater than 0.9 and FC-A and FC-B, greater than 3.5 and 2.5, respectively; see 'Materials and Methods' section) were excluded. Moreover, it was determined that the fold change between the spectral counts obtained from the LC/MS between GST-RHOA wt and GST-RHOA E40Q (FC GST-RHOA wt vs GST-RHOA E40Q) had to be higher than 4. Finally, proteins that appeared in a $\geq 5\%$ in the

CRAPome repository were considered as contaminants and eliminated for further analysis.

Importantly, after this filtering, 8 proteins binding to RHOA wt, but not to RHOA E40Q, were identified (**Table 14**).

Table 14. RHOA interacting proteins identified by MS analysis.

Accession	Protein	GST-RhoA wt	GST-RhoA E40Q	FC (#Spec. Counts)		CRAPome (%)
		#Spec Counts	#Spec Counts	GST-RhoA wt	vs GST-RhoA E40Q	
PKN1_HUMAN	Serine/threonine-protein kinase N1	12		NA		0.73%
PKN2_HUMAN	Serine/threonine-protein kinase N2	74	8	9,25		2.92%
PKN3_HUMAN	Serine/threonine-protein kinase N3	5		NA		3.89%
RIPOR1_HUMAN	Rho family-interacting cell polarization regulator 1	10	2	5		0.001%
ARHG2_HUMAN	Rho guanine nucleotide exchange factor 2	9		NA		4.62%
ARHGB_HUMAN	Rho guanine nucleotide exchange factor 11	4		NA		1.22%
ARHGC_HUMAN	Rho guanine nucleotide exchange factor 12	3		NA		0.49%
PGAP1_HUMAN	GPI inositol-deacylase	8		NA		0%
GRN_HUMAN	Progranulin		2	NA		2.19%
PURB_HUMAN	Transcriptional activator protein Pur-beta		3	NA		5.60%

#: number; vs: *versus*; FC (#Spec Counts): Fold change of the Spectral counts; CRAPome (%): percentage of presence in CRAPome repository; NA: not applicable.

Interestingly, PKN family proteins PKN1, PKN2 and PKN3 were in this short list, suggesting that inactivation of PKN signalling may be involved in the biological role of this hotspot RHOA mutation. To validate this observation, the levels of PKN1 and PKN2 in the protein lysate pulled down with GST-RHOA wt or GST-RHOA E40Q beads, were assessed by Western blot. In good agreement with the LC/MS results, it was observed robust binding of RHOA wt to PKN1 and PKN2, whereas no binding was detected to the recurrent E40Q RHOA mutant (**Figure 54**).

In addition, two proteins were found that do not bind to RHOA wt but bind to RHOA E40Q, following the same criteria described above. There were progranulin and the transcriptional activator protein Pur-beta (green-coloured, **Table 14**).

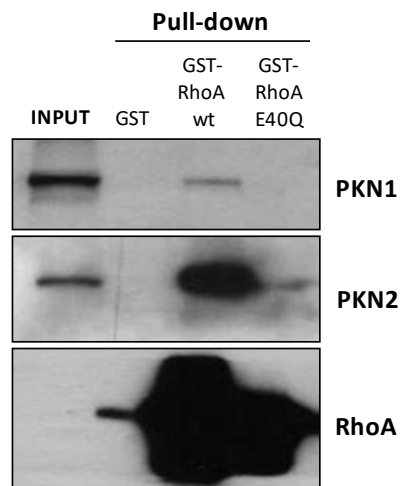


Figure 54. PKN1, PKN2 and RHOA pull down in HNSCC cells. PKN1 and PKN2 binding to RHOA wt and the lack of interaction with the RHOA E40Q mutant was confirmed by Western blot using the lysate from 10 HNSCC cell lines (FaDu, Detroit562, 92VU040, 92VU041, 92VU078, 92VU080, 92VU094, 92VU120, JHU029 and SCC25). RHOA antibody was used as a positive control.

The Small GTPase RHOA in cancer

Chapter I & Chapter II

DISCUSSION

DISCUSSION

Cancer is a leading cause of death worldwide, accounting for nearly 10 million deaths in 2020¹⁸⁶. In other words, one in six deaths is caused by cancer. A correct cancer diagnosis is essential for an appropriate and effective treatment. Each cancer type, an even in every different stage of the disease, requires a specific treatment aiming to maximize the cure rate.

Cancer is a multistep process that arises over the course of several years, resulting from the accumulation and selection of successive genetic and epigenetic changes that lead to the gain-of-function of oncogenes, and to the loss-of-function of tumor suppressor genes. Genomic profiling for cancer precision medicine has been a very useful tool to find discreet driver mutations that are associated with therapeutic targets, or with a diagnostic or prognostic value. The identification of driving changes and the way they participate or orchestrate the tumorigenic process facilitates the development of targeted therapies to improve survival outcomes of cancer patients.

Over the past decade, our laboratory has been focused in studying the role of RHOA GTPase in cancer. Although RHOA was vastly described as an oncogene, we could convincingly demonstrate a tumor suppressor role in colorectal cancer^{102, 103}. Furthermore, recent studies in our laboratory provide clear evidence of the tumor suppressor role of RHOA in diffuse type gastric cancer (unpublished data). Specifically, the downregulation or deletion of RHOA results in increased proliferation and invasion of diffuse cancer cells, both *in vitro* and *in vivo*. Interestingly, the opposite effect was observed when the wild type or the constitutively active (G14V) form of RHOA were overexpressed in diffuse gastric cancer cell lines with low endogenous levels of RHOA protein. Thereby, it is now realized that the role of RHOA in tumorigenesis is highly determined by the context, acting as an oncogene or tumor suppressor depending on the tumor context.

RHOA is a small GTPase protein participating in important cellular functions, such as cytoskeletal rearrangement and transcriptional regulation related with cell growth, survival, migration and invasion^{21, 22}. RHOA acts as a switch protein cycling between an active (when bound to GTP) and inactive (when bound to GDP) forms. This cycle and consequently its activity, is highly regulated by guanine nucleotide exchange factors (GEFs) and GTPase activating proteins (GAPs) that promote RHOA activation and inactivation, respectively. Furthermore, guanine nucleotide dissociation inhibitors (GDIs) sequester GDP-RHOA in the cytosol supporting protein inactivation and preventing degradation. Contrary, the active GTP-RHOA form is generally associated to the plasma membrane where binds and activates different effector proteins, such as

Discussion

Rho-associated coiled coil protein kinase (ROCK), Diaphanous Homologue 1 (DIAPH) and Protein Kinase N (PKN), among others^{51, 56}.

Recently, with the extensive use of sequencing technologies, it has been found that RHOA is mutated in a large list of cancer types^{125, 299}. Interestingly, the distribution of the mutations along RHOA coding sequence is not arbitrary, but in a clear hotspot pattern mimicking the mutational pattern observed in oncogenes. Our group has focused on the study of the hotspot mutations found in three liquid tumors: adult T-cell lymphoma/leukemia (ATLL), angioimmunoblastic T-cell lymphoma (AITL) and Burkitt lymphoma (BL); and two solid tumors: diffuse-gastric cancer (DGC) and head and neck squamous cell carcinoma (HNSCC). According to The Cancer Genome Atlas (TCGA), the frequency of RHOA mutations in tumors ranges from about 2% to over 50%. But, surprisingly, RHOA hotspot mutations are different among tumor types: C16R (ATLL); G17V (AITL); R5Q (BL and DGC); G17E, L57V, Y42C (DGC); and E40Q (HNSCC) (**Figure 55**). The selection of these specific mutations in particular tumor types suggest distinctive roles of each mutant in the carcinogenic process of each tumor type.

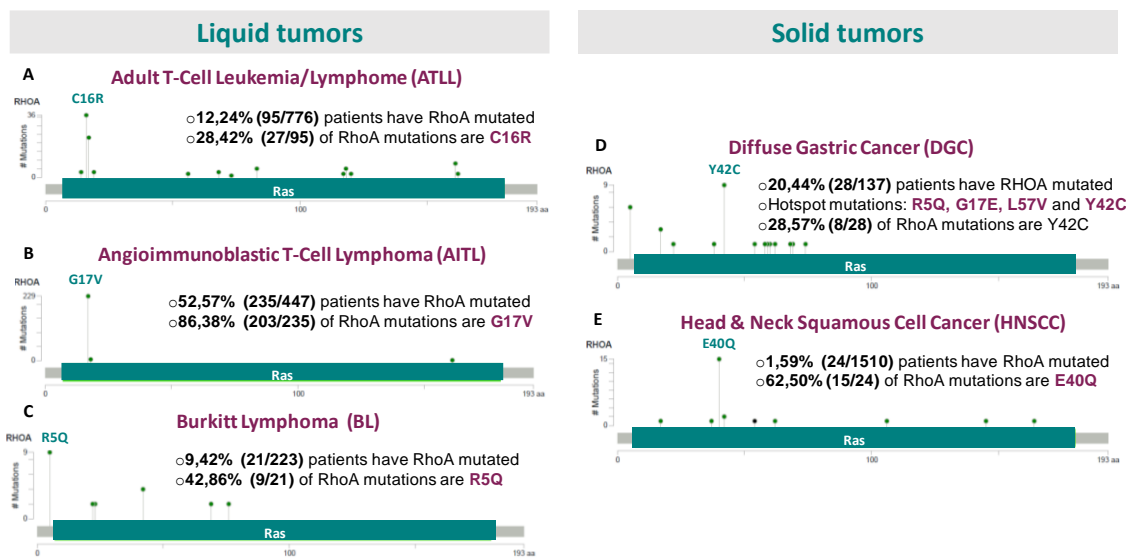


Figure 55 RHOA mutation mapper in different tumor types. Summary of RHOA mutations found in adult T-cell leukemia/lymphoma^{125, 309} (A), angioimmunoblastic T-cell lymphoma^{152, 309-312} (B), Burkitt lymphoma^{148, 309} (C), diffuse type gastric cancer^{128, 313} (D) and head & neck squamous cell cancer^{125, 210, 211, 301, 302} (E). Ras: RAS gene. Data was plotted using 'Mutation Mapper' in cbiportal.org.

In DGC, published data shows that 14%-24% of tumors display RHOA mutations^{128, 129}. The analysis of the localization of these mutations indicates that there are four clear mutation hotspots (Tyr42, Arg5, Gly17 and Leu57); being Y42C the most frequent missense substitution. To investigate the role of RHOA mutations in gastric tumorigenesis we engineered a transgenic mouse model expressing RHOA Y42C conditionally in the gastric mucosa. RHOA Y42C mutation accelerated the oncogenic process initiated by N-methyl-N-nitrosourea (MNU) in the gastric epithelium, as

evidenced by an increased number of tumors compared to control littermates (unpublished data). RHOA seems to have a dual role in the gastric cancer context, as a tumor suppressor in the wild-type form, and as an oncogene in the Y42C mutant form.

The peculiar and intriguing context-dependent role and the puzzling mutational profile exhibited by RHOA have promoted the study of the role of these mutations in their respective tumor-contexts. Results from these studies indicate that these hotspot mutations are affecting some, but not all RHOA functions. Otherwise, RHOA would be overexpressed or silenced, as it happens in other tumor types. As an example, our group has recently found that the RHOA Y42C mutation frequently found in diffuse gastric tumors specifically interferes with the binding of the downstream effector PKN, while largely preserving the binding capacity of RHOA to other effectors (unpublished data). This leads to the specific inactivation of PKN signaling, which we have shown to have strong tumor suppressor activity (unpublished data). Alternatively, some of these RHOA hotspot mutations could be neomorphic, thus leading to new functions. The study of the RHOA G17V mutation in AITL led to the finding that this mutant creates a binding site to the GEF VAV1 promoting the carcinogenic process in this tumor type¹⁵⁷. Therefore, we hypothesize that these mutations must be conferring an oncogenic potential through the targeted overactivation of RHOA oncogenic functions, the targeted inactivation of tumor-suppressive RHOA functions while preserving others that would be oncogenic, and/or by the acquisition of new oncogenic activities.

To elucidate possible differences in the signaling pathways modified by these tissue-specific RHOA recurrent mutations, we decided to study in a single cell context the functional characterization of RHOA wt and the following RHOA mutations: C16R, G17V, R5Q, G17E, L57V, Y42C and E40Q.

1. Functional characterization of RHOA hotspot mutants

The functional characterization of the different RHOA mutants was approached through the transient transfection of the fibroblastic-like HEK293T and COS1 cell lines with the different RHOA mutants fused to the green fluorescent protein (GFP) in its N-terminal end. The use of these cell line models guaranteed a reliable and efficient transfection rate. Moreover, the use of a fluorescent tag (GFP) fused to our protein of interest allowed the tracking, specifically the assessment of the transfection efficiency and the monitorization of the subcellular localization of the different RHOA mutants into the cells.

In addition to the pathogenic hotspot mutants listed before, two further RHOA mutants were included: G14V and T19N. These mutations are not found recurrently in tumors but constitute excellent models for comparison purposes. G14V and T19N

Discussion

mutants have been widely characterized as constitutive-active and dominant-negative RHOA forms, respectively^{314, 315}.

RHOA G17 mutants exhibit a lower protein stability

RHOA expression and activity are tightly regulated. At the transcriptional level, the Myc-Skp2-Miz1-p300 transcriptional complex and other transcription factors such as HIF-1, NFκB and STAT6 binds to the *RHOA* promoter for expressing RHOA⁵¹. Moreover, it is well-known that RHOA activity is highly regulated by GEFs and GAPs that promotes the activation or inactivation of this GTPase, respectively. However, the activity of RHOA can be modified also at posttranslational level by the phosphorylation, ubiquitination and AMPylation of this protein. In addition, the stability of RHOA protein is regulated. On the one hand, it is known that the cytosolic and inactive RHOA forms are degraded through the proteasome. This process is prevented by the binding of inactive RHOA to GDIs³⁰³. On the other hand, the membrane-associated and active RHOA is degraded through autophagy pathway^{40, 41}.

We first interrogated if the mutations in RHOA affected the protein levels. Significantly lower protein levels of RHOA with G17 mutations (G17E and G17V) were evidenced through two different approaches (Western blot and cytometry analysis). To rule out a possible technical artifact, the transfection material, new plasmid preparations and even new mutagenesis reactions were prepared and tested. However, although a similar transfection efficacy between GFP-RHOA mutants tested was obtained, the result showing reduced protein expression was maintained. To finally discard a possible technical artifact, the determination of GFP-RHOA transgene copy number (on total DNA) and transcript levels (on total RNA) was carried out. However, no differences were found between RHOA mutants at this level, and correlation analysis demonstrated no association between DNA copies/RNA transcript levels and GFP-RHOA protein levels. Moreover, these differences in the protein expression levels of G17 RHOA mutants were observed in two different cell lines, HEK293T and COS1, and thus, the result obtained did not seem context-dependent.

To further support this, we decided to check the levels of RHOA wt and RHOA G17 mutants in the specific cellular context where these mutations are normally found (G17E in gastric cells, and G17V in lymphoid cells). Similarly to the results obtained with the fibroblastic lines, G17 mutants displayed a decrease in protein levels compared to the wild-type form of RHOA. These results are consistent with some reports identified upon an exhaustive survey of the literature available on RHOA mutants in which a decrease in RHOA G17V protein levels was observed when compared to RHOA wild-type in a Jurkat overexpression model^{157, 316}. Thereby our results suggested a posttranscriptional and/or posttranslational deregulation mechanisms in the expression of G17E/V mutant forms.

Then, we decide to focus our attention into the study of the biology of RHOA G17E and RHOA G17V forms. The posttranslational regulation of exogenous RHOA proteins was addressed evaluating GFP-RHOA protein half-life. Results showed a clear decrease in the stability of RHOA protein when mutated in codon G17 compared to wild-type RHOA, a fact that could explain the reduction of RHOA G17E and RHOA G17V protein levels. RHOA G17E mutation is characteristic of DGC, whereas G17V is the hotspot RHOA mutation found in AITL. Therefore, it is unlikely that the oncogenic role of RHOA G17 mutations drives tumorigenesis solely through reducing RHOA expression, as then RHOA G17E and G17V mutations would be observed in both, DGC and AITL tumors and not specifically selected in different tumor types.

RHOA G17 mutants tend to localize into the nucleus

The subcellular localization of a protein is directly linked with its function. Specifically, it determines the accessibility of this protein to interact with specific partners that could modulate its activity or participate in a signal transduction pathway within the cell.

RHOA localizes mainly in the cytosol and plasma membrane. The localization in these two compartments is determined by the activity state of the GTPase, since GDP-bound RHOA remains into the cytosol and GTP-bound RHOA is found anchored to the plasma membrane to carry out its function. Nevertheless, some studies have demonstrated that RHOA also localizes into the nucleus¹⁶²⁻¹⁶⁵. We found interesting to investigate how the different hotspot RHOA mutations could affect its subcellular localization. To obtain robust results, two different approaches were used: co-localization of DAPI (nuclear staining) and GFP (GFP-RHOA) through confocal microscopy, and flow cytometry analysis of isolated nuclei. Results demonstrate that the G17E mutant has a significantly increased nuclear localization compared to wild type RHOA and other hotspot RHOA mutants investigated. Moreover, RHOA G17V and the constitutive-active RHOA G14V forms exhibited a clear trend to localize into the nucleus.

Little is known about the role of RHOA in the nucleus, but as this GTPase has been involved in the DNA damage response (DDR) promoting cell cycle arrest and cell survival, and we hypothesized that nuclear shuttling might be required to undertake these particular functions. According to the literature, nuclear RHOA localization is tightly regulated through its binding to GDP Dissociation Inhibitor 1 (GDI1). Specifically, binding of GDI1 to RHOA inhibits its translocation to the nucleus^{166, 304}. Furthermore, the nuclear activity of RHOA in DDR seems to be dependent on ataxia telangiectasia-mutated (ATM) and flap structure-specific endonuclease 1 (FEN1) proteins. Reactive oxygen species (ROS) may also promote the activation of the nuclear form of this GTPase. Interestingly, Rho-specific GEFs Net1 and Ect2 also participate in DDR. Indeed, Net1 has a key role in the activation of nuclear RHOA. Downstream of this GTPase, it

Discussion

seems that cell cycle arrest is driven by mitogen-activated protein kinases (MAPK), especially p38 and ROCK¹⁶⁸.

Interestingly, the lower protein stability found and the higher nuclear localization of G17 RHOA mutants could be related to the results obtained by Dubash et al¹⁶⁶. GDIs (guanine nucleotide dissociation inhibitor) are Rho regulators with three important functions: i) inhibition of nucleotide dissociation, ii) inhibition of GTP hydrolysis, and iii) protein release from the plasma membrane³⁰⁴. Moreover, GDIs have been involved in the stabilization of GTPases preventing its degradation through the proteasome³⁰³. In this study, authors showed how GDIs maintain RHOA sequestered in the cytosol of the cells, restricting the translocation of this protein to the nucleus. Then, one of the possible hypotheses that would be interesting to test is whether RHOA G17 mutants have lost the GDI capacity binding. If so, this could contribute to a decrease in protein stability and increased nuclear localization. Moreover, it could be evaluated if RHOA G17 mutants drive AITL and DGC tumors by mediating DNA damage response (DDR), thus promoting cell cycle arrest and cell survival, as these are the main reported roles of RHOA wt into the nucleus¹⁶⁸.

RHOA hotspot mutants display reduced cytoskeletal dynamics

The metastatic capacity of cancer cells is directly related with the ability to detach from the bulk tumor mass, as well as migrate and invade to both, neighboring and distant tissues. Tumor cell plasticity is thus required for efficient tumor spreading. RHOA is well known to regulate the formation of filamentous actin (F-actin), triggering morphology and adhesion changes, through the activation of ROCK and mDia effectors proteins, and as a result, promoting tumor progression. mDia is a formin, a protein that nucleates and polymerizes long actin filaments. ROCK is a kinase that phosphorylates MLCP (myosin-light-chain phosphatase) and the non-muscle myosin II light chain (MLC), leading to the inactivation and activation of these proteins, respectively. These events promote the accumulation of activated myosin motor proteins, which bind to the actin filaments polymerized by mDia, to create actomyosin bundles. In addition, ROCK phosphorylates and activates LIM-kinase. LIM-kinase will in turn phosphorylate and inactivate cofilin, which prevents the breakdown and recycling of actin filaments, maintaining the integrity of cytoskeletal structures^{174, 317, 318} (**Figure 56**).

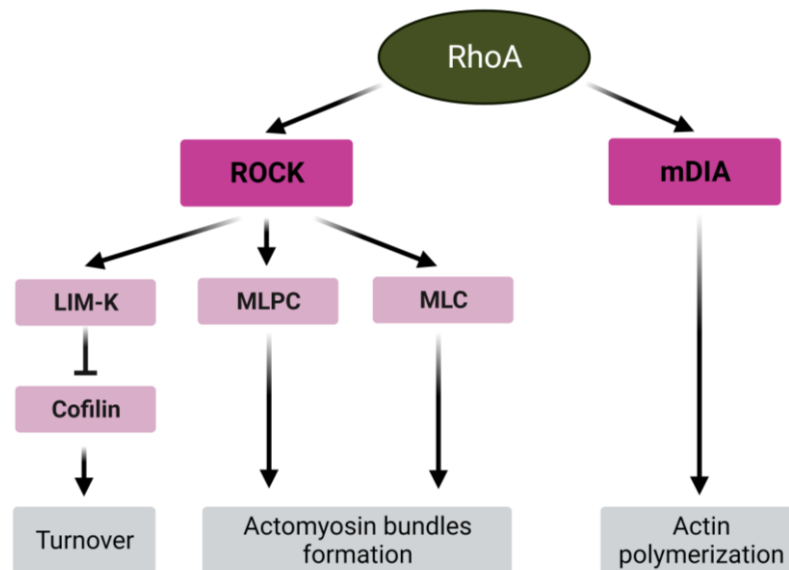


Figure 56. Signaling from RHOA to the cytoskeleton. Direct activating signals are presented by arrows. Inhibitory signals are depicted as truncated arrows. LIMK: LIM kinase; MLPC: Myosin light-chain phosphatase; MLC: myosin light chain³¹⁹.

COS1 cells transiently transfected with the different RHOA forms and F-actin staining (phalloidin) were used to characterize the cytoskeletal dynamics. Overexpression of RHOA wt and the constitutive-active form of RHOA promoted the increase of F-actin formation, as previously reported¹³⁶. However, a general impairment of F-actin formation was observed when overexpressing the different RHOA mutants under study. The RHOA C16R protein present in ATLL, was the only mutant maintaining a RHOA wild-type-like activity on cytoskeleton dynamics.

In our transiently transfected HEK293T cell line models, overexpression of RHOA wt and the constitutive-active RHOA G14V form promoted a change in morphology noticeable at the macroscopic level. This change towards cell roundness was indeed previously reported^{173, 320}. Contrary, the overexpression of the rest of the mutants did not affect the normal fibroblastic-like morphology of HEK293T cells. The acquisition of a roundness morphology and the consequent detachment from the substrate are well known signs of resistance to anoikis, the apoptosis program activated when cells lose their attachment to the substrate or to surrounding cells³²¹. We reasoned that the morphological phenotype could underline the aggressiveness capacity of cells.

In multicellular organisms, it is important that the cells are able to adhere to the extracellular matrix proteins and to surrounding cells. However, for cancer cells to metastasize and colonize other organs and tissues, the opposite scenario is needed. Similarly, to the results observed in the F-actin formation assay, all the mutants interrogated, except RHOA C16R (ATLL) and RHOA L57V (DGC), downregulated the detachment capacity. Unfortunately, significant differences were found only in one of the two approaches used to measure the adhesion capability, number of cells attached

Discussion

to the substrate, while results obtained through the cell adhesion under well-calibrated detachment forces were not significant. Further studies are required to investigate in detail the differences in adhesive properties observed, such as characterizing the plasma membrane proteins possibly regulated by RHOA that are involved in cell-to-cell and/or cell-to-matrix adhesion.

Collectively, RHOA hotspot mutants, except RHOA C16R, did not exhibit the upregulation of cytoskeletal rearrangement expected for an oncogene with a strong impact in cellular migration and invasion, compared to RHOA wt. Therefore, the oncogenic process in ATTL tumors, driven by a RHOA C16R mutation, could be related with this overactivation of the cytoskeletal dynamics. Nevertheless, migration and invasion assays must be performed in the specific tumor context where these mutations are found to truly describe the impact of the mutations in the establishment of distant tumors.

RHOA hotspot mutations downregulate SRF and NFκB signaling

As described before, RHOA activity is highly regulated by several proteins, such as GEFs, GAPs and GDIs, posttranslational modifications and through transcriptional factors. Interestingly, RHOA, in turn, is able to regulate the transcriptional activity of certain transcription factors, such as SRF and NFκB, through signaling cascades modulated by different RHOA effectors⁵¹.

The activity of the transcription factor SRF is regulated directly by the cytoskeletal rearrangements occurring within cells that, as described before, are tightly orchestrated by RHOA. Specifically, activated RHOA promotes F-actin formation, by the incorporation of globular actin (G-actin) into actin filaments. This leads to the release of SRF cofactors retained in the cytoplasm by G-actin (such as myocardin-related transcription factors; MRTFs), and its translocation from the cytoplasm into the nucleus, where they can bind and activate the transcription factor SRF. This transcription factor then activates the transcription of genes strongly related to the cytoskeletal dynamics, such as actin and gelsolin, among others. The expression of these target genes stimulates cytoplasmic actin polymerization (**Figure 57**). Interestingly, SRF activity has been related with the carcinogenic process^{180, 181}, so the regulation of this transcription factor by the different RHOA hotspot mutants resulted interesting for us.

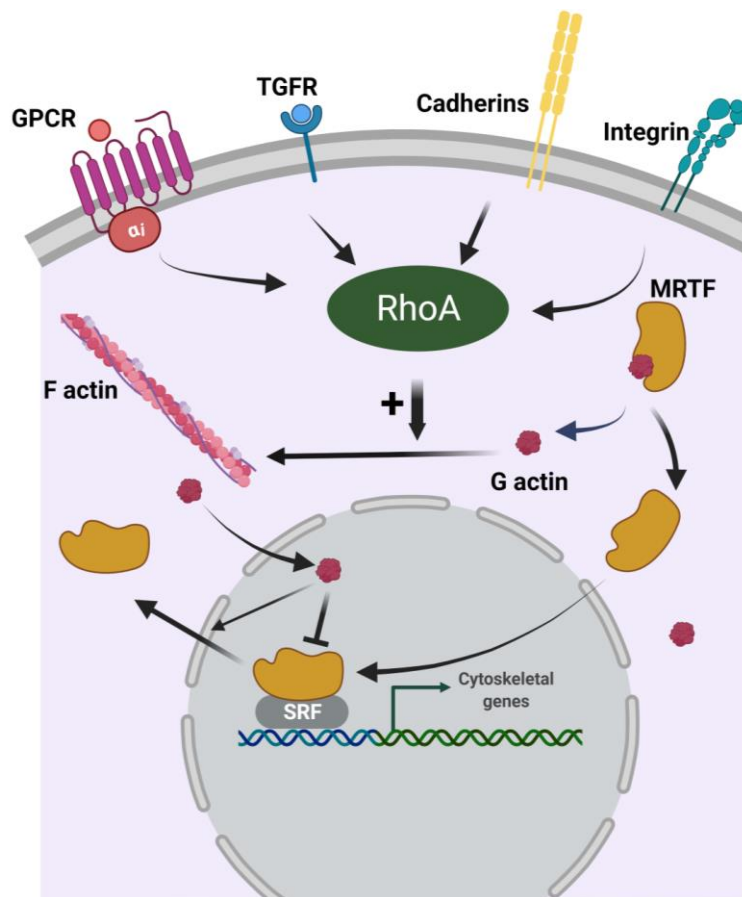


Figure 57 Cytoskeletal dynamics and SRF signaling. Cytoskeletal actin microfilaments dynamics is triggered by the activation of different membrane receptors such as G protein-coupled receptors (GPCRs), integrins, transforming growth factor- β receptors (TGFRs) and E-cadherins, among others. Integrins and E-cadherins are structural mediators of focal adhesions and adherent junctions, respectively. All these receptors modulate the activity of Rho GTPases through Rho guanine nucleotide exchange factors (GEFs). Effectors of Rho GTPases, including Rho-associated kinases (ROCKs) and formins (such as Diaphanous-related formins; mDia/DIAPH), orchestrate actin polymerization by incorporating globular actin (G-actin) into the filamentous actin (F-actin). High levels of free G-actin retain the serum response factor (SRF) cofactor proteins, *i.e.*, myocardin-related transcription factors (MRTFs) in the cytoplasm. Incorporation of G-actin into the F-actin filaments releases MRTFs, prompting their shuttling into the nucleus to interact with the transcription factor SRF. This triggers expression of a subset of SRF target genes, namely cytoskeletal genes. Furthermore, nuclear MRTF can be complexed with nuclear G-actin, which inhibits MRTF-mediated stimulation of SRF-dependent transcription, promoting MRTF nuclear export. Created with BioRender.com.

The NF κ B pathway is a conserved signaling cascade involved in different cellular processes, such as inflammation and cell survival. Moreover, it is extensively involved in cancer development and progression through controlling the expression of key target genes, such as *TNFA*, *IL6*, *VEGF* or *BCL2*, that mediate cell proliferation, survival and angiogenesis¹⁸³. In normal resting cells, cytosolic I κ B (inhibitory κ B) binds and inhibits NF κ B from translocating to the nucleus for transcription of target genes. During activation of the canonical NF κ B pathway, the NF κ B transcription factor must be released from the I κ B proteins. I κ B is phosphorylated by the IKK complex (Inhibitory

Discussion

κ B kinase), consisting of IKK1, IKK2 and NEMO (NF κ B essential modulator) and then ubiquitinated and degraded by the proteasome. Degradation of I κ B is the main regulatory mechanism of the canonical NF κ B pathway, and RHOA is reported to regulate NF κ B specifically acting on I κ B^{51, 322}.

Knowing that both transcription factors, SRF and NF κ B, have been associated with the carcinogenic process, we next evaluated the impact of the different *RHOA* mutations on the activation of these signaling pathways. Results, using luciferase reporter assays, demonstrated that all *RHOA* hotspot mutants, except *RHOA* C16R, significantly downregulate SRF signaling when compared with *RHOA* wt. As expected, the constitutive-active *RHOA* G14V and the dominant-negative *RHOA* T19N forms, up- and down-regulated SRF activity, respectively. Because SRF signaling directly regulates actin filaments, the transcriptional activity of SRF would be expected to correlate with the cellular levels of F-actin. Indeed, the results obtained in the SRF luciferase assays strongly correlated with the capacity of *RHOA* mutant forms to promote the formation of F-actin. Thereby, there is a general downregulation of the *RHOA*-actin-SRF pathway upon *RHOA* mutation, except for *RHOA* C16R, which does not affect this activity of *RHOA*. Hence, unlike for other tumor types, in ATLL F-actin/SRF pathway downregulation does not seem to be needed for the oncogenic activity. Contrastingly, NF κ B activation resulted inhibited when *RHOA* was mutated. Although *RHOA* G14V did not change NF κ B activation capacity, the dominant-negative *RHOA* T19N decreased it. This general downregulation of NF κ B in the presence of *RHOA* hotspot mutants reveals that the deregulation of this signaling pathway could be relevant for the oncogenic activities of these *RHOA* mutations.

Collectively, the results obtained are consistent with the reduction of SRF/NF κ B signaling contributing to the oncogenic process of DGC, BL, HNSCC and AITL. Importantly, however, this is not the case for ATLL, since F-actin/SRF pathway resulted unaffected by the *RHOA* C16R hotspot mutant.

RHOA mutations affect the binding to known interactors

As mentioned before, *RHOA* is an important molecular switch that acts through binding and activation of several downstream effectors⁵². *RHOA* needs to be bound to GTP to acquire an active conformation allowing effector interaction. As shown in **Figure 12**, *RHOA* mutations are allocated in different regions of the *RHOA* protein. Some are in the GTP/GDP binding and other in the effector binding domain. We reasoned that the different *RHOA* hotspot mutations found could affect either the intrinsic GTPase activity or the binding ability to effectors and regulators. So, an alternative way to evaluate how these *RHOA* hotspot mutations could drive carcinogenesis was to investigate changes in the binding capacity to well-known *RHOA* interacting proteins.

The interactome of RHOA hotspot mutants was evaluated using two different approaches. First, a pull-down assay was used to measure the interaction capacity of the different RHOA forms to the effector protein Rhotekin. Furthermore, a yeast-two-hybrid approach was used to investigate the binding capacity of the DGC (R5Q, G17E, L57V and Y42C), BL (R5Q) and the HNSCC (E40Q) RHOA mutants to ROCK, DIAPH2, PKN1 and Kinectin effector proteins, and the Rho activity regulator NET1.

The pull-down assay with a Rhotekin binding domain is a widely used approach to measure indirectly the catalytic activity of Rho GTPases, due the fact that no primary antibodies are available to detect the active form of this GTPase. Rhotekin is a scaffold protein involved in physiological functions as cell growth and cytokinesis³²³. Moreover, it has been linked with cancer in several studies. There are reports describing the abnormal expression of Rhotekin in cancer types, such as gastric³²⁴, colorectal³²⁵ or bladder³²⁶ carcinomas. Indeed, in gastric cancer, it was demonstrated that the overexpression of Rhotekin confers cell resistance to apoptosis through the activation of NFκB signaling pathway³²⁷. To evaluate the binding to Rhotekin, protein lysates from HEK293T cells with forced overexpression RHOA wt or the different RHOA hotspot mutants were used. Results showed that the mutations in codon 17 of RHOA found in DGC (G17E) and in AITL (G17V) significantly reduced the cellular levels RHOA-bound Rhotekin. However, as these two mutants displayed lower RHOA expression levels in all the cell line models tested, including HEK293T cells, at present we cannot distinguish whether the reduction in Rhotekin is caused by a lower affinity to effector caused by the mutation, or due to the reduced RHOA levels within the cells.

In addition, the interactome of RHOA and the frequent mutants found in DGC (R5Q, G17E, L57V and Y42C), BL (R5Q) and HNSCC (E40Q) was characterized through a yeast-two-hybrid assay. This experiment allowed us to assess the presence and the strength of the interaction of the different RHOA mutants to the RHOA effectors proteins that are best characterized (ROCK³²⁸⁻³³¹, DIAPH2³³², PKN1^{333, 334} and Kinectin^{332, 335}) and the RhoGEF NET1³³⁶. We demonstrated the feasibility of this screening approach validating the binding of RHOA wt to all the proteins tested.

The predominant RHOA hotspot mutant HNSCC, RHOA E40Q, showed a total lack of binding to the kinectin effector protein and Net1 GEF protein. Kinectin 1 (KTN1) is a multifunctional protein that interacts with Kinesin and participates in multiple processes of cellular dynamics such as organelle motility and focal adhesion growth of cellular lamella^{332, 337, 338}. The interaction of Kinectin and kinesin is one of the key events in the cytoskeleton dynamics and essential for maintaining cell shape and sustaining cell migration. Recently studies indicated that in cutaneous squamous cell carcinoma, Kinectin promotes cell proliferation, associating this protein with tumor progression³³⁹. In turn, Net1 is a guanine exchange factor (GEF) for RHOA whose function is to enhance its GTPase activity. This GEF has been related with the carcinogenic processes. Specifically, it has been found up-regulated in gastric cancer,

Discussion

driving its aggressive phenotype by sustaining migration and invasion¹³⁷. Moreover, Net1 is essential for the formation of stress fibers. Its expression is induced after the activation of TGF β signaling pathway. Net1, as RHOA GEF, activates this GTPase promoting stress fiber formation²³⁶.

Regarding the performance of DGC RHOA mutants in the yeast-two-hybrid assay, we could confirm that RHOA Y42C was unable to bind to PKN1, as previously reported¹³⁶, while retaining its binding capacity to almost all the other effector proteins tested (ROCK, DIAPH2 and Kinectin). Interestingly, G17E and L57V mutants were also deficient at binding PKN1. Moreover, it was interesting to observe global differences between RHOA mutants. Namely, RHOA G17E lost the binding capacity to all the binders tested, except mDIA and NET1; whereas, on the contrary, the DGC R5Q RHOA mutant did not exhibit any change to the binding capacity to any of the tested interactors. This could indicate how the different RHOA mutations found in DGC could have common and/or different oncogenic roles in the DGC carcinogenic process.

Taken all together, these results demonstrate that the *RHOA* mutations described in HNSCC and DGC solid tumors, lack the ability to bind to important effectors and/or RHOA pathway regulators, predicting an impairment of downstream RHOA signaling. Binding to PKN was lost in most DGC RHOA mutants, highlighting the possible RHOA downstream effector involved in the carcinogenesis of this tumor type. Then, we decided to further investigate the relevance role of PKN1 in DGC. PKN1 is a PKC-related serine/threonine-protein kinase involved in processes such as regulation of actin intermediate filaments, cell migration, tumor cell invasion and transcription regulation³⁴⁰⁻³⁴². The results obtained within the group convincingly demonstrate that PKN1 negatively regulates the growth and the invasion capacity of diffuse type gastric cancer cells (data not shown). We hypothesized that the tumor suppressive role of *RHOA* in diffuse-gastric cancer could be driven, at least in part, by its downstream effector PKN1. Therefore, *RHOA* mutations found in DGC could have an oncogenic role through the inhibition of the binding to this tumor suppressive effector. Interestingly, it has been recently reported that Y42C RHOA also contributes to DGC oncogenesis through ROCK overactivation¹³⁹, indicating that at least some of these hotspot mutations may have multiple oncogenic effects.

Overview and future perspectives

RHOA mutations are different between tumor types and are distributed in distinctive hotspots: C16R (ATLL); G17V (AITL), R5Q (BL and DGC); G17E, L57V, Y42C (DGC); and E40Q (HNSCC)¹²⁵. We have hypothesized that these mutations have been selected because of its oncogenic role in the carcinogenic process of the different tumor types. These hotspot mutations must confer an oncogenic potential to RHOA by affecting some, but not all of its functions, and the oncogenic functions of RHOA varies depending of the different tumor types. Results from all the experiments discussed

above, comparing the effects between the different RHOA mutants tested and RHOA wt, are summarized in **Table 15**.

Table 15. Summary of the functional characterization studies and the interactome analysis for the different RHOA hotspot mutants.

RhoA mutant	Tumor context	Protein stability	Nuclear Localization	Cytoskeletal dynamycs			NFkB activity	Binding strength known interactors						
				Factin Formation	Detachment capacity	SRF activity		Rhotekin	ROCK	mDia	PKN1	Kinectin	NET1	
Constitutive-active (G14V)	-	=	Yes	=	↑	↑	=	=	N/A	N/A	N/A	N/A	N/A	N/A
Dominant-negative (T19N)	-	=	No	↓	↓	↓	↓	↓	N/A	N/A	N/A	N/A	N/A	N/A
C16R	ATLL	=	No	=	=	=	↓	=	N/A	N/A	N/A	N/A	N/A	N/A
G17V	AITL	↓	Yes	↓	↓	↓	↓	↓	N/A	N/A	N/A	N/A	N/A	N/A
R5Q	BL, DGC	=	No	↓	↓	↓	↓	=	=	=	=	=	=	=
G17E	DGC	↓	Yes	↓	↓	↓	↓	↓	↓	=	↓	↓	↓	=
L57V	DGC	=	No	↓	=	↓	↓	=	=	=	↓	=	=	=
Y42C	DGC	=	No	↓	↓	↓	↓	=	=	=	↓	=	=	=
E40Q	HNSCC	=	No	↓	↓	↓	↓	=	=	=	=	↓	↓	↓

Up and downregulation of the different features studied is summarized in the table. Purple color indicates downregulation. Green color indicates upregulation. Grey color indicates an equivalent phenotype to the RHOA wt. N/A: non available. (-): not found in patient tumors.

Altogether, results point-out to RHOA hotspot mutations as loss-of-function or inactivating mutations (predominantly purple colored in the table), except for ATLL hotspot mutant RHOA C16R (predominantly grey colored in the table). BL, AITL, DGC and HNSCC tumors could be driven by a downregulation of the cytoskeletal dynamics and NFkB signaling by the different RHOA hotspot mutations. However, ATLL oncogenic process seems not to be promoted by the cytoskeletal rearrangement deregulation. Moreover, the nuclear localization of RHOA G17 mutants could be important for the DGC and AITL tumorigenesis. In addition, interesting results have been found through the study of the interactome of mutant RHOA. PKN1 is a tumor suppressor in DGC and RHOA hotspot mutation found in DGC could drive this tumor type in part by their inability to bind it. Further experiments to characterize and study more in detail these findings must be performed. The study of the role and the interactome of the different RHOA mutants in the specific tumor-context in which they have been described would be extremely useful to identify new actionable targets for further development of personalized cancer therapies.

2. RHOA in head & neck squamous cell carcinoma

Head & neck squamous cell carcinoma (HNSCC) is the seventh most common type of cancer. It comprises a heterogeneous group of malignancies of the upper aerodigestive tract, salivary glands and thyroid. It is estimated that approximately 950,000 cases will

Discussion

be diagnosed in 2022 worldwide, but only 40–50% of patients will survive upon 5 years of the diagnostic¹⁸⁶. Tobacco and alcohol consumption, and HPV infection are the main risk factors in HNSCC development. Interestingly, the etiology of the HNSCC tumors, specifically the HPV status, conditions the specific anatomical region where the tumor develops, the prognosis and the associated molecular alterations³⁴³. The genetic profile of HNSCC tumors revealed a strong skewing towards alteration of tumor suppressor genes, such as *TP53*, *CDKN2A*, *FAT1*, *NOTCH1*, among others²⁰¹. The most common genetic abnormalities found in HNSCC differ from other solid tumors in the sense that are frequently driven by mutations in oncogenes.

Head and neck cancer treatment is based on radiation and surgery, and has not evolved substantially over the years. Consequently, patient survival has not improved significantly in the last 60 years. To identify molecular biomarkers with prognostic or predictable value, it is essential to identify and describe in detail molecular alterations occurring and driving the HNSCC tumorigenic process. Changes in key cellular functions, mainly cell cycle deregulation and cell death evasion, arising due to alterations in the *TP53* and PI3K pathway, respectively, are crucial for the onset and development of HNSCC. But changes in cell growth (EGFR and TGF β) and dedifferentiation (NOTCH1) pathways have also been shown to be important in the progression of HNSCC²⁰⁴. Nevertheless, the limited information on the molecular carcinogenesis of HNSCC, and the genetic and biological heterogeneity of the disease has hindered the development of successful targeted therapies.

RHOA is one of the most extensively investigated member of the Rho GTPase family. It has long been involved in the malignant transformation of cells, as well as in tumor invasion and metastasis. Although there is little literature related with RHOA and HNSCC, this GTPase seems to be expressed at higher levels in HNSCC cells compared with healthy cells^{85, 281}. Moreover, there is a study reporting that RHOA downregulation in tongue cancer cells reduces cell proliferation, migration and invasion⁸⁵. According to these data, RHOA is predicted to have an oncogenic role in HNSCC tumors.

As mentioned in the previous section, high-throughput profiling of large number of tumors has revealed frequent *RHOA* mutations distributed as hotspots in a wide variety of liquid and solid human cancers, including HNSCC. *RHOA* is mutated in 1.5% of HNSCC patients, but remarkably, E40Q represents more than 60% of the mutations^{293, 294}. Therefore, the selection of this mutation in HNSCC tumors predicts a determinant oncogenic role in the tumorigenic process.

RHOA evaluation as a biomarker in HNSCC

Biomarkers are defined as biological molecules found in blood, other body fluids, or tissues that are a sign of a normal or abnormal process, condition or disease. Biomarkers represent important tools for diagnosis, prognosis and/or treatment

response. Regarding HNSCC, some biomarkers have been suggested to impact the diagnosis and prognosis, but few of them have been validated. HPV DNA/p16 status, used for the determination of HPV infection, and PD-L1 levels are examples of validated diagnostic and prognostic/predictive biomarkers currently used in the clinic for HNSCC cases³⁴⁴ (**Table 16**). However, to improve patient outcomes, better understanding of the molecular pathogenesis of HNSCC is still necessary for the development of prognostic biomarkers and therapeutic advances.

Table 16. Role of (bio)markers in HNSCC.

Marker	Mechanism	Prognostic role	Predictive role	Diagnostic role	Limitations	Validated
HPV	Oncogenesis-driver in OSCC	Yes	No (2 clinical trials negative, other trials still ongoing)	Yes (Cancer of unknown primary presenting with cervical LNs)	Lack of specificity, applicable only in OSCC	Yes
PET imaging	-	Yes (high pretreatment SUV)	Yes (indication of residual disease for performing LN dissection)	Yes (stage, treatment response)	Appropriate interval between treatment completion and PET unclear, not always available	Yes
Tobacco	Inflammation and tobacco carcinogen-induced DNA damage	Yes (inferior treatment outcomes)	No	No	Demographic parameter	Yes
Immunoscore	Quantification of CD3+ and CD8+ TILs in the tumor core and the invasive margin of resected tumors	Yes (high number of TILs improve survival)	No (being assessed for response to immunotherapy)	No	Not always available	Yes
PD-L1	Mediates the inhibition of T cell activity	Yes (conflicting)	Yes (response to immunotherapy)	No	Technical issues in measurement	Yes
Skeletal muscle mass	Abnormal body composition	Yes (poor survival)	Yes (wound complication, fistula after laryngectomy, chemotherapy toxicity)	No		No
Next generation sequencing	Oncogenesis drivers	Yes (TP53, NOTCH1, CDKN2A mutations)	No	No	Cost, Not always available	No

HPV, Human Papilloma Virus; LN: lymph node; OSCC: Oropharyngeal Squamous Cell Carcinoma; PD-L1: Programmed Death-Cell; SUV: Standardized Uptake Value; TILs: Tumor Infiltrating Lymphocytes³⁴⁴.

The association of Rho GTPases and clinical data from HNSCC patients has been evaluated in several studies. Elevated RhoC levels in patients is associated with a metastatic phenotype²⁸³. Accordingly, the downregulation of RhoC in HNSCC cell lines resulted in a reduction of migration and invasion HNSCC cells *in vitro* and *in vivo*²⁸⁴. On the contrary, RhoB has been described as a tumor suppressor in HNSCC. Specifically, RhoB expression was detected in normal epithelium, carcinomas *in situ*, and well-differentiated tumors, but it becomes undetectable as tumors become invasive and poorly differentiated⁸⁴.

Here, the association of tumor RHOA protein and RHOA mRNA expression with clinical variables was studied. Surprisingly, although RHOA expression was not a good biomarker for survival prediction, it was for the first time significantly associated with the degree of differentiation of the tumor. Specifically, poorly differentiated tumors had higher levels of RHOA, compared to well and moderately differentiated ones. In HNSCC, it has been demonstrated that tumor differentiation has prognosis value, as poorly laryngeal differentiated tumors are associated with shorter survival outcomes³⁴⁵. According to this, poorly differentiated HNSCC tumor patients presented

Discussion

shorter survival outcomes than patients with good or moderately differentiated tumors.

Due the fact that HNSCC comprises a heterogeneous group of tumors arising in different head and neck anatomical regions, we decided to investigate whether RHOA expression was dependent on the localization of the primary tumor. Significant differences were found in the expression of RHOA when comparing oropharynx, hypopharynx and larynx tumors. Therefore, we stratified the patients in the tissue microarray according to the HNSCC anatomical subtype, and conducted new association studies. RHOA levels were associated with the degree of tumor differentiation in oropharynx and hypopharynx tumors, but not in larynx tumors. Disease-specific and disease-free survival outcomes were associated with RHOA protein levels exclusively in larynx tumor patients. Precisely, high RHOA protein in tumors significantly associated with shorter survival.

To further confirm these associations, we used the data available in The Cancer Genome Atlas (TCGA). Importantly, again, survival outcomes (disease-specific and disease-free survival outcomes) were associated with RHOA mRNA levels exclusively in larynx cancer patients, namely, higher RHOA levels predicted poor patient prognosis. However, surprisingly, RHOA mRNA expression did not associate with tumor differentiation degree, as shown before with RHOA protein analysis in TMAs. Differently to immunohistochemical studies, transcriptomic high-throughput expression data, such as microarray analysis, assess the levels of gene expression in bulk tumors. Therefore, the varying amounts of 'contaminating' non-epithelial cells could hinder the real association of a given gene expression in tumors with certain clinicopathological features.

Collectively, here we have demonstrated for the first time that RHOA has a prognostic value predicting survival and recurrence in larynx tumors. Moreover, RHOA could be used as a novel biomarker to predict the aggressiveness of the tumor in oral and pharynx tumors, as RHOA protein levels correlate with poorly differentiated tumors and poorer survival as consequence. Further validation studies to confirm these associations are required. Interestingly, the incorporation of this biomarker into the clinics would allow tailored treatment based on the use of a more aggressive treatment for patients with higher levels of RHOA to diminish the risk for recurrence and improve patient survival. On the other hand, patients with low levels of RHOA could benefit from a less intensive treatment. HNSCC treatment is mainly based on radiotherapy. Patients with a better survival prognosis could receive lower or more spaced radiotherapy doses, reducing the side effects of this treatment.

RHOA role in HNSCC cell lines

Historically, RHOA has been extensively associated with tumor prognosis in different solid tumor types, such as gastric, hepatic, urinary or breast cancer^{65, 69, 78, 89}, among

others. However, our group has demonstrated that the role of RHOA in the carcinogenic process is context-dependent, since RHOA acts as a tumor suppressor gene in colorectal^{102, 103} and diffuse-gastric cancer. The role of RHOA has not been widely studied in head and neck cancer. Downregulation of RHOA in tongue-derived cancer cell lines demonstrated a reduction in cell growth, migration and invasion *in vitro* and *in vivo*⁸⁵, but our data indicates that the role of RHOA may vary depending on the location of the tumor and there are not studies reporting the effect of the modulation of RHOA levels in malignant cell lines established from other head and neck anatomical regions.

SCC25 and JHU012 cell lines isolated from tongue and larynx cancers, respectively, and with moderate expression of RHOA protein, were selected to downregulate RHOA by two approaches, a targeted downregulation of RHOA through shRNAs and by CRISPR/Cas9 editing. The downregulation of RHOA through shRNA (RHOA KD) carried out in SCC25 cells impaired cell growth and colony formation capacity. This impairment was not significant in cell proliferation assays, but the trend was robust. Furthermore, lower tumor volume and weight were obtained when SCC25 RHOA KD cells were grown as subcutaneous xenograft in mice compared to control SCC25 cells, although this difference statistically significant. To confirm previous reported results indicating that RHOA is an oncogene in tongue tumoral cells, we decided to generate cellular system in which we completely eliminate the expression of RHOA. Knocking-out of RHOA by CRISPR/Cas9 in SCC25 cells, henceforth called RHOA KO, significantly impaired cell growth of these tongue cancer cells. These results confirmed the trend for lower growth observed in SCC25 RHOA KD cells. As the effect of modulating RHOA levels in larynx cells was not addressed before, growth (cell proliferation and colony formation), as well as migration (wound healing) assays were performed using newly engineered JHU012 RHOA KO clones. We demonstrated for the first time that the depletion of RHOA in larynx tumor cells are consistent with the results obtained in tongue tumor cells, *i.e.*, a significant reduction in both, cell growth and migration.

Altogether, the results obtained from the downregulation of RHOA expression in HNSCC cell lines demonstrate that RHOA has an oncogenic role in the HNSCC carcinogenic process. These results reinforce the observations obtained from the cohorts of HNSCC patients.

RHOA E40Q mutation in HNSCC cancer cells

The use of genome-wide sequencing technologies in cancer, has evidenced recently that RHOA is frequently mutated in several liquid and solid tumor types¹²⁵, opening an important new field of research. Curiously, the distribution of RHOA mutations across its coding sequence is not random, as occurs in tumor suppressor genes such as *TP53*, but mimics the mutational profile of a oncogenes, with clear mutational hotspots, such as *PI3KCA* (**Figure 58**).

Discussion

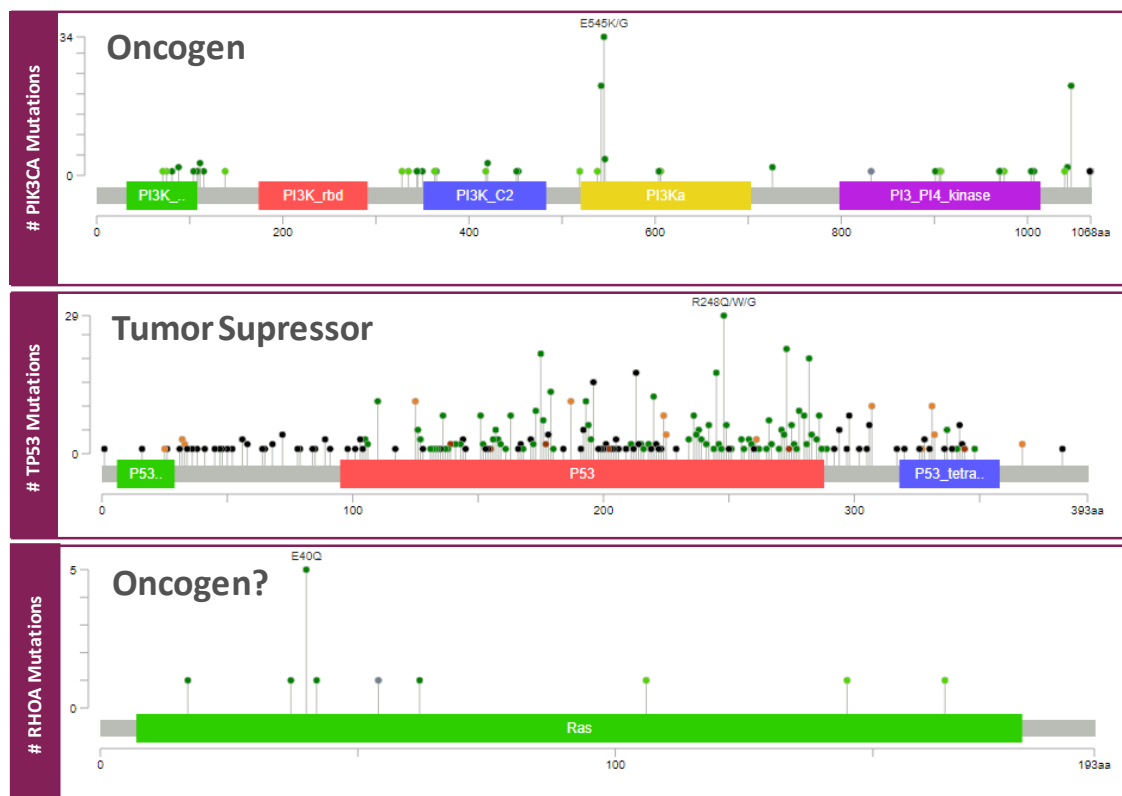


Figure 58. Distribution of mutations in *PI3KCA* oncogene, *TP53* tumor suppressor and *RHOA* along the coding sequence. Figures represent the mutational profile of *PI3KCA*, *TP53* and *RHOA* in 825 HNSCC patients from 5 different independent studies^{127, 210, 211, 301}. Figure created with TCGA data in cBioPortal.com.

Importantly, E40Q mutation has a predominant penetrance in HNSCC. Then, we wondered if RHOA E40Q mutation could have an oncogenic role in HNSCC.

In order to study the effect of RHOA in HNSCC, we proceeded with the reintroduction of RHOA wt or RHOA E40Q in RHOA KO tongue and larynx cell systems. For this purpose, we used the doxycycline-inducible overexpression of wild-type RHOA or RHOA E40Q mutant fused to GFP (GFP-RHOA wt and GFP-RHOA E40Q, respectively). Doxycycline concentration was accurately adjusted to achieve two different levels of exogenous RHOA: one close to the endogenous protein expression, and other significantly higher trying to exacerbate any possible phenotype dependent of RHOA expression. We decided to proceed in this way because it has been recently described that the stability of Rho GTPases highly depends on GDI1, a guanosine dissociation inhibitor that protects them from degradation. GDI1 levels are limited in the cells and consequently, Rho members compete for the binding to RhoGDI1. The overexpression of exogenous Rho GTPases displaces the endogenous pool of Rho proteins bound to RhoGDI1, inducing their degradation and inactivation^{303, 304}.

Surprisingly, however, reintroduction of RHOA wt at the physiological levels did not recover with none of the dox conditions tested, neither the parental cell growth, nor

migration and invasion when tested *in vitro*. Only a trend towards decreased cell growth was observed when using higher dox concentration. This result complicated the investigation of the role of the hotspot mutant RHOA E40Q, which showed the same phenotype seen in cells expressing RHOA wt.

In an attempt to clarify the reason of our unexpected results, we moved forward trying to discard possible artefactual issues that could explain why reintroduction of wt RHOA did not recover the growth pattern of the parental cells, as routinely reported extensively in similar 'rescue experiments' in the literature. First, we could rule out the hypothesis of a misbalance in the endogenous pool of Rho GTPases due to a supraphysiological RHOA expression, as explained before, because we adjusted the expression levels of RHOA to avoid this.

Therefore, we argued that in the experimental set up described above we are not putting back into the cells the same that was taken out by the CRISPR/Cas9 technology when RHOA KO cell systems were generated. Analysis of the human genome has revealed that only about 1.5% of the genetic material codes for proteins. Most genomic DNA participates in the regulation of gene expression at the transcriptional and posttranscriptional level. In eukaryotic cells, mature mRNAs contain a 5' untranslated region (5'-UTR), a coding region made up of triplet codons and a 3' untranslated region (3'-UTR). UTRs are relevant in the post-transcriptional regulation of gene expression, being highly involved in the transport of mRNAs out of the nucleus, the subcellular localization and stability, and in the control of the translation efficiency³⁰⁵. The lentiviral vectors used for the reintroduction of GFP-RHOA wt and GFP-RHOA E40Q in the SCC25 and JHU012 HNSCC RHOA KO cell line systems contained exclusively the RHOA protein coding sequence. Hence, we wondered whether the inability of exogenous GFP-RHOA to restore RHOA-deficiency could be related to the lack of these regulatory sequences. Also, it has been reported that GFP and other tags, such as His-tag might affect the bioactivity of the protein to which it is bound^{306, 307}. GFP is fused to RHOA in its N-terminal end, which corresponds to the extreme closer to E40Q mutation. Although this tag did not impair RHOA function in other cell line models such as gastric cancer, we could not rule out that key binding or catalytic sites in HNSCC could be masked by fusion and folding of GFP. Accordingly, we considered introducing into RHOA KO cell systems RHOA wt or its mutant in HNSCC, RHOA E40Q, lacking GFP tag in the coding sequencing and containing the full length 5'- and 3'-UTRs. Nevertheless, again we could not recover the parental features in cell growth and migration *in vitro* assays.

Unfortunately, the role of RHOA E40Q could not be elucidated because, despite the different approaches used, we could not archive the restoration of parental phenotype upon the reintroduction of RHOA wt into RHOA-depleted cell systems. However, in the experiments that were carried out, no differences were observed in cell growth when RHOA wt or E40Q RHOA was reintroduced into RHOA KO cells. There are multiple

Discussion

ways to study the role of a protein in a cellular system. The study of the interactome of a protein in the specific tumor-context provides interesting clues of the cell signaling networks and thus functional processes. Guided by the idea that RHOA hotspot mutations affect to part of the functions of RHOA but not all, because otherwise they would not naturally selected, we used an independent-unbiased method to identify changes in the RHOA interactome caused by the recurrent RHOA E40Q mutation. So, a pull-down assay coupled with liquid chromatography/mass spectrometry (LC/MS) analysis was performed to compare RHOA wt and RHOA E40Q binders in a HNSCC cellular context.

As expected, wild type RHOA was found to bind to multiple proteins that are known RHOA interactors, effectors and regulators (data not shown). But surprisingly, there were some notable absences in the interactome of RHOA such as ROCK, which is one the best-known RHOA effectors. For an LC/MS system to detect a protein, it must ionize well under the conditions used. This relies on many things, including the concentration of the protein, the type of MS system used and/or the settings and parameters used to run LC/MS. Therefore, the absence of ROCK protein binding could be due to many factors. Interestingly, lack binding of RHOA to known interactors such as ROCK under the conditions used, was also observed in our lab for other tumor types such as DGC or AITL, indicating a possible technical issue (settings or parameters used) rather than a biological one (protein concentration). Further investigations are needed in this regard. Interestingly, however, we found some known effectors and regulators that bind exclusively, or to much higher proportion (>4-fold) to wild type RHOA than to RHOA E40Q (**Table X**). Among them, we found RIPOR protein 1 (RIPOR1). RIPOR (RHO family interacting cell polarization regulators) family of proteins are emerging binders of Rho protein involved in cell polarity. Ripor1 specifically regulates Golgi apparatus reorientation during cell migration. The relocalization of Golgi-localized proteins from the Golgi apparatus towards the leading edge of cells during directional cell migration, is important for the efficient motility of the cells³⁴⁶.

In the proteomic assay carried out, RHOA E40Q lost the binding capacity to the three members of PKN family of proteins (PKN1, PKN2 and PKN 3). To confirm this finding, we tested by Western blot the levels of PKN1 and PKN2 in a pull-down assay with GST-RHOA wt and GST-RHOA E40Q beads in the very same cell lysates interrogated by shotgun proteomics. In good agreement with the LC/MS results, we observed a robust binding of RHOA wt to PKN1 and PKN2, while no binding was detected to the recurrent hotspot mutant RHOA E40Q.

PKN proteins, as described before, are PKC-related serine/threonine-protein kinases. They are involved in key cell function such as migration, invasion and gene transcriptional regulation^{340, 342, 347, 348}. However, nothing is known about the role of these family of proteins in HNSCC. According to the results obtained in our group, PKN1 acts as a tumor suppressor in diffuse-gastric cancer cells, inhibiting cell growth

and invasion. Therefore, RHOA E40Q could be acting as an oncogene in HNSCC abrogating the activation of a putative tumor suppressor activity of PKN in HNSCC.

Interestingly, two proteins bound to RHOA E40Q mutant but not to the wild-type RHOA were identified: Progranulin and the transcriptional activator protein Pur β (**Table 15**). Progranulin is a growth factor that has been related with the carcinogenic process in different types of cancer, stimulating cell proliferation, migration, invasion and angiogenesis, among other cancer-related features³⁴⁹. Interestingly, Progranulin promotes *in vitro* and *in vivo* tumorigenesis of poorly tumorigenic epithelial cancer cells^{350, 351}. No supporting literature was found connecting Pur β and cancer. Purine-rich element binding protein B is a nucleic acid-binding protein whose main biochemical function is to form high affinity nucleoprotein complexes with single-stranded DNA (ssDNA) or mRNA sequences containing repeats of the so-called PUR element. It has been implicated in regulating gene expression both at the level of transcription and translation. Previous reports have suggested a mechanistic connection between *PURB* loss-of-function and aberrant leukocyte function. However, in acute myelogenous leukemia, increased levels of Pur β disrupt myeloid cell homeostasis³⁵².

So, analyzing RHOA E40Q interactome, through the yeast-two-hybrid assay and shotgun proteomics, we can conclude that the RHOA interactome is deregulated when RHOA is mutated in that specific codon. Interestingly, the consistent lack of binding of RHOA E40Q to PKN family and Ripor1 proteins led us to reason that the RHOA oncogenic role observed in head and neck cancer cells could be mediated by a deregulation of downstream PKN and/or Ripor1 signalings. Moreover, if the impairment of NET1 and kinectin interactions with RHOA E40Q, found through yeast-two-hybrid screening, and the acquisition of progranulin and Pur β binding capacity, found in the shotgun proteomics analysis, are confirmed in HNSCC cell lines, we could address the relevance of these proteins into HNSCC carcinogenesis.

Overview and future perspectives

The lack of improvement in the survival rates, and the reduced number of personalized treatments in head & neck squamous cell carcinoma (HNSCC) have promoted active research into the molecular mechanisms leading to HNSCC. Interestingly, it has been recently discovered the hotspot RHOA E40Q mutation in this tumor type, indicating that deregulation of RHOA is important for the HNSCC carcinogenic process.

Here, we have demonstrated for the first time the interesting prognostic value of RHOA as biomarker predicting poorer survival in larynx tumors and aggressiveness of oral and pharynx tumors. According to this, we have confirmed that RHOA acts as an oncogene in HNSCC cancer cells, since its depletion impairs cell growth and migration. However, the results of our experiments were inconclusive with regards to the role of RHOA E40Q mutant because the parental phenotype was not restored after the

Discussion

reintroduction of RHOA what physiological levels. Possible artifactual reasons, as the presence of GFP or the lack of UTRs have been ruled out. Nevertheless, further experiments should be performed to know if these results have a biological or artefactual explanation. An alternative approach to study the role of RHOA E40Q would be to specifically edit E40 in the endogenous RHOA of HNSCC cells. However, despite this unexpected issue, we concentrated our efforts in studying the differential interactome of RHOA wt and the hotspot mutant RHOA E40Q, which has revealed important differences that require further investigation.

The Small GTPase RHOA in cancer

Chapter I & Chapter II

CONCLUSIONS

CONCLUSIONS

The main conclusions of this thesis regarding the functional characterization of the recurrent *RHOA* mutations in cancer, and the study of *RHOA* wt and *RHOA* E40Q in head and neck tumors are:

1. *RHOA* hotspot mutants G17E and G17V display a lower protein stability and have a strong tendency to localize into the cell nucleus, when compared with wild-type *RHOA*.
2. *RHOA* hotspot mutations act as loss-of function or inactivating mutations in the assays conducted:
 - a. *RHOA* hotspot mutants, except *RHOA* C16R, inhibit the F-actin-*RHOA*-SRF signaling pathway and detachment cell capability, when compared with wild-type *RHOA*.
 - b. *RHOA* hotspot mutants investigated inhibit NF κ B signaling, when compared with wild-type *RHOA*.
3. Hotspot *RHOA* mutations found in diffuse-gastric cancer affect specifically the binding to the effector PKN, whereas *RHOA* E40Q mutation found in HNSCC affect the binding to NET1 and kinectin.
4. The value of *RHOA* as a biomarker depends on the specific location of the head and neck tumors studied.
 - a. *RHOA* is associated with the differentiation grade in oral and pharynx cancers. High *RHOA* protein levels are associated with poorly differentiated oral and pharynx tumors.
 - b. *RHOA* predicts survival in larynx cancer. High *RHOA* tumor expression is associated with shorter disease-free and disease-specific survival in patients with a larynx cancer.
5. *RHOA* inactivation results in reduced proliferation and migration capacity in head and neck cancer cells.
6. *RHOA* E40Q fails to bind effector proteins of the PKN family and Ripor1, among other interactors; and acquires the capacity to bind to the growth factor Progranulin and Pur β .

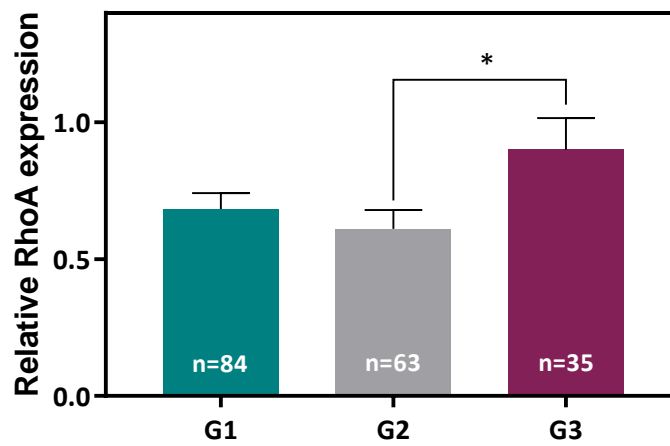
SUPPLEMENTARY RESULTS

Supplementary Table 1. Clinicopathological features of 182 oropharynx cancer patients and association with RHOA protein expression.

	Total	High RHOA	Low RHOA	p value
Sex, n (%)				
Female	5	2 (6.9)	3 (2)	0.18 ^a
Male	177	27 (93.1)	150 (98)	
Age at diagnosis (years), mean±SD	57,1 ± 10,1	56,6 ± 10,8	57,2 ± 10	0.76 ^b
Degree of differentiation, n (%)				
Good	84	12 (41,4)	72 (47,1)	0.01 ^a
Moderate	63	6 (20,7)	57 (37,2)	
Poor	35	11 (37,9)	24 (15,7)	
Mean follow up (years), mean±SD	2,8 ± 3,1	3,6 ± 4,3	2,6 ± 2,8	0.92 ^b
Five-year survival				
Alive	51	11 (37,9)	40 (26,1)	0.26 ^a
Dead	131	18 (62,1)	113 (73,9)	
Adjuvant treatment, n (%)				
Yes	130	24 (82,8)	106 (69,3)	0.18 ^a
No	52	5 (17,2)	47 (30,7)	
Stages, n (%)				
1	2	1 (3,4)	1 (0,7)	0.49 ^a
2	13	1 (3,4)	12 (7,8)	
3	30	5 (17,3)	25 (16,3)	
4	137	22 (75,9)	115 (75,2)	
1,2,3	45	7 (24,1)	38 (24,8)	0.16 ^a
4	137	22 (75,9)	115 (75,2)	
Recidiva, n (%)				
Yes	138	19 (65,5)	119 (77,8)	0.16 ^a
No	44	10 (34,5)	34 (22,2)	
Distant metastasis, n (%)				
Yes	66	10 (34,5)	56 (36,6)	1 ^a
No	116	19 (65,5)	97 (63,4)	
Tobacco consumption, n (%)				
>50 PA	78	14 (51,9)	64 (42,1)	1 ^a
<50 PA	101	13 (48,1)	88 (57,9)	
Alcohol consumption, n (%)				
Yes	171	25 (92,6)	146 (96,1)	0.35 ^a
No	8	2 (7,4)	6 (3,9)	
HPV status, n (%)				
Positive	8	2 (6,9)	6 (3,9)	0.36 ^a
Negative	174	27 (93,1)	147 (96,1)	

^aFisher's exact test; ^bMann-Whitney test; ^cChi-square test.

Supplementary Results



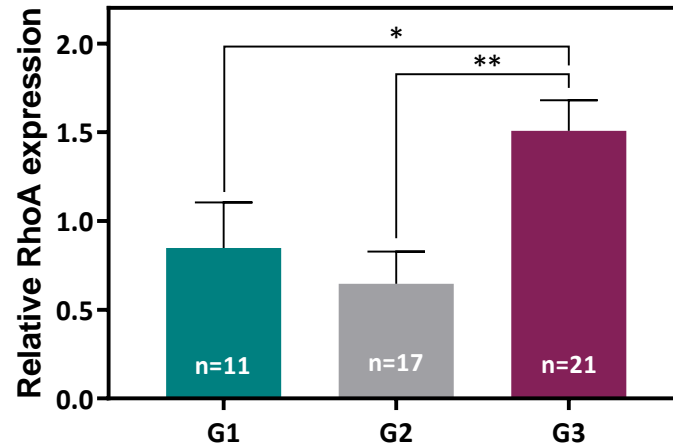
Supplementary Figure 1. RHOA tumor expression and grade of differentiation of primary oropharynx tumors. The levels of RHOA immunostaining in tissue microarrays containing triplicate tumor samples from 182 patients with oropharynx primary tumors were quantified blinded from the clinical patient data. The histogram shows the average intensity (\pm SEM) of RHOA immunostaining in tumors that are well (grade 1, G1), moderately (grade 2, G2) and poorly (grade 3, G3) differentiated. * Student's t-test $p < 0.05$.

Supplementary Table 2. Clinicopathological features of 49 hypopharynx cancer patients and association with RHOA protein expression.

	Total	High RHOA	Low RHOA	p value
Sex, n (%)				
Female	1	0	1 (3.1)	1 ^a
Male	48	17 (100)	31 (96.9)	
Age at diagnosis (years), mean±SD	58.3 ± 9.0	60.1 ± 11.4	57.4 ± 7.0	0.62 ^b
Degree of differentiation, n (%)				
Good	11	3 (17.6)	8 (25.0)	0.01 ^a
Moderate	17	2 (11.8)	15 (46.9)	
Poor	21	12 (70.6)	9 (28.1)	
Mean follow up (years), mean±SD	2.4 ± 2.1	2.5 ± 2.2	2.3 ± 2.1	0.70 ^b
Five-year survival				
Alive	4	1 (7.1)	3 (10.3)	1 ^a
Dead	39	13 (92.9)	26 (89.6)	
Adjuvant treatment, n (%)				
Yes	36	13 (76.5)	23 (71.9)	1 ^a
No	13	4 (23.5)	9 (28.1)	
Stages, n (%)				
1	1	0	1 (3.1)	N.A.
2	2	0	2 (6.2)	
3	3	3 (17.6)	0	
4	43	14 (82.4)	29 (90.7)	
1,2,3	5	3 (17.6)	3 (9.4)	0.40 ^a
4	43	14 (82.4)	29 (90.6)	
Recidiva, n (%)				
Yes	40	13 (76.5)	27 (84.4)	0.70 ^a
No	9	4 (23.5)	5 (15.6)	
Distant metastasis, n (%)				
Yes	36	13 (76.5)	23 (71.9)	1 ^a
No	13	4 (23.5)	9 (28.1)	
Tobacco consumption, n (%)				
>50 PA	16	4 (23.5)	12 (37.5)	0.36 ^a
<50 PA	33	13 (76.5)	20 (62.5)	
Alcohol consumption, n (%)				
Yes	48	17 (100)	31 (96.9)	1 ^a
No	1	0	1 (3.1)	

^aFisher's exact test; ^bMann-Whitney test; ^cChi-square test; N.A.: not applicable

Supplementary Results



Supplementary Figure 2. RHOA tumor expression and grade of differentiation of primary hypopharynx tumors. The levels of RHOA immunostaining in tissue microarrays containing triplicate tumor samples from 49 patients with hypopharynx primary tumors were quantified blinded from the clinical patient data. The histogram shows the average intensity (\pm SEM) of RHOA immunostaining in tumors that are well (grade 1, G1), moderately (grade 2, G2) and poorly (grade 3, G3) differentiated. * Student's t-test $p < 0.05$; ** $p < 0.01$.

Supplementary Table 3. Clinicopathological features of 315 oral cavity cancer patients from TCGA and association with RHOA transcript expression.

	Total	High RHOA	Low RHOA	p value
Sex, n (%)				
Female	102	84 (38.2)	18 (19.0)	0.001 ^a
Male	213	136 (61.8)	77 (81.0)	
Age at diagnosis (years), mean±SD	61.6 ± 13.1	61.0 ± 10.4	61.9 ± 14.1	0.43 ^b
Degree of differentiation, n (%)				
Good	49	35 (16.1)	14 (14.9)	0.59 ^a
Moderate	196	133 (61.3)	63 (67.0)	
Poor	66	49 (22.6)	17 (18.1)	
Mean follow up (years), mean±SD	2.5 ± 2.4	2.5 ± 2.7	2.4 ± 1.7	0.47 ^b
Five-year survival				
Alive	148	101 (52.1)	47 (53.4)	0.9 ^a
Dead	134	93 (47.9)	41 (46.6)	
Adjuvant treatment, n (%)				
Yes	67	46 (59.7)	21 (63.6)	0.83 ^a
No	43	31 (40.3)	12 (36.4)	
Stages, n (%)				
1	21	9 (4.6)	12 (12.5)	0.06 ^a
2	53	40 (20.4)	13 (13.5)	
3	56	39 (19.9)	17 (17.7)	
4	162	108 (55.1)	54 (56.3)	
1,2,3	130	88 (44.9)	42 (43.7)	0.90 ^a
4	162	108 (55.1)	54 (56.3)	
Recidiva, n (%)				
Yes	92	65 (29.5)	27 (28.4)	0.90 ^a
No	223	155 (70.5)	68 (71.6)	
Distant etastasis, n (%)				
Yes	2	1 (0.5)	1 (1.1)	0.50 ^a
No	298	209 (99.5)	89 (98.9)	
Tobacco consumption, n (%)				
>50 PA	55	34 (30.9)	21 (38.9)	0.38 ^a
<50 PA	109	76 (69.1)	33 (61.1)	
Alcohol consumption, n (%)				
Yes	96	65 (71.4)	31 (73.8)	0.84 ^a
No	37	26 (28.6)	11 (26.2)	

^aFisher's exact test; ^bMann-Whitney test; ^cChi-square test.

Supplementary Results

Supplementary Table 4. Clinicopathological features of 79 oropharynx cancer patients from TCGA and association with RHOA transcript expression.

	Total	High RHOA	Low RHOA	p value
Sex, n (%)				
Female	11	7 (12.1)	4 (19.0)	0.47 ^a
Male	68	51 (87.9)	17 (81.0)	
Age at diagnosis (years), mean±SD	55.9±9.3	56.1±9.8	55.3±7.9	0.93 ^b
Degree of differentiation, n (%)				
Good	5	2 (4.4)	3 (15.8)	0.17 ^a
Moderate	31	20 (44.4)	10 (52.6)	
Poor	29	23 (51.2)	6 (31.6)	
Mean follow up (years), mean±SD	2.2±1.6	2.2±1.6	2.3±1.6	0.71 ^b
Five-year survival				
Alive	55	40 (71.4)	15 (75.0)	1 ^a
Dead	21	16 (28.6)	5 (25.0)	
Adjuvant treatment, n (%)				
Yes	23	18 (69.2)	5 (62.5)	1 ^a
No	11	8 (30.8)	3 (37.5)	
Stages, n (%)				
1	5	4 (6.9)	1 (5.3)	0.24 ^a
2	10	5 (8.6)	5 (26.3)	
3	13	11 (19.0)	2 (10.5)	
4	49	38 (65.5)	11 (57.9)	
1,2,3	28	20 (34.5)	8 (42.1)	0.59 ^a
4	49	38 (65.5)	11 (57.9)	
Recidiva, n (%)				
Yes	19	15 (25.9)	4 (19.0)	0.77 ^a
No	60	43 (74.1)	17 (81.0)	
Distant metastasis, n (%)				
Yes	1	0	1 (5.6)	0.24 ^a
No	73	56 (100)	17 (94.4)	
Tobacco consumption, n (%)				
>50 PA	8	6 (18.7)	2 (14.3)	1 ^a
<50 PA	38	26 (81.3)	12 (85.7)	
Alcohol consumption, n (%)				
Yes	28	24 (80.0)	4 (50.0)	0.17 ^a
No	10	6 (20.0)	4 (50.0)	
HPV status, n (%)				
Positive	19	12 (75.0)	7 (87.5)	0.63 ^a
Negative	5	4 (25.0)	1 (12.5)	

^aFisher's exact test; ^bMann-Whitney test; ^cChi-square test.

The Small GTPase RHOA in cancer

Chapter I & Chapter II

BIBLIOGRAPHY

BIBLIOGRAPHY

1. SIEGEL, R. L., MILLER, K. D., FUCHS, H. E. & JEMAL, A. 2022. Cancer statistics, 2022. *CA Cancer J Clin*, 72, 7-33.
2. *National Cancer Institute (NIH)* (<https://www.cancer.gov/>).
3. HANAHAHAN, D. 2022. Hallmarks of Cancer: New Dimensions. *Cancer Discov*, 12, 31-46.
4. HANAHAHAN, D. & WEINBERG, R. A. 2000. The hallmarks of cancer. *Cell*, 100, 57-70.
5. HANAHAHAN, D. & WEINBERG, R. A. 2011. Hallmarks of cancer: the next generation. *Cell*, 144, 646-74.
6. KNUDSON, A. G., JR. 1971. Mutation and cancer: statistical study of retinoblastoma. *Proc Natl Acad Sci U S A*, 68, 820-3.
7. VOGELSTEIN, B. & KINZLER, K. W. 2004. Cancer genes and the pathways they control. *Nat Med*, 10, 789-99.
8. DREESEN, O. & BRIVANLOU, A. H. 2007. Signaling pathways in cancer and embryonic stem cells. *Stem Cell Rev*, 3, 7-17.
9. CARGNELLO, M. & ROUX, P. P. 2011. Activation and function of the MAPKs and their substrates, the MAPK-activated protein kinases. *Microbiol Mol Biol Rev*, 75, 50-83.
10. DHILLON, A. S., HAGAN, S., RATH, O. & KOLCH, W. 2007. MAP kinase signalling pathways in cancer. *Oncogene*, 26, 3279-90.
11. DU, Z. & LOVLY, C. M. 2018. Mechanisms of receptor tyrosine kinase activation in cancer. *Mol Cancer*, 17, 58.
12. JIANG, N., DAI, Q., SU, X., FU, J., FENG, X. & PENG, J. 2020. Role of PI3K/AKT pathway in cancer: the framework of malignant behavior. *Mol Biol Rep*, 47, 4587-4629.
13. FRITSCH, R., DE KRIJGER, I., FRITSCH, K., GEORGE, R., REASON, B., KUMAR, M. S., DIEFENBACHER, M., STAMP, G. & DOWNWARD, J. 2013. RAS and RHO families of GTPases directly regulate distinct phosphoinositide 3-kinase isoforms. *Cell*, 153, 1050-63.
14. REVATHIDEVI, S. & MUNIRAJAN, A. K. 2019. Akt in cancer: Mediator and more. *Semin Cancer Biol*, 59, 80-91.
15. BOUTELLE, A. M. & ATTARDI, L. D. 2021. p53 and Tumor Suppression: It Takes a Network. *Trends Cell Biol*, 31, 298-310.
16. VIVANCO, I. & SAWYERS, C. L. 2002. The phosphatidylinositol 3-Kinase AKT pathway in human cancer. *Nat Rev Cancer*, 2, 489-501.
17. MILELLA, M., FALCONE, I., CONCIATORI, F., CESTA INCANI, U., DEL CURATOLO, A., INZERILLI, N., NUZZO, C. M., VACCARO, V., VARI, S., COGNETTI, F. & CIUFFREDA, L. 2015. PTEN: Multiple Functions in Human Malignant Tumors. *Front Oncol*, 5, 24.
18. GIL, M., RAMIL, F. & AGÍS, J. A. 2020. Hydroids (Cnidaria, Hydrozoa) from Mauritanian Coral Mounds. *Zootaxa*, 4878, zootaxa 4878 3 2.
19. ÁLVAREZ-GARCIA, V., TAWIL, Y., WISE, H. M. & LESLIE, N. R. 2019. Mechanisms of PTEN loss in cancer: It's all about diversity. *Semin Cancer Biol*, 59, 66-79.
20. MUNDI, P. S., SACHDEV, J., MCCOURT, C. & KALINSKY, K. 2016. AKT in cancer: new molecular insights and advances in drug development. *Br J Clin Pharmacol*, 82, 943-56.
21. JAFFE, A. B. & HALL, A. 2005. Rho GTPases: biochemistry and biology. *Annu Rev Cell Dev Biol*, 21, 247-69.
22. BUSTELO, X. R., SAUZEAU, V. & BERENJENO, I. M. 2007. GTP-binding proteins of the Rho/Rac family: regulation, effectors and functions in vivo. *Bioessays*, 29, 356-70.
23. VEGA, F. M. & RIDLEY, A. J. 2008. Rho GTPases in cancer cell biology. *FEBS Lett*, 582, 2093-101.
24. LARTEY, J. & LOPEZ BERNAL, A. 2009. RHO protein regulation of contraction in the human uterus. *Reproduction*, 138, 407-24.
25. RIDLEY, A. J. 2006. Rho GTPases and actin dynamics in membrane protrusions and vesicle trafficking. *Trends Cell Biol*, 16, 522-9.

Bibliography

26. KIM, J. G., ISLAM, R., CHO, J. Y., JEONG, H., CAP, K. C., PARK, Y., HOSSAIN, A. J. & PARK, J. B. Regulation of RHOA GTPase and various transcription factors in the RHOA pathway. *J Cell Physiol*, 233, 6381-6392.
27. OLSON, M. F. 2018. Rho GTPases, their post-translational modifications, disease-associated mutations and pharmacological inhibitors. *Small GTPases*, 9, 203-215.
28. LANG, P., GESBERT, F., DELESPINE-CARMAGNAT, M., STANCOU, R., POUCHELET, M. & BERTOGLIO, J. 1996. Protein kinase A phosphorylation of RHOA mediates the morphological and functional effects of cyclic AMP in cytotoxic lymphocytes. *EMBO J*, 15, 510-9.
29. KIM, J. G., CHOI, K. C., HONG, C. W., PARK, H. S., CHOI, E. K., KIM, Y. S. & PARK, J. B. 2017. Tyr42 phosphorylation of RHOA GTPase promotes tumorigenesis through nuclear factor (NF)-kappaB. *Free Radic Biol Med*, 112, 69-83.
30. CHAN, C. H., LEE, S. W., LI, C. F., WANG, J., YANG, W. L., WU, C. Y., WU, J., NAKAYAMA, K. I., KANG, H. Y., HUANG, H. Y., HUNG, M. C., PANDOLFI, P. P. & LIN, H. K. 2010. Deciphering the transcriptional complex critical for RHOA gene expression and cancer metastasis. *Nat Cell Biol*, 12, 457-67.
31. KIM, J. G., KWON, H. J., WU, G., PARK, Y., LEE, J. Y., KIM, J., KIM, S. C., CHOE, M., KANG, S. G., SEO, G. Y., KIM, P. H. & PARK, J. B. 2017. RHOA GTPase oxidation stimulates cell proliferation via nuclear factor-kappaB activation. *Free Radic Biol Med*, 103, 57-68.
32. BERENJENO, I. M., NUNEZ, F. & BUSTELO, X. R. 2007. Transcriptomal profiling of the cellular transformation induced by Rho subfamily GTPases. *Oncogene*, 26, 4295-305.
33. SAUZEAU, V., BERENJENO, I. M., CITTERIO, C. & BUSTELO, X. R. 2010. A transcriptional cross-talk between RHOA and c-Myc inhibits the RHOA/Rock-dependent cytoskeleton. *Oncogene*, 29, 3781-92.
34. GILKES, D. M., XIANG, L., LEE, S. J., CHATURVEDI, P., HUBBI, M. E., WIRTZ, D. & SEMENZA, G. L. 2014. Hypoxia-inducible factors mediate coordinated RHOA-ROCK1 expression and signaling in breast cancer cells. *Proc Natl Acad Sci U S A*, 111, E384-93.
35. GADEA, G., DE TOLEDO, M., ANGUILLE, C. & ROUX, P. 2007. Loss of p53 promotes RHOA-ROCK-dependent cell migration and invasion in 3D matrices. *J Cell Biol*, 178, 23-30.
36. XIA, M. & LAND, H. 2007. Tumor suppressor p53 restricts Ras stimulation of RHOA and cancer cell motility. *Nat Struct Mol Biol*, 14, 215-23.
37. BARABUTIS, N. 2020. P53 in RHOA regulation. *Cytoskeleton (Hoboken)*.
38. INGALLINA, E., SORRENTINO, G., BERTOLIO, R., LISEK, K., ZANNINI, A., AZZOLIN, L., SEVERINO, L. U., SCAINI, D., MANO, M., MANTOVANI, F., ROSATO, A., BICCIATO, S., PICCOLO, S. & DEL SAL, G. 2018. Mechanical cues control mutant p53 stability through a mevalonate-RHOA axis. *Nat Cell Biol*, 20, 28-35.
39. GOTO, K., CHIBA, Y., MATSUSUE, K., HATTORI, Y., MAITANI, Y., SAKAI, H., KIMURA, S. & MISAWA, M. 2010. The proximal STAT6 and NF-kappaB sites are responsible for IL-13- and TNF-alpha-induced RHOA transcriptions in human bronchial smooth muscle cells. *Pharmacol Res*, 61, 466-72.
40. BELAID, A., CERZO, M., CHARGUI, A., CORCELLE-TERMEAU, E., PEDEUTOUR, F., GIULIANO, S., ILIE, M., RUBERA, I., TAUC, M., BARALE, S., BERTOLOTTI, C., BREST, P., VOURET-CRAVIARI, V., KLIONSKY, D. J., CARLE, G. F., HOFMAN, P. & MOGRABI, B. 2013. Autophagy plays a critical role in the degradation of active RHOA, the control of cell cytokinesis, and genomic stability. *Cancer Res*, 73, 4311-22.
41. BELAID, A., NDIAYE, P. D., CERZO, M., CAILLETEAU, L., BREST, P., KLIONSKY, D. J., CARLE, G. F., HOFMAN, P. & MOGRABI, B. 2014. Autophagy and SQSTM1 on the RHOA(d) again: emerging roles of autophagy in the degradation of signaling proteins. *Autophagy*, 10, 201-8.
42. SIT, S. T. & MANSER, E. 2011. Rho GTPases and their role in organizing the actin cytoskeleton. *J Cell Sci*, 124, 679-83.
43. HIGGS, H. N. & POLLARD, T. D. 1999. Regulation of actin polymerization by Arp2/3 complex and WASp/Scar proteins. *J Biol Chem*, 274, 32531-4.
44. VAN AELST, L. & D'SOUZA-SCHOREY, C. 1997. Rho GTPases and signaling networks. *Genes Dev*, 11, 2295-322.
45. RIDLEY, A. J., PATERSON, H. F., JOHNSTON, C. L., DIEKMANN, D. & HALL, A. 1992. The small GTP-binding protein rac regulates growth factor-induced membrane ruffling. *Cell*, 70, 401-10.
46. PHUYAL, S. & FARHAN, H. 2019. Multifaceted Rho GTPase Signaling at the Endomembranes. *Front Cell Dev Biol*, 7, 127.
47. LAMAZE, C., CHUANG, T. H., TERLECKY, L. J., BOKOCH, G. M. & SCHMID, S. L. 1996. Regulation of receptor-mediated endocytosis by Rho and Rac. *Nature*, 382, 177-9.

48. CHI, X., WANG, S., HUANG, Y., STAMNES, M. & CHEN, J. L. 2013. Roles of rho GTPases in intracellular transport and cellular transformation. *Int J Mol Sci*, 14, 7089-108.
49. CROISÉ, P., ESTAY-AHUMADA, C., GASMAN, S. & ORY, S. 2014. Rho GTPases, phosphoinositides, and actin: a tripartite framework for efficient vesicular trafficking. *Small GTPases*, 5, e29469.
50. RAJAKYLÄ, E. K. & VARTIAINEN, M. K. 2014. Rho, nuclear actin, and actin-binding proteins in the regulation of transcription and gene expression. *Small GTPases*, 5, e27539.
51. KIM, J. G., ISLAM, R., CHO, J. Y., JEONG, H., CAP, K. C., PARK, Y., HOSSAIN, A. J. & PARK, J. B. 2018. Regulation of RHOA GTPase and various transcription factors in the RHOA pathway. *J Cell Physiol*, 233, 6381-6392.
52. BISHOP, A. L. & HALL, A. 2000. Rho GTPases and their effector proteins. *Biochem J*, 348 Pt 2, 241-55.
53. THUMKEO, D., WATANABE, S. & NARUMIYA, S. 2013. Physiological roles of Rho and Rho effectors in mammals. *Eur J Cell Biol*, 92, 303-15.
54. ASPENSTRÖM, P. 1999. Effectors for the Rho GTPases. *Curr Opin Cell Biol*, 11, 95-102.
55. BURRIDGE, K. & WENNERBERG, K. 2004. Rho and Rac take center stage. *Cell*, 116, 167-79.
56. HEASMAN, S. J. & RIDLEY, A. J. 2008. Mammalian Rho GTPases: new insights into their functions from in vivo studies. *Nat Rev Mol Cell Biol*, 9, 690-701.
57. MUKAI, H., KITAGAWA, M., SHIBATA, H., TAKANAGA, H., MORI, K., SHIMAKAWA, M., MIYAHARA, M., HIRAO, K. & ONO, Y. 1994. Activation of PKN, a novel 120-kDa protein kinase with leucine zipper-like sequences, by unsaturated fatty acids and by limited proteolysis. *Biochem Biophys Res Commun*, 204, 348-56.
58. AVRAHAM, H. & WEINBERG, R. A. 1989. Characterization and expression of the human rhoH12 gene product. *Mol Cell Biol*, 9, 2058-66.
59. PERONA, R., ESTEVE, P., JIMENEZ, B., BALLESTERO, R. P., RAMON Y CAJAL, S. & LACAL, J. C. 1993. Tumorigenic activity of rho genes from *Aplysia californica*. *Oncogene*, 8, 1285-92.
60. PRENDERGAST, G. C., KHOSRAVI-FAR, R., SOLSKI, P. A., KURZAWA, H., LEBOWITZ, P. F. & DER, C. J. 1995. Critical role of Rho in cell transformation by oncogenic Ras. *Oncogene*, 10, 2289-96.
61. VILLALONGA, P. & RIDLEY, A. J. 2006. Rho GTPases and cell cycle control. *Growth Factors*, 24, 159-64.
62. ESTEVE, P., EMBADE, N., PERONA, R., JIMENEZ, B., DEL PESO, L., LEON, J., ARENDS, M., MIKI, T. & LACAL, J. C. 1998. Rho-regulated signals induce apoptosis in vitro and in vivo by a p53-independent, but Bcl2 dependent pathway. *Oncogene*, 17, 1855-69.
63. WHEELER, A. P. & RIDLEY, A. J. 2004. Why three Rho proteins? RHOA, RhoB, RhoC, and cell motility. *Exp Cell Res*, 301, 43-9.
64. BRYAN, B. A. & D'AMORE, P. A. 2007. What tangled webs they weave: Rho-GTPase control of angiogenesis. *Cell Mol Life Sci*, 64, 2053-65.
65. FRITZ, G., BRACHETTI, C., BAHLMANN, F., SCHMIDT, M. & KAINA, B. 2002. Rho GTPases in human breast tumours: expression and mutation analyses and correlation with clinical parameters. *Br J Cancer*, 87, 635-44.
66. FRITZ, G., JUST, I. & KAINA, B. 1999. Rho GTPases are over-expressed in human tumors. *Int J Cancer*, 81, 682-7.
67. ABRAHAM, M. T., KURIAKOSE, M. A., SACKS, P. G., YEE, H., CHIRIBOGA, L., BEARER, E. L. & DELACURE, M. D. 2001. Motility-related proteins as markers for head and neck squamous cell cancer. *Laryngoscope*, 111, 1285-9.
68. HORIUCHI, A., IMAI, T., WANG, C., OHIRA, S., FENG, Y., NIKAIDO, T. & KONISHI, I. 2003. Up-regulation of small GTPases, RHOA and RhoC, is associated with tumor progression in ovarian carcinoma. *Lab Invest*, 83, 861-70.
69. PAN, Y., BI, F., LIU, N., XUE, Y., YAO, X., ZHENG, Y. & FAN, D. 2004. Expression of seven main Rho family members in gastric carcinoma. *Biochem Biophys Res Commun*, 315, 686-91.
70. FUKUI, K., TAMURA, S., WADA, A., KAMADA, Y., SAWAI, Y., IMANAKA, K., KUDARA, T., SHIMOMURA, I. & HAYASHI, N. 2006. Expression and prognostic role of RHOA GTPases in hepatocellular carcinoma. *J Cancer Res Clin Oncol*, 132, 627-33.
71. WANG, H. B., LIU, X. P., LIANG, J., YANG, K., SUI, A. H. & LIU, Y. J. 2009. Expression of RHOA and RhoC in colorectal carcinoma and its relations with clinicopathological parameters. *Clin Chem Lab Med*, 47, 811-7.
72. JEONG, D., PARK, S., KIM, H., KIM, C. J., AHN, T. S., BAE, S. B., KIM, H. J., KIM, T. H., IM, J., LEE, M. S., KWON, H. Y. & BAEK, M. J. 2016. RHOA is associated with invasion and poor prognosis in colorectal cancer. *Int J Oncol*, 48, 714-22.

Bibliography

73. SAYAGUES, J. M., CORCHETE, L. A., GUTIERREZ, M. L., SARASQUETE, M. E., DEL MAR ABAD, M., BENGOCHEA, O., FERMINAN, E., ANDUAGA, M. F., DEL CARMEN, S., IGLESIAS, M., ESTEBAN, C., ANGOSO, M., ALCAZAR, J. A., GARCIA, J., ORFAO, A. & MUNOZ-BELLVIS, L. 2016. Genomic characterization of liver metastases from colorectal cancer patients. *Oncotarget*, 7, 72908-72922.
74. LIU, N., BI, F., PAN, Y., SUN, L., XUE, Y., SHI, Y., YAO, X., ZHENG, Y. & FAN, D. 2004. Reversal of the malignant phenotype of gastric cancer cells by inhibition of RHOA expression and activity. *Clin Cancer Res*, 10, 6239-47.
75. CHANG, K. K., CHO, S. J., YOON, C., LEE, J. H., PARK, D. J. & YOON, S. S. 2016. Increased RHOA Activity Predicts Worse Overall Survival in Patients Undergoing Surgical Resection for Lauren Diffuse-Type Gastric Adenocarcinoma. *Ann Surg Oncol*, 23, 4238-4246.
76. FARIED, A., FARIED, L. S., USMAN, N., KATO, H. & KUWANO, H. 2007. Clinical and prognostic significance of RHOA and RhoC gene expression in esophageal squamous cell carcinoma. *Ann Surg Oncol*, 14, 3593-601.
77. LI, X. R., JI, F., OUYANG, J., WU, W., QIAN, L. Y. & YANG, K. Y. 2006. Overexpression of RHOA is associated with poor prognosis in hepatocellular carcinoma. *Eur J Surg Oncol*, 32, 1130-4.
78. WANG, D., DOU, K., XIANG, H., SONG, Z., ZHAO, Q., CHEN, Y. & LI, Y. 2007. Involvement of RHOA in progression of human hepatocellular carcinoma. *J Gastroenterol Hepatol*, 22, 1916-20.
79. DELLA PERUTA, M., GIAGULLI, C., LAUDANNA, C., SCARPA, A. & SORIO, C. 2010. RHOA and PRKCD control different aspects of cell motility in pancreatic cancer metastatic clones. *Mol Cancer*, 9, 61.
80. TIMPSON, P., MCGHEE, E. J., MORTON, J. P., VON KRIEGSHEIM, A., SCHWARZ, J. P., KARIM, S. A., DOYLE, B., QUINN, J. A., CARRAGHER, N. O., EDWARD, M., OLSON, M. F., FRAME, M. C., BRUNTON, V. G., SANSOM, O. J. & ANDERSON, K. I. 2011. Spatial regulation of RHOA activity during pancreatic cancer cell invasion driven by mutant p53. *Cancer Res*, 71, 747-57.
81. LI, Z., CHANG, Z., CHIAO, L. J., KANG, Y., XIA, Q., ZHU, C., FLEMING, J. B., EVANS, D. B. & CHIAO, P. J. 2009. TrkB1 induces liver metastasis of pancreatic cancer cells by sequestering Rho GDP dissociation inhibitor and promoting RHOA activation. *Cancer Res*, 69, 7851-9.
82. YANG, X., ZHENG, F., ZHANG, S. & LU, J. 2015. Loss of RHOA expression prevents proliferation and metastasis of SPCA1 lung cancer cells in vitro. *Biomed Pharmacother*, 69, 361-6.
83. KONSTANTINIDOU, G., RAMADORI, G., TORTI, F., KANGASNIEMI, K., RAMIREZ, R. E., CAI, Y., BEHRENS, C., DELLINGER, M. T., BREKKEN, R. A., WISTUBA, II, HEGUY, A., TERUYA-FELDSTEIN, J. & SCAGLIONI, P. P. 2013. RHOA-FAK is a required signaling axis for the maintenance of KRAS-driven lung adenocarcinomas. *Cancer Discov*, 3, 444-57.
84. ADNANE, J., MURO-CACHO, C., MATHEWS, L., SEBTI, S. M. & MUÑOZ-ANTONIA, T. 2002. Suppression of rho B expression in invasive carcinoma from head and neck cancer patients. *Clin Cancer Res*, 8, 2225-32.
85. YAN, G., ZOU, R., CHEN, Z., FAN, B., WANG, Z., WANG, Y., YIN, X., ZHANG, D., TONG, L., YANG, F., JIANG, W., FU, W., ZHENG, J., BERGO, M. O., DALIN, M., ZHENG, J., CHEN, S. & ZHOU, J. 2014. Silencing RHOA inhibits migration and invasion through Wnt/beta-catenin pathway and growth through cell cycle regulation in human tongue cancer. *Acta Biochim Biophys Sin (Shanghai)*, 46, 682-90.
86. DUA, P. & GUDE, R. P. 2008. Pentoxifylline impedes migration in B16F10 melanoma by modulating Rho GTPase activity and actin organisation. *Eur J Cancer*, 44, 1587-95.
87. HEO, J. C., PARK, J. Y., WOO, S. U., RHO, J. R., LEE, H. J., KIM, S. U., KHO, Y. H. & LEE, S. H. 2006. Dykellic acid inhibits cell migration and tube formation by RHOA-GTP expression. *Biol Pharm Bull*, 29, 2256-9.
88. KOSLA, J., PANKOVA, D., PLACHY, J., TOLDE, O., BICANOVA, K., DVORAK, M., ROSEL, D. & BRABEK, J. 2013. Metastasis of aggressive amoeboid sarcoma cells is dependent on Rho/ROCK/MLC signaling. *Cell Commun Signal*, 11, 51.
89. KAMAI, T., KAWAKAMI, S., KOGA, F., ARAI, G., TAKAGI, K., ARAI, K., TSUJII, T. & YOSHIDA, K. I. 2003. RHOA is associated with invasion and lymph node metastasis in upper urinary tract cancer. *BJU Int*, 91, 234-8.
90. KAMAI, T., TSUJII, T., ARAI, K., TAKAGI, K., ASAMI, H., ITO, Y. & OSHIMA, H. 2003. Significant association of Rho/ROCK pathway with invasion and metastasis of bladder cancer. *Clin Cancer Res*, 9, 2632-41.
91. WANG, J., WU, Q., ZHANG, L. H., ZHAO, Y. X. & WU, X. 2016. The role of RHOA in vulvar squamous cell carcinoma: a carcinogenesis, progression, and target therapy marker. *Tumour Biol*, 37, 2879-90.

92. CHEN, S., WANG, J., GOU, W. F., XIU, Y. L., ZHENG, H. C., ZONG, Z. H., TAKANO, Y. & ZHAO, Y. 2013. The involvement of RHOA and Wnt-5a in the tumorigenesis and progression of ovarian epithelial carcinoma. *Int J Mol Sci*, 14, 24187-99.
93. HORIUCHI, A., KIKUCHI, N., OSADA, R., WANG, C., HAYASHI, A., NIKAIIDO, T. & KONISHI, I. 2008. Overexpression of RHOA enhances peritoneal dissemination: RHOA suppression with Lovastatin may be useful for ovarian cancer. *Cancer Sci*, 99, 2532-9.
94. WANG, X., JIANG, W., KANG, J., LIU, Q. & NIE, M. 2015. Knockdown of RHOA expression alters ovarian cancer biological behavior in vitro and in nude mice. *Oncol Rep*, 34, 891-9.
95. GHOSH, P. M., GHOSH-CHOUDHURY, N., MOYER, M. L., MOTT, G. E., THOMAS, C. A., FOSTER, B. A., GREENBERG, N. M. & KREISBERG, J. I. 1999. Role of RHOA activation in the growth and morphology of a murine prostate tumor cell line. *Oncogene*, 18, 4120-30.
96. GHOSH, P. M., BEDOLLA, R., MIKHAILOVA, M. & KREISBERG, J. I. 2002. RHOA-dependent murine prostate cancer cell proliferation and apoptosis: role of protein kinase Czeta. *Cancer Res*, 62, 2630-6.
97. KAMAI, T., YAMANISHI, T., SHIRATAKI, H., TAKAGI, K., ASAMI, H., ITO, Y. & YOSHIDA, K. 2004. Overexpression of RHOA, Rac1, and Cdc42 GTPases is associated with progression in testicular cancer. *Clin Cancer Res*, 10, 4799-805.
98. ZHAO, X., LU, L., POKHRIYAL, N., MA, H., DUAN, L., LIN, S., JAFARI, N., BAND, H. & BAND, V. 2009. Overexpression of RHOA induces preneoplastic transformation of primary mammary epithelial cells. *Cancer Res*, 69, 483-91.
99. PILLE, J. Y., DENOYELLE, C., VARET, J., BERTRAND, J. R., SORIA, J., OPOLON, P., LU, H., PRITCHARD, L. L., VANNIER, J. P., MALVY, C., SORIA, C. & LI, H. 2005. Anti-RHOA and anti-RhoC siRNAs inhibit the proliferation and invasiveness of MDA-MB-231 breast cancer cells in vitro and in vivo. *Mol Ther*, 11, 267-74.
100. PILLE, J. Y., LI, H., BLOT, E., BERTRAND, J. R., PRITCHARD, L. L., OPOLON, P., MAKSIMENKO, A., LU, H., VANNIER, J. P., SORIA, J., MALVY, C. & SORIA, C. 2006. Intravenous delivery of anti-RHOA small interfering RNA loaded in nanoparticles of chitosan in mice: safety and efficacy in xenografted aggressive breast cancer. *Hum Gene Ther*, 17, 1019-26.
101. BELLIZZI, A., MANGIA, A., CHIRIATTI, A., PETRONI, S., QUARANTA, M., SCHITTULLI, F., MALFETTON, A., CARDONE, R. A., PARADISO, A. & RESHKIN, S. J. 2008. RHOA protein expression in primary breast cancers and matched lymphocytes is associated with progression of the disease. *Int J Mol Med*, 22, 25-31.
102. ARANGO, D., LAIHO, P., KOKKO, A., ALHOPURO, P., SAMMALKORPI, H., SALOVAARA, R., NICORICI, D., HAUTANIEMI, S., ALAZZOUZI, H., MECKLIN, J. P., JARVINEN, H., HEMMINKI, A., ASTOLA, J., SCHWARTZ, S., JR. & AALTONEN, L. A. 2005. Gene-expression profiling predicts recurrence in Dukes' C colorectal cancer. *Gastroenterology*, 129, 874-84.
103. RODRIGUES, P., MACAYA, I., BAZZOCCO, S., MAZZOLINI, R., ANDRETTA, E., DOPESO, H., MATEO-LOZANO, S., BILIC, J., CARTON-GARCIA, F., NIETO, R., SUAREZ-LOPEZ, L., AFONSO, E., LANDOLFI, S., HERNANDEZ-LOSA, J., KOBAYASHI, K., RAMON Y CAJAL, S., TABERNEO, J., TEBBUTT, N. C., MARIADASON, J. M., SCHWARTZ, S., JR. & ARANGO, D. 2014. RHOA inactivation enhances Wnt signalling and promotes colorectal cancer. *Nat Commun*, 5, 5458.
104. CHEW, T. W., LIU, X. J., LIU, L., SPITSBERGEN, J. M., GONG, Z. & LOW, B. C. 2014. Crosstalk of Ras and Rho: activation of RHOA abates Kras-induced liver tumorigenesis in transgenic zebrafish models. *Oncogene*, 33, 2717-27.
105. DITTERT, D. D., KIELISCH, C., ALLDINGER, I., ZIETZ, C., MEYER, W., DOBROWOLSKI, F., SAEGER, H. D. & BARETTON, G. B. 2008. Prognostic significance of immunohistochemical RHOA expression on survival in pancreatic ductal adenocarcinoma: a high-throughput analysis. *Hum Pathol*, 39, 1002-10.
106. ZANDVAKILI, I., DAVIS, A. K., HU, G. & ZHENG, Y. 2015. Loss of RHOA Exacerbates, Rather Than Dampens, Oncogenic K-Ras Induced Lung Adenoma Formation in Mice. *PLoS One*, 10, e0127923.
107. KALPANA, G., FIGY, C., YEUNG, M. & YEUNG, K. C. 2019. Reduced RHOA expression enhances breast cancer metastasis with a concomitant increase in CCR5 and CXCR4 chemokines signaling. *Sci Rep*, 9, 16351.
108. LAWSON, C. D., FAN, C., MITIN, N., BAKER, N. M., GEORGE, S. D., GRAHAM, D. M., PEROU, C. M., BURRIDGE, K., DER, C. J. & ROSSMAN, K. L. 2016. Rho GTPase Transcriptome Analysis Reveals Oncogenic Roles for Rho GTPase-Activating Proteins in Basal-like Breast Cancers. *Cancer Res*, 76, 3826-37.

Bibliography

109. HUMPHRIES, B., WANG, Z., LI, Y., JHAN, J. R., JIANG, Y. & YANG, C. 2017. ARHGAP18 Downregulation by miR-200b Suppresses Metastasis of Triple-Negative Breast Cancer by Enhancing Activation of RHOA. *Cancer Res*, 77, 4051-4064.
110. KACZOROWSKI, M., BIECEK, P., DONIZY, P., PIENIAZEK, M., MATKOWSKI, R. & HALON, A. 2019. Low RHOA expression is associated with adverse outcome in melanoma patients: a clinicopathological analysis. *Am J Transl Res*, 11, 4524-4532.
111. KLEIN, R. M. & HIGGINS, P. J. 2011. A switch in RND3-RHOA signaling is critical for melanoma cell invasion following mutant-BRAF inhibition. *Mol Cancer*, 10, 114.
112. DIAZ-NUNEZ, M., DIEZ-TORRE, A., DE WEVER, O., ANDRADE, R., ARLUZZA, J., SILIO, M. & ARECHAGA, J. 2016. Histone deacetylase inhibitors induce invasion of human melanoma cells in vitro via differential regulation of N-cadherin expression and RHOA activity. *BMC Cancer*, 16, 667.
113. GARCIA-MARISCAL, A., LI, H., PEDERSEN, E., PEYROLLIER, K., RYAN, K. M., STANLEY, A., QUONDAMATTEO, F. & BRAKEBUSCH, C. 2018. Loss of RHOA promotes skin tumor formation and invasion by upregulation of RhoB. *Oncogene*, 37, 847-860.
114. OSTROM, Q. T., GITTLEMAN, H., DE BLANK, P. M., FINLAY, J. L., GURNEY, J. G., MCKEAN-COWDIN, R., STEARNS, D. S., WOLFF, J. E., LIU, M., WOLINSKY, Y., KRUCHKO, C. & BARNHOLTZ-SLOAN, J. S. 2016. American Brain Tumor Association Adolescent and Young Adult Primary Brain and Central Nervous System Tumors Diagnosed in the United States in 2008-2012. *Neuro Oncol*, 18 Suppl 1, i1-i50.
115. TABU, K., OHBA, Y., SUZUKI, T., MAKINO, Y., KIMURA, T., OHNISHI, A., SAKAI, M., WATANABE, T., TANAKA, S. & SAWA, H. 2007. Oligodendrocyte lineage transcription factor 2 inhibits the motility of a human glial tumor cell line by activating RHOA. *Mol Cancer Res*, 5, 1099-109.
116. GOLDBERG, L. & KLOOG, Y. 2006. A Ras inhibitor tilts the balance between Rac and Rho and blocks phosphatidylinositol 3-kinase-dependent glioblastoma cell migration. *Cancer Res*, 66, 11709-17.
117. FORGET, M. A., DESROSIERS, R. R., DEL, M., MOUMDJIAN, R., SHEDID, D., BERTHELET, F. & BELIVEAU, R. 2002. The expression of rho proteins decreases with human brain tumor progression: potential tumor markers. *Clin Exp Metastasis*, 19, 9-15.
118. PU, Y. S., WANG, C. W., LIU, G. Y., KUO, Y. Z., HUANG, C. Y., KANG, W. Y., SHUN, C. T., LIN, C. C., WU, W. J. & HOUR, T. C. 2008. Down-regulated expression of RHOA in human conventional renal cell carcinoma. *Anticancer Res*, 28, 2039-43.
119. MIYAZAKI, J., ITO, K., FUJITA, T., MATSUZAKI, Y., ASANO, T., HAYAKAWA, M., ASANO, T. & KAWAKAMI, Y. 2017. Progression of Human Renal Cell Carcinoma via Inhibition of RHOA-ROCK Axis by PARG1. *Transl Oncol*, 10, 142-152.
120. RIHET, S., VIELH, P., CAMONIS, J., GOUD, B., CHEVILLARD, S. & DE GUNZBURG, J. 2001. Mutation status of genes encoding RHOA, Rac1, and Cdc42 GTPases in a panel of invasive human colorectal and breast tumors. *J Cancer Res Clin Oncol*, 127, 733-8.
121. PARK, B., NGUYEN, N. T., DUTT, P., MERDEK, K. D., BASHAR, M., STERPETTI, P., TOSOLINI, A., TESTA, J. R. & TOKSOZ, D. 2002. Association of Lbc Rho guanine nucleotide exchange factor with alpha-catenin-related protein, alpha-catulin/CTNNA1, supports serum response factor activation. *J Biol Chem*, 277, 45361-70.
122. PALOMERO, T., COURONNE, L., KHIABANIAN, H., KIM, M. Y., AMBESI-IMPIOMBATO, A., PEREZ-GARCIA, A., CARPENTER, Z., ABATE, F., ALLEGRETTA, M., HAYDU, J. E., JIANG, X., LOSSOS, I. S., NICOLAS, C., BALBIN, M., BASTARD, C., BHAGAT, G., PIRIS, M. A., CAMPO, E., BERNARD, O. A., RABADAN, R. & FERRANDO, A. A. 2014. Recurrent mutations in epigenetic regulators, RHOA and FYN kinase in peripheral T cell lymphomas. *Nat Genet*, 46, 166-70.
123. YOO, H. Y., SUNG, M. K., LEE, S. H., KIM, S., LEE, H., PARK, S., KIM, S. C., LEE, B., RHO, K., LEE, J. E., CHO, K. H., KIM, W., JU, H., KIM, J., KIM, S. J., KIM, W. S., LEE, S. & KO, Y. H. 2014. A recurrent inactivating mutation in RHOA GTPase in angioimmunoblastic T cell lymphoma. *Nat Genet*, 46, 371-5.
124. MANSO, R., SANCHEZ-BEATO, M., MONSALVO, S., GOMEZ, S., CERECEDA, L., LLAMAS, P., ROJO, F., MOLLEJO, M., MENARGUEZ, J., ALVES, J., GARCIA-COSIO, M., PIRIS, M. A. & RODRIGUEZ-PINILLA, S. M. 2014. The RHOA G17V gene mutation occurs frequently in peripheral T-cell lymphoma and is associated with a characteristic molecular signature. *Blood*, 123, 2893-4.
125. KATAOKA, K. & OGAWA, S. 2016. Variegated RHOA mutations in human cancers. *Exp Hematol*, 44, 1123-1129.
126. LAUREN, P. 1965. THE TWO HISTOLOGICAL MAIN TYPES OF GASTRIC CARCINOMA: DIFFUSE AND SO-CALLED INTESTINAL-TYPE CARCINOMA. AN ATTEMPT AT A HISTO-CLINICAL CLASSIFICATION. *Acta Pathol Microbiol Scand*, 64, 31-49.

127. 2014. Comprehensive molecular characterization of gastric adenocarcinoma. *Nature*, 513, 202-9.
128. KAKIUCHI, M., NISHIZAWA, T., UEDA, H., GOTOH, K., TANAKA, A., HAYASHI, A., YAMAMOTO, S., TATSUNO, K., KATOH, H., WATANABE, Y., ICHIMURA, T., USHIKU, T., FUNAHASHI, S., TATEISHI, K., WADA, I., SHIMIZU, N., NOMURA, S., KOIKE, K., SETO, Y., FUKAYAMA, M., ABURATANI, H. & ISHIKAWA, S. 2014. Recurrent gain-of-function mutations of RHOA in diffuse-type gastric carcinoma. *Nat Genet*, 46, 583-7.
129. WANG, K., YUEN, S. T., XU, J., LEE, S. P., YAN, H. H., SHI, S. T., SIU, H. C., DENG, S., CHU, K. M., LAW, S., CHAN, K. H., CHAN, A. S., TSUI, W. Y., HO, S. L., CHAN, A. K., MAN, J. L., FOGLIZZO, V., NG, M. K., CHAN, A. S., CHING, Y. P., CHENG, G. H., XIE, T., FERNANDEZ, J., LI, V. S., CLEVERS, H., REJTO, P. A., MAO, M. & LEUNG, S. Y. 2014. Whole-genome sequencing and comprehensive molecular profiling identify new driver mutations in gastric cancer. *Nat Genet*, 46, 573-82.
130. CHO, S. Y., PARK, J. W., LIU, Y., PARK, Y. S., KIM, J. H., YANG, H., UM, H., KO, W. R., LEE, B. I., KWON, S. Y., RYU, S. W., KWON, C. H., PARK, D. Y., LEE, J. H., LEE, S. I., SONG, K. S., HUR, H., HAN, S. U., CHANG, H., KIM, S. J., KIM, B. S., YOON, J. H., YOO, M. W., KIM, B. S., LEE, I. S., KOOK, M. C., THIESSEN, N., HE, A., STEWART, C., DUNFORD, A., KIM, J., SHIH, J., SAKSENA, G., CHERNIACK, A. D., SCHUMACHER, S., WEINER, A. T., ROSENBERG, M., GETZ, G., YANG, E. G., RYU, M. H., BASS, A. J. & KIM, H. K. 2017. Sporadic Early-Onset Diffuse Gastric Cancers Have High Frequency of Somatic CDH1 Alterations, but Low Frequency of Somatic RHOA Mutations Compared With Late-Onset Cancers. *Gastroenterology*, 153, 536-549 e26.
131. HASHIMOTO, T., OGAWA, R., TANG, T. Y., YOSHIDA, H., TANIGUCHI, H., KATAI, H., ODA, I. & SEKINE, S. 2019. RHOA mutations and CLDN18-ARHGAP fusions in intestinal-type adenocarcinoma with anastomosing glands of the stomach. *Mod Pathol*, 32, 568-575.
132. LIM, B., KIM, C., KIM, J. H., KWON, W. S., LEE, W. S., KIM, J. M., PARK, J. Y., KIM, H. S., PARK, K. H., KIM, T. S., PARK, J. L., CHUNG, H. C., RHA, S. Y. & KIM, S. Y. 2016. Genetic alterations and their clinical implications in gastric cancer peritoneal carcinomatosis revealed by whole-exome sequencing of malignant ascites. *Oncotarget*, 7, 8055-66.
133. CHOI, J. H., KIM, Y. B., AHN, J. M., KIM, M. J., BAE, W. J., HAN, S. U., WOO, H. G. & LEE, D. 2018. Identification of genomic aberrations associated with lymph node metastasis in diffuse-type gastric cancer. *Exp Mol Med*, 50, 6.
134. HU, B., EL HAJJ, N., SITTNER, S., LAMMERT, N., BARNES, R. & MELONI-EHRIG, A. 2012. Gastric cancer: Classification, histology and application of molecular pathology. *J Gastrointest Oncol*, 3, 251-61.
135. USHIKU, T., ISHIKAWA, S., KAKIUCHI, M., TANAKA, A., KATOH, H., ABURATANI, H., LAUWERS, G. Y. & FUKAYAMA, M. 2016. RHOA mutation in diffuse-type gastric cancer: a comparative clinicopathology analysis of 87 cases. *Gastric Cancer*, 19, 403-411.
136. SAHAI, E., ALBERTS, A. S. & TREISMAN, R. 1998. RHOA effector mutants reveal distinct effector pathways for cytoskeletal reorganization, SRF activation and transformation. *EMBO J*, 17, 1350-61.
137. MURRAY, D., HORGAN, G., MACMATHUNA, P. & DORAN, P. 2008. NET1-mediated RHOA activation facilitates lysophosphatidic acid-induced cell migration and invasion in gastric cancer. *Br J Cancer*, 99, 1322-9.
138. NISHIZAWA, T., NAKANO, K., HARADA, A., KAKIUCHI, M., FUNAHASHI, S. I., SUZUKI, M., ISHIKAWA, S. & ABURATANI, H. 2018. DGC-specific RHOA mutations maintained cancer cell survival and promoted cell migration via ROCK inactivation. *Oncotarget*, 9, 23198-23207.
139. ZHANG, H., SCHAEFER, A., WANG, Y., HODGE, R. G., BLAKE, D. R., DIEHL, J. N., PAPAGEORGE, A. G., STACHLER, M. D., LIAO, J., ZHOU, J., WU, Z., AKARCA, F. G., DE KLERK, L. K., DERKS, S., PIEROBON, M., HOADLEY, K. A., WANG, T. C., CHURCH, G., WONG, K. K., PETRICOIN, E. F., COX, A. D., LOWY, D. R., DER, C. J. & BASS, A. J. 2020. Gain-of-Function RHOA Mutations Promote Focal Adhesion Kinase Activation and Dependency in Diffuse Gastric Cancer. *Cancer Discov*, 10, 288-305.
140. NISHIZAWA, T., NAKANO, K., FUJII, E., KOMURA, D., KUROIWA, Y., ISHIMARU, C., MONNAI, M., ABURATANI, H., ISHIKAWA, S. & SUZUKI, M. 2019. In vivo effects of mutant RHOA on tumor formation in an orthotopic inoculation model. *Oncol Rep*, 42, 1745-1754.
141. GHERARDI, E., BIRCHMEIER, W., BIRCHMEIER, C. & VANDE WOUDE, G. 2012. Targeting MET in cancer: rationale and progress. *Nat Rev Cancer*, 12, 89-103.
142. LIU, J., LI, S., CHEN, S., CHEN, S., GENG, Q. & XU, D. 2019. c-Met-dependent phosphorylation of RHOA plays a key role in gastric cancer tumorigenesis. *J Pathol*, 249, 126-136.
143. ISHIKAWA, S. 2016. Opposite RHOA functions within the ATLL category. *Blood*, 127, 524-5.
144. SVENSMARK, J. H. & BRAKEBUSCH, C. Rho GTPases in cancer: friend or foe? *Oncogene*.

Bibliography

145. DE RIENZO, A., ARCHER, M. A., YEAP, B. Y., DAO, N., SCIARANGHELLA, D., SIDERIS, A. C., ZHENG, Y., HOLMAN, A. G., WANG, Y. E., DAL CIN, P. S., FLETCHER, J. A., RUBIO, R., CROFT, L., QUACKENBUSH, J., SUGARBAKER, P. E., MUNIR, K. J., BATTILANA, J. R., GUSTAFSON, C. E., CHIRIEAC, L. R., CHING, S. M., WONG, J., TAY, L. C., RUDD, S., HERCUS, R., SUGARBAKER, D. J., RICHARDS, W. G. & BUENO, R. 2016. Gender-Specific Molecular and Clinical Features Underlie Malignant Pleural Mesothelioma. *Cancer Res*, 76, 319-28.
146. BURKHARDT, B., ZIMMERMANN, M., OSCHLIES, I., NIGGLI, F., MANN, G., PARWARESCH, R., RIEHM, H., SCHRAPPE, M. & REITER, A. 2005. The impact of age and gender on biology, clinical features and treatment outcome of non-Hodgkin lymphoma in childhood and adolescence. *Br J Haematol*, 131, 39-49.
147. RICHTER, J., SCHLESNER, M., HOFFMANN, S., KREUZ, M., LEICH, E., BURKHARDT, B., ROSOŁOWSKI, M., AMMERPOHL, O., WAGENER, R., BERNHART, S. H., LENZE, D., SZCZEPANOWSKI, M., PAULSEN, M., LIPINSKI, S., RUSSELL, R. B., ADAM-KLAGES, S., APIC, G., CLAVIEZ, A., HASENCLEVER, D., HOVESTADT, V., HORNIG, N., KORBEL, J. O., KUBE, D., LANGENBERGER, D., LAWERENZ, C., LISFELD, J., MEYER, K., PICELLI, S., PISCHIMAROV, J., RADLWIMMER, B., RAUSCH, T., ROHDE, M., SCHILHABEL, M., SCHOLTYSIK, R., SPANG, R., TRAUTMANN, H., ZENZ, T., BORKHARDT, A., DREXLER, H. G., MOLLER, P., MACLEOD, R. A., POTT, C., SCHREIBER, S., TRUMPER, L., LOEFFLER, M., STADLER, P. F., LICHTER, P., EILS, R., KUPPERS, R., HUMMEL, M., KLAPPER, W., ROSENSTIEL, P., ROSENWALD, A., BRORS, B. & SIEBERT, R. 2012. Recurrent mutation of the ID3 gene in Burkitt lymphoma identified by integrated genome, exome and transcriptome sequencing. *Nat Genet*, 44, 1316-20.
148. ROHDE, M., RICHTER, J., SCHLESNER, M., BETTS, M. J., CLAVIEZ, A., BONN, B. R., ZIMMERMANN, M., DAMM-WELK, C., RUSSELL, R. B., BORKHARDT, A., EILS, R., HOELL, J. I., SZCZEPANOWSKI, M., OSCHLIES, I., KLAPPER, W., BURKHARDT, B. & SIEBERT, R. 2014. Recurrent RHOA mutations in pediatric Burkitt lymphoma treated according to the NHL-BFM protocols. *Genes Chromosomes Cancer*, 53, 911-6.
149. SNYDER, J. T., WORTHYLAKE, D. K., ROSSMAN, K. L., BETTS, L., PRUITT, W. M., SIDEROVSKI, D. P., DER, C. J. & SONDEK, J. 2002. Structural basis for the selective activation of Rho GTPases by Dbp exchange factors. *Nat Struct Biol*, 9, 468-75.
150. O'HAYRE, M., INOUE, A., KUFAREVA, I., WANG, Z., MIKELIS, C. M., DRUMMOND, R. A., AVINO, S., FINKEL, K., KALIM, K. W., DIPASQUALE, G., GUO, F., AOKI, J., ZHENG, Y., LIONAKIS, M. S., MOLINOLO, A. A. & GUTKIND, J. S. 2016. Inactivating mutations in GNA13 and RHOA in Burkitt's lymphoma and diffuse large B-cell lymphoma: a tumor suppressor function for the G13/RHOA axis in B cells. *Oncogene*, 35, 3771-80.
151. NAGATA, Y., KONTANI, K., ENAMI, T., KATAOKA, K., ISHII, R., TOTOKI, Y., KATAOKA, T. R., HIRATA, M., AOKI, K., NAKANO, K., KITANAKA, A., SAKATA-YANAGIMOTO, M., EGAMI, S., SHIRAISHI, Y., CHIBA, K., TANAKA, H., SHIOZAWA, Y., YOSHIZATO, T., SUZUKI, H., KON, A., YOSHIDA, K., SATO, Y., SATO-OTSUBO, A., SANADA, M., MUNAKATA, W., NAKAMURA, H., HAMA, N., MIYANO, S., NUREKI, O., SHIBATA, T., HAGA, H., SHIMODA, K., KATADA, T., CHIBA, S., WATANABE, T. & OGAWA, S. 2016. Variegated RHOA mutations in adult T-cell leukemia/lymphoma. *Blood*, 127, 596-604.
152. SAKATA-YANAGIMOTO, M., ENAMI, T., YOSHIDA, K., SHIRAISHI, Y., ISHII, R., MIYAKE, Y., MUTO, H., TSUYAMA, N., SATO-OTSUBO, A., OKUNO, Y., SAKATA, S., KAMADA, Y., NAKAMOTO-MATSUBARA, R., TRAN, N. B., IZUTSU, K., SATO, Y., OHTA, Y., FURUTA, J., SHIMIZU, S., KOMENO, T., SATO, Y., ITO, T., NOGUCHI, M., NOGUCHI, E., SANADA, M., CHIBA, K., TANAKA, H., SUZUKAWA, K., NANMOKU, T., HASEGAWA, Y., NUREKI, O., MIYANO, S., NAKAMURA, N., TAKEUCHI, K., OGAWA, S. & CHIBA, S. 2014. Somatic RHOA mutation in angioimmunoblastic T cell lymphoma. *Nat Genet*, 46, 171-5.
153. IHARA, K., MURAGUCHI, S., KATO, M., SHIMIZU, T., SHIRAKAWA, M., KURODA, S., KAIBUCHI, K. & HAKOSHIMA, T. 1998. Crystal structure of human RHOA in a dominantly active form complexed with a GTP analogue. *J Biol Chem*, 273, 9656-66.
154. SHIMIZU, T., IHARA, K., MAESAKI, R., KURODA, S., KAIBUCHI, K. & HAKOSHIMA, T. 2000. An open conformation of switch I revealed by the crystal structure of a Mg²⁺-free form of RHOA complexed with GDP. Implications for the GDP/GTP exchange mechanism. *J Biol Chem*, 275, 18311-7.
155. CHIBA, S., ENAMI, T., OGAWA, S. & SAKATA-YANAGIMOTO, M. 2015. G17V RHOA: Genetic evidence of GTP-unbound RHOA playing a role in tumorigenesis in T cells. *Small GTPases*, 6, 100-3.
156. GARCIA-MATA, R., WENNERBERG, K., ARTHUR, W. T., NOREN, N. K., ELLERBROEK, S. M. & BURRIDGE, K. 2006. Analysis of activated GAPs and GEFs in cell lysates. *Methods Enzymol*, 406, 425-37.

157. FUJISAWA, M., SAKATA-YANAGIMOTO, M., NISHIZAWA, S., KOMORI, D., GERSHON, P., KIRYU, M., TANZIMA, S., FUKUMOTO, K., ENAMI, T., MURATANI, M., YOSHIDA, K., OGAWA, S., MATSUE, K., NAKAMURA, N., TAKEUCHI, K., IZUTSU, K., FUJIMOTO, K., TESHIMA, T., MIYOSHI, H., GAULARD, P., OHSHIMA, K. & CHIBA, S. 2018. Activation of RHOA-VAV1 signaling in angioimmunoblastic T-cell lymphoma. *Leukemia*, 32, 694-702.
158. COOLS, J. 2014. RHOA mutations in peripheral T cell lymphoma. *Nat Genet*, 46, 320-1.
159. LUKER, K. E. & PIWNICA-WORMS, D. 2004. Optimizing luciferase protein fragment complementation for bioluminescent imaging of protein-protein interactions in live cells and animals. *Methods Enzymol*, 385, 349-60.
160. DEL RE, D. P., MIYAMOTO, S. & BROWN, J. H. 2007. RHOA/Rho kinase up-regulate Bax to activate a mitochondrial death pathway and induce cardiomyocyte apoptosis. *J Biol Chem*, 282, 8069-78.
161. ALTHOEFER, H., EVERSOLE-CIRE, P. & SIMON, M. I. 1997. Constitutively active Galphaq and Galpha13 trigger apoptosis through different pathways. *J Biol Chem*, 272, 24380-6.
162. BOIVIN, D. & BÉLIVEAU, R. 1995. Subcellular distribution and membrane association of Rho-related small GTP-binding proteins in kidney cortex. *Am J Physiol*, 269, F180-9.
163. ADAMSON, P., PATERSON, H. F. & HALL, A. 1992. Intracellular localization of the P21rho proteins. *J Cell Biol*, 119, 617-27.
164. KRANENBURG, O., POLAND, M., GEBBINK, M., OOMEN, L. & MOOLENAAR, W. H. 1997. Dissociation of LPA-induced cytoskeletal contraction from stress fiber formation by differential localization of RHOA. *J Cell Sci*, 110 (Pt 19), 2417-27.
165. MICHAELSON, D., SILLETTI, J., MURPHY, G., D'EUSTACHIO, P., RUSH, M. & PHILIPS, M. R. 2001. Differential localization of Rho GTPases in live cells: regulation by hypervariable regions and RhoGDI binding. *J Cell Biol*, 152, 111-26.
166. DUBASH, A. D., GUILLUY, C., SROUGI, M. C., BOULTER, E., BURRIDGE, K. & GARCÍA-MATA, R. 2011. The small GTPase RHOA localizes to the nucleus and is activated by Net1 and DNA damage signals. *PLoS One*, 6, e17380.
167. BALDASSARE, J. J., JARPE, M. B., ALFERES, L. & RABEN, D. M. 1997. Nuclear translocation of RHOA mediates the mitogen-induced activation of phospholipase D involved in nuclear envelope signal transduction. *J Biol Chem*, 272, 4911-4.
168. CHENG, C., SEEN, D., ZHENG, C., ZENG, R. & LI, E. 2021. Role of Small GTPase RHOA in DNA Damage Response. *Biomolecules*, 11.
169. MANDERS, E. M. M., VERBEEK, F. J. & ATEN, J. A. 1993. Measurement of co-localization of objects in dual-colour confocal images. *J Microsc*, 169, 375-382.
170. CAVALLARO, U. & CHRISTOFORI, G. 2004. Cell adhesion and signalling by cadherins and Ig-CAMs in cancer. *Nat Rev Cancer*, 4, 118-32.
171. KOZMA, R., AHMED, S., BEST, A. & LIM, L. 1995. The Ras-related protein Cdc42Hs and bradykinin promote formation of peripheral actin microspikes and filopodia in Swiss 3T3 fibroblasts. *Mol Cell Biol*, 15, 1942-52.
172. NOBES, C. D., HAWKINS, P., STEPHENS, L. & HALL, A. 1995. Activation of the small GTP-binding proteins rho and rac by growth factor receptors. *J Cell Sci*, 108 (Pt 1), 225-33.
173. PATERSON, H. F., SELF, A. J., GARRETT, M. D., JUST, I., AKTORIES, K. & HALL, A. 1990. Microinjection of recombinant p21rho induces rapid changes in cell morphology. *J Cell Biol*, 111, 1001-7.
174. NARUMIYA, S., TANJI, M. & ISHIZAKI, T. 2009. Rho signaling, ROCK and mDia1, in transformation, metastasis and invasion. *Cancer Metastasis Rev*, 28, 65-76.
175. HYNES, R. O. 2002. Integrins: bidirectional, allosteric signaling machines. *Cell*, 110, 673-87.
176. HYNES, R. O. 1992. Integrins: versatility, modulation, and signaling in cell adhesion. *Cell*, 69, 11-25.
177. REYES, C. D. & GARCÍA, A. J. 2003. A centrifugation cell adhesion assay for high-throughput screening of biomaterial surfaces. *J Biomed Mater Res A*, 67, 328-33.
178. CHOI, H. N., KIM, K. R., LEE, J. H., PARK, H. S., JANG, K. Y., CHUNG, M. J., HWANG, S. E., YU, H. C. & MOON, W. S. 2009. Serum response factor enhances liver metastasis of colorectal carcinoma via alteration of the E-cadherin/beta-catenin complex. *Oncol Rep*, 21, 57-63.
179. KIM, H. J., KIM, K. R., PARK, H. S., JANG, K. Y., CHUNG, M. J., SHONG, M. & MOON, W. S. 2009. The expression and role of serum response factor in papillary carcinoma of the thyroid. *Int J Oncol*, 35, 49-55.
180. PARK, M. Y., KIM, K. R., PARK, H. S., PARK, B. H., CHOI, H. N., JANG, K. Y., CHUNG, M. J., KANG, M. J., LEE, D. G. & MOON, W. S. 2007. Expression of the serum response factor in hepatocellular carcinoma: implications for epithelial-mesenchymal transition. *Int J Oncol*, 31, 1309-15.

Bibliography

181. PHIEL, C. J., GABBETA, V., PARSONS, L. M., ROTHBLAT, D., HARVEY, R. P. & MCHUGH, K. M. 2001. Differential binding of an SRF/NK-2/MEF2 transcription factor complex in normal versus neoplastic smooth muscle tissues. *J Biol Chem*, 276, 34637-50.
182. MIRALLES, F., POSERN, G., ZAROMYTIDOU, A. I. & TREISMAN, R. 2003. Actin dynamics control SRF activity by regulation of its coactivator MAL. *Cell*, 113, 329-42.
183. XIA, L., TAN, S., ZHOU, Y., LIN, J., WANG, H., OYANG, L., TIAN, Y., LIU, L., SU, M., WANG, H., CAO, D. & LIAO, Q. 2018. Role of the NFκB-signaling pathway in cancer. *Onco Targets Ther*, 11, 2063-2073.
184. FIELDS, S. & SONG, O. 1989. A novel genetic system to detect protein-protein interactions. *Nature*, 340, 245-6.
185. BOSE, P., BROCKTON, N. T. & DORT, J. C. 2013. Head and neck cancer: from anatomy to biology. *Int J Cancer*, 133, 2013-23.
186. SUNG, H., FERLAY, J., SIEGEL, R. L., LAVERSANNE, M., SOERJOMATARAM, I., JEMAL, A. & BRAY, F. 2021. Global Cancer Statistics 2020: GLOBOCAN Estimates of Incidence and Mortality Worldwide for 36 Cancers in 185 Countries. *CA Cancer J Clin*, 71, 209-249.
187. LEEMANS, C. R., SNIJDERS, P. J. F. & BRAKENHOFF, R. H. 2018. The molecular landscape of head and neck cancer. *Nat Rev Cancer*, 18, 269-282.
188. GILLISON, M. L., CHATURVEDI, A. K., ANDERSON, W. F. & FAKHRY, C. 2015. Epidemiology of Human Papillomavirus-Positive Head and Neck Squamous Cell Carcinoma. *J Clin Oncol*, 33, 3235-42.
189. CHOW, L. Q. M. 2020. Head and Neck Cancer. *N Engl J Med*, 382, 60-72.
190. PAI, S. I. & WESTRA, W. H. 2009. Molecular pathology of head and neck cancer: implications for diagnosis, prognosis, and treatment. *Annu Rev Pathol*, 4, 49-70.
191. EDMANS, J. G., CLITHEROW, K. H., MURDOCH, C., HATTON, P. V., SPAIN, S. G. & COLLEY, H. E. 2020. Mucoadhesive Electrospun Fibre-Based Technologies for Oral Medicine. *Pharmaceutics*, 12.
192. JOHNSON, D. E., BURTNES, B., LEEMANS, C. R., LUI, V. W. Y., BAUMAN, J. E. & GRANDIS, J. R. 2020. Head and neck squamous cell carcinoma. *Nat Rev Dis Primers*, 6, 92.
193. NAPIER, S. S. & SPEIGHT, P. M. 2008. Natural history of potentially malignant oral lesions and conditions: an overview of the literature. *J Oral Pathol Med*, 37, 1-10.
194. VAN DER WAAL, I. 2009. Potentially malignant disorders of the oral and oropharyngeal mucosa; terminology, classification and present concepts of management. *Oral Oncol*, 45, 317-23.
195. SCHAAIJ-VISSER, T. B., BREMMER, J. F., BRAAKHUIS, B. J., HECK, A. J., SLIJPER, M., VAN DER WAAL, I. & BRAKENHOFF, R. H. 2010. Evaluation of cornulin, keratin 4, keratin 13 expression and grade of dysplasia for predicting malignant progression of oral leukoplakia. *Oral Oncol*, 46, 123-7.
196. TORRES-RENDON, A., STEWART, R., CRAIG, G. T., WELLS, M. & SPEIGHT, P. M. 2009. DNA ploidy analysis by image cytometry helps to identify oral epithelial dysplasias with a high risk of malignant progression. *Oral Oncol*, 45, 468-73.
197. SLAUGHTER, D. P., SOUTHWICK, H. W. & SMEJKAL, W. 1953. Field cancerization in oral stratified squamous epithelium; clinical implications of multicentric origin. *Cancer*, 6, 963-8.
198. CALIFANO, J., VAN DER RIET, P., WESTRA, W., NAWROZ, H., CLAYMAN, G., PIANTADOSI, S., CORIO, R., LEE, D., GREENBERG, B., KOCH, W. & SIDRANSKY, D. 1996. Genetic progression model for head and neck cancer: implications for field cancerization. *Cancer Res*, 56, 2488-92.
199. LEEMANS, C. R., BRAAKHUIS, B. J. & BRAKENHOFF, R. H. 2011. The molecular biology of head and neck cancer. *Nat Rev Cancer*, 11, 9-22.
200. CHUNG, C. H., PARKER, J. S., KARACA, G., WU, J., FUNKHOUSER, W. K., MOORE, D., BUTTERFOSS, D., XIANG, D., ZANATION, A., YIN, X., SHOCKLEY, W. W., WEISSLER, M. C., DRESSLER, L. G., SHORES, C. G., YARBROUGH, W. G. & PEROU, C. M. 2004. Molecular classification of head and neck squamous cell carcinomas using patterns of gene expression. *Cancer Cell*, 5, 489-500.
201. WALTER, V., YIN, X., WILKERSON, M. D., CABANSKI, C. R., ZHAO, N., DU, Y., ANG, M. K., HAYWARD, M. C., SALAZAR, A. H., HOADLEY, K. A., FRITCHIE, K., SAILEY, C. J., WEISSLER, M. C., SHOCKLEY, W. W., ZANATION, A. M., HACKMAN, T., THORNE, L. B., FUNKHOUSER, W. D., MULDREW, K. L., OLSHAN, A. F., RANDELL, S. H., WRIGHT, F. A., SHORES, C. G. & HAYES, D. N. 2013. Molecular subtypes in head and neck cancer exhibit distinct patterns of chromosomal gain and loss of canonical cancer genes. *PLoS One*, 8, e56823.
202. KECK, M. K., ZUO, Z., KHATTRI, A., STRICKER, T. P., BROWN, C. D., IMANGULI, M., RIEKE, D., ENDHARDT, K., FANG, P., BRÄGELMANN, J., DEBOER, R., EL-DINALI, M., AKTOLGA, S., LEI, Z., TAN, P., ROZEN, S. G., SALGIA, R., WEICHELBAUM, R. R., LINGEN, M. W., STORY, M. D., ANG, K. K., COHEN, E. E., WHITE, K. P., VOKES, E. E. & SEIWERT, T. Y. 2015. Integrative analysis of head and neck cancer identifies two biologically distinct HPV and three non-HPV subtypes. *Clin Cancer Res*, 21, 870-81.

203. DE CECCO, L., NICOLAU, M., GIANNOCCARO, M., DAIDONE, M. G., BOSSI, P., LOCATI, L., LICITRA, L. & CANEVARI, S. 2015. Head and neck cancer subtypes with biological and clinical relevance: Meta-analysis of gene-expression data. *Oncotarget*, 6, 9627-42.
204. 2015. Comprehensive genomic characterization of head and neck squamous cell carcinomas. *Nature*, 517, 576-82.
205. CHUNG, C. H., PARKER, J. S., ELY, K., CARTER, J., YI, Y., MURPHY, B. A., ANG, K. K., EL-NAGGAR, A. K., ZANATION, A. M., CMELAK, A. J., LEVY, S., SLEBOS, R. J. & YARBROUGH, W. G. 2006. Gene expression profiles identify epithelial-to-mesenchymal transition and activation of nuclear factor-kappaB signaling as characteristics of a high-risk head and neck squamous cell carcinoma. *Cancer Res*, 66, 8210-8.
206. SMEETS, S. J., BRAKENHOFF, R. H., YLSTRA, B., VAN WIERINGEN, W. N., VAN DE WIEL, M. A., LEEMANS, C. R. & BRAAKHUIS, B. J. 2009. Genetic classification of oral and oropharyngeal carcinomas identifies subgroups with a different prognosis. *Cell Oncol*, 31, 291-300.
207. DE MARTEL, C., FERLAY, J., FRANCESCHI, S., VIGNAT, J., BRAY, F., FORMAN, D. & PLUMMER, M. 2012. Global burden of cancers attributable to infections in 2008: a review and synthetic analysis. *Lancet Oncol*, 13, 607-15.
208. SLEBOS, R. J., YI, Y., ELY, K., CARTER, J., EVJEN, A., ZHANG, X., SHYR, Y., MURPHY, B. M., CMELAK, A. J., BURKEY, B. B., NETTERVILLE, J. L., LEVY, S., YARBROUGH, W. G. & CHUNG, C. H. 2006. Gene expression differences associated with human papillomavirus status in head and neck squamous cell carcinoma. *Clin Cancer Res*, 12, 701-9.
209. POETA, M. L., MANOLA, J., GOLDWASSER, M. A., FORASTIERE, A., BENOIT, N., CALIFANO, J. A., RIDGE, J. A., GOODWIN, J., KENADY, D., SAUNDERS, J., WESTRA, W., SIDRANSKY, D. & KOCH, W. M. 2007. TP53 mutations and survival in squamous-cell carcinoma of the head and neck. *N Engl J Med*, 357, 2552-61.
210. AGRAWAL, N., FREDERICK, M. J., PICKERING, C. R., BETTEGOWDA, C., CHANG, K., LI, R. J., FAKHRY, C., XIE, T. X., ZHANG, J., WANG, J., ZHANG, N., EL-NAGGAR, A. K., JASSER, S. A., WEINSTEIN, J. N., TREVIÑO, L., DRUMMOND, J. A., MUZNY, D. M., WU, Y., WOOD, L. D., HRUBAN, R. H., WESTRA, W. H., KOCH, W. M., CALIFANO, J. A., GIBBS, R. A., SIDRANSKY, D., VOGELSTEIN, B., VELCULESCU, V. E., PAPADOPOULOS, N., WHEELER, D. A., KINZLER, K. W. & MYERS, J. N. 2011. Exome sequencing of head and neck squamous cell carcinoma reveals inactivating mutations in NOTCH1. *Science*, 333, 1154-7.
211. STRANSKY, N., EGLOFF, A. M., TWARD, A. D., KOSTIC, A. D., CIBULSKIS, K., SIVACHENKO, A., KRYUKOV, G. V., LAWRENCE, M. S., SOUGNEZ, C., MCKENNA, A., SHEFLER, E., RAMOS, A. H., STOJANOV, P., CARTER, S. L., VOET, D., CORTÉS, M. L., AUCLAIR, D., BERGER, M. F., SAKSENA, G., GUIDUCCI, C., ONOFRIO, R. C., PARKIN, M., ROMKES, M., WEISSFELD, J. L., SEETHALA, R. R., WANG, L., RANGEL-ESCARÉÑO, C., FERNANDEZ-LOPEZ, J. C., HIDALGO-MIRANDA, A., MELENDEZ-ZAJGLA, J., WINCKLER, W., ARDLIE, K., GABRIEL, S. B., MEYERSON, M., LANDER, E. S., GETZ, G., GOLUB, T. R., GARRAWAY, L. A. & GRANDIS, J. R. 2011. The mutational landscape of head and neck squamous cell carcinoma. *Science*, 333, 1157-60.
212. ZHOU, G., LIU, Z. & MYERS, J. N. 2016. TP53 Mutations in Head and Neck Squamous Cell Carcinoma and Their Impact on Disease Progression and Treatment Response. *J Cell Biochem*, 117, 2682-2692.
213. OPITZ, O. G., SULIMAN, Y., HAHN, W. C., HARADA, H., BLUM, H. E. & RUSTGI, A. K. 2001. Cyclin D1 overexpression and p53 inactivation immortalize primary oral keratinocytes by a telomerase-independent mechanism. *J Clin Invest*, 108, 725-32.
214. RHEINWALD, J. G., HAHN, W. C., RAMSEY, M. R., WU, J. Y., GUO, Z., TSAO, H., DE LUCA, M., CATRICALÀ, C. & O'TOOLE, K. M. 2002. A two-stage, p16(INK4A)- and p53-dependent keratinocyte senescence mechanism that limits replicative potential independent of telomere status. *Mol Cell Biol*, 22, 5157-72.
215. SMEETS, S. J., VAN DER PLAS, M., SCHAAIJ-VISSER, T. B., VAN VEEN, E. A., VAN MEERLOO, J., BRAAKHUIS, B. J., STEENBERGEN, R. D. & BRAKENHOFF, R. H. 2011. Immortalization of oral keratinocytes by functional inactivation of the p53 and pRb pathways. *Int J Cancer*, 128, 1596-605.
216. REED, A. L., CALIFANO, J., CAIRNS, P., WESTRA, W. H., JONES, R. M., KOCH, W., AHRENDT, S., EBY, Y., SEWELL, D., NAWROZ, H., BARTEK, J. & SIDRANSKY, D. 1996. High frequency of p16 (CDKN2/MTS-1/INK4A) inactivation in head and neck squamous cell carcinoma. *Cancer Res*, 56, 3630-3.
217. SMEETS, S. J., BRAAKHUIS, B. J., ABBAS, S., SNIJDERS, P. J., YLSTRA, B., VAN DE WIEL, M. A., MEIJER, G. A., LEEMANS, C. R. & BRAKENHOFF, R. H. 2006. Genome-wide DNA copy number alterations in

Bibliography

- head and neck squamous cell carcinomas with or without oncogene-expressing human papillomavirus. *Oncogene*, 25, 2558-64.
218. BRAAKHUIS, B. J., SNIJDERS, P. J., KEUNE, W. J., MEIJER, C. J., RUIJTER-SCHIPPERS, H. J., LEEMANS, C. R. & BRAKENHOFF, R. H. 2004. Genetic patterns in head and neck cancers that contain or lack transcriptionally active human papillomavirus. *J Natl Cancer Inst*, 96, 998-1006.
219. BERNS, K., HIJMANS, E. M., MULLENDERS, J., BRUMMELKAMP, T. R., VELDS, A., HEIMERIKX, M., KERKHOVEN, R. M., MADIREDO, M., NIJKAMP, W., WEIGELT, B., AGAMI, R., GE, W., CAVET, G., LINSLEY, P. S., BEIJERSBERGEN, R. L. & BERNARDS, R. 2004. A large-scale RNAi screen in human cells identifies new components of the p53 pathway. *Nature*, 428, 431-7.
220. HYNES, N. E. & LANE, H. A. 2005. ERBB receptors and cancer: the complexity of targeted inhibitors. *Nat Rev Cancer*, 5, 341-54.
221. LIN, S. Y., MAKINO, K., XIA, W., MATIN, A., WEN, Y., KWONG, K. Y., BOURGUIGNON, L. & HUNG, M. C. 2001. Nuclear localization of EGF receptor and its potential new role as a transcription factor. *Nat Cell Biol*, 3, 802-8.
222. LO, H. W., HSU, S. C., ALI-SEYED, M., GUNDUZ, M., XIA, W., WEI, Y., BARTHOLOMEUSZ, G., SHIH, J. Y. & HUNG, M. C. 2005. Nuclear interaction of EGFR and STAT3 in the activation of the iNOS/NO pathway. *Cancer Cell*, 7, 575-89.
223. OZANNE, B., RICHARDS, C. S., HENDLER, F., BURNS, D. & GUSTERSON, B. 1986. Over-expression of the EGF receptor is a hallmark of squamous cell carcinomas. *J Pathol*, 149, 9-14.
224. GRANDIS, J. R. & TWEARDY, D. J. 1993. Elevated levels of transforming growth factor alpha and epidermal growth factor receptor messenger RNA are early markers of carcinogenesis in head and neck cancer. *Cancer Res*, 53, 3579-84.
225. BONNER, J. A., HARARI, P. M., GIRALT, J., AZARNIA, N., SHIN, D. M., COHEN, R. B., JONES, C. U., SUR, R., RABEN, D., JASSEM, J., OVE, R., KIES, M. S., BASELGA, J., YOUSOUFIAN, H., AMELLAL, N., ROWINSKY, E. K. & ANG, K. K. 2006. Radiotherapy plus cetuximab for squamous-cell carcinoma of the head and neck. *N Engl J Med*, 354, 567-78.
226. TEMAM, S., KAWAGUCHI, H., EL-NAGGAR, A. K., JELINEK, J., TANG, H., LIU, D. D., LANG, W., ISSA, J. P., LEE, J. J. & MAO, L. 2007. Epidermal growth factor receptor copy number alterations correlate with poor clinical outcome in patients with head and neck squamous cancer. *J Clin Oncol*, 25, 2164-70.
227. SHEU, J. J., HUA, C. H., WAN, L., LIN, Y. J., LAI, M. T., TSENG, H. C., JINAWATH, N., TSAI, M. H., CHANG, N. W., LIN, C. F., LIN, C. C., HSIEH, L. J., WANG, T. L., SHIH IE, M. & TSAI, F. J. 2009. Functional genomic analysis identified epidermal growth factor receptor activation as the most common genetic event in oral squamous cell carcinoma. *Cancer Res*, 69, 2568-76.
228. HAMA, T., YUZA, Y., SAITO, Y., J. O. U., KONDO, S., OKABE, M., YAMADA, H., KATO, T., MORIYAMA, H., KURIHARA, S. & URASHIMA, M. 2009. Prognostic significance of epidermal growth factor receptor phosphorylation and mutation in head and neck squamous cell carcinoma. *Oncologist*, 14, 900-8.
229. SOK, J. C., COPPELLI, F. M., THOMAS, S. M., LANGO, M. N., XI, S., HUNT, J. L., FREILINO, M. L., GRANER, M. W., WIKSTRAND, C. J., BIGNER, D. D., GOODING, W. E., FURNARI, F. B. & GRANDIS, J. R. 2006. Mutant epidermal growth factor receptor (EGFRvIII) contributes to head and neck cancer growth and resistance to EGFR targeting. *Clin Cancer Res*, 12, 5064-73.
230. DERYNCK, R. & AKHURST, R. J. 2007. Differentiation plasticity regulated by TGF-beta family proteins in development and disease. *Nat Cell Biol*, 9, 1000-4.
231. MASSAGUÉ, J. 2008. TGFbeta in Cancer. *Cell*, 134, 215-30.
232. WANG, D., SONG, H., EVANS, J. A., LANG, J. C., SCHULLER, D. E. & WEGHORST, C. M. 1997. Mutation and downregulation of the transforming growth factor beta type II receptor gene in primary squamous cell carcinomas of the head and neck. *Carcinogenesis*, 18, 2285-90.
233. HUNTLEY, S. P., DAVIES, M., MATTHEWS, J. B., THOMAS, G., MARSHALL, J., ROBINSON, C. M., EVESON, J. W., PATERSON, I. C. & PRIME, S. S. 2004. Attenuated type II TGF-beta receptor signalling in human malignant oral keratinocytes induces a less differentiated and more aggressive phenotype that is associated with metastatic dissemination. *Int J Cancer*, 110, 170-6.
234. QIU, W., SCHÖNLEBEN, F., LI, X. & SU, G. H. 2007. Disruption of transforming growth factor beta-Smad signaling pathway in head and neck squamous cell carcinoma as evidenced by mutations of SMAD2 and SMAD4. *Cancer Lett*, 245, 163-70.
235. BORNSTEIN, S., WHITE, R., MALKOSKI, S., OKA, M., HAN, G., CLEAVER, T., REH, D., ANDERSEN, P., GROSS, N., OLSON, S., DENG, C., LU, S. L. & WANG, X. J. 2009. Smad4 loss in mice causes

- spontaneous head and neck cancer with increased genomic instability and inflammation. *J Clin Invest*, 119, 3408-19.
236. SHEN, X., LI, J., HU, P. P., WADDELL, D., ZHANG, J. & WANG, X. F. 2001. The activity of guanine exchange factor NET1 is essential for transforming growth factor-beta-mediated stress fiber formation. *J Biol Chem*, 276, 15362-8.
237. ZHANG, Y. E. 2009. Non-Smad pathways in TGF-beta signaling. *Cell Res*, 19, 128-39.
238. KOZAKI, K., IMOTO, I., PIMKHAOKHAM, A., HASEGAWA, S., TSUDA, H., OMURA, K. & INAZAWA, J. 2006. PIK3CA mutation is an oncogenic aberration at advanced stages of oral squamous cell carcinoma. *Cancer Sci*, 97, 1351-8.
239. MURUGAN, A. K., HONG, N. T., FUKUI, Y., MUNIRAJAN, A. K. & TSUCHIDA, N. 2008. Oncogenic mutations of the PIK3CA gene in head and neck squamous cell carcinomas. *Int J Oncol*, 32, 101-11.
240. OKAMI, K., WU, L., RIGGINS, G., CAIRNS, P., GOGGINS, M., EVRON, E., HALACHMI, N., AHRENDT, S. A., REED, A. L., HILGERS, W., KERN, S. E., KOCH, W. M., SIDRANSKY, D. & JEN, J. 1998. Analysis of PTEN/MMAC1 alterations in aerodigestive tract tumors. *Cancer Res*, 58, 509-11.
241. MOLINOLO, A. A., HEWITT, S. M., AMORNPHIMOLTHAM, P., KEELAWAT, S., RANGDAENG, S., MENESES GARCÍA, A., RAIMONDI, A. R., JUFE, R., ITOIZ, M., GAO, Y., SARANATH, D., KALEEBI, G. S., YOO, G. H., LEAK, L., MYERS, E. M., SHINTANI, S., WONG, D., MASSEY, H. D., YEUDALL, W. A., LONARDO, F., ENSLEY, J. & GUTKIND, J. S. 2007. Dissecting the Akt/mammalian target of rapamycin signaling network: emerging results from the head and neck cancer tissue array initiative. *Clin Cancer Res*, 13, 4964-73.
242. AVAN, A., NARAYAN, R., GIOVANNETTI, E. & PETERS, G. J. 2016. Role of Akt signaling in resistance to DNA-targeted therapy. *World J Clin Oncol*, 7, 352-369.
243. ZUMSTEG, Z. S., MORSE, N., KRIGSFELD, G., GUPTA, G., HIGGINSON, D. S., LEE, N. Y., MORRIS, L., GANLY, I., SHIAO, S. L., POWELL, S. N., CHUNG, C. H., SCALTRITI, M. & BASELGA, J. 2016. Taselisib (GDC-0032), a Potent β -Sparing Small Molecule Inhibitor of PI3K, Radiosensitizes Head and Neck Squamous Carcinomas Containing Activating PIK3CA Alterations. *Clin Cancer Res*, 22, 2009-19.
244. MARQUARD, F. E. & JÜCKER, M. 2020. PI3K/AKT/mTOR signaling as a molecular target in head and neck cancer. *Biochem Pharmacol*, 172, 113729.
245. SHAH, P. A., HUANG, C., LI, Q., KAZI, S. A., BYERS, L. A., WANG, J., JOHNSON, F. M. & FREDERICK, M. J. 2020. NOTCH1 Signaling in Head and Neck Squamous Cell Carcinoma. *Cells*, 9.
246. FUKUSUMI, T. & CALIFANO, J. A. 2018. The NOTCH Pathway in Head and Neck Squamous Cell Carcinoma. *J Dent Res*, 97, 645-653.
247. LUUKKAA, M., VIHINEN, P., KRONQVIST, P., VAHLBERG, T., PYRHÖNEN, S., KÄHÄRI, V. M. & GRÉNMAN, R. 2006. Association between high collagenase-3 expression levels and poor prognosis in patients with head and neck cancer. *Head Neck*, 28, 225-34.
248. PATEL, B. P., SHAH, S. V., SHUKLA, S. N., SHAH, P. M. & PATEL, P. S. 2007. Clinical significance of MMP-2 and MMP-9 in patients with oral cancer. *Head Neck*, 29, 564-72.
249. VIRÓS, D., CAMACHO, M., ZARRAONANDIA, I., GARCÍA, J., QUER, M., VILA, L. & LEÓN, X. 2013. Prognostic role of MMP-9 expression in head and neck carcinoma patients treated with radiotherapy or chemoradiotherapy. *Oral Oncol*, 49, 322-5.
250. FABER, A., BARTH, C., HÖRMANN, K., KASSNER, S., SCHULTZ, J. D., SOMMER, U., STERN-STRAETER, J., THORN, C. & GOESSLER, U. R. 2011. CD44 as a stem cell marker in head and neck squamous cell carcinoma. *Oncol Rep*, 26, 321-6.
251. STERZ, C. M., KULLE, C., DAKIC, B., MAKAROVA, G., BÖTTCHER, M. C., BETTE, M., WERNER, J. A. & MANDIC, R. 2010. A basal-cell-like compartment in head and neck squamous cell carcinomas represents the invasive front of the tumor and is expressing MMP-9. *Oral Oncol*, 46, 116-22.
252. PELTANOVA, B., RAUDENSKA, M. & MASARIK, M. 2019. Effect of tumor microenvironment on pathogenesis of the head and neck squamous cell carcinoma: a systematic review. *Mol Cancer*, 18, 63.
253. NIJKAMP, M. M., SPAN, P. N., HOOGSTEEN, I. J., VAN DER KOGEL, A. J., KAANDERS, J. H. & BUSSINK, J. 2011. Expression of E-cadherin and vimentin correlates with metastasis formation in head and neck squamous cell carcinoma patients. *Radiother Oncol*, 99, 344-8.
254. ZHANG, Z., FILHO, M. S. & NÖR, J. E. 2012. The biology of head and neck cancer stem cells. *Oral Oncol*, 48, 1-9.
255. SWARTZ, J. E., POTHEN, A. J., VAN KEMPEN, P. M., STEGEMAN, I., FORMSMA, F. K., CANN, E. M., WILLEMS, S. M. & GROLMAN, W. 2016. Poor prognosis in human papillomavirus-positive

Bibliography

- oropharyngeal squamous cell carcinomas that overexpress hypoxia inducible factor-1 α . *Head Neck*, 38, 1338-46.
256. NEIVA, K. G., ZHANG, Z., MIYAZAWA, M., WARNER, K. A., KARL, E. & NÖR, J. E. 2009. Cross talk initiated by endothelial cells enhances migration and inhibits anoikis of squamous cell carcinoma cells through STAT3/Akt/ERK signaling. *Neoplasia*, 11, 583-93.
257. KYZAS, P. A., CUNHA, I. W. & IOANNIDIS, J. P. 2005. Prognostic significance of vascular endothelial growth factor immunohistochemical expression in head and neck squamous cell carcinoma: a meta-analysis. *Clin Cancer Res*, 11, 1434-40.
258. ALSAHAFI, E., BEGG, K., AMELIO, I., RAULF, N., LUCARELLI, P., SAUTER, T. & TAVASSOLI, M. 2019. Clinical update on head and neck cancer: molecular biology and ongoing challenges. *Cell Death Dis*, 10, 540.
259. CRAMER, J. D., BURTNES, B., LE, Q. T. & FERRIS, R. L. 2019. The changing therapeutic landscape of head and neck cancer. *Nat Rev Clin Oncol*, 16, 669-683.
260. GILLISON, M. L., KOCH, W. M., CAPONE, R. B., SPAFFORD, M., WESTRA, W. H., WU, L., ZAHURAK, M. L., DANIEL, R. W., VIGLIONE, M., SYMER, D. E., SHAH, K. V. & SIDRANSKY, D. 2000. Evidence for a causal association between human papillomavirus and a subset of head and neck cancers. *J Natl Cancer Inst*, 92, 709-20.
261. MEHANNA, H., BEECH, T., NICHOLSON, T., EL-HARIRY, I., MCCONKEY, C., PALERI, V. & ROBERTS, S. 2013. Prevalence of human papillomavirus in oropharyngeal and nonoropharyngeal head and neck cancer--systematic review and meta-analysis of trends by time and region. *Head Neck*, 35, 747-55.
262. ANG, K. K., HARRIS, J., WHEELER, R., WEBER, R., ROSENTHAL, D. I., NGUYEN-TÂN, P. F., WESTRA, W. H., CHUNG, C. H., JORDAN, R. C., LU, C., KIM, H., AXELROD, R., SILVERMAN, C. C., REDMOND, K. P. & GILLISON, M. L. 2010. Human papillomavirus and survival of patients with oropharyngeal cancer. *N Engl J Med*, 363, 24-35.
263. O'SULLIVAN, B., HUANG, S. H., SU, J., GARDEN, A. S., STURGIS, E. M., DAHLSTROM, K., LEE, N., RIAZ, N., PEI, X., KOYFMAN, S. A., ADELSTEIN, D., BURKEY, B. B., FRIBORG, J., KRISTENSEN, C. A., GOTHELF, A. B., HOEBERS, F., KREMER, B., SPEEL, E. J., BOWLES, D. W., RABEN, D., KARAM, S. D., YU, E. & XU, W. 2016. Development and validation of a staging system for HPV-related oropharyngeal cancer by the International Collaboration on Oropharyngeal cancer Network for Staging (ICON-S): a multicentre cohort study. *Lancet Oncol*, 17, 440-451.
264. AMIN, M. B., EDGE, S., GREENE, F., BYRD, D. R., BROOKLAND, R. K., WASHINGTON, M. K., GERSHENWALD, J. E., COMPTON, C. C., HESS, K. R., SULLIVAN, D. C., JESSUP, J. M., BRIERLEY, J. D., GASPARI, L. E., SCHILSKY, R. L., BALCH, C. M. 2017. AJCC Cancer Staging Manual (8th edition). *Springer International Publishing: American Joint Commission on Cancer*.
265. EDGE, S. B. & COMPTON, C. C. 2010. The American Joint Committee on Cancer: the 7th edition of the AJCC cancer staging manual and the future of TNM. *Ann Surg Oncol*, 17, 1471-4.
266. AMIN, M. B., GREENE, F. L., EDGE, S. B., COMPTON, C. C., GERSHENWALD, J. E., BROOKLAND, R. K., MEYER, L., GRESS, D. M., BYRD, D. R. & WINCHESTER, D. P. 2017. The Eighth Edition AJCC Cancer Staging Manual: Continuing to build a bridge from a population-based to a more "personalized" approach to cancer staging. *CA Cancer J Clin*, 67, 93-99.
267. PFISTER, D. G., SPENCER, S., BRIZEL, D. M., BURTNES, B., BUSSE, P. M., CAUDELL, J. J., CMELAK, A. J., COLEVAS, A. D., DUNPHY, F., EISELE, D. W., GILBERT, J., GILLISON, M. L., HADDAD, R. I., HAUGHEY, B. H., HICKS, W. L., JR., HITCHCOCK, Y. J., JIMENO, A., KIES, M. S., LYDIATT, W. M., MAGHAMI, E., MARTINS, R., MCCAFFREY, T., MELL, L. K., MITTAL, B. B., PINTO, H. A., RIDGE, J. A., RODRIGUEZ, C. P., SAMANT, S., SCHULLER, D. E., SHAH, J. P., WEBER, R. S., WOLF, G. T., WORDEN, F., YOM, S. S., MCMILLIAN, N. R. & HUGHES, M. 2014. Head and neck cancers, Version 2.2014. Clinical practice guidelines in oncology. *J Natl Compr Canc Netw*, 12, 1454-87.
268. LACAS, B., CARMEL, A., LANDAIS, C., WONG, S. J., LICITRA, L., TOBIAS, J. S., BURTNES, B., GHI, M. G., COHEN, E. E. W., GRAU, C., WOLF, G., HITT, R., CORVÒ, R., BUDACH, V., KUMAR, S., LASKAR, S. G., MAZERON, J. J., ZHONG, L. P., DOBROWSKY, W., GHADJAR, P., FALLAI, C., ZAKOTNIK, B., SHARMA, A., BENSADOUN, R. J., RUO REDDA, M. G., RACADOT, S., FOUNTZILAS, G., BRIZEL, D., ROVEA, P., ARGIRIS, A., NAGY, Z. T., LEE, J. W., FORTPIED, C., HARRIS, J., BOURHIS, J., AUPÉRIN, A., BLANCHARD, P. & PIGNON, J. P. 2021. Meta-analysis of chemotherapy in head and neck cancer (MACH-NC): An update on 107 randomized trials and 19,805 patients, on behalf of MACH-NC Group. *Radiother Oncol*, 156, 281-293.

269. GUAN, J., LI, Q., ZHANG, Y., XIAO, N., CHEN, M., ZHANG, Y., LI, L. & CHEN, L. 2016. A meta-analysis comparing cisplatin-based to carboplatin-based chemotherapy in moderate to advanced squamous cell carcinoma of head and neck (SCCHN). *Oncotarget*, 7, 7110-9.
270. ARGIRIS, A., KARAMOUZIS, M. V., RABEN, D. & FERRIS, R. L. 2008. Head and neck cancer. *Lancet*, 371, 1695-709.
271. ADELSTEIN, D., GILLISON, M. L., PFISTER, D. G., SPENCER, S., ADKINS, D., BRIZEL, D. M., BURTNES, B., BUSSE, P. M., CAUDELL, J. J., CMELAK, A. J., COLEVAS, A. D., EISELE, D. W., FENTON, M., FOOTE, R. L., GILBERT, J., HADDAD, R. I., HICKS, W. L., HITCHCOCK, Y. J., JIMENO, A., LEIZMAN, D., LYDIATT, W. M., MAGHAMI, E., MELL, L. K., MITTAL, B. B., PINTO, H. A., RIDGE, J. A., ROCCO, J., RODRIGUEZ, C. P., SHAH, J. P., WEBER, R. S., WITEK, M., WORDEN, F., YOM, S. S., ZHEN, W., BURNS, J. L. & DARLOW, S. D. 2017. NCCN Guidelines Insights: Head and Neck Cancers, Version 2.2017. *J Natl Compr Canc Netw*, 15, 761-770.
272. LARKINS, E., BLUMENTHAL, G. M., YUAN, W., HE, K., SRIDHARA, R., SUBRAMANIAM, S., ZHAO, H., LIU, C., YU, J., GOLDBERG, K. B., MCKEE, A. E., KEEGAN, P. & PAZDUR, R. 2017. FDA Approval Summary: Pembrolizumab for the Treatment of Recurrent or Metastatic Head and Neck Squamous Cell Carcinoma with Disease Progression on or After Platinum-Containing Chemotherapy. *Oncologist*, 22, 873-878.
273. COHEN, E. E. W., SOULIÈRES, D., LE TOURNEAU, C., DINIS, J., LICITRA, L., AHN, M. J., SORIA, A., MACHIÈLS, J. P., MACH, N., MEHRA, R., BURTNES, B., ZHANG, P., CHENG, J., SWABY, R. F. & HARRINGTON, K. J. 2019. Pembrolizumab versus methotrexate, docetaxel, or cetuximab for recurrent or metastatic head-and-neck squamous cell carcinoma (KEYNOTE-040): a randomised, open-label, phase 3 study. *Lancet*, 393, 156-167.
274. FERRIS, R. L., BLUMENSCHNEIN, G., JR., FAYETTE, J., GUIGAY, J., COLEVAS, A. D., LICITRA, L., HARRINGTON, K., KASPER, S., VOKES, E. E., EVEN, C., WORDEN, F., SABA, N. F., IGLESIAS DOCAMPO, L. C., HADDAD, R., RORDORF, T., KIYOTA, N., TAHARA, M., MONGA, M., LYNCH, M., GEESE, W. J., KOPIT, J., SHAW, J. W. & GILLISON, M. L. 2016. Nivolumab for Recurrent Squamous-Cell Carcinoma of the Head and Neck. *N Engl J Med*, 375, 1856-1867.
275. BURTNES, B., HARRINGTON, K. J., GREIL, R., SOULIÈRES, D., TAHARA, M., DE CASTRO, G., JR., PSYRRI, A., BASTÉ, N., NEUPANE, P., BRATLAND, Å., FUEREDER, T., HUGHES, B. G. M., MESÍA, R., NGAMPHAIBOON, N., RORDORF, T., WAN ISHAK, W. Z., HONG, R. L., GONZÁLEZ MENDOZA, R., ROY, A., ZHANG, Y., GUMUSCU, B., CHENG, J. D., JIN, F. & RISCHIN, D. 2019. Pembrolizumab alone or with chemotherapy versus cetuximab with chemotherapy for recurrent or metastatic squamous cell carcinoma of the head and neck (KEYNOTE-048): a randomised, open-label, phase 3 study. *Lancet*, 394, 1915-1928.
276. FERRIS, R. L., BLUMENSCHNEIN, G., JR., FAYETTE, J., GUIGAY, J., COLEVAS, A. D., LICITRA, L., HARRINGTON, K. J., KASPER, S., VOKES, E. E., EVEN, C., WORDEN, F., SABA, N. F., DOCAMPO, L. C. I., HADDAD, R., RORDORF, T., KIYOTA, N., TAHARA, M., LYNCH, M., JAYAPRAKASH, V., LI, L. & GILLISON, M. L. 2018. Nivolumab vs investigator's choice in recurrent or metastatic squamous cell carcinoma of the head and neck: 2-year long-term survival update of CheckMate 141 with analyses by tumor PD-L1 expression. *Oral Oncol*, 81, 45-51.
277. MOK, T. S. K., WU, Y. L., KUDABA, I., KOWALSKI, D. M., CHO, B. C., TURNA, H. Z., CASTRO, G., JR., SRIMUNINIMIT, V., LAKTIONOV, K. K., BONDARENKO, I., KUBOTA, K., LUBINIECKI, G. M., ZHANG, J., KUSH, D. & LOPES, G. 2019. Pembrolizumab versus chemotherapy for previously untreated, PD-L1-expressing, locally advanced or metastatic non-small-cell lung cancer (KEYNOTE-042): a randomised, open-label, controlled, phase 3 trial. *Lancet*, 393, 1819-1830.
278. PLAVC, G., JESENKO, T., ORAŽEM, M. & STROJAN, P. 2020. Challenges in Combining Immunotherapy with Radiotherapy in Recurrent/Metastatic Head and Neck Cancer. *Cancers (Basel)*, 12.
279. NOWICKI, T. S., HU-LIESKOVAN, S. & RIBAS, A. 2018. Mechanisms of Resistance to PD-1 and PD-L1 Blockade. *Cancer J*, 24, 47-53.
280. BHAVE, S. L., TEKNOS, T. N. & PAN, Q. 2011. Molecular parameters of head and neck cancer metastasis. *Crit Rev Eukaryot Gene Expr*, 21, 143-53.
281. PATEL, V., ROSENFELDT, H. M., LYONS, R., SERVITJA, J. M., BUSTELO, X. R., SIROFF, M. & GUTKIND, J. S. 2007. Persistent activation of Rac1 in squamous carcinomas of the head and neck: evidence for an EGFR/Vav2 signaling axis involved in cell invasion. *Carcinogenesis*, 28, 1145-52.
282. PAN, Q., BAO, L. W., TEKNOS, T. N. & MERAJVER, S. D. 2006. Targeted disruption of protein kinase C epsilon reduces cell invasion and motility through inactivation of RHOA and RhoC GTPases in head and neck squamous cell carcinoma. *Cancer Res*, 66, 9379-84.

Bibliography

283. KLEER, C. G., TEKNOS, T. N., ISLAM, M., MARCUS, B., LEE, J. S., PAN, Q. & MERAJVER, S. D. 2006. RhoC GTPase expression as a potential marker of lymph node metastasis in squamous cell carcinomas of the head and neck. *Clin Cancer Res*, 12, 4485-90.
284. ISLAM, M., LIN, G., BRENNER, J. C., PAN, Q., MERAJVER, S. D., HOU, Y., KUMAR, P. & TEKNOS, T. N. 2009. RhoC expression and head and neck cancer metastasis. *Mol Cancer Res*, 7, 1771-80.
285. LIU, X., WANG, C., CHEN, Z., JIN, Y., WANG, Y., KOLOKYTHAS, A., DAI, Y. & ZHOU, X. 2011. MicroRNA-138 suppresses epithelial-mesenchymal transition in squamous cell carcinoma cell lines. *Biochem J*, 440, 23-31.
286. SKVORTSOV, S., DUDAS, J., EICHBERGER, P., WITSCH-BAUMGARTNER, M., LOEFFLER-RAGG, J., PRITZ, C., SCHARTINGER, V. H., MAIER, H., HALL, J., DEBBAGE, P., RIECHELMANN, H., LUKAS, P. & SKVORTSOVA, I. 2014. Rac1 as a potential therapeutic target for chemo-radioresistant head and neck squamous cell carcinomas (HNSCC). *Br J Cancer*, 110, 2677-87.
287. SKVORTSOV, S., JIMENEZ, C. R., KNOL, J. C., EICHBERGER, P., SCHIESTL, B., DEBBAGE, P., SKVORTSOVA, I. & LUKAS, P. 2011. Radioresistant head and neck squamous cell carcinoma cells: intracellular signaling, putative biomarkers for tumor recurrences and possible therapeutic targets. *Radiother Oncol*, 101, 177-82.
288. CAO, C., CHEN, Y., MASOOD, R., SINHA, U. K. & KOBIELAK, A. 2012. alpha-Catulin marks the invasion front of squamous cell carcinoma and is important for tumor cell metastasis. *Mol Cancer Res*, 10, 892-903.
289. ZHANG, Z., YANG, X. F., HUANG, K. Q., REN, L., ZHAO, S., GOU, W. F., SHEN, D. F., SUN, H. Z., TAKANO, Y. & ZHENG, H. C. 2016. The upregulated alpha-catulin expression was involved in head-neck squamous cell carcinogenesis by promoting proliferation, migration, invasion, and epithelial to mesenchymal transition. *Tumour Biol*, 37, 1671-81.
290. BOURGUIGNON, L. Y., GILAD, E., BRIGHTMAN, A., DIETRICH, F. & SINGLETON, P. 2006. Hyaluronan-CD44 interaction with leukemia-associated RhoGEF and epidermal growth factor receptor promotes Rho/Ras co-activation, phospholipase C epsilon-Ca²⁺ signaling, and cytoskeleton modification in head and neck squamous cell carcinoma cells. *J Biol Chem*, 281, 14026-40.
291. TORRE, C., WANG, S. J., XIA, W. & BOURGUIGNON, L. Y. 2010. Reduction of hyaluronan-CD44-mediated growth, migration, and cisplatin resistance in head and neck cancer due to inhibition of Rho kinase and PI-3 kinase signaling. *Arch Otolaryngol Head Neck Surg*, 136, 493-501.
292. WANG, S. J. & BOURGUIGNON, L. Y. 2011. Role of hyaluronan-mediated CD44 signaling in head and neck squamous cell carcinoma progression and chemoresistance. *Am J Pathol*, 178, 956-63.
293. LAWRENCE, M. S., STOJANOV, P., MERMEL, C. H., ROBINSON, J. T., GARRAWAY, L. A., GOLUB, T. R., MEYERSON, M., GABRIEL, S. B., LANDER, E. S. & GETZ, G. 2014. Discovery and saturation analysis of cancer genes across 21 tumour types. *Nature*, 505, 495-501.
294. CHANG, M. T., ASTHANA, S., GAO, S. P., LEE, B. H., CHAPMAN, J. S., KANDOTH, C., GAO, J., SOCCI, N. D., SOLIT, D. B., OLSHEN, A. B., SCHULTZ, N. & TAYLOR, B. S. 2016. Identifying recurrent mutations in cancer reveals widespread lineage diversity and mutational specificity. *Nat Biotechnol*, 34, 155-63.
295. CAMP, R. L., DOLLED-FILHART, M. & RIMM, D. L. 2004. X-tile: a new bio-informatics tool for biomarker assessment and outcome-based cut-point optimization. *Clin Cancer Res*, 10, 7252-9.
296. RAN, F. A., HSU, P. D., WRIGHT, J., AGARWALA, V., SCOTT, D. A. & ZHANG, F. 2013. Genome engineering using the CRISPR-Cas9 system. *Nat Protoc*, 8, 2281-2308.
297. SKEHAN, P., STORENG, R., SCUDIERO, D., MONKS, A., MCMAHON, J., VISTICA, D., WARREN, J. T., BOKESCH, H., KENNEY, S. & BOYD, M. R. 1990. New colorimetric cytotoxicity assay for anticancer-drug screening. *J Natl Cancer Inst*, 82, 1107-12.
298. LLOMBART, V., TREJO, S. A., BRONSOMS, S., MORANCHO, A., FEIFEI, M., FAURA, J., GARCÍA-BERROCOSO, T., SIMATS, A., ROSELL, A., CANALS, F., HERNÁNDEZ-GUILLAMÓN, M. & MONTANER, J. 2017. Profiling and identification of new proteins involved in brain ischemia using MALDI-imaging-mass-spectrometry. *J Proteomics*, 152, 243-253.
299. ZHOU, J., HAYAKAWA, Y., WANG, T. C. & BASS, A. J. 2014. RHOA mutations identified in diffuse gastric cancer. *Cancer Cell*, 26, 9-11.
300. YAN, G., ZOU, R., CHEN, Z., FAN, B., WANG, Z., WANG, Y., YIN, X., ZHANG, D., TONG, L., YANG, F., JIANG, W., FU, W., ZHENG, J., BERGO, M. O., DALIN, M., ZHENG, J., CHEN, S. & ZHOU, J. 2014. Silencing RHOA inhibits migration and invasion through Wnt/ β -catenin pathway and growth through cell cycle regulation in human tongue cancer. *Acta Biochim Biophys Sin (Shanghai)*, 46, 682-90.

301. MORRIS, L. G. T., CHANDRAMOHAN, R., WEST, L., ZEHIR, A., CHAKRAVARTY, D., PFISTER, D. G., WONG, R. J., LEE, N. Y., SHERMAN, E. J., BAXI, S. S., GANLY, I., SINGH, B., SHAH, J. P., SHAHA, A. R., BOYLE, J. O., PATEL, S. G., ROMAN, B. R., BARKER, C. A., MCBRIDE, S. M., CHAN, T. A., DOGAN, S., HYMAN, D. M., BERGER, M. F., SOLIT, D. B., RIAZ, N. & HO, A. L. 2017. The Molecular Landscape of Recurrent and Metastatic Head and Neck Cancers: Insights From a Precision Oncology Sequencing Platform. *JAMA Oncol*, 3, 244-255.
302. PICKERING, C. R., ZHANG, J., YOO, S. Y., BENGTSSON, L., MOORTHY, S., NESKEY, D. M., ZHAO, M., ORTEGA ALVES, M. V., CHANG, K., DRUMMOND, J., CORTEZ, E., XIE, T. X., ZHANG, D., CHUNG, W., ISSA, J. P., ZWEIDLER-MCKAY, P. A., WU, X., EL-NAGGAR, A. K., WEINSTEIN, J. N., WANG, J., MUZNY, D. M., GIBBS, R. A., WHEELER, D. A., MYERS, J. N. & FREDERICK, M. J. 2013. Integrative genomic characterization of oral squamous cell carcinoma identifies frequent somatic drivers. *Cancer Discov*, 3, 770-81.
303. BOULTER, E., GARCIA-MATA, R., GUILLUY, C., DUBASH, A., ROSSI, G., BRENNWALD, P. J. & BURRIDGE, K. 2010. Regulation of Rho GTPase crosstalk, degradation and activity by RhoGDI1. *Nat Cell Biol*, 12, 477-83.
304. CHO, H. J., KIM, J. T., BAEK, K. E., KIM, B. Y. & LEE, H. G. 2019. Regulation of Rho GTPases by RhoGDIs in Human Cancers. *Cells*, 8.
305. MIGNONE, F., GISSI, C., LIUNI, S. & PESOLE, G. 2002. Untranslated regions of mRNAs. *Genome Biol*, 3, REVIEWS0004.
306. BENDEZÚ, F. O., VINCENZETTI, V., VAVYLONIS, D., WYSS, R., VOGEL, H. & MARTIN, S. G. 2015. Spontaneous Cdc42 polarization independent of GDI-mediated extraction and actin-based trafficking. *PLoS Biol*, 13, e1002097.
307. WU, J. & FILUTOWICZ, M. 1999. Hexahistidine (His₆)-tag dependent protein dimerization: a cautionary tale. *Acta Biochim Pol*, 46, 591-9.
308. MELLACHERUVU, D., WRIGHT, Z., COUZENS, A. L., LAMBERT, J. P., ST-DENIS, N. A., LI, T., MITEVA, Y. V., HAURI, S., SARDIU, M. E., LOW, T. Y., HALIM, V. A., BAGSHAW, R. D., HUBNER, N. C., AL-HAKIM, A., BOUCHARD, A., FAUBERT, D., FERMIN, D., DUNHAM, W. H., GOUDREAU, M., LIN, Z. Y., BADILLO, B. G., PAWSON, T., DUROCHER, D., COULOMBE, B., AEBERSOLD, R., SUPERTI-FURGA, G., COLINGE, J., HECK, A. J., CHOI, H., GSTAIGER, M., MOHAMMED, S., CRISTEA, I. M., BENNETT, K. L., WASHBURN, M. P., RAUGHT, B., EWING, R. M., GINGRAS, A. C. & NESVIZHSKII, A. I. 2013. The CRAPome: a contaminant repository for affinity purification-mass spectrometry data. *Nat Methods*, 10, 730-6.
309. TATE, J. G., BAMFORD, S., JUBB, H. C., SONDKA, Z., BEARE, D. M., BINDAL, N., BOUTSELAKIS, H., COLE, C. G., CREATORE, C., DAWSON, E., FISH, P., HARSHA, B., HATHAWAY, C., JUPE, S. C., KOK, C. Y., NOBLE, K., PONTING, L., RAMSHAW, C. C., RYE, C. E., SPEEDY, H. E., STEFANCIK, R., THOMPSON, S. L., WANG, S., WARD, S., CAMPBELL, P. J. & FORBES, S. A. 2019. COSMIC: the Catalogue Of Somatic Mutations In Cancer. *Nucleic Acids Res*, 47, D941-D947.
310. WANG, C., MCKEITHAN, T. W., GONG, Q., ZHANG, W., BOUSKA, A., ROSENWALD, A., GASCOYNE, R. D., WU, X., WANG, J., MUHAMMAD, Z., JIANG, B., ROHR, J., CANNON, A., STEIDL, C., FU, K., LI, Y., HUNG, S., WEISENBURGER, D. D., GREINER, T. C., SMITH, L., OTT, G., ROGAN, E. G., STAUDT, L. M., VOSE, J., IQBAL, J. & CHAN, W. C. 2015. IDH2R172 mutations define a unique subgroup of patients with angioimmunoblastic T-cell lymphoma. *Blood*, 126, 1741-52.
311. WANG, M., ZHANG, S., CHUANG, S. S., ASHTON-KEY, M., OCHOA, E., BOLLI, N., VASSILIOU, G., GAO, Z. & DU, M. Q. 2017. Angioimmunoblastic T cell lymphoma: novel molecular insights by mutation profiling. *Oncotarget*, 8, 17763-17770.
312. NGUYEN, T. B., SAKATA-YANAGIMOTO, M., ASABE, Y., MATSUBARA, D., KANO, J., YOSHIDA, K., SHIRAIISHI, Y., CHIBA, K., TANAKA, H., MIYANO, S., IZUTSU, K., NAKAMURA, N., TAKEUCHI, K., MIYOSHI, H., OHSHIMA, K., MINOWA, T., OGAWA, S., NOGUCHI, M. & CHIBA, S. 2017. Identification of cell-type-specific mutations in nodal T-cell lymphomas. *Blood Cancer J*, 7, e516.
313. ZHANG, W. 2014. TCGA divides gastric cancer into four molecular subtypes: implications for individualized therapeutics. *Chin J Cancer*, 33, 469-70.
314. ASPENSTROM, P. 2018. Activated Rho GTPases in Cancer-The Beginning of a New Paradigm. *Int J Mol Sci*, 19.
315. STRASSHEIM, D., PORTER, R. A., PHELPS, S. H. & WILLIAMS, C. L. 2000. Unique in vivo associations with SmgGDS and RhoGDI and different guanine nucleotide exchange activities exhibited by RHOA, dominant negative RHOA(Asn-19), and activated RHOA(Val-14). *J Biol Chem*, 275, 6699-702.

Bibliography

316. CORTES, J. R., AMBESI-IMPIOMBATO, A., COURONNE, L., QUINN, S. A., KIM, C. S., DA SILVA ALMEIDA, A. C., WEST, Z., BELVER, L., MARTIN, M. S., SCOURZIC, L., BHAGAT, G., BERNARD, O. A., FERRANDO, A. A. & PALOMERO, T. 2018. RHOA G17V Induces T Follicular Helper Cell Specification and Promotes Lymphomagenesis. *Cancer Cell*, 33, 259-273 e7.
317. MAEKAWA, M., ISHIZAKI, T., BOKU, S., WATANABE, N., FUJITA, A., IWAMATSU, A., OBINATA, T., OHASHI, K., MIZUNO, K. & NARUMIYA, S. 1999. Signaling from Rho to the actin cytoskeleton through protein kinases ROCK and LIM-kinase. *Science*, 285, 895-8.
318. KIMURA, K., ITO, M., AMANO, M., CHIHARA, K., FUKATA, Y., NAKAFUKU, M., YAMAMORI, B., FENG, J., NAKANO, T., OKAWA, K., IWAMATSU, A. & KAIBUCHI, K. 1996. Regulation of myosin phosphatase by Rho and Rho-associated kinase (Rho-kinase). *Science*, 273, 245-8.
319. BROS, M., HAAS, K., MOLL, L. & GRABBE, S. 2019. RHOA as a Key Regulator of Innate and Adaptive Immunity. *Cells*, 8.
320. VEGA, F. M., FRUHWIRTH, G., NG, T. & RIDLEY, A. J. 2011. RHOA and RhoC have distinct roles in migration and invasion by acting through different targets. *J Cell Biol*, 193, 655-65.
321. PAOLI, P., GIANNONI, E. & CHIARUGI, P. 2013. Anoikis molecular pathways and its role in cancer progression. *Biochim Biophys Acta*, 1833, 3481-3498.
322. TONG, L. & TERGAONKAR, V. 2014. Rho protein GTPases and their interactions with NFκB: crossroads of inflammation and matrix biology. *Biosci Rep*, 34.
323. ITO, H., MORISHITA, R. & NAGATA, K. I. 2018. Functions of Rhotekin, an Effector of Rho GTPase, and Its Binding Partners in Mammals. *Int J Mol Sci*, 19.
324. LIU, C. A., WANG, M. J., CHI, C. W., WU, C. W. & CHEN, J. Y. 2004. Overexpression of rho effector rhotekin confers increased survival in gastric adenocarcinoma. *J Biomed Sci*, 11, 661-70.
325. YING-TAO, Z., YI-PING, G., LU-SHENG, S. & YI-LI, W. 2005. Proteomic analysis of differentially expressed proteins between metastatic and non-metastatic human colorectal carcinoma cell lines. *Eur J Gastroenterol Hepatol*, 17, 725-32.
326. FAN, J., MA, L. J., XIA, S. J., YU, L., FU, Q., WU, C. Q., HUANG, X. H., JIANG, J. M. & TANG, X. D. 2005. Association between clinical characteristics and expression abundance of RTKN gene in human bladder carcinoma tissues from Chinese patients. *J Cancer Res Clin Oncol*, 131, 157-62.
327. LIU, C. A., WANG, M. J., CHI, C. W., WU, C. W. & CHEN, J. Y. 2004. Rho/Rhotekin-mediated NF-kappaB activation confers resistance to apoptosis. *Oncogene*, 23, 8731-42.
328. LEUNG, T., CHEN, X. Q., MANSER, E. & LIM, L. 1996. The p160 RHOA-binding kinase ROK alpha is a member of a kinase family and is involved in the reorganization of the cytoskeleton. *Mol Cell Biol*, 16, 5313-27.
329. LEUNG, T., MANSER, E., TAN, L. & LIM, L. 1995. A novel serine/threonine kinase binding the Ras-related RHOA GTPase which translocates the kinase to peripheral membranes. *J Biol Chem*, 270, 29051-4.
330. NAKAGAWA, O., FUJISAWA, K., ISHIZAKI, T., SAITO, Y., NAKAO, K. & NARUMIYA, S. 1996. ROCK-I and ROCK-II, two isoforms of Rho-associated coiled-coil forming protein serine/threonine kinase in mice. *FEBS Lett*, 392, 189-93.
331. ISHIZAKI, T., NAITO, M., FUJISAWA, K., MAEKAWA, M., WATANABE, N., SAITO, Y. & NARUMIYA, S. 1997. p160ROCK, a Rho-associated coiled-coil forming protein kinase, works downstream of Rho and induces focal adhesions. *FEBS Lett*, 404, 118-24.
332. ALBERTS, A. S., BOUQUIN, N., JOHNSTON, L. H. & TREISMAN, R. 1998. Analysis of RHOA-binding proteins reveals an interaction domain conserved in heterotrimeric G protein beta subunits and the yeast response regulator protein Skn7. *J Biol Chem*, 273, 8616-22.
333. AMANO, M., MUKAI, H., ONO, Y., CHIHARA, K., MATSUI, T., HAMAJIMA, Y., OKAWA, K., IWAMATSU, A. & KAIBUCHI, K. 1996. Identification of a putative target for Rho as the serine-threonine kinase protein kinase N. *Science*, 271, 648-50.
334. WATANABE, G., SAITO, Y., MADAULE, P., ISHIZAKI, T., FUJISAWA, K., MORII, N., MUKAI, H., ONO, Y., KAKIZUKA, A. & NARUMIYA, S. 1996. Protein kinase N (PKN) and PKN-related protein rhopilin as targets of small GTPase Rho. *Science*, 271, 645-8.
335. HOTTA, K., TANAKA, K., MINO, A., KOHNO, H. & TAKAI, Y. 1996. Interaction of the Rho family small G proteins with kinectin, an anchoring protein of kinesin motor. *Biochem Biophys Res Commun*, 225, 69-74.
336. CHAN, A. M., TAKAI, S., YAMADA, K. & MIKI, T. 1996. Isolation of a novel oncogene, NET1, from neuroepithelioma cells by expression cDNA cloning. *Oncogene*, 12, 1259-66.

337. TOYOSHIMA, I., YU, H., STEUER, E. R. & SHEETZ, M. P. 1992. Kinectin, a major kinesin-binding protein on ER. *J Cell Biol*, 118, 1121-31.
338. VIGNAL, E., BLANGY, A., MARTIN, M., GAUTHIER-ROUVIÈRE, C. & FORT, P. 2001. Kinectin is a key effector of RhoG microtubule-dependent cellular activity. *Mol Cell Biol*, 21, 8022-34.
339. GAO, L., CHEN, S., HONG, M., ZHOU, W., WANG, B., QIU, J., XIA, J., ZHAO, P., FU, L., WANG, J., DAI, Y., XIE, N., YANG, Q., HUANG, H. D., GAO, X. & ZOU, C. 2021. Kinectin 1 promotes the growth of triple-negative breast cancer via directly co-activating NF-kappaB/p65 and enhancing its transcriptional activity. *Signal Transduct Target Ther*, 6, 250.
340. MUKAI, H., MORI, K., TAKANAGA, H., KITAGAWA, M., SHIBATA, H., SHIMAKAWA, M., MIYAHARA, M. & ONO, Y. 1995. Xenopus PKN: cloning and sequencing of the cDNA and identification of conserved domains. *Biochim Biophys Acta*, 1261, 296-300.
341. TAKAHASHI, M., MUKAI, H., TOSHIMORI, M., MIYAMOTO, M. & ONO, Y. 1998. Proteolytic activation of PKN by caspase-3 or related protease during apoptosis. *Proc Natl Acad Sci U S A*, 95, 11566-71.
342. PALMER, R. H., RIDDEN, J. & PARKER, P. J. 1995. Cloning and expression patterns of two members of a novel protein-kinase-C-related kinase family. *Eur J Biochem*, 227, 344-51.
343. SABATINI, M. E. & CHIOCCA, S. 2020. Human papillomavirus as a driver of head and neck cancers. *Br J Cancer*, 122, 306-314.
344. ECONOMOPOULOU, P., DE BREE, R., KOTSANTIS, I. & PSYRRI, A. 2019. Diagnostic Tumor Markers in Head and Neck Squamous Cell Carcinoma (HNSCC) in the Clinical Setting. *Front Oncol*, 9, 827.
345. CHEN, P., YU, W., HUANG, J., XU, H., LI, G., CHEN, X. & HUANG, Z. 2017. Matched-pair analysis of survival in patients with poorly differentiated versus well-differentiated glottic squamous cell carcinoma. *Oncotarget*, 8, 14770-14776.
346. LV, Z., DING, Y., CAO, W., WANG, S. & GAO, K. 2022. Role of RHO family interacting cell polarization regulators (RIPORs) in health and disease: Recent advances and prospects. *Int J Biol Sci*, 18, 800-808.
347. FROST, J. A., STEEN, H., SHAPIRO, P., LEWIS, T., AHN, N., SHAW, P. E. & COBB, M. H. 1997. Cross-cascade activation of ERKs and ternary complex factors by Rho family proteins. *EMBO J*, 16, 6426-38.
348. BAGRODIA, S., DÉRIJARD, B., DAVIS, R. J. & CERIONE, R. A. 1995. Cdc42 and PAK-mediated signaling leads to Jun kinase and p38 mitogen-activated protein kinase activation. *J Biol Chem*, 270, 27995-8.
349. ARECHA VALETA-VELASCO, F., PEREZ-JUAREZ, C. E., GERTON, G. L. & DIAZ-CUETO, L. 2017. Progranulin and its biological effects in cancer. *Med Oncol*, 34, 194.
350. HE, Z. & BATEMAN, A. 1999. Progranulin gene expression regulates epithelial cell growth and promotes tumor growth in vivo. *Cancer Res*, 59, 3222-9.
351. HE, Z. & BATEMAN, A. 2003. Progranulin (granulin-epithelin precursor, PC-cell-derived growth factor, acrogranin) mediates tissue repair and tumorigenesis. *J Mol Med (Berl)*, 81, 600-12.
352. KELM, R. J., JR., LAMBA, G. S., LEVIS, J. E. & HOLMES, C. E. 2018. Characterization of purine-rich element binding protein B as a novel biomarker in acute myelogenous leukemia prognostication. *J Cell Biochem*, 119, 2073-2083.

